Posttranscriptional regulation of the components of the human leukocyte antigen class I antigen processing and presentation machinery as an immune escape mechanism in melanoma

Dissertation

zur Erlangung des
Doktorgrades der Naturwissenschaften (Dr. rer. nat.)

der

Naturwissenschaftlichen Fakultät I – Biowissenschaften –

der Martin-Luther-Universität
Halle-Wittenberg,

vorgelegt

von Frau Maria-Filothei Lazaridou

geb. am 29.04.1991 in Athen (Griechenland)

Gutachter:

1. Prof. Dr. Stefan Hüttelmaier, Institut für Molekulare Medizin, Martin-Luther-Universität Halle-Wittenberg

2. Prof. Dr. Barbara Seliger, Institut für Medizinische Immunologie, Martin-Luther-Universität Halle-Wittenberg

3. Prof. Dr. Ourania E. Tsitsilonis, Department of Animal and Human Physiology, Faculty of Biology, National and Kapodistrian University of Athens

Tag der öffentlichen Verteidigung: 07.04.2021

Table of contents

1. Introduction

Human melanoma is one of the most immunogenic type of cancers and thereby frequently used as an experimental prototype and model for the identification of the major principles in tumour immunology[1]. Tumours are characterised by an aberrant cell proliferation with the potential to invade or spread to other parts of the body. Currently, ten hallmarks of cancer have been described, which tumour cells can acquire during their development[2], including the capacity of tumours to evade destruction by the host's immune system. In addition, the tumour microenvironment (TME) consisting of soluble and cellular components of the adaptive and innate immune system, plays an important role in the initiation and progression of melanoma. Tumour cells can develop immune escape strategies, such as the deregulation of the components of the human leukocyte antigen class I (HLA-I) antigen processing and presentation machinery (APM)[3], in order to evade immune destruction by T-cells. This deregulation could occur at the posttranscriptional level via microRNAs (miRs) and RNA binding proteins (RBPs) affecting the expression of the components of the APM but also other immune modulatory molecules in tumour and immune cells[4]. Therefore, miRs and RBPs might serve as prognostic and/or predictive tumour markers or as therapeutic tools alone or in combination with immunotherapies.

1.1 Melanoma

Skin cancer could be categorised in melanoma and non-melanoma. The most common types of non-melanoma tumours are basal cell carcinoma and squamous cell carcinoma[5]. Melanoma is the most dangerous type of skin cancer, being currently the 19th most common cancer, while 100350 new cases and 6850 deaths are predicted to occur in United States of America in 2020[6]. Melanoma is more common in men than women[7]. In men it develops often on the back, while in women on the legs[8].

Melanocytes are pigment-containing basal cells[9] originating from the neural crest during embryogenesis and migrating to peripheral sites such as the skin, where they populate hair follicles and epidermis[10]. Moles occur when melanocytes grow in a cluster instead of being spread throughout the skin. Melanoma develops due to abnormal proliferation of melanocytes and is observed when a mole changes in size, colour, itchiness or skin breakdown[9] (Fig. 1.1). Melanocytes are also located in the mucous membranes of the mouth, nose, anus, vagina and, to a lesser extent in the intestine, conjunctiva, retina and meninges. Thus, although melanoma mainly occurs in the skin[9], it also rarely develops in the mouth, intestines, or eye[8].
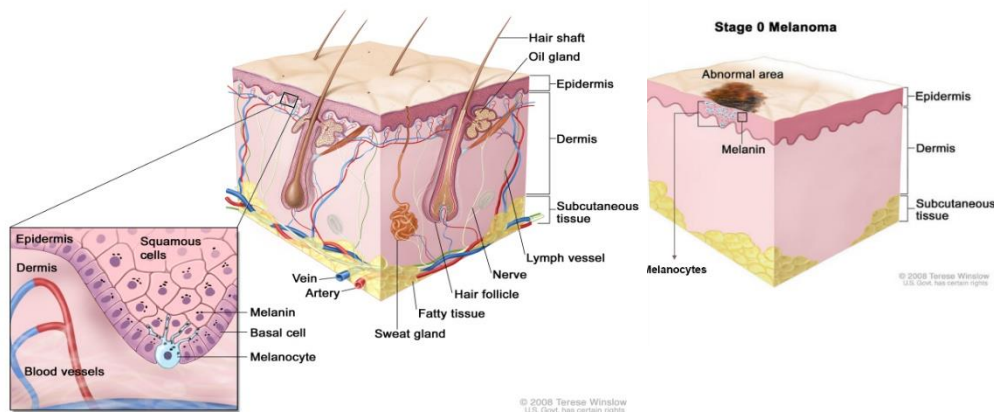
Figure 1.1. Anatomy of the skin, showing the epidermis, dermis, and subcutaneous tissue. Melanocytes are in the layer of basal cells at the deepest part of the epidermis. (edited from Terese Winslow, 2008)

The morphological classification system for melanoma defines four main types with various incidence: superficial spreading melanoma (70%), nodular melanoma (<5%), acral-lentiginous melanoma (15-20%) and lentigo maligna melanoma (15-20%). There exist also some very rare types: mucosal lentiginous melanoma, intraocular melanoma and desmoplastic melanoma. However, this classification has been superseded by a system based on the histopathological parameters of the excised lesion[11]. The figure 1.2 depicts the different melanoma stages. Also important are the risk factors of invasion: "Clark level"[12,13] and "Breslow's depth"[14]. Recently, additional prognostic information has been obtained by sentinel lymph node (SLN) biopsy, a minimally invasive procedure that determines the regional node field status with great accuracy[12,15].
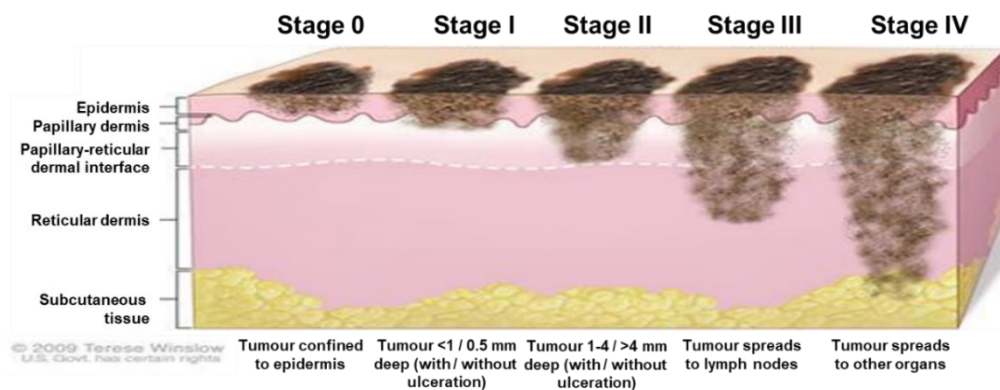
Figure 1.2. The different stages of malignant melanoma and their characteristics[16,17]. (edited from Terese Winslow, 2008)

The earliest stage melanomas are stage 0 (melanoma in situ), and then range from stages I (1) through IV (4) (Fig. 1.2). Some stages are further divided, using capital letters (A, B, etc.). The lower the number, the less the cancer has spread. In stage IV melanoma, the cancer has spread and there exist distant metastases. Within a stage, a lower letter means a lower stage[9].

The most known risk factor for melanoma is the exposure of the skin to ultraviolet (UV) light leading to DNA damage[18], despite being quite variable due to racial background

(skin pigmentation) and geography (sunlight derived ultraviolet irradiation)[8]. During the last years, the importance of the genetic background was underlined by high-throughput assays[19], resulting in the identification of molecules serving as diagnostic, prognostic and predictive biomarkers. Several genes have been mutated with a highly variable incidence, including the serine/threonine kinase B-Raf proto-oncogene (BRAF, 40-50%). The most frequent BRAF mutation is the V600E variant (up to 90%) in which the crucial valin residue at position 600 is substituted by a glutamic acid residue, followed by the V600K variant (5%) carrying a lysine residue at position 600 or in rare cases V600R or V600D variants where position 600 is replaced by either arginine or aspartic acid residues, respectively[20-22]. Apart from the BRAF mutations, other genes have also been mutated in cutaneous melanoma, such as the cyclin dependent kinase inhibitor 2A (CDKN2A, (20-40%)[23], NRAS proto-oncogene (15-20%)[22,24] and tumour protein p53 (TP53, 10%)[25]. BRAF (20%)[26], NRAS (14%)[27] and neurofibromin 1 (NF1,14%)[28] in acral melanoma, while the splicing factor 3B subunit 1 (SF3B1, 37%)[29] in mucosal melanoma[30] and KIT (also known as CD117) in *in situ* melanoma[31]. BRAF mutations are associated with increased tumour growth and proliferation through activation of the mitogen-activating protein kinase (MAPK) signalling pathway[22]. MAPK pathway inhibition by tyrosine-kinase inhibitors (TKIs) including BRAF, KIT or MEK inhibitors has been a breakthrough in the treatment of mainly advanced/inoperable melanoma regarding the response and survival of patients with disease harbouring BRAF V600 activating mutations[10]. At the functional level, receptor tyrosine kinases (RTKs) and their tyrosine kinase enzymes compete with TKIs, which compete with the ATP binding site of the catalytic domain of several tyrosine kinases and inhibit their phosphorylation[32]. Nevertheless, the antiproliferative effect of these inhibitors is limited, despite robust early clinical efficacy, due to the development of various resistance mechanisms[10], which appear to be MAPK pathway-dependent or independent. In the majority of cases, the MAPK pathway is reactivated, either due to the appearance of concomitant NRAS mutations, most likely through the proto-oncogene c-RAF[33], or due to MEK mutations[34]. Additionally, mechanisms of resistance appear to be related with COT, a MAPK downstream of BRAF[35] or the PI3K pathway, through the upregulation of platelet-derived growth factor receptor (PDGF-R) and insulin-like growth factor receptor (IGFR), and the genomic loss of phosphatase and tensin homolog (PTEN)[34,36].

Hanahan and Weinberg were the first that referred to the hallmarks of cancer, consisting today of ten biological features, which tumour cells can acquire during their multistep development. The hallmarks constitute an organizing principle for rationalizing the complexities of neoplastic disease[2]. Initially they included sustained proliferative signalling, evasion of growth suppressors, resistance to cell death, replicative immortality, induction of angiogenesis and activation of invasion and metastasis[37]. Recently, the list was further extended by adding the following hallmarks: reprogram of energy metabolism, escape of immune destruction, genome instability and promotion of inflammation. This knowledge could lead to the development of novel modalities to treat human cancer[2].

Melanoma is one of the most immunogenic tumours due to its high (UV-driven) mutational burden, which generates neoantigens that can be recognized as "non-self" by the host immune system[38]. However, many immune modulatory mechanisms have been described to favour the genesis and progression of melanoma and to interfere with the immune recognition resulting in immune resistance and

immunosuppression[39]. The interrelationship between the immune system and malignancy is now better understood through the concept of tumour immunoediting[40], which exists in continuum from immune elimination to immune equilibrium and further to tumour escape[41]. Melanoma is a target for immunotherapies because it is frequently infiltrated with cluster of differentiation 8^{+} (CD8^{+}) effector T-cells[42] and occasionally undergo spontaneous regressions[43]. Metastatic melanoma is known for its resistance to traditional cancer treatments, including chemotherapy and radiotherapy[38], as well as for its responsiveness to immunotherapy[44] (Table 1.1).

Table 1.1. Different strategies for cancer treatment

	Therapy	Drugs for melanoma treatment
Targeted therapies	TKIs (MAPK pathway inhibition) (FDA approved)	BRAF Inhibitors: binimetinib, sorafenib, vemurafenib, dabrafenib mesylate, encorafenib, KIT inhibitors: dasatinib (Sprycel), imatinib (Gleevec), nilotinib (Tasigna) MEK inhibitors: cobinetinib
Active immuno-therapies	DC-based immunotherapies	
	peptide- and DNA-based anticancer vaccines	cell-based vaccines (Canvaxin™ (CancerVax Corp.,USA)[53], GVAXR (Aduro Bio Tech, Berkeley, CA)[54]) peptide-based vaccine (gp100)
	immunostimulatory cytokines immune modulatory mAbs inhibitors of the immunosuppressive metabolism PRRs agonists immunogenic cell death inducers	IL-2, IFN-α
Passive immuno-therapies	tumour-targeting mAbs ACT	
	oncolytic viruses	talimogenela herparepvec (T Vec, Amgen (Thousand Oaks, CA))
ICPs	anti-CTLA-4	ipilimumab (anti-CTLA-4, B-M Squibb)
	anti-PD1	nivolumab (anti-PD1, B-M Squibb) pembrolizumab (anti-PD1, Merck/MSD)

Although several tumour-targeting mAbs, ACT and oncolytic viruses have been classified as passive, they may de facto constitute active forms of immunotherapy[45]. (TKIs = tyrosine-kinase inhibitors, BRIM-3 = BRAF inhibitor in melanoma-3, DC = dendritic cell, PRRs = pattern recognition receptors, ACT = adoptive cell transfer)

Cancer immunotherapy refers to a number of approaches intended to activate the immune system, to induce the immune response and the disease stabilization[46]. During the past three decades, cancer immunotherapy has become a clinical reality[47,48] and is currently transforming several types of cancer, such as metastatic melanoma from a death sentence to a chronic disease[49]. Cancer immunotherapies are generally classified as "active" or "passive". Active immunotherapies aim to stimulate the host immune system or a specific immune response against tumour cells, while donated or laboratory-made immune system components or cellular proteins are given to the patients during passive immunotherapies[44,47].

Recent clinical trials have been focused on a series of molecules known as immune checkpoints, whose natural function is to restrain a potentially over-exuberant response and harbour immunosuppressive functions[50]. Blocking immune checkpoint (ICP) molecules with monoclonal antibodies (mAb) has emerged as a viable clinical strategy, mediating tumour shrinkage in several cancer types, including melanoma[46]. Neoadjuvant and adjuvant therapies may include chemotherapy, hormone therapy, radiation therapy, immunotherapy and targeted therapy. Neoadjuvant therapies are delivered before the main treatment, to help reduce the size of a tumour or kill spread tumour cells, while adjuvant therapies are delivered after the primary treatment, to destroy remaining tumour cells. Current challenges include incorporating immunotherapy into adjuvant and neoadjuvant cancer therapy, refining dose, schedule and duration of treatments and developing novel surrogate endpoints that accurately capture overall survival benefit early in treatment[49].

1.2 The immune system

Immunity can be defined very roughly as resistance to malignancies, in particular to infectious diseases and cancer. The immune system consists of various cell populations (such as T-cells, B-cells, macrophages, DCs and NK cells), tissues and molecules that maintain the host's healthy status, mediate protection against pathogens and tumour cells, and induce immunological tolerance against self antigens[51]. The coordinated action of immune cells and molecules comprises the immune response. Thus, one important physiologic task of the immune system is to prevent and/or eradicate infections and neoplastic transformed cells.

The immune system is classically divided into the innate immunity[52], which provides fast reactive first line of defence mechanisms, and the adaptive immunity, which provides a more specific, but slower second line of defence and generates a more specialized protection[53]. The innate immunity is the first line of defence mediated by cells and molecules to eliminate highly diverse infectious microbes through a limited repertoire of germline-encoded receptors (PRRs)[53-55]. The basic protective strategy of the innate immune system for the organism is to constitutively produce a limited series of generic receptors, such as the toll-like receptors (TLRs) and other PRRs, triggering inflammatory response against pathogen invasion[55,56]. A variety of different molecules produced by pathogens can serve as pathogen-associated molecular patterns (PAMPs), including glycans, glycoconjugates[57], single-stranded (ss) and double-stranded (ds) nucleic acids (DNA and RNA) or RNA viruses[58]. Such PAMPs can be recognized by PRRs, inducing receptor oligomerization and subsequently triggering intracellular signal transduction cascades, which induce inflammatory responses[56].

In contrast, the adaptive immune system is characterized by memory, specificity, diversity, clonal expansion, but also immunological tolerance and is divided into humoral and cell-mediated responses[51,54]. Specific adaptive immunity depends upon the somatic diversification of antigen-receptor genes to generate a vast repertoire of cells, each expressing different, highly specific antigen receptors[59]. Lymphocytes are responsible for the specificity of adaptive immune responses[60] using their cell surface receptors to recognize specific pathogens and then respond to the antigen triggering by clonal amplification, cellular differentiation, and production of antibodies with the same antigen binding specificity[59,61]. B-lymphocytes (humoral immune response) and T-lymphocytes (cellular immune response) derive from stem cells in the bone marrow[62]. B-lymphocytes mature in the bone marrow, while T-lymphocytes migrate to

the thymus to complete their antigen-independent maturation into functional T-cells. In the thymus, T-cells develop specific markers, such as the T-cell receptor (TCR), CD3, CD4 and CD8. They also undergo thymic education through positive and negative selection[63]. T-lymphocytes are divided into CD8^{+} cytotoxic T-lymphocytes (CTL or T_c), which mediate highly specific cytotoxicity, and CD4^{+} helper T-lymphocytes (T_h)[62], which are essential to mount an effective humoral response and to establish humoral memory.

CD8^{+} T-cells and NK cells are the key players in anti-tumour immune response[64]. CD8^{+} T-cells receive an activation signal when their TCR recognizes peptide antigen bound to the major histocompatibility complex class I (MHC-I), presented on the surface of antigen presenting cells (APCs), notably professional APCs (pAPCs) such as dendritic cells (DCs)[65]. Engagement of antigenic ligands by the TCR induces intracellular signalling responses, leading within minutes to the formation of an immunological synapse between the lymphocyte and the APC[66]. However, this interaction is of low-affinity and a second (co-stimulatory) signal is generally indispensable for their full activation and survival[67]. The prototype of co-stimulatory factors is the interaction of CD28 (on the surface of the T-cell) and CD86 or CD80 (on the surface of the APCs)[65]. The delivery of appropriate activation signals to naive CD8^{+} T-cells by pAPCs leads to their proliferation and concomitant differentiation into effector CD8^{+} T-cells (or CTLs)[68,69] and central memory CD8^{+} T-cells[70]. After binding to the target cell, CTLs release granules containing perforin and granzyme. Perforin forms pores on the cellular membrane. Granzymes are structurally related serine proteases and they pass through the pores[71], activating caspase enzymes that induce DNA fragmentation and cell apoptosis[62]. CTLs also bind the death inducing receptor Fas through their Fas ligand (FasL) thereby activating apoptosis (Fig. 1.3). Fas belongs to the TNF receptor family, is expressed on lymphoid, myeloid and non-hemopoietic cells and induces apoptosis in different cell types[72], such as pathogen infected target cells, as well as potentially deleterious and autoreactive lymphocytes[73]. The majority of T-cells recognize peptide antigens bound and presented by the MHC[74] (Fig. 1.3). All nucleated cells can present antigens on MHC-I to CD8^{+} T-cells[51]. Alternatively, MHC-I can serve as an inhibitory ligand for NK cells (Fig. 1.3).
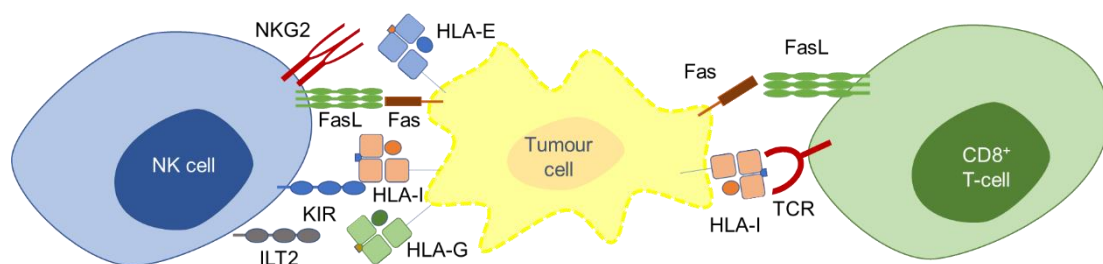
Figure 1.3. Tumour recognition by CTLs and NK cells
CD8^{+} T-cells express TCRs and recognize tumour antigen peptides associated with MHC-I cell surface proteins. NK cells interact with a wide range of activating and inhibitory receptors, such as the NCRs, KIRs and ILTs.

NK cells have been classified as lymphocytes[75,76] on the basis of their morphology, their expression of many lymphoid markers[53], and their origin from the common lymphoid progenitor cell in the bone marrow[77]. However, they are considered to be components of innate immune defence because they lack antigen-specific cell surface

receptors. In addition, they have been shown in humans and mice to participate in the early response against virus infection[78] and in tumour immunosurveillance[79]. NK cell receptors can be either activating or inhibitory[80]. Activating receptors include receptors that interact with soluble ligands such as cytokines, or cell surface molecules[81]. Such are the natural cytotoxicity receptors (NCRs: NKp30, NKp44, and NKp46), killer cell immunoglobulin-like receptors (KIRs) and NKG2D, while the Ig-like transcripts receptors (ILTs) belong to the inhibitory receptors. Several of the KIRs and CD94-NKG2C receptors are capable of recognizing self-major MHC-I by signalling through intracytoplasmic immunoreceptor tyrosine-based inhibition motifs (ITIMs)[80]. KIR ligands are the HLA-C and HLA-B molecules. Based on the aa sequence determining the KIR-binding epitope, HLA-C alleles have been assigned to HLA-C group 1 (C1) or group 2 (C2), while most HLA-B alleles can be distinguished by the presence of the serological epitopes Bw4 and Bw6 but only those bearing the HLA-Bw4 motif serve as ligands for KIRs[82], such as KIR3DL1 and HLA-Bw4[83]. NKG2D receptor interacts also with various ligands expressed at low levels in most tissues[84], such as NKG2DA and HLA-E, but they are overexpressed upon initiation of cellular distress, for example after initiation of the DNA damage response[85]. NK cells express also Fc receptors (FcR), recognizing the invariable Fc region of immunoglobulins, and they can bind also to tumour cells via tumour-bound antibodies.

NK cell receptors specific for MHC-I molecules appear to be stochastically expressed in the NK-cell population[84,86], in a process characterised as 'NK cell education', a process whereby the effector functions of developing NK cells are adapted to the levels of MHC-I expressed by a host[87] facilitating the surveillance of target cells with downregulated MHC-I expression due to infection or malignancy[83,88].

The ability of NK cells to specifically recognize cells lacking expression of self-MHC-I molecules was discovered over 30 years ago (the "missing self" hypothesis[89]), where NK cells can detect the lack of MHC-I, "missing self", a situation occurring when cells are perturbed by viral infection or cellular transformation[90]. Since healthy nucleated cells express self MHC-I molecules, KIRs ensure that NK cells do not attack normal cells but eliminate infected or tumour cells (which may have reduced MHC-I expression)[91]. Thus, NK cells selectively kill target cells with downregulated MHC-I molecules and/or upregulated stress-induced self-molecules such as NKG2D ligands[85] (Fig. 1.3).

Despite the recent remarkable breakthroughs in clinical cancer immunotherapy, the cytolytic potential of NK cells still remains largely untapped in clinical settings. There is abundant evidence demonstrating partial or complete loss of MHC-I expression in a wide spectrum of human tumour types. Such loss may result in immune selection of escape variants by tumour-specific CD8+ T-cells and acquired resistance to checkpoint inhibition therapy, giving rise to potential NK cell-based adoptive immunotherapies to convert checkpoint inhibitor therapy-resistant patients into clinical responders[89]. Various NK cell sources are currently being used for the development of adoptive cancer immunotherapy, including autologous or allogeneic NK cells, NK cell lines from peripheral blood and stem cells, and genetically engineered NK cells[92,93].

1.3 Characteristics of MHC-I molecules and the antigen processing and presentation machinery (APM)

Antigen presentation can be subdivided into MHC-I and MHC-II dependent pathways. On the one hand, extracellular proteins internalized by APCs are processed in late

endosomes and lysosomes, displayed by MHC-II molecules and can be recognized by CD4^{+} T-cells. On the other hand, proteins in the cytosol of nucleated cells are processed by the multicatalytic proteasome and the yielded peptides are presented on MHC-I molecules via the antigen processing and presentation machinery (APM), a multitasking key player, and can be recognized by CD8^{+} T-cells or NK cells[94,95]. Cross-presentation is an alternative pathway to establish the presentation of antigenic peptides via MHC-I molecules but herefore requires the uptake, processing and presentation of exogenous antigens by pAPCs. In addition, it has been demonstrated that also endogenous antigens can also be presented by MHC-II when they are degraded through autophagy[95].

The MHC is a set of genes, which is divided into three subgroups: MHC-I, MHC-II and MHC-III molecules[74]. MHC-I and MHC-II molecules are membrane proteins, highly polymorphic[51], while MHC-III molecules are structurally poorly defined and functionally, which are not involved in antigen presentation, but include several secreted proteins with immune functions, such as components of the complement system, cytokines and heat shock proteins[96]. The human leukocyte antigen (HLA) system is the gene complex encoding MHC proteins in humans and the HLA-I system includes the "classical" HLA-A, -B, -C[97] and the "non-classical" HLA-E, -F, -G and –H molecules[98]. Key functions for classical HLA-I molecules are to present antigenic peptide ligands to CD8^{+} T-cells, whereas non-classical HLA-I molecules mediate inhibitory or activating stimuli in NK, B- or selected T-cells[98].

MHC-I molecules are heterodimers that consist of a heavy chain (HC) not covalently bound to the β2-microglobulin (β2-m) chain. The MHC-I HC is composed of the α1, α2, and α3 domains[99]. The MHC-I HC is polymorphic and encoded by the MHC-I genes, while the β2-m subunit is not polymorphic and encoded by the β2-m gene[100]. B2-m has no transmembrane region and it lies below the α1 domain, while the α3 domain is plasma membrane-spanning and interacts with the CD8 co-receptor of T-cells. The α3-CD8 interaction holds the MHC-I molecule in place, while the TCR binds its α1-α2 heterodimer ligand, and monitors the coupled peptide for antigenicity. The α1 and α2 domains yield the peptide binding groove and the peptide presented is held in the central region of the α1/α2 heterodimer[101].

The APM consists of several components: the transporter associated with antigen processing (TAP), the MHC-I HC, β2-m, the adapter chaperone tapasin (TPN), the endoplasmic reticulum (ER)-resident oxidoreductase ERp57, the binding immunoglobulin protein (BiP), the lectin-like chaperone calreticulin (CRT), the calcium-binding protein calnexin (CNX) and the genes encoding the proteasome subunits, among them the low molecular weight proteins (LMPs)[102,103]. TAP is a heterodimer transporter consisting of the TAP1 (ABCB2) and TAP2 (ABCB3) subunits[104], which are members of the superfamily of ATP-binding cassette (ABC) transporters translocating antigenic peptides into the ER lumen[105]. A heterodimeric TAP complex is essential and sufficient for peptide binding and translocation, whereas TAP1 or TAP2 homodimers are non-functional[106] and a mutated TAP complex showed a drastically diminished transport rate[107]. TAP1 and TAP2 are found in all nucleated cells of jawed vertebrates[107]. Together with HLA-DR, -DQ, -DP, -DM, and -DO molecules, which belong to the HLA-II molecules, TPN, LMP2 and LMP7, TAP1 and TAP2 genes are located on chromosome 6 (6p21.32)[108,109]. Two transcript variants encoding different isoforms have been identified for TAP1, differing in the 5'-UTR and coding sequence (CDS) and resulting into a shorter isoform at the N-terminus[110], while three transcript

variants encoding different isoforms have been found for TAP2, differing either at 3 nt positions and resulting in a 17 amino acid shorter isoform at the C-terminus or in the 5'-UTR and CDS[110,111]. For TPN, three transcript variants have been documented either differing in the 3'-CDS and 3'-UTR or lacking an alternate in-frame exon in the central coding region[112].

The NLR family CARD domain containing 5 (NLRC5) is member of the NLR family that acts as a transcriptional activator of MHC-I genes[113], while Nlrc5-deficient knock-out mice showed reduced MHC-I, exhibiting the greatest effect in cells in the immune system[114]. Activation of adaptive immune responses by interferon (IFN) is partially due to transcriptional activation of genes encoding the MHC-I and MHC-II antigens and respective APM components such as the TAP, TPN, the LMPs and the endoplasmic reticulum aminopeptidases 1 and 2 (ERAP1/2), since the promoter of these MHC-I APM components contain a combination of distinct transcription factor-binding sites (TFBS), like Sp1, the cAMP responsive element binding protein 1 (CREB1), the nuclear factor (NF)-κB, E2F, and the E1A binding protein p300, exhibiting IFN-response elements, which suggested a regulation by interferon-regulated factors (IRFs)[115]. The APM components are induced by stimulation with IFN type I (IFN-α and β) and type II (IFN-γ) [116,117]. Among them, IFN-γ can promote the upregulation of the specific catalytic immunoproteasome subunits LMP2 (also called *β*1i or PSMB9), LMP7 (*β*2i or PSMB8) and LMP10 (*β*5i or PSMB10), which are incorporated into the 20S proteasome thereby replacing the constitutive *β*1, *β*2, and *β*5 proteasome subunits[118]. The exchange of these subunits results in the generation of the immunoproteasome and an altered peptide repertoire[119,120].

The four main steps of the antigen processing and presentation via MHC-I molecules are summarised in figure 1.4.

 1) Peptide generation and trimming

MHC-I molecules present a wide repertoire of peptides to CD8+ T-cells. These peptides are not randomly chosen, but rather selected for their ability to bind to the polymorphic MHC-I peptide binding groove[121]. Peptides presented by MHC-I molecules are mainly derived from endogenously cytosolic proteins generated by proteasomes during the degradation of intracellular proteins[122] (Fig. 1.4). The proteasome is a multicatalytic protein complex[104] located in the nucleus and the cytosol[123-125]. Its shape is cylindrical and contains a catalytic core and regulatory domains. Proteasome subtypes are defined by their catalytic subunits[118]. Particularly, the immunoproteasomes consist of LMP2, LMP7 and LMP10[120]. Regulatory particles bind to one or both ends of the 20S proteasome. Two 19S regulatory particles (or PA700) bind to both sides of the 20S proteasome and they form the 26S proteasome[126]. Other regulatory particles, such as PA28αβ (proteasome activator subunit 1 and 2, PSME1-2)[127], PA200 (PSME3)[128] and PI31 (proteasome inhibitor subunit 1, PSMF1)[129] can also associate with the 20S regulatory particle. Different groups of genes encode the different subunits of the proteasome. Particularly, the 20S proteasome is encoded by the proteasome 20S subunit alpha 1-8 (PSMA1-8) and proteasome 20S subunit beta 1-10 (PSMB1-10) genes[130,131], while the 26S proteasome by the proteasome 26S subunit, ATPase 1-6 (PSMC1-6) and proteasome 26S subunit, non-ATPase 1 (PSMD1-14) genes[132].

Ubiquitin acts as a tag that signals the protein-transport machinery to ferry the protein to the proteasome for degradation[133]. Upon activation of the immunoproteasome, ubiquitinated proteins pass unfold, spread along, and lose the polyubiquitin chain

(deubiquitination) through the action of deubiquitinating enzymes (DUBs)[134]. They are subsequently broken down into peptides ranging from 2 to 25 residues with a correct C-terminus, whereas the N-termini might be are further trimmed by peptidases localized in the cytosol[102,134]. Several cytosolic peptidases, such as the tripeptidyl peptidase II (TPPII), the bleomycin hydrolase (BLH), the puromycin-sensitive aminopeptidase and the IFN-γ-inducible leucine aminopeptidase 3 (LAP3), play a role in trimming of the N-extended proteasome products[135,136]. A big variety of peptides is created in terms of amino acid sequence, length and quantity[137], depending on whether the proteasome or immunoproteasome is involved.

Two mechanisms exist for the trimming of peptides to a size suitable for association with MHC-I molecules by trimming in the ER and by cytosolic peptidases during peptide recycling over the ER membrane[138]. The ER resident aminopeptidases associated with antigen processing (ERAAP), ERAP1 and 2 in humans, are involved in the final N-terminal trimming of peptides in the ER and are considered as "molecular rulers" due to their substrate preference[139-141]. ERAP1 is thought to be the main trimming enzyme of the ER, responsible for fitting peptides that need to be shortened to the required length, while ERAP2 seems to be responsible for shaping a smaller subset of the peptidome[142]. Longer peptides often undergo further trimming in the ER lumen by the ERAP1/2 or transported back to the cytosol where they are trimmed by the cytosolic peptidases and recycle back to the ER by Sec61 translocon[143,144] and Derlin-1[145] or in a TAP-dependent fashion for association with MHC-I molecules[134,138]. Such peptides are more rapidly translocated from the ER to the cytosol than degraded in the ER lumen[144].
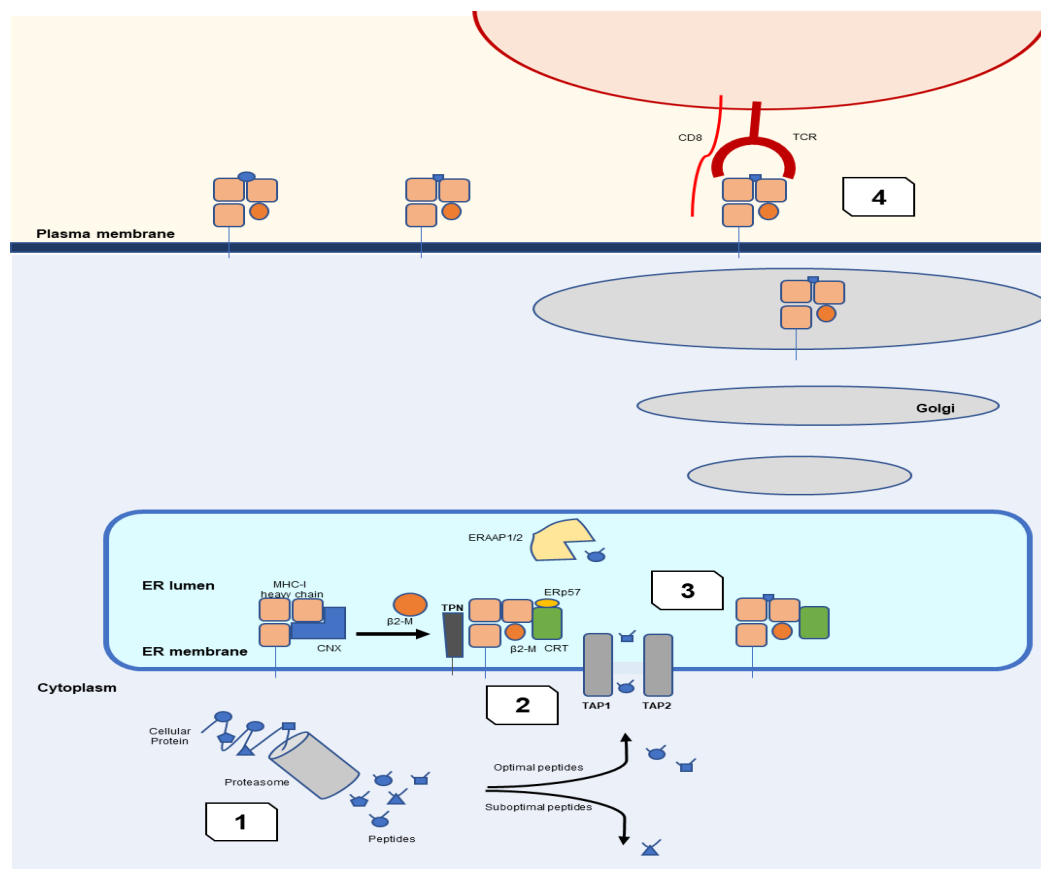
Figure 1.4. Schematic representation of the four MHC-I antigen processing and presentation steps 1) peptide generation and trimming, 2) peptide transport, 3) formation of the MHC-I loading complex, 4) antigen presentation.

2) Peptide transport

After their cytosolic cleavage, the peptides are transported from the cytosol into the ER via the TAP[134] (Fig. 1.4). TAP1 and TAP2 consist of two domains: a hydrophobic, N-terminal transmembrane domain (TMD) harbouring the substrate-binding site and a cytosolic, C-terminal nucleotide-binding domain (NBD) responsible for ATP binding and hydrolysis[146] (Fig. 1.5). The TMDs of TAP1 and TAP2 contain 10 and 9 transmembrane helices, respectively. The N-terminal 4 TM helices of TAP1 and the N-terminal 3 TM helices TAP2, known as TMD0s, recruit TPN[147]. Each coreTAP subunit consists of six TM helices plus the NBD[148]. The coreTAP shares significant homology with other ABC transporters and is necessary and sufficient for peptide binding and transport[149]. Deletion of the first transmembrane-spanning segment of TAP destroys its ability to interact with TPN[150], however, the core TAP subunits lacking these TMD0s are sufficient for TAP assembly, peptide binding and translocation[149,150].
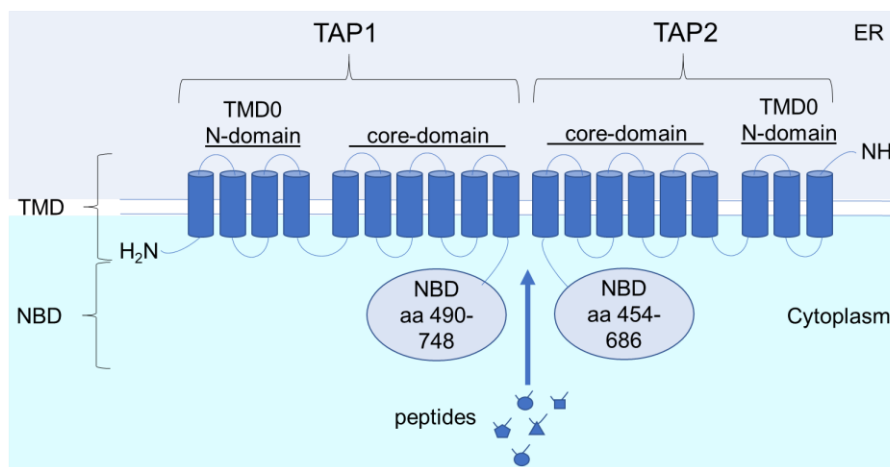
Figure 1.5. Schematic presentation of the TAP heterodimer
The transmembrane domains (TMDs) and nucleotide-binding domains (NBDs) domains of TAP1 and TAP2 are shown in dark and light blue, respectively. The TMDs are subdivided into a core-domain, which comprises the peptide translocation pore, and a N-terminal domain (TMD0), which recruit TPN[151] (edited from Plewnia, G. *et al.* Journal of molecular biology 2007).

TAP forms a transmembrane pore in the ER membrane and upon ATP binding or hydrolysis the pore opens or close, respectively (ATP switch model)[152-154]. Peptide binding to the TMDs is independent from ATP binding to the NBDs[155], while peptide binding and translocation induce ATP hydrolysis. Under physiological conditions, the transport complex is loaded with two ATP-Mg in the resting state. Peptide binding of TAP triggers an allosteric cross talk between NBDs and TMDs. The adopted substrate-bound state induces dimerization of the NBDs and presumably the formation of an occluded state. A subsequent conformational rearrangement of the TMDs switches TAP from the inward-facing state (cytosol) to the outward-facing state (ER). The tight NBD dimer sandwiches two ATP molecules at its interface. ATP hydrolysis by TAP is strictly coupled to peptide binding and release into the ER lumen. After ATP hydrolysis, the NBD dimer is destabilized and the transporter resets to its inward-open, "resting" state, in which inorganic phosphate and ADP are exchanged by ATP-Mg[107]. The peptide length and sequence play an important role in the transport by TAP1 and TAP2, since peptides of a relatively short length (8–12 residues), positively charged or aromantic residues at the N-terminus and hydrophobic or basic C-terminus are more

efficiently transported to the ER lumen[102,134,156,157]. At high ER peptide concentrations (16 µM), TAP is blocked by trans-inhibition[107].

Apart from endogenously derived cytosolic peptides, exogenous peptides can be processed and presented to CD8^{+} T-cells via the cross-presentation pathway. There are two main pathways for cross-presentation. While the cytosolic pathway is proteasome- and TAP-dependent, the vacuolar pathway depends on neither the TAP dimer nor the proteasome[95]. Moreover, the HLA-A2 molecules are TAP-independently expressed in the TAP1^{-}/TAP2^{-} T2 cell line. There exist also a TAP-independent pathway that does involve proteasomal degradation of proteins, such as the Epstein–Barr nuclear antigens (EBNAs) 1, 2, 3A, 3B, 3C and -LP, and the latent membrane proteins 1 and 2 (LMP-1, LMP-2), constitutively expressed in Epstein-Barr virus (EBV)-transformed B-lymphoblastoid cell lines *in vitro*[158],

Mutations in TAP can been related to ankylosing spondylitis, insulin-dependent diabetes mellitus, celiac disease and the bare lymphocyte syndrome type I (BLS I), where patients generally have a severe reduction of HLA-I surface expression and they exhibit granulomatous skin lesions. In most cases, this low expression is due to a homozygous inactivating mutation in either TAP1 or TAP2. TAP deficiencies are usually characterized by chronic bacterial infections of the upper and lower airways, evolving to bronchiectasis[159]. Despite the defect in HLA-I mediated presentation of viral antigens to CD8^{+} T-cells, patients with defects in TAP do not suffer from severe viral infection. Although the proportion of T-cells may be reduced in patients with TAP deficiencies, they have normal humoral response and they tend to have a higher proportion of immune cells, such γδ T-cells, NK cells and neutrophils[111].

Nevertheless, viruses that maintain life-long infections, such as herpes- and poxviruses have developed distinct methods to block TAP. Through a long period of coevolution with their hosts, such DNA viruses have independently acquired highly efficient means of blocking TAP-mediated peptide transport and/or subsequent peptide loading onto MHC-I assembly. Particularly *Herpesviridae* express numerous immune evasion molecules that (i) cause degradation of MHC-I, (ii) lead to retention of immature molecules in the cis-Golgi, (iii) induce enhanced endocytosis of MHC-I and (iv) block MHC-I protein synthesis reducing its surface expression[160]. To date, four herpesvirus-encoded TAP inhibitors have been identified: (i) ICP47 encoded by herpes simplex virus (HSV) 1 and 2, (ii) BNLF2a encoded by the EBV, (iii) US6 encoded by human and rhesus cytomegalovirus (HCMV and RhCMV), and (iv) UL49.5 encoded by a broad range of varicelloviruses[147].

Moreover, in TAP1 knockout mice, peptides for MHC-I presentation are unable to be actively transported into the ER via the TAP complex and are therefore not available for binding to the MHC molecule, preventing its presentation on the cell surface. In TPN knockout mice, appropriate peptides enter the ER, but the various functions of TPN are not available[161].

3) Formation of the MHC-I loading complex

With the help of the chaperones BiP, CNX[162], the thiol oxidoreductase ERp57[163,164], CRT[165] and TPN[109,165], the peptides transported into the ER are loaded onto nascent MHC-I molecules[166] (Fig. 1.4). TAP and TPN are critical for the binding of peptides[165,167], since TAP stabilizes the HC/β2-m heterodimers and TPN facilitates the optimal peptide loading onto MHC-I molecules[104,109] and the efficient processing. The number of TPN per TAP dimer can vary from 1 to 4 molecules[168]. Inappropriate pairing

of TAP alleles with MHC-I alleles led to reduced expression of MHC-I, which could be detected at the cell surface[111].

MHC-I HC encounters the chaperones BiP and CNX. The MHC-I HC interacts with CNX, which facilitates its complete folding and, by acting in concert with ERp57, ensures its correct oxidation[169]. After β2-m association[170], CNX is replaced by CRT[135] and, subsequently, the remaining peptide loading complex (PLC) components, including the protein disulfide isomerase (PDI), TPN, ERp57, and TAP, form a macromolecular complex (MHC-I assembly)[171]. The optimisation of the MHC-I peptide cargo is suggested to be dependent on TPN[172]. However, HLA-I molecules vary in their dependence on the protein[173], since the anchor positions of the given HLA-allele largely define the peptides which can be stably bound and subsequently presented, as well as to its conformational flexibility[174]. After TPN-catalysed proofreading, stable peptide–MHC-I complexes are released from the PLC and traffic via the Golgi to the cell surface[175]. After epitope proofreading and quality control within the PLC, kinetically stable peptide–MHC complexes are released to shuttle their antigenic cargo via the secretory pathway to the plasma membrane[107].

Peptides bound in the groove of MHC-I molecules serve two functions: to structurally stabilize MHC molecules for long-lived display at the cell surface and to form part of a composite peptide-MHC ligand recognized by the TCRs. However, genetic lesions in the peptide-loading steps of the APM pathway, particularly in major components of the PLC including TAP and TPN can result in the production of "empty" MHC-I molecules. For this reason, the molecular flexibility in peptide loading onto MHC, the MHC/chaperone interaction and the interaction of the peptide-MHC complex with the TCR form a set of dynamic events contributing to their biological and potentially pathogenic role[176].

As a key component of the PLC, the importance of TPN in peptide selection and loading is apparent in TPN knock-out mice and cell lines in which expression of MHC-I molecules is often severely reduced due to a lack of appropriate peptide loading[177]. However, apart from TPN, the tapasin-related protein (TAPBPR or TAPBPL) functions also as a peptide editor, which influences the selected peptides displayed by MHC-I molecules for immune recognition. It is located on chromosome 12 (12p13.3), is inducible by IFN-γ and has 22% identity to TPN. Despite their differences in their aa sequence composition, they are located similarly on the MHC-I assembly [111]. The effect of TAPBPR on MHC-I expression and peptide selection appears less profound in comparison to TPN, since the steady state levels of MHC-I are similar in the presence or absence of TAPBPR and TAPBPR deficient cell lines, such as HeLa or KBM-7 cells, do not have impaired peptide loading onto MHC-I. In the absence of TAPBPR, the recovered peptide repertoire appears broader, while upon its overexpression TAPBPR is detectable at the cell surface[177]. In addition, TPN functions only in a near neutral pH, while TAPBPR seems to operate within a wider range (ER: pH 7.2, cis- Golgi: pH 6.7, trans-Golgi: pH 6.0)[178].

4) Antigen presentation

After successful peptide loading, MHC-I molecules are released from the PLC and the trimer, consisting of MHC-I HC, β2-m and the peptide, is then transported through the trans-Golgi apparatus to the cell surface, where it can be recognised by immune cells. Thus, proper expression of the HLA-I APM components is obligatory for effective T-cell recognition of tumours[136,179] (Fig. 1.4).

The fact that it took around 40 years after the discovery of MHC molecules to form a coherent picture of how MHC-I and MHC-II molecules really work highlights the complexity of these pathways[180]. A broader and deeper knowledge about the molecular mechanisms underlying APM defects can enlighten the mechanisms behind the immune escape of the tumours and its progression and ultimately help to develop personalized immunotherapies. A fine tuning of this pathway via the proper pharmacological manipulation of tumour cells is mandatory. Therefore, further studies should be directed at investigating strategies to modulate *in vivo* the APM expression in tumour cells[134].

1.4 Defects of MHC-I expression as an immune escape mechanism

After the publication of the first[37] and second[2] version of the hallmarks of cancer by Hanahan and Weinberg, it is widely acknowledged, that manipulation of immune mechanisms and evasion of immune surveillance are skills acquired by the cancer cells. Furthermore, according to Cavallo and co-authors, tumour cells should be able to thrive in a chronically inflamed microenvironment, to evade immune recognition and to suppress immune reactivity[181]. Concerning the evasion of immune recognition and destruction, cancers can develop various mechanisms to protect themselves from immune cell attacks[119], such as T- and B-cells, macrophages and NK cells[2]. Indeed, the frequency and the functionality of CD8$^+$ effector T-cells and pAPCs, such as DCs, B-cells and macrophages, are often downregulated in the peripheral blood of tumour patients. In contrast, the numbers of immune suppressive myeloid-derived suppressor cells (MDSCs), natural killer T-cells (NKT-cells), T_{regs} and tumour-associated macrophages (TAMs) are upregulated[182,183].

The tumour-mediated escape mechanisms include alterations in (Fig. 1.6)[184,185]:

1. the generation, processing and presentation of T-cell epitopes derived from tumour associated antigens (TAAs) by HLA-I and/or HLA-II molecules
2. signal transduction pathways, such as the PI3K-Akt and Ras-ERK pathways via the RTKs
3. the expression of co-inhibitory molecules, such as B7.1 (CD80), B7.2 (CD86), CD28, PD-1 ligand (PD-L1), PD-L2, ICOSL (inducible T cell costimulator ligand), B7-H3, B7-H4, B7-H6, VISTA (V-domain Ig suppressor of T cell activation), GAL9 and CD47[186]
4. the expression of apoptosis-related molecules e.g. via the inhibitor of apoptosis proteins (IAP)
5. the secretion of immune suppressive mediators and exosomes, conditioning the local microenvironment and intercellular communication, such as the transforming growth factor β (TGF-β) or IL-10
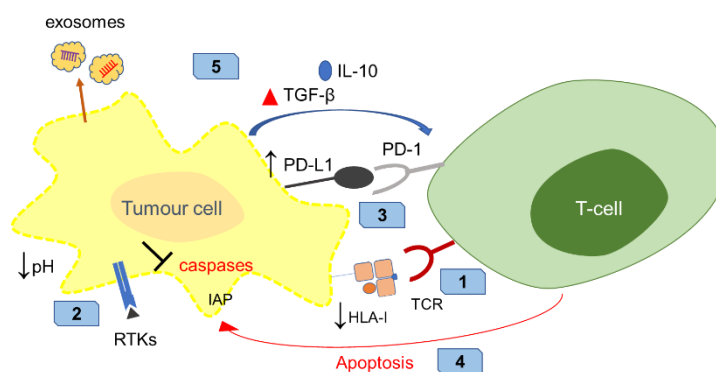
Figure 1.6. Scheme of the 5 main immune escape mechanisms

The cancer cells avoid recognition and destruction by defecting the generation, processing and presentation of TAAs by HLA-I APM components[119]. Defects within the APM can occur at any step of this complicated pathway and eventually affect HLA-I surface expression and the recognition of the tumour cells by effector immune cells[3]. The downregulation of APM components has been often characterised as tumour-dependent, and more pronounced in metastasis compared to primary lesions[134]. The clinical relevance of the aberrant expression of HLA-I APM components can be correlated with altered HLA-I surface expression, tumour immune escape, bad prognosis, reduced overall survival and reduced / inefficient T-cell responses. The percentage of human tumours with HLA-I loss, including total loss, haplotype loss, or allelic loss, varies from 65% to 90% in different types of malignancy[187].

Based on the components of the tumour microenvironment (TME), if the TME is rich of T-cells and myeloid cells, the tumour is "hot" and the tumour-infiltrating lymphocytes (TILs) are implicated in killing the tumour. Tumour-infiltrating T-cells can be activated by checkpoint inhibitors[188]. "Hot" tumours often produce neoantigens that can cause a strong immune response and they are often found in the bladder, head and neck, kidney, liver, melanoma and NSCLC, as well as cancers with high microsatellite instability (MSI)[189]. On the contrary, a TME with a high frequency of T_{regs}, myeloid suppressor cells, M2 macrophages and few T-cells forms the "cold" tumours. These tumours can create an immunosuppressive environment. "Cold" tumours include glioblastoma, ovarian, prostate and pancreatic cancers[190]. HLA-I abnormalities due to structural alterations, such as loss of heterozygosity (LOH), homozygous deletions, MSI and gene mutations are quite rare[191]. Deregulations of the epigenetic, transcriptional or posttranscriptional level of HLA-I APM components have been also described in several types of cancers[192] and are further discussed in §1.5. Most of the "hot" tumours are associated with better patients' prognosis and therapies' response, compared to the "cold" tumours[193].

1.5 Posttranscriptional regulation of gene expression

The regulation of gene expression defines the development and homeostasis of cells and tissues[194,195]. The genomic DNA localized in the cell nucleus is a central component of this process, serving as a template for the transcription of messenger RNAs (mRNAs) that is then translated into proteins[194].

Posttranscriptional regulation is named as the control of gene expression at the RNA level, between the transcription and the translation of the gene[196]; while posttranslational regulation refers to the control of the protein levels, due to various posttranslational modifications, such as phosphorylation, sequestration or proteolysis[197]. Posttranscriptional gene regulation concerns processes involved in the maturation, transport, stability and translation of all classes of RNAs, coding and non-coding (ncRNAs)[198]. Non-coding RNAs (ncRNAs) are classified into two major categories: structural and regulatory ncRNAs[199]. Structural ncRNAs comprise of rRNAs and tRNAs. Regulatory ncRNAs are divided into three classes, small (20-50nt), medium (50-200nt) and long (>200nt) ncRNAs, according to the length of their chain[200]. MicroRNAs (miRs) belong to the small ncRNAs and together with the RNA binding proteins (RBPs) they function as guide molecules for posttranscriptional gene regulation.

1.5.1 MicroRNAs

MiRs are endogenous ~22 nt RNAs existing in animals[201], plants[202] and protozoa[203]. MiRs target mRNAs and direct their posttranscriptional regulation[204], resulting in translational repression or mRNA degradation[205]. Despite the fact that the majority of published studies concentrate on the inhibitory effect of miRs on gene expression, miRs and their associated protein complexes, called microribonucleoproteins (microRNPs), have been recently reported to additionally stimulate directly or indirectly the gene expression[206] either by heterochromatin formation[207] or by activation of translation[208,209] under specific conditions. MiRs are characterized by specific maturation processes defined by canonical and non-canonical biogenic pathways[210]. Since their discovery in 1993 by the Ambrose laboratory[211], the knowledge about miRs and their functions has increased exponentially[212]. Nowadays, they represent one of the well-known classes of small ncRNAs in multicellular organisms, while the current version (v22.1) of the databank "miRBase"[213] comprises 38589 miR entries from 223 different species. Concerning their nomenclature, the unbiased "5p/3p" strand annotation indicates the position of the strand in the pre-miR hairpin independently of its expression status[214].

During dynamic interactions, miR binding sites can be located not only in the 3'-untranslated region (3'-UTR)[205], but also in the 5'-untranslated region (5'-UTR) or the CDS[215]. The 5' region of the miR centred on nucleotides 2–7 is named as the canonical seeding region and reduces considerably the occurrence of false-positive predictions of binding sites[204,216-219]. However, non-canonical interactions have been demonstrated by computational and *in vivo* UV crosslinking approaches to take also place[220]. Therefore, miRs can bind to their mRNA targets via (a) canonical sites, divided into three groups: 7mer-A1, 7mer-m8 and 8mer[221], (b) atypical sites, with productive 3′ pairing, consisting of two groups: 3' supplementary and 3' compensatory, (c) marginal sites, 6 nt sites matching the seed region, and (d) recently characterised exceptions, such as "centered" and "G-bulge" sites or interactions in the CDS[204,220].

Most miRs are known to be synthesized by the canonical pathway, passing through two sequential maturation steps[212] (Fig. 1.7). Briefly, canonical miRs are genomically encoded and transcribed in the nucleus as relatively long primary transcripts (pri-miRs)[222]. The pri-miR is then processed by the microprocessor complex, consisting of the binding protein DiGeorge critical region 8 (DGCR8), which recognize the pri-miR, and the RNAse III enzyme Drosha[223], which cleaves at the base of the hairpin embedded within the pri-miR[212]. The resulting ~60-70 nt hairpin molecule precursor miR (pre-miR) is translocated from the nucleus to the cytoplasm by the high-resolution export factor Exportin-5/RanGTP[224,225]. In the cytoplasm, the RNAse III enzyme Dicer and one of its two mammalian cofactors, the HIV-1 TAR RNA-binding protein (TRBP) or the protein activator of the interferon induced protein kinase EIF2AK2 (PACT), remove the terminal loop of the pre-miR to release the mature double-stranded ~22 nt miR molecule[226]. Subsequently, either arm of this dsRNA is incorporated into the RNA induced silencing complex (RISC). Within this complex, the mature single-stranded miR directly binds a member of the Argonaute (AGO) protein family[214] and acts as a guide to the target mRNA[227], while the other (passenger) strand is degraded[228]. Subsequent binding of the trinucleotide repeat containing 6A (TNRC6) and interaction with the poly(A)-binding protein (PABP) plays a pivotal role for all downstream events of the target mRNA in animals[229,230]. In general, based on the sequence complementarity, partially complementary base pairing of a miR seed region with a

target mRNA induces translational repression, while perfect base pairing results in endonucleolytic cleavage of target mRNA[231]. Subsequently, the degradation of the target mRNA is initiated by deadenylation and decapping, making the mRNAs accessible for exoribonucleases[194].
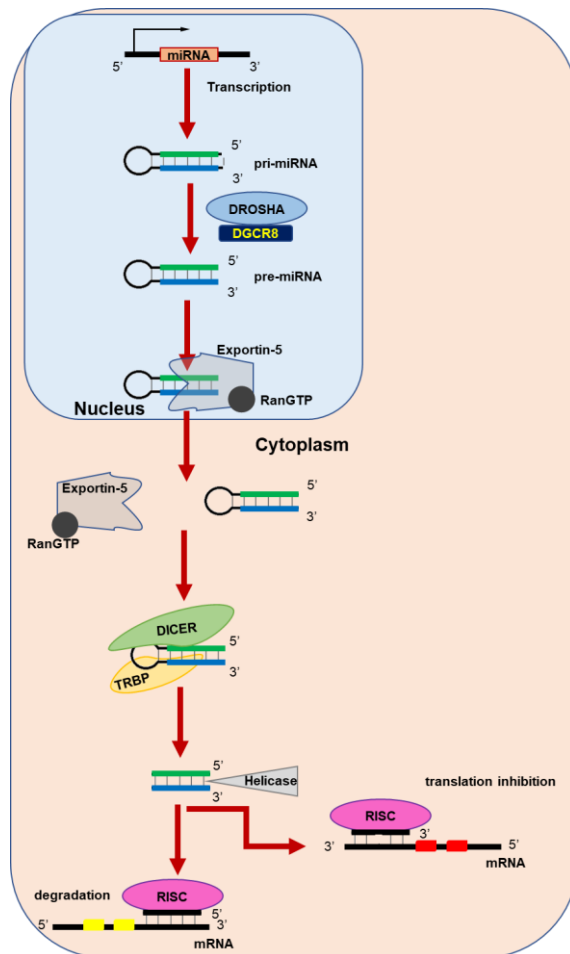
Figure 1.7. Biogenesis pathway of miRs
Canonical miR genes are usually transcribed by RNA Pol II to generate the pri-miRs transcripts. Pre-miRs are generated by the Drosha–DGCR8 complex. and recognized by Exportin 5. In the cytoplasm, Dicer catalyses the production of miR duplexes. Dicer, TRBP and AGO1–4 mediate the processing of pre-miR and the assembly of the RISC. One strand of the duplex remains on the AGO as the mature miR, whereas the other strand is degraded. Binding of the miR to the target mRNA can lead to mRNA degradation or to translational inhibition[228].

Non-canonical miRs are a subset of miRs, which have been recently discovered by small RNA deep sequencing approaches to take part in several cellular processes, such as immune responses and cell proliferation[210,212]. They structurally and functionally resemble canonical miRs, although their origins are diverse, including introns, small nucleolar RNAs (snoRNAs), endogenous short hairpin RNAs (shRNAs) and tRNAs. Regarding their biogenesis, non-canonical miRs are following distinct maturation pathways, typically bypassing one or more steps of the classic canonical biogenesis pathway[212]. Dicer is almost always present in the generation of both canonical and non-canonical miRs, respectively, and without it almost all functional miRs are lost. Drosha and DGCR8 are needed to process canonical miRs, while non-canonical miRs can be generated in their absence[212,226,232].

In the last years, miRs are increasingly reported to be involved in the development of a multitude of diseases[233], such as different types of cancers[234,235], auto-immune diseases[236], heart diseases, like hypertrophy and ischemia[237] and mental disorders, like schizophrenia or major depression disorders[238]. Under different physiological or pathological conditions, miRs could switch from translational inhibition to activation and *vice versa*[215]. In the tumour development, miRs play often a crucial role, since they act as either oncogenes or tumour suppressor genes thereby affecting tumour growth, metastasis formation and disease progression[239]. Many miRs abnormally

expressed in hematologic and solid tumours[240] including melanoma are summarized in figure 1.8. Furthermore, miRs could also have immune modulatory functions[192], leading to escape from immune surveillance or altered immune responses by affecting the expression of immune modulatory molecules in tumour and immune cells[4].

Immune modulatory miRs (im-miRs) have been recently identified to control the expression of immune modulatory molecules as well as the function of tumour and immune cell populations, enabling tumours to escape from immune surveillance[4]. Using distinct strategies including *in silico* prediction, miR arrays, small RNA sequencing, RNA affinity approaches and luciferase reporter assays, several im-miRs have been recently identified. However, despite their emerging role as fine tuners in the gene regulation of cancer cells, there exists limited information about im-miRs regulating the HLA-I APM components[241,242]. Table 1.2 lists im-miRs, which have been already published to regulate HLA-I APM components. Interestingly, members of the miR-148/-152 family were shown to posttranscriptionally regulate several members of the HLA-I APM components[243], such as the ERP57[244], the HLA-A, -B, -C as well as the non-classical HLA-G molecules[241,245,246]. Nucleotide variations within the 3'-UTR of HLA-C regulate miR-148a binding and directly correlate to surface expression. Binding of miR-148/-152 to the 3'-UTR of HLA-G downregulates mRNA and protein expression levels, followed by an altered immune cell infiltration and immune response[247], while a direct interaction of HLA-A with miR-148/-152 was also reported[248]. Recently, miR-744 and miR-16 have been reported to regulate HLA-G CDS in choriocarcinoma cell line JEG3.
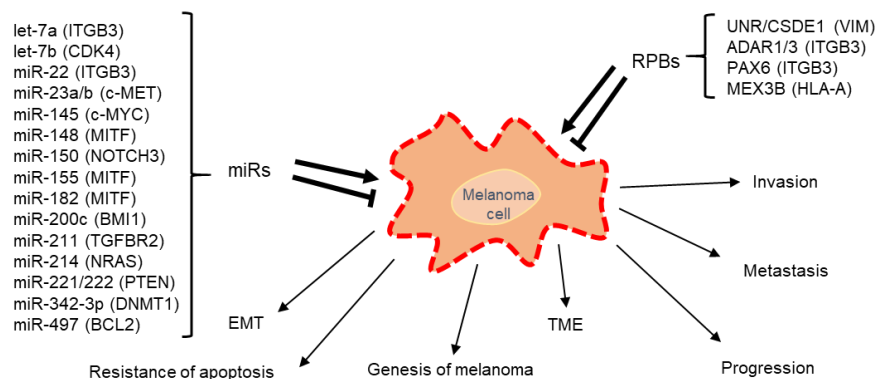
Figure 1.8. Posttranscriptional regulation by miRs and RBPs in melanoma
Distinct profiles of miRs and RNA binding proteins (RBPs) expression are detected at each step of melanoma development. Several miRs and RBPs can impair a wide array of processes. Acting either as oncogenic or tumour suppressive, they can affect the tumour progression and the possible response to therapies even by slight alterations in their expression levels. The names of validated targets are given in parentheses.
(BCL2: BCL2 apoptosis regulator, BMI1: BMI1 proto-oncogene, c-MET: MET proto-oncogene, c-MYC: MYC proto-oncogene, CDK4: cyclin dependent kinase 4, DNMT1: DNA methyltransferase 1, ITGB3: integrin subunit beta 3, MITF: melanocyte inducing transcription factor, NOTCH3: Notch receptor 3, TGFBR2: transforming growth factor beta receptor 2, VIM: Vimentin)

Moreover, the mimic-based overexpression of the tumour suppressive miR-9 in nasopharyngeal carcinoma (NPC) exerts a broad effect to many well-known IFN-induced genes. TAP1, β2-m, proteasome subunits (e.g. LMP2 and LMP10), classical (e.g. HLA-B, HLA-C) and non-classical HLA-I molecules (e.g. HLA-F) are upregulated by miR-9[249], but details of the underlying mechanism of this deregulation remain unknown. It could also be shown that overexpression of the ER stress-induced miR-

346 in Calu-3 and HeLa cells resulted in TAP1 mRNA reduction, which correlated with decreased expression of HLA-I surface antigens[250]. Apart from tumour-related miRs, exogenous miRs derived from pathogens, were shown to target human mRNAs and decrease the expression of key players originally thought to control infections. In this context, the EBV derived miR-BHRF1–3 has been reported to directly target TAP2 and indirectly reduce HLA-I surface expression, which results in the inhibition of recognition and killing of infected B-cells by EBV-specific CD8^{+} T cells[251]. Additionally, the human cytomegalovirus miR-US4-1 targets ERAP1 thereby affecting the CD8^{+} T cell responses[252].

Table 1.2. List of im-miRs regulating HLA-I and APM components

Target mRNA	miR	Reference
CRT	miR-455	[253]
	miR-27a	[254]
	miR-1275	[255]
ERAAP	miR-US4-1 (CMV)	[252]
ERP57	miR-148a	[244]
HLA-A	miR-148a	[242]
	miR-181a	[256]
HLA-B	miR-148a	[242]
HLA-C	miR-148a	[242]
	miR-9	[249]
	miR-148a	[241]
HLA-E	miR-376a(e)	[257]
HLA-G	miR-148/-152	[245]
	miR-152	[258]
	miR-133	[247]
	miR-548q	[259]
	miR-628-5p	[259]
	HOTAIR (lncRNA)	[260,261]
	miR-744	[262]
	miR-16	[262]
LMP7	miR-451a	[263]
TAP1	miR-346	[250]
TAP2	miR-BHRF1–3 (EBV)	[251]
	miR-125a-5p	[242]
	miR-1270	[264]

(adapted from Friedrich M., Jasinski-Bergner S., Lazaridou M.F. *et al*, Cancer Immunol Immunother, 2019[3])

1.5.2 RNA binding proteins

Next to miRs, RNA binding proteins (RBPs) can also posttranscriptionally regulate gene expression by binding to mRNA[265] and forming ribonucleoprotein (RNP) complexes[266]. The localization of RBPs is important in determining their function and consequently, RBPs can be divided into nuclear and cytoplasmic RBPs. Nuclear RBPs primarily regulate nascent mRNA (pre-mRNA) processing events, including 5'-capping by addition of a 7 methylguanosine (m^{7}G), 3'-polyadenylation and pre-mRNA splicing[267], while cytoplasmic RBPs bind mature mRNA sequences upon their release from the nucleus. Cytoplasmic RBPs operate more directly in the translation via directing mRNA transport, competitive or co-operative interactions with the translation machinery, and regulation of mRNA stability. Despite the categorization, a number of RBPs can be characterized as both nuclear and cytoplasmic [268] (Fig. 1.9).
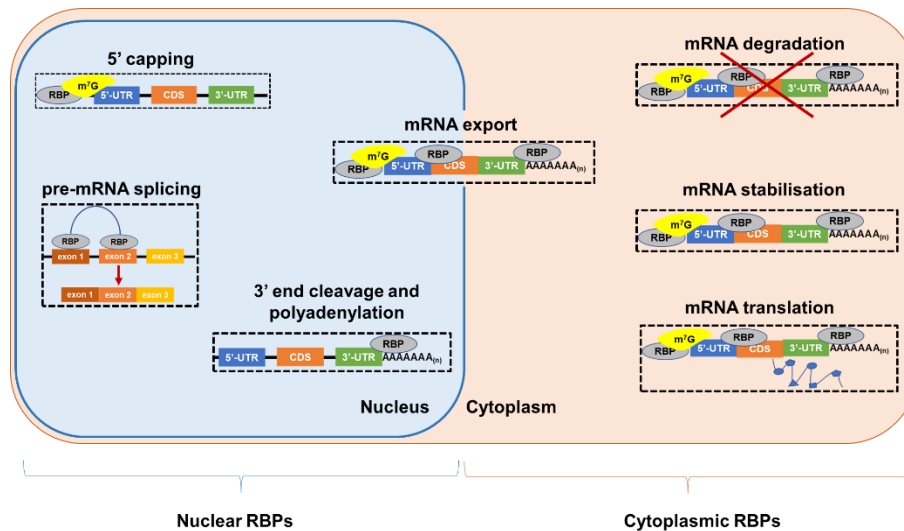
Figure 1.9. Mechanisms of posttranscriptional control regulated by either nuclear or cytoplasmic RBPs

Molecular functions controlled by RBP include gene transcription, 5′ capping, pre-mRNA splicing, 3' end cleavage, polyadenylation and methylation, mRNA export, mRNA translation initiation or inhibition, mRNA stabilization or degradation[269].

RBPs are proteins binding RNA through one or multiple globular RNA-binding domains (RBDs) and, subsequently, changing the fate or function of the bound RNAs[270]. An RBP can bind to sequence and/or structural motifs in the RNA via modular combinations of a limited set of structurally well-defined RBDs[271] such as the RNA recognition motif (RRM, 4 nt)[272], the hnRNP K homology domain (KH, 4 nt), the DEAD box helicase domain (6 nt)[273] or the Pumilio domain (8-10 nt)[274]. Upon the introduction of large-scale quantitative methods, such as next-generation sequencing and mass spectrometry (MS), several RBPs have been discovered and their number increases, since additional RBPs lacking conventional RBDs are currently identified by recent proteome-wide studies. Based on high-throughput screens conducted in various cell types, 1542 human RBPs, have been so far experimentally validated representing ~7.5% of all protein-coding genes[198,275].

Eukaryotic cells encode a large number of RBPs[271,276], which play crucial roles in the cellular biogenesis, stability, function, transport and localization[266]. Depending on their binding preferences, RBPs are classified as ssRNA and dsRNA[276] binders and show different RNA-sequence specificities and affinities, resulting in being as diverse as their

targets and functions[266]. These targets include mRNA as well as a number of functional ncRNAs, which cannot circulate as "naked" RNAs, but they can form RNP complexes with the RBPs[277]. Hence, RBPs can further be categorized into mRNA-binding[278], pre-rRNA-binding, tRNA-binding, small nuclear RNA (snRNA)-binding and snoRNA-binding proteins, as well as a residual ncRNA-binding category[198].

The combinatorial action of RBPs and miRs on target mRNAs is suspected to form a posttranscriptional regulatory code[265]. RBPs and miRs regulate their targets in either a positive or negative manner[279]. RBPs can also bind pre-miRs and regulate their expression and thus the depletion of distinct RBPs can change the expression of mature miRs and indirectly modulate the targeted mRNA expression levels[280]. The basic steps of the miR processing and gene regulation pathway are highly regulated by RBPs[281], such as DGCR8 in the pri-miR processing[282], PACT[283] and TRBP[284] in pre-miR processing, the family of the four AGO proteins in the RISC complex and the TNRC6C/GW182 protein family[285]. Depletion of these RBPs can positively or negatively affect the levels of miRs[280]. Particularly in cancer, a quite complicated network has been reported between miRs and RBPs[286]. On the one hand, miRs can regulate the expression of RBPs, such as PUM1 in glioblastoma and breast cancer[287] and PUM2 in bladder cancer[288]. On the other hand, RBPs, such as Dicer, can precisely regulate the expression of specific miRs in acute myeloid leukemia[289], chronic lymphocytic leukemia[290] or hepatocellular carcinoma[291]. Both miRs and RBPs target mRNAs and they can cooperate or counteract in the regulation of a specific mRNA target, resulting into the cooperative or competitive ribonucleosome model, respectively[292-294]. In the cooperative model, RBPs can enhance the impact of miRs on shared low-accessibility target mRNAs as guides that mediate the opening of the structure (synergistical action), while in the competitive model, RBPs can counteract miRs for neighbouring mRNA binding sites (antagonistic action) [295,296].

RBPs play also a dynamic role in a wide range of biological processes, such as development, homeostasis and differentiation, signalling, metabolism, infection and other disease-related processes and the effects of drugs[275,297,298]. The impact of altered RBPs activities affects cellular development and diseases, in which there are either a gain-of-function or loss-of-function causes pathogenesis[297]. Recently, RBPs have been found to be essential also for the development and function of the immune system, the development of autoimmune and inflammatory diseases[269]. RBPs directly mediate intracellular immunity and may be the targets of infectious agents for inactivation or exploitation[299]. The RBPs AUF1 and IGF2BP3 may contribute to immune evasion by tumour cells by binding to RNAs that encode stress-induced ligands for NKG2D and inhibiting their expression, promoting immune evasion by damaged or malignant cells[300,301].

Cancer cells also exploit posttranscriptional molecules to their advantage, as has been shown for miRs[235] and more recently for lncRNAs[302]. In this context, RBPs are not an exception, and there is already ample experimental evidence that altered RBP function has a significant effect on cancer phenotypes[2]. Particularly in cancer development and progression, RBPs are dysregulated in different cancer types, thus impacting on the expression and function of oncoproteins and tumour-suppressor proteins[303]. Particularly, the RBPs mechanisms of posttranscriptional regulation in cancer can result in the development and progression of cancer by sustained cell proliferation,

evasion of apoptosis, avoiding immune surveillance, inducing angiogenesis, and activating metastasis[304].

Several RBPs have been published to target and deregulate the HLA-I molecules. Briefly, the muscle excess (MEX)-3 RNA-binding family, particularly MEX-3B in melanoma[305] and MEX-3C regulated HLA-I at the posttranscriptional level[306] (Fig. 1.8). The RBP SYNCRIP regulated the HLA-A protein expression by alternative polyadenylation signals, while its specific blocking reduced HLA-A surface expression[307]. Recently, the heterogeneous nuclear ribonucleoprotein R (HNRNPR) was identified as the first positive posttranscriptional regulator for classical and non-classical HLA-I molecules in several cancer cell lines[259], while the expression of HLA-B27 HC has been reported to modulate the intracellular environment of U937 monocyte/ macrophages by altering the human antigen R (HuR) regulation[308]. Interestingly, no RBPs have been reported to regulate at any level the expression of APM components[3], underlining the need for more extensive research. The table 1.3 lists known interactions of RBPs with HLA-I molecules.

Table 1.3. List of RBPs regulating the HLA-I molecules

RBP	Target mRNA	Reference
HNRNPR	HLA-I	[309]
	HLA-G	[310]
MEX-3B	HLA-A	[305]
MEX-3C	HLA-A	[306]
Syncrip	HLA-A	[307]
ELAV1/HuR	HLA-B27	[308]

(adapted from Friedrich M., Jasinski-Bergner S., Lazaridou M.F. *et al*, Cancer Immunol Immunother, 2019[3])

2. Aims

Loss or downregulation of HLA-I molecules on the cell surface can be due to an impaired expression and/or function of APM components and thus lead to the evasion of tumour cells from immune recognition. Next to structural alterations (mutations, deletions, insertions) or LOHs the posttranscriptional control might play a role in modulating the surface expression rate of HLA-I molecules in tumours. The latter can be partly mediated by miRs and/or RBPs.

Thus, the aim of this thesis is to investigate the posttranscriptional regulation of immune modulatory molecules in human melanoma with focus on three key components of the HLA-I APM pathway, namely TAP1, TAP2 and TPN. For this reason, miRs and RBPs potentially targeting these HLA-I APM components will be identified using both *in silico* analysis by employing various databases and miTRAP assays for the enrichment of miRs or RNA affinity purification assays for the enrichment of RBPs, followed by small RNA sequencing or MS analyses, respectively.

Based on small RNA sequencing data obtained from the generated miTRAP eluates, a number of putative novel miRs targeting these APM components, will be identified. The specific binding of selected candidate miRs to the 3'-UTRs of TAP1, TAP2 or TPN will be validated by dual luciferase reporter assays. Using melanoma cell lines displaying distinct HLA-I surface expression levels and discordant APM expression levels, candidate miRs will be transfected as miR-mimics or inhibitors, respectively. Their effect will be evaluated on overexpressed or inhibited cells regarding the modulation of the expression and/or function of (i) APM components by performing qPCR and Western blot analyses, (ii) the HLA-I surface expression using flow cytometry and (iii) the T- or NK cell targeting susceptibility by conducting CD107 degranulation assays. Moreover, the clinical relevance of these miRs and APM components will be assessed in melanoma patients by analysis of relevant TCGA datasets. Additionally, the expression pattern of selected miRs targeting TAP1 will be determined in FFPE sections of primary melanoma patients and correlated with both the observed TAP1 expression levels and the immune cell infiltration rates.

Concerning the identification of RBPs, RNA affinity purification assays will be established for their enriched binding to TAP1 or TPN 3'-UTRs. Mass spectrometry will allow to identify RBPs, which target the TAP1 or TPN 3'-UTR. To further validate their effects on the TAP1, TPN and HLA-I surface expression rates by performing qPCR, Western blot or flow cytometry analyses, either recombinant plasmids or short interfering RNAs (siRNAs) will be transfected into three melanoma model cell lines displaying distinct HLA-I surface expression rates. Furthermore, upon the overexpression or knock down of the selected RBPs additional proteomic profilings had to be performed in order to identify potential downstream target proteins.

To briefly summarize, this study provides further evidence that three key APM components can be deregulated by miRs or RBPs, thereby resulting in modulations of the HLA-I surface expression rates in melanoma tumours. These findings suggest that the posttranscriptional control of HLA-I APM components might indeed play a role in mediating the immune escape of melanoma tumour cells and thus as a consequence promote tumour growth. Finally, such target molecules might be not only beneficial as predictive biomarkers but even as potential therapeutic targets for novel cancer immunotherapies.

3. Materials

3.1 Chemicals

Chemical	Distributor
2-Iodacetamide (C_2H_4INO)	AppliChem GmbH, Darmstadt, Germany
Acetone $(CH_3)_2CO$	Sigma-Aldrich, St. Louis, MO, USA
Acetonitrile (ACN)	AppliChem GmbH, Darmstadt, Germany
Acrylamide/Bis solution, 29:1 (40 %)	SERVA Electrophoresis GmbH, Heidelberg, Germany
a-cyano-4-hydroxycinnamic acid	Bruker Daltonik GmbH, Bremen, Germany
Agarose	SERVA Electrophoresis GmbH, Heidelberg, Germany
Ammonium acetate ($C_2H_7NO_2$)	Sigma-Aldrich, St. Louis, MO, USA
Ammonium bicarbonate (NH_4HCO_3)	Sigma-Aldrich, St. Louis, MO, USA
Ammonium persulfate (APS)	CARL ROTH GmbH & Co. KG, Karlsruhe, Germany
Ampicillin	CARL ROTH GmbH & Co. KG, Karlsruhe, Germany
Ampuwa® water	Fresenius Kabi GmbH, Bad Homburg, Germany
Amylose Resin	NEB, Ipswich, MA, USA
Annexin V	MACS, Merck, Darmstadt, Germany
β-mercaptoethanol (C_2H_6OS)	AppliChem GmbH, Darmstadt, Germany
Bromophenol blue ($C_{19}H_{10}Br_4O_5S$)	SERVA Electrophoresis GmbH, Heidelberg, Germany
Bovine Serum Albumin (BSA), ultra pure	Invitrogen, Carlsbad, CA, USA
Calcium chloride ($CaCl_2$)	Sigma-Aldrich, St. Louis, MO, USA
Carboxyfluorescein succinimidyl ester (CFSE)	Invitrogen, Carlsbad, CA, USA
CHAPS	AppliChem GmbH, Darmstadt, Germany
Chloroform ($CHCl_3$)	Sigma-Aldrich, St. Louis, MO, USA
Coomassie-Brilliantblue G-250	AppliChem GmbH, Darmstadt, Germany
D-(+)-Maltose monohydrate	Sigma-Aldrich, St. Louis, MO, USA
Dimethyl sulfoxide (DMSO)	Sigma-Aldrich, St. Louis, MO, USA
Dimethylethylammoniumpropane sulfonate ($C_7H_{17}NO_3S$)	Merck, Darmstadt, Germany
Dithiothreitol (DTT)	Promega, Madison, Washington, USA
Dulbecco's modified eagle's medium (DMEM) (with or without Phenol red)	Gibco® Invitrogen, Carlsbad, CA, USA
Dulbecco's phosphate buffered saline (DPBS)	Sigma-Aldrich, St. Louis, MO, USA
Ethanol (C_2H_6O)	Sigma-Aldrich, St. Louis, MO, USA
Ethidium bromide ($C_{21}H_{20}BrN_3$)	AppliChem GmbH, Darmstadt, Germany
Ethylenediaminetetraacetic acid (EDTA)	Thermo Scientific, Rockford, IL, USA
Fetal calf serum (FCS)	Gibco® Invitrogen, Carlsbad, CA, USA
Ficoll gradient	Biochrom AG, Berlin, Germany
G-418/ Geneticin	PAA Laboratories GmbH, Pasching
Glycerin ($C_3H_8O_3$)	AppliChem GmbH, Darmstadt, Germany
Glycine ($C_2H_5NO_2$)	AppliChem GmbH, Darmstadt, Germany
Glycogen	Thermo Scientific, Rockford, IL, USA
Guanidinium thiocyanate	CARL ROTH GmbH & Co. KG, Karlsruhe, Germany
Halt Protease and phosphatase inhibitor cocktail (100x)	Thermo Scientific, Rockford, IL, USA
Heparin	Biochrom AG, Berlin, Germany
HEPES	Gibco® Invitrogen, Carlsbad, CA, USA

Chemical	Distributor
Horse serum	CC pro, Oberdorla, Germany
Human serum	CC pro, Oberdorla, Germany
Hydrochloric acid (HCl)	CARL ROTH GmbH & Co. KG, Karlsruhe, Germany
Interleukin-7 (IL-7)	Immunotools, Friesoythe, Germany
Interleukin-12 (IL-12)	Immunotools, Friesoythe, Germany
Interleukin-15 (IL-15)	Immunotools, Friesoythe, Germany
Interleukin-18 (IL-18)	BioVision, Ilmenau, Germany
Isopropanol (C_3H_8O)	Sigma-Aldrich, St. Louis, MO, USA
Kanamycin	CARL ROTH GmbH & Co. KG, Karlsruhe, Germany
LB-agar	CARL ROTH GmbH & Co. KG, Karlsruhe, Germany
LB-medium	CARL ROTH GmbH & Co. KG, Karlsruhe, Germany
L-glutamine	Lonza, Basel, Schweiz
LMW calibration kit for SDS electrophoresis	GE Healthcare, Easton Turnpike, Fairfield, CT, USA
Low melting agarose	BioLine GmbH, Luckenwalde, Germany
Magnesium chloride ($MgCl_2$)	CARL ROTH GmbH & Co. KG, Karlsruhe, Germany
MelanA/Mart1 peptide, H2N-AAGIGLTV-COOH, 10mg immunograde	Peptides&elephants, Hennigsdorf, Germany
Methanol	Sigma-Aldrich, St. Louis, MO, USA
Natrium chloride (NaCl)	CARL ROTH GmbH & Co. KG, Karlsruhe, Germany
N-butanol	CARL ROTH GmbH & Co. KG, Karlsruhe, Germany
NDSB-201	Calbiochem®, Merck, Darmstadt, Germany
Nonidet P40 (NP-40)	Roche Applied Science, Mannheim, Germany
Optimem	Gibco® Invitrogen, Carlsbad, CA, USA
Ortho-phosphoric acid (H_3PO_4)	Merck, Darmstadt, Germany
PageRuler Prestained Protein Ladder	Thermo Scientific, Rockford, IL, USA
Penicillin/Streptomycin (100x)	PAA, Pasching, Austria
Pierce protease inhibitor mini tablets	Thermo Scientific, Rockford, IL, USA
Pharmalite (pH 3.0 to 10)	VWR®, Darmstadt, Germany
Phenol	Thermo Scientific, Rockford, IL, USA
Phosphatase inhibitor cocktail	Sigma-Aldrich, St. Louis, MO, USA
Phytohemagglutinin-L (PHA-L)	Sigma-Aldrich, St. Louis, MO, USA
Plus one dry strip cover fluid	GE Healthcare, Easton Turnpike, Fairfield, CT, USA
Ponceau S	AppliChem GmbH, Darmstadt, Germany
Potassium chloride (KCl)	Merck, Darmstadt, Germany
Potassium dihydrogen phosphate (KH_2PO_4)	Merck, Darmstadt, Germany
Propidium iodide	Sigma-Aldrich, St. Louis, MO, USA
Puromycin	Sigma-Aldrich, St. Louis, MO, USA
RPMI 1640 (without or with Phenol red)	Gibco® Invitrogen, Carlsbad, CA, USA
Skim milk powder	BD Biosciences, Heidelberg, Germany
Sodium deoxycholate	Sigma-Aldrich, St. Louis, MO, USA
Sodium dodecyl sulfate (SDS)	AppliChem GmbH, Darmstadt, Germany
Sodium hydroxide (NaOH)	CARL ROTH GmbH & Co. KG, Karlsruhe, Germany
Sodium phosphate dibasic dihydrate ($Na_2HPO_4 * 2H_2O$)	CARL ROTH GmbH & Co. KG, Karlsruhe, Germany
Sodium pyruvate (100 mM)	Gibco® Invitrogen, Carlsbad, CA, USA
Sodium thiosulfate ($Na_2S_2O_3$)	Sigma-Aldrich, St. Louis, MO, USA

Chemical	Distributor
Streptavidin-coated agarose beads	GE Healthcare, Chicago, USA
T-cell growth factor (TCGF)	ZeptoMetrix, New York, USA
Tetramethylethylenediamine (TEMED)	AppliChem GmbH, Darmstadt, Germany
Thiourea (CH_4N_2S)	Sigma-Aldrich, St. Louis, MO, USA
Trichloroacetic acid ($C_2HCl_3O_2$)	AppliChem GmbH, Darmstadt, Germany
Trifluoroacetic acid (CF_3CO_2H)	AppliChem GmbH, Darmstadt, Germany
Trifluoroacetic acid (TFA)	AppliChem GmbH, Darmstadt, Germany
Tris(hydroxymethyl)aminomethane (TRIS, $C_4H_{11}NO_3$)	AppliChem GmbH, Darmstadt, Germany
Trizol	Invitrogen, Carlsbad, CA, USA
Trypan bleu ($C_{34}H_{28}N_6Na_4O_{14}S_4$)	Gibco® Invitrogen, Carlsbad, CA, USA
Trypsin/EDTA (10 x)	PAA, Pasching, Austria
Tween® 20	AppliChem GmbH, Darmstadt, Germany
Urea ($CO(NH_2)_2$)	AppliChem GmbH, Darmstadt, Germany
X-vivo 15-Medium	Lonza, Basel, Schweiz
Xylene cyanole FF ($C_{25}H_{27}N_2NaO_6S_2$)	Sigma-Aldrich, St. Louis, MO, USA
Yeast tRNA	Invitrogen, Carlsbad, CA, USA

3.2 Buffers

Buffer	Composition
2x Laemmli buffer	125 mM Tris HCl (pH 6.8), 4% SDS, 20% glycerol, 0.0025% bromophenol blue
4x Laemmli buffer	125 mM Tris HCl (pH 6.8), 4% SDS, 40% glycerol, 0.005% bromophenol blue
Annexin V-Binding buffer	140 mM NaCl, 2.5 mM $CaCl_2$, 10 mM HEPES/NaOH, pH 7.4
Beads binding and wash buffer	Cell lysis buffer supplemented with 11 µg/mL heparin
Beads blocking buffer	Cell lysis buffer supplemented with 250 µg/mL BSA and 20 µg/mL yeast tRNA
Binding buffer	20 mM HEPES/KOH pH 7.9, 200 mM KCl, 1 mM EDTA supplemented with one tablet Pierce protease inhibitor mini tablets, EDTA-free, per 10 mL buffer
Blocking buffer	20mM HEPES pH 7.9, 0.1 M KCl, 10 mM $MgCl_2$, 0.01% NP-40, 1 mM DTT, 1 mg/mL BSA, 0.09 mg/mL glycogen, 20 µg/mL yeast tRNA
Cell lysis buffer	20 mM Tris HCl pH 7.5, 150 mM NaCl, 1.5 mM $MgCl_2$, 8.7% glycerol, 0.05% NP-40, protease inhibitor cocktail (1:100)
Cell storage buffer	Cell lysis buffer supplemented with 22 µg/mL heparin, 2 mM DTT, 80U RNasin
Colloidal coomassie staining solution	2.55% phosphoric acid, 150 mM aluminum sulfate, 0.5 mM coomassie brilliant blue G-250, 5 M methanol
cytoplasmic buffer	0.3 M HEPES pH 7.9, 1.4 M KCl, 30 mM $MgCl_2$
Extract binding buffer	cell lysis buffer supplemented with 22 µg/mL heparin
High salt 300 (HS300) washing buffer	20 mM HEPES pH 7.9, 0.3 M KCl, 10 mM $MgCl_2$, 0.01% NP-40, 1 mM DTT
High salt 400 (HS400) washing buffer	20 mM HEPES pH 7.9, 0.4 M KCl, 10 mM $MgCl_2$, 0.01% NP-40, 1 mM DTT
Hypotonic buffer	10mM HEPES pH 7.9, 1.5 mM $MgCl_2$, 10 mM KCl
Low salt (LS) washing buffer	20 mM HEPES pH 7.9, 0.1 M KCl, 10 mM $MgCl_2$, 0.01% NP-40, 1 mM DTT
Phosphate buffered saline (PBS) (10-fold)	684 mM NaCl, 13.4 mM KCl, 7,3 mM KH_2PO_4, 40.4 mM $Na_2HPO_4*2H_2O$, pH 7.4

Buffer	Composition
Protein sample buffer (4x)	187.7 mM Tris HCl pH 6.8, 1.9 mM β-mercaptoethanol, 0.2 mM bromophenol blue
Rabilloud buffer	7 M urea, 2 M thiurea, 0.2 M NDSB-201, 4 % (w/V) CHAPS, 1 % (w/V) DTT, 0.5 % (V/V) pharmalyte, bromophenol blue
Radioimmunoperci pitation assay (RIPA) buffer	25 mM Tris HCl (pH 7,6), 150mM NaCl, 1% (V/V) NP-40, 1% (w/V) sodium deoxycholate, 0.1% (w/V) SDS
RNA elution buffer	15 mM maltose solution
RNA sample buffer (3x)	10 mM Tris HCl pH 7.6, 80% (v/v) formamide, 0.025% (w/V) xylene cyanole FF, 0.025% bromophenol blue
SDS-running buffer (10-fold)	250mM Tris, 2M glycine, 1% (w/v) SDS
SDS-running buffer (1-fold)	100 mL 10-fold SDS running buffer, 900 mL H_2O
TAE (50-fold)	2 M Tris, 0.05 M EDTA, 5.7 % (v/v) acetic acid
TBS (10-fold)	0.2 M Tris, 1.4 M NaCl (pH 7.6 with HCl)
TBST-T	100 mL 10-fold TBS, 900 mL H_2O, 1 mL Tween-20-solution
Transfer buffer	100 mL 10-fold running buffer (without SDS), 200 mL methanol, 700 mL H_2O

3.3 Oligonucleotides

Name	Application	Sequence	Condition
TAP1-3'-UTR fw	Cloning	AAAGAATTCCTCCAGAATGAAAGCCTTCTC	63°C
TAP1-3'-UTR rev	Cloning	AAACTCGAGACAAAACACCAATTTTATTA	63°C
TAP2-3'-UTR-1 fw	Cloning	AAAGAATTCTCTTCTCAGGGGCGTCTCCA	67°C
TAP2-3'-UTR-1 rev	Cloning	AAACTCGAGCAGGGCTTGAGAGCACCTGA AG	71°C
TAP2-3'-UTR-2 fw	Cloning	AAAGGATCCACATACGATGATGGCATTTCT GG	66°C
TAP2-3'-UTR-2 rev	Cloning	AAACTCGAGGCCCCTGAGATAAGAAACTTT CAGG	68°C
TAP2-3'-UTR-3 fw	Cloning	AAAGAATTCCAGTACAGGAAGATGCAGTAG ACC	66°C
TAP2-3'-UTR-3 rev	Cloning	AAACTCGAGAGTTCAGAACAGTGAACTTAG ACAG	66°C
TPN-3'-UTR-1 fw	Cloning	AAAGGATCCCCACCTGCAAGGATTCAAAG	67°C
TPN-3'-UTR-1 rev	Cloning	AAACTCGAGCGGATCACCAGGTTAGGAGA	68°C
TPN-3'-UTR-2 fw	Cloning	AAAGAATTCCTCGGACTACAGGCGTCCTC	67°C
TPN-3'-UTR-2 rev	Cloning	AAAGGATCCTCTGGCCGACCGTCCTGACT	71°C
TAP1-3'-UTR LUC fw	Cloning	AAAGCTAGCCTCCAGAATGAAAGCCTTCTC	66°C
TAP1-3'-UTR LUC rev	Cloning	AAAGTCGACACAAAACACCAATTTTATTA	60°C
Del TAP1 miR-200a-5p fw	Cloning	ATCAGCTATTTTCAACATAACTGAAG	56°C
Del TAP1 miR-200a-5p rev	Cloning	CACACCAAAGCATCAGCC	56°C
Del TAP1 miR-26b-5p fw	Cloning	TTTGCCTTGAGTGTGTTACCTC	58°C
Del TAP1 miR-26b-5p rev	Cloning	GCTGCCTACTCTGCAGCT	59°C

Name	Application	Sequence	Condition
Del TAP1 miR-21-3p fw	Cloning	GTGTCGACCTGCAGGCAT	60ºC
Del TAP1 miR-21-3p rev	Cloning	ACAGGGTGTTTATGGGCC	56ºC
T7 TAP1 fw	PCR	GCGGAGATCTAATACGACTCACTATAGGAAGCCTTCTCAGACCTGCG	63ºC
T7 TAP2-3'-UTR-1 fw	PCR	GCGGAGATCTAATACGACTCACTATAGGTCTTCTCAGGGGCGTCTC	67ºC
T7 TAP2-3'-UTR-2 fw	PCR	GCGGAGATCTAATACGACTCACTATAGGACATACGATGATGGCATTTCTGG	66ºC
T7 TAP2-3'-UTR-3 fw	PCR	GCGGAGATCTAATACGACTCACTATAGGCAGTACAGGAAGATGCAGTAG	66ºC
T7 TPN-3'-UTR-1 fw	PCR	GCGGAGATCTAATACGACTCACTATAGGCCACCTGCAAGGATTC	66ºC
T7 TPN-3'-UTR-2 fw	PCR	GCGGAGATCTAATACGACTCACTATAGGCCACCTGCAAGGATTCAAAG	67ºC
T7 HLA-G-3'-UTR fw	PCR	GCGGAGATCTAATACGACTCACTATAGGAAAGGAGGGAGCTACTCTCAG	68ºC
HLA-G-3'-UTR rev	PCR	AAAGTTCTCATGTCTTCCATTTATTTTG	57ºC
T7 TGFBR2-3'-UTR-2 fw	PCR	AAACTTAAGCACTTTATAAATATTTGGAGATTTTGC	51ºC
TGFBR2-3'-UTR-2 rev	PCR	AAACTCGAGTTTAGCTACTAGGAATGGGAACAGG	59ºC
TAP1 fw	qPCR	GGAATCTCTGGCAAAGTCCA	60ºC
TAP1 rev	qPCR	TGGGTGAACTGCATCTGGTA	60ºC
TAP2 fw	qPCR	CCAAGACGTCTCCTTTGCAT	60ºC
TAP2 rev	qPCR	TTCATCCAGCAGCACCTGTC	60ºC
TPN fw	qPCR	TGGGTAAGGGACATCTGCTC	60ºC
TPN rev	qPCR	ACCTGTCCTTGCAGGTATGG	60ºC
LMP2 fw	qPCR	TGTGCACTCTCTGGTTCAGC	60ºC
LMP2 rev	qPCR	TGCTGCATCCACATAACCAT	60ºC
LMP7 fw	qPCR	TCTGCGTCATCAGCAAGAAC	60ºC
LMP7 rev	qPCR	GCCATTCAGGAAGTGTCCAT	60ºC
LMP10 fw	qPCR	GGGCTTCTCCTTCGAGAACT	60ºC
LMP10 rev	qPCR	CAGCCCCACAGCAGTAGATT	60ºC
B2M fw	qPCR	CTCGCGCTACTCTCTCTT	60ºC
B2M rev	qPCR	AAGACCAGTCCTTGCTGA	60ºC
HLA-ABC fw	qPCR	GCCTACCACGGCAAGGATTAC	60ºC
HLA-ABC rev	qPCR	GGTGGCCTCATGGTCAGAGA	60ºC
HLA-A fw	qPCR	GGCAGCTCAGATCACCAAGC	60ºC
HLA-A rev	qPCR	TGGGGTGGTGGGTCATATGT	60ºC
HLA-B fw	qPCR	CTACCCTGCGGAGATCA	60ºC
HLA-B rev	qPCR	ACAGCCAGGCCAGCAACA	60ºC
HLA-C fw	qPCR	TGGTGGTGCCTTCTGGACAA	60ºC
HLA-C rev	qPCR	CCAAGGACAGCTAGGACAACC	60ºC
ALAS1 fw	qPCR	TGAGACAGATGCTAATGGATGC	60ºC
ALAS1 rev	qPCR	CACCGTAGGGTAATTGATTGCT	60ºC
ACTB fw	qPCR	TCCTGTGGCATCCACGAAACT	60ºC

Name	Application	Sequence	Condition
ACTB rev	qPCR	GAAGCATTTGCGGTGGACGAT	60ºC
GAPDH fw	qPCR	GAGAAGGCTGGGGCTCATTTG	60ºC
GAPDH rev	qPCR	GGACTGTGGTCATGAGTCCTTC	60ºC
IGF2BP1 fw	qPCR	GCCTCCATCAAGATTGCACC	60ºC
IGF2BP1 rev	qPCR	CTGCCGTCAAATTCTGCAAC	60ºC
IGF2BP2 fw	qPCR	TTACATCGGGAACCTGAGCC	60ºC
IGF2BP2 rev	qPCR	GGTAGTCCACGAAGGCGTAG	60ºC
IGF2BP3 fw	qPCR	GCTACGCGTTCGTGGACTG	60ºC
IGF2BP3 rev	qPCR	CCAGCACCTCCCACTGTAAAT	60ºC
HNRNPC fw	qPCR	TCGAAACGTCAGCGTGTATC	60ºC
HNRNPC rev	qPCR	TCCAGGTTTTCCAGGAGAGA	60ºC
general reverse miR-primer	qPCR	GTGCAGGGTCCGAGGT	60ºC
miR-9-5p fw	qPCR	GCCCGCTCTTTGGTTATCTAGC	60ºC
miR-9-5p SLRT	stem-loop primer	GTCGTATCCAGTGCAGGGTCCGAGGTATT CGCACTGGATACGACTCATAC	42ºC
miR-21-3p fw	qPCR	GCCCAACACCAGTCGATGG	60ºC
miR-21-3p SLRT	stem-loop primer	GTCGTATCCAGTGCAGGGTCCGAGGTATT CGCACTGGATACGACACAGCC	42ºC
miR-21-5p fw	qPCR	GCCGTAGCTTATCAGACTGATG	60ºC
miR-21-5p SLRT	stem-loop primer	GTCGTATCCAGTGCAGGGTCCGAGGTATT CGCACTGGATACGACTCAACA	42ºC
miR-22-3p fw	qPCR	GCACAAGCTGCCAGTTGAAG	60ºC
miR-22-3p SLRT	stem-loop primer	GTCGTATCCAGTGCAGGGTCCGAGGTATT CGCACTGGATACGACACAGTT	42ºC
miR-24-3p fw	qPCR	GGAGTTGGCTCAGTTCAGCAG	60ºC
miR-24-3p SLRT	stem-loop primer	GTCGTATCCAGTGCAGGGTCCGAGGTATT CGCACTGGATACGACCTGTTC	42ºC
miR-26a-5p fw	qPCR	GCCCGTTCAAGTAATCCAGGA	60ºC
miR-26a-5p SLRT	stem-loop primer	GTCGTATCCAGTGCAGGGTCCGAGGTATT CGCACTGGATACGACAGCCTA	42ºC
miR-26b-5p fw	qPCR	GCCCGCTTCAAGTAATTCAGG	60ºC
miR-26b-5p SLRT	stem-loop primer	GTCGTATCCAGTGCAGGGTCCGAGGTATT CGCACTGGATACGACACCTAT	42ºC
miR-29a-3p fw	qPCR	GCCCTAGCACCATCTGAAATC	60ºC
miR-29a-3p SLRT	stem-loop primer	GTCGTATCCAGTGCAGGGTCCGAGGTATT CGCACTGGATACGACTAACCG	42ºC
miR-107 fw	qPCR	CACGCATAGCAGCATTGTACAG	60ºC
miR-107 SLRT	stem-loop primer	GTCGTATCCAGTGCAGGGTCCGAGGTATT CGCACTGGATACGACTGATAG	42ºC
miR-125a-5p fw	qPCR	GATCCCTGAGACCCTTTAACC	60ºC
miR-125a-5p SLRT	stem-loop primer	GTCGTATCCAGTGCAGGGTCCGAGGTATT CGCACTGGATACGACTCACAG	42ºC
miR-125b-5p fw	qPCR	GATCCCTGAGACCCTTTAACC	60ºC
miR-125b-5p SLRT	stem-loop primer	GTCGTATCCAGTGCAGGGTCCGAGGTATT CGCACTGGATACGACTCACAG	42ºC
miR-128-3p fw	qPCR	GCCAGTCACAGTGAACCGG	60ºC
miR-128-3p SLRT	stem-loop primer	GTCGTATCCAGTGCAGGGTCCGAGGTATT CGCACTGGATACGACAAAGAG	42ºC

Name	Application	Sequence	Condition
miR-181b-5p fw	qPCR	GCCCAACATTCATTGCTGTCG	60ºC
miR-181b-5p SLRT	stem-loop primer	GTCGTATCCAGTGCAGGGTCCGAGGTATT CGCACTGGATACGACACCCAC	42ºC
miR-200a-5p qPCR fw	qPCR	GCCCCATCTTACCGGACAGT	60ºC
miR-200a-5p SLRT	stem-loop primer	GTCGTATCCAGTGCAGGGTCCGAGGTATT CGCACTGGATACGACTCCAGC	42ºC
miR-200b-3p fw	qPCR	GCCCTAATACTGCCTGGTAA	60ºC
miR-200b-3p SLRT	stem-loop primer	GTCGTATCCAGTGCAGGGTCCGAGGTATT CGCACTGGATACGACTCATCA	42ºC
miR-200c-3p fw	qPCR	GCCCTAATACTGCCGGGTAA	60ºC
miR-200c-3p SLRT	stem-loop primer	GTCGTATCCAGTGCAGGGTCCGAGGTATT CGCACTGGATACGACTCCATC	42ºC
miR-340-5p fw	qPCR	GCCCGGTTATAAAGCAATGAGAC	60ºC
miR-340-5p SLRT	stem-loop primer	GTCGTATCCAGTGCAGGGTCCGAGGTATT CGCACTGGATACGACAATCAG	42ºC
miR-452-5p fw	qPCR	CACGCAAACTGTTTGCAGAGG	60ºC
miR-452-5p SLRT	stem-loop primer	GTCGTATCCAGTGCAGGGTCCGAGGTATT CGCACTGGATACGACTCAGTT	42ºC
miR-516b-5p fw	qPCR	GCGCAATCTGGAGGTAAGAAGC	60ºC
miR-516b-5p SLRT	stem-loop primer	GTCGTATCCAGTGCAGGGTCCGAGGTATT CGCACTGGATACGACAAAGTG	42ºC
miR-532-5p fw	qPCR	GCCCCATGCCTTGAGTGTAG	60ºC
miR-532-5p SLRT	stem-loop primer	GTCGTATCCAGTGCAGGGTCCGAGGTATT CGCACTGGATACGACACGGTC	42ºC
miR-542-3p fw	qPCR	GCCCTGTGACAGATTGATAA	60ºC
miR-542-3p SLRT	stem-loop primer	GTCGTATCCAGTGCAGGGTCCGAGGTATT CGCACTGGATACGACTTTCAG	42ºC
miR-584-5p fw	qPCR	CACGCATTATGGTTTGCCTGG	60ºC
miR-584-5p SLRT	stem-loop primer	TCGTATCCAGTGCAGGGTCCGAGGTATTC GCACTGGATACGACCTCAGT	42ºC
miR-590-3p fw	qPCR	GCCCGGGTAATTTTATGTATAAGC	60ºC
miR-590-3p SLRT	stem-loop primer	GTCGTATCCAGTGCAGGGTCCGAGGTATT CGCACTGGATACGAC ACTAGC	42ºC
miR-629-5p fw	qPCR	CGCATGGGTTTACGTTGGG	60ºC
miR-629-5p SLRT	stem-loop primer	TCGTATCCAGTGCAGGGTCCGAGGTATTC GCACTGGATACGACAGTTCT	42ºC
miR-744-5p fw	qPCR	GCATGCGGGGCTAGGGC	60ºC
miR-744-5p SLRT	stem-loop primer	TCGTATCCAGTGCAGGGTCCGAGGTATTC GCACTGGATACGAC TGCTGT	42ºC
miR-3180-3p fw	qPCR	GATATGGGGCGGAGCTTCC	60ºC
miR-3180-3p SLRT	stem-loop primer	GTCGTATCCAGTGCAGGGTCCGAGGTATT CGCACTGGATACGACGGCCTC	42ºC
U6 snRNA fw	qPCR	CGGCAGCACATATACTAAAATTGGA	60ºC
U6 snRNA rev	qPCR	AATATGGAACGCTTCACGAATTTGC	60ºC

3.4 Antibodies

Antibody	Company	Clone/ Conjugate	Application
ACTB	Sigma	monoclonal, AC-74	Western Blot
AGO2	Abcam	monoclonal, ab156870	Western Blot
anti-mouse IgG HRP-linked	Cell Signalling, Danvers, Massachusetts, USA	polyclonal, #7076/HRP	Western Blot
anti-rabbit IgG HRP-linked	Cell Signalling	polyclonal, #7074/HRP	Western Blot
CD107a	Biolegend (San Diego, California, USA)	monoclonal, 1D4B/APC	Flow Cytometry
CD16	Biolegend	monoclonal, Brilliant Violet 510 / 3G8	Flow Cytometry
CD3	Biolegend	monoclonal, Pacific blue / OKT3	Flow Cytometry
CD8a	Biolegend	monoclonal, PE / RPA-T8	Flow Cytometry
CD56 (NCAM)	Biolegend	monoclonal, Pe-Cy7 / CMSSB	Flow Cytometry
GAPDH	Cell Signalling	monoclonal, 14C10	Western Blot
Goat anti-mouse IgG	Dako	polyclonal, P0447/HRP	Western Blot
HLA-A2	Kindly provided by Prof. Dr. Soldano Ferrone	monoclonal, SB00-147	Flow Cytometry
HLA-ABC	Biolegend	monoclonal, W6/32 / Pe-Cy7	Flow Cytometry
HLA-BC	Biolegend	monoclonal, B1.23.2 / APC	Flow Cytometry
HLA-C	Biolegend	monoclonal, DT-9 / unconjugated	Flow Cytometry
HLA-I HC	Kindly provided by Prof. Dr. Soldano Ferrone	polyclonal, sp08-222	Western Blot
IGF2BP1	Kindly provided by Prof. Dr. Stefan Hüttelmeier	monoclonal, 6A9	Western Blot
IGF2BP2	Kindly provided by Prof. Dr. Stefan Hüttelmeier	monoclonal, 4E5	Western Blot
IGF2BP3	Kindly provided by Prof. Dr. Stefan Hüttelmeier	monoclonal, 6G8	Western Blot
LMP10	Kindly provided by Prof. Dr. Soldano Ferrone	polyclonal, sb07-71	Western Blot
LMP2	Kindly provided by Prof. Dr. Soldano Ferrone	polyclonal, sb07.019	Western Blot
LMP7	ENZO	polyclonal, PW 8200	Western Blot
MBP	Abcam	polyclonal, ab9084	Western Blot
Swine anti-rabbit IgG	Dako	polyclonal, P0217/HRP	Western Blot
TAP1	Abcam	polyclonal, ab13516	Western Blot
TAP2	Kindly provided by Prof. Dr. Soldano Ferrone	monoclonal, sp12-157	Western Blot
TPN	Abcam	polyclonal, ab13518	Western Blot

3.5 Enzymes

Enzyme	Company	Application
ApaI	NEB	Cloning
BamHI	NEB	Cloning
BclI	NEB	Cloning

Enzyme	Company	Application
BglII	Thermo Scientific	Cloning
DNase I	NEB	RNA preparation
	Promega	miTRAP, RNA-AP
DpnI	NEB	Cloning
EcoRI	NEB	Cloning
HindIII	Thermo Scientific	Cloning
KpnI	Thermo Scientific	Cloning
MluI	NEB	Cloning
NheI	Thermo Scientific	Cloning
PciI	NEB	Cloning
Phusion® High-Fidelity DNA-Polymerase	NEB	Cloning
Proteinase K	Promega	Cloning
PspOMI	NEB	Cloning
Q5® High-Fidelity DNA-Polymerase	NEB	Cloning
Reverse-Transcriptase	Thermo Scientific	Reverse transcription
Ribolock Rnase Inhibitors	Thermo Scientific	cDNA synthesis
RNase A	Macherey-Nagel	Plasmid preparation
Rnasin	Promega	miTRAP, RNA-AP
SalI	Thermo Scientific	Cloning
Shrimp Alkaline Phosphatase (rSAP)	NEB	Phosphorylation
SpeI	NEB	Cloning
T4 DNA-Ligase	Promega	Cloning
T4 Polynucleotide-Kinase	NEB	Cloning
T7 RNA Polymerase	Promega	*in vitro* transcription
Taq DNA-Polymerase	Invitrogen	PCR
Trypsin	Promega	Cell culture
XbaI	NEB	Cloning
XhoI	NEB	Cloning

3.6 Kits

Kit	Distributor	Application
2x SYBR Green qPCR Master Mix	Biotool	qPCR
4-20% Mini-PROTEAN® TGX™ precast protein gel	SERVA Electrophoresis GmbH	SDS-PAGE
auto-MACS kit	Miltenyi Biotec	Isolation of NK cells
BCA Protein Assay Reagent	Thermo Scientific	Determination of protein concentration
Calibration standard II kit (700-3500 Da)	Bruker Daltonics, Inc.	Mass spectormetry
DNaseI (Rnase-free)	NEB	DNase treatment
Dual-Luciferase® Reporter Assay System	Promega	Measurement of Luciferase
Effectene Transfection Reagent	Qiagen	Transfection
GoTaq® G2 Flexi DNA Polymerase	Promega	PCR
Lipofectamine 2000	Invitrogen	Transfection
Lipofectamine RNAimax	Invitrogen	Transfection
MEGAclear™ Transcription Clean Up Kit	Invitrogen	RNA purification
NK Cell Isolation Kit, human	Miltenyi Biotec	Isolation of NK cells
NucleoBond® Xtra midi	Macherey-Nagel	Plasmid extraction
NucleoSpin® Gel and PCR Clean-up	Macherey-Nagel	DNA purification
NucleoSpin® Plasmid	Macherey-Nagel	Plasmid extraction

Kit	Distributor	Application
NucleoSpin® RNA kit	Macherey-Nagel	RNA extraction
NucleoSpin® Tissue kit	Macherey-Nagel	RNA extraction
PCR Mastermix Taq	Invitrogen	PCR
Pierce™ ECL Western Blotting Substrate	Thermo Scientific	Western Blot
Platinum®Taq DNA Polymerase	Invitrogen	PCR
Q5® High-Fidelity DNA Polymerase kit	NEB	PCR
Q5® Site-Directed Mutagenesis Kit	NEB	DNA mutagenesis
QIAamp DNA Mini Kit	Qiagen	DNA extraction
RevertAid First Strand cDNA Synthesis Kit	Thermo Scientific	cDNA synthesis
RiboMAX™ Large Scale RNA Production System-T7	Promega	*in vitro* transcription
RQ1 RNase-free DNase	Promega	DNase treatment
Turbofect	Thermo Scientific	Transfection

3.7 Consumables

Name	Company	Application
0.2 mL tubes	Dr. Ilona Schubert Laborfachhandel	Molecular biology
1.5 mL tubes	Dr. Ilona Schubert Laborfachhandel	Molecular biology
10 mL serological pipettes	TPP Techno Plastic Products AG	Cell culture
15 mL Greiner tubes	Greiner Bio-One GmbH	Cell culture
2.0 mL tubes	Dr. Ilona Schubert Laborfachhandel	Molecular biology
25, 75 and 175 cm² cell culture flasks	Sarstedt	Cell culture
25 mL serological pipettes	TPP Techno Plastic Products AG	Cell culture
5 mL serological pipettes	TPP Techno Plastic Products AG	Cell culture
50 mL Greiner tubes	Greiner Bio-One GmbH	Cell culture
6-, 12- and 96- well plates (flat bottom)	Sarstedt	Cell culture
96-well plate (round bottom)	Sarstedt	Cell culture
FACS tubes	Sarstedt	Flow cytometry
LS column	Miltenyi	Cell culture
Neubauer hemocytometer (0.0025 mm2)	Marienfeld-Superior	Cell culture
Nitrocellular membrane	Schleicher & Schuell	Western Blot
PARAFILM® M	Sigma-Aldrich	Microbiology
Pasteur pipette	Hirschmann laboratory equipment GmbH & Co KG	Cell culture
Pipettes	Eppendorf, Gilson	Molecular biology/ Cell culture
Pipettes' tips (0-10 µL, 10-100 µL, 20-200 µL, 100-1000 µL)	Sarstedt	Molecular biology/ Cell culture
Semi-micro cuvettes	Dr. Ilona Schubert Laborfachhandel	Molecular biology
Whatman paper	Whatman	Western Blot

3.8 Equipment

Name	Company	Application
96-well labcycler gradient	Sensoquest	PCR
Allegra® X-15R Centrifuge	Beckman Coulter	Cell culture
Balance	Ohaus Europe, GmbH	Molecular biology
BD FACSCanto™	BD Biosciences	Flow cytometry
BD LSRFortessa™	BD Biosciences	Flow cytometry
BIO-RAD 96-well iCycler	BIO-RAD Laboratories, Inc.	qPCR
Blue Shake 3D gel shaker	SERVA, Heidelberg, Germany	Coomassie staining
Cell dounce homogenizer		RNA-affinity purification
CO_2-Incubator	Binder	Cell culture
DigestPro MSi	Intavis	Mass spectrometry
GelPal spot picker	Genetix	Mass spectrometry
GloMax 96-microplate luminometer	Promega (kindly provided by Prof. Possern)	Measurement of luciferase activity
Herolab spot hunter	Herolab GmbH	Mass spectrometry
Horizontal Electrophoresis Systems (Agarosegel running chamber)	BIO-RAD Laboratories, Inc	Molecular biology
Infinite® 200Pro microplate reader	TECAN	Molecular biology
LAS 3000 CCD camera system	FUJIFILM	Western Blot
Microcentrifuge Z233 MK-2	Hermle Labortechnik	Cell culture
Mini-PROTEAN® Tetra Cell	BIO-RAD Laboratories, Inc.	Western Blot
MTP 384 ground steel target	Bruker Daltonics, Inc.	Mass spectrometry
Navios flow cytometer	Beckman Coulter, Krefeld, Germany	Flow cytometry
Power supply	BIO-RAD Laboratories, Inc	Molecular biology
Rotor-Gene	Qiagen	qPCR
Sterile working bench: HERA safe	Heraeus Sepatech GmbH	Cell culture
Suction pump	KNF Neuberger, GmbH	Cell culture
Telaval 3 inverted microscope	Carl Zeiss Jena	Cell culture
Thermoblock	Eppendorf AG	Molecular biology
Trans-Blot® Tank	BIO-RAD Laboratories, Inc., California, USA	Western Blot
ultrafleXtreme™	Bruker Daltonics, Inc.	Mass spectrometry
Ultraschall-Homogenizator	SONOPULS Bandelin	Cell disruption
UV-table	Hoefer	Molecular biology
ZipTips®	Millipore	Mass spectrometry

3.9 Software

Name	Company	Application
Acrobat Reader DC	Adobe	PDF files reading
Adobe Photoshop Elements 4.0	Adobe	Image editing
BD CellQuest Pro Software	BD Biosciences	Flow cytometry
Bio-Rad CFX Maestro 1.0	Bio-Rad Laboratories	qPCR analysis
Clone Manager 5	Sci-Ed Software	Cloning
ENCORI	http://starbase.sysu.edu.cn/rbpClipRNA.php	Expression analysis
Endnote	Thomson Reuters	Reference's editing
FACSDiva software package	BD Biosciences	Flow cytometry
flexAnalysis software (3.3.80.0)	Bruker Daltonics, Inc.	Mass spectrometry

Name	Company	Application
FlowJo_V10.0.7r2	DONGLE	Flow cytometry
GIMP 2.8.16	Spencer Kimball	Image editing
GraphPad Prism 8.0.1	GraphPad Software, LLC	Designing of diagrams
Image Reader LAS3000 software	Fuji LAS3000, Fuji GmbH, Düsseldorf	Western blot
Image Studio Lite Ver 5.2	LI-COR Biosciences	Image editing
ImageJ 1.51j8	National Institute of Health	Image editing
Kaluza® Flow Analysis Software	Beckman-Coulter	Flow cytometry
MASCOT search engine	Matrix Science	Mass spectrometry
Mendeley Desktop	Mendeley	Reference editing
MetaVue™ Research Imaging Software	Molecular Devices, LLC	Cell culture
Microsoft Excel 2010	Microsoft	Calculation of values
Microsoft PowerPoint 2010	Microsoft	Image editing
Microsoft Word 2010	Microsoft	Text editing
miRBase	http://mirbase.org/	MiR prediction
miRDB	http://www.mirdb.org/	MiR prediction
miRwalk	http://zmf.umm.uni-heidelberg.de/apps/zmf/mirwalk2/index.html	MiR prediction
Primer Premier 5.00	PREMIER Biosoft International	Primer designing
R2: microarray analysis and visualization platform	http://r2.amc.nl	Analysis of gene expression
RNA hybrid	BiBiServ	MiR prediction
Rotor-Gene 6000 Series Software 1.7	Corbett	qPCR analysis
Serial Cloner 2.6.1	Serial basics	Primer designing
Starbase v2.0	http://starbase.sysu.edu.cn/starbase2/index.php	Expression analysis
STRING	https://string-db.org/cgi/input.pl?sessionId=MQcAlaxDE5F4&input_page_show_search=on	Analysis of protein interactions
Targetscan	Whitehead Institute for Biomedical Research	MiR prediction
Winglow Software	Berthold Technologies	Measurement of Luciferase activity
Xenabrowser	https://xenabrowser.net/	Expression analysis

4. Methods

4.1 Cell culture conditions and cell lines

The human embryonic kidney cell line HEK293T, the NK cell-sensitive erythroleukemic cell line K-562 (ATCC® CCL-243™) and the human TAP-negative T2 cell line (ATCC® CRL-1992™) were purchased from the American Tissue Culture Collection (ATCC, Manassas, USA), while the human melanoma cell line MKR from the German Cancer Research Centre (DKFZ, Heidelberg, Germany). The human melanoma cell lines FM3 (ESTDAB-007), FM81 (ESTDAB-026), Mel-1359 (ESTDAB-047) and MZ-Mel2 (CVCL-1435)[311] were obtained from the European Searchable Tumour Cell Line and Data Bank (ESTDAB project; www.ebi.ac.uk/ipd/estdab)[312,313]. The human melanoma cell line BUF1379 was kindly provided by Professor Dr. Soldano Ferrone (Department of Surgery, Massachusetts General Hospital, Harvard Medical School, Boston, USA). The NK cell-sensitive erythroleukemic cell line K562 served as a control in functional assays and T2 cells negative for TAP1, TAP2, LMP2, LMP7 and MHC-II antigens as a control for peptide pulsing[314]. This deficiency of T2 cells in TAP1, TAP2, LMP2, LMP7 and MHC-II antigens results in failure to correctly translocate endogenous, processed peptides to the site of MHC loading in the ER/Golgi apparatus[315].

HEK293T cells were cultured in Dulbecco's Modified Eagles Medium (DMEM, Invitrogen, Carlsbad, CA, USA), while all other cell lines were maintained in Roswell Park Memorial Institute 1640 medium (RPMI 1640, Invitrogen). DMEM and RPMI were supplemented with 10 % (v/v) fetal calf serum (FCS) (PAN, Aidenbach, Germany), 2 mM L-glutamine (Lonza, Basel, Switzerland) and 1 % penicillin/streptomycin (v/v, Sigma-Aldrich, Missouri, US) at 37 °C in 5 % (v/v) CO_2 humidified air. For IFN-γ treatment, the cell lines were cultured in the presence of recombinant 200 U/mL IFN-γ (PAN) for 24h or 48h.

Peripheral blood mononuclear cells were purified from peripheral blood samples of healthy donors using a Ficoll gradient (BiochromAG, Berlin, Germany) according to manufacturers' instructions. Total PBMCs were cultured in X-VIVO 15 medium (Lonza) supplemented with 1% (v/v) sodium pyruvate, 2mM L-glutamine and 1% (v/v) penicillin/streptomycin as well as with the 3 different cytokines IL-12 (Immunotools, Friesoythe, Germany), IL-15 (Immunotools) and IL-18 (Biovision, Ilmenau, Germany) in order to stimulate the NK cells within the PBMCs. The experiments were performed with PBMCs from at least three different donors.

T-cells specific for the HLA-A2-restricted Melan A/Mart-1 epitope were kindly provided by Pedro Romero (Ludwig Institute for Cancer Research, Lausanne, Switzerland) and cultured in RPMI 1640 supplemented with 8% human serum.

For cryopreservation all cultured cells were harvested, washed with phosphate-buffered saline (PBS), resuspended in pure FCS supplemented with 10% (v/v) dimethyl sulfoxide (DMSO, Sigma-Aldrich) and stored in cryogenic vessels at -80° C until further use.

Cultured cells were harvested by trypsinization, washed twice with PBS and frozen at -80°C until further use. The cell pellets for the RNA affinity purification (RNA-AP) assays (miTRAP and RNA-AP for RBPs) were harvested by trypsinization, washed twice with PBS, immediately frozen in liquid nitrogen and subsequently stored at -80°C until further use.

4.2 Transient transfection

For transient transfection of miR mimics (30 nM), miR inhibitors (100 nM), siRNAs (2 ng/mL) or plasmids (2 µg/mL) 0.25 – 1x10^6 cells were seeded in 6-well plates and transiently transfected after 12-16 h with the respective amount of the nucleic acid using the appropriate volume of Lipofectamine RNAiMAX (Invitrogen), Lipofectamine 2000 (Invitrogen) or Effectene (Giagen, Hilden, Germany) according to the manufacturer's instructions. The cells were harvested 48 h post-transfection for subsequent RNA, protein, flow cytometric analyses or luciferase reporter assays.

4.3 Isolation of DNA, RNA and miRs

Plasmid DNA was isolated either with the NucleoSpin® Plasmid or the NucleoBond® Xtra Midi kits (Macherey-Nagel, Schkeuditz, Germany) for small or medium scale plasmid preparation, respectively. The NucleoSpin® Gel and PCR Clean-up kit (Macherey-Nagel) was employed for the purification of the PCR products or plasmids. Total cellular RNA from cell cultures was isolated using the NucleoSpin® RNA kit (Macherey-Nagel) according to the manufacturer's instructions. Total cellular RNA and miRs from cell cultures were extracted using the TRIzol reagent (Invitrogen) according to the manufacturer's instructions. For RNA isolation from paraffin-embedded tissue sections, total RNA was extracted using the NucleoSpin® Tissue kit (Macherey-Nagel) according to the manufacturers' protocol. The isolated RNA was treated with DNase I (New England Biolabs (NEB), Ipswich, MA, USA) for 30 min at 37°C. The DNase I was subsequently inactivated with 50 mM EDTA (Thermo Scientific, Waltham, Massachusetts, USA) by incubation for 10 min at 75°C and the RNA was used as template for cDNA synthesis.

The concentration of DNA or RNA samples was determined with the Infinite® 200Pro absorbance microplate reader (TECAN). As an indicator of samples purity, the ratios of the absorbance values of 260 nm vs 280 nm (A260/A280) and the 260 nm vs 230 nm (A260/A230) were determined.

4.4 cDNA synthesis and quantitative qPCR

The reverse transcription quantitative polymerase chain reaction (RT-qPCR) was performed as previously described[313]. For cDNA synthesis, 500ng DNase I treated RNA was reversed transcribed into cDNA using the RevertAid^{TM} H Minus first strand cDNA synthesis kit (Thermo Scientific). For miR-specific cDNA synthesis, miR-specific stem-loop primers[316,317] (§ 3.3) have been designed and used, whereas for the reverse transcription reaction of mRNA, oligo dT primers (Thermo Scientific) were used. The reverse transcription reactions and semi-quantitative PCRs were carried out in a 96-well labcycler (Sensoquest, Göttingen, Germany).

For the quantitative PCR (qPCR) reactions, the 2x SYBR Green qPCR Master Mix (Absource, Munich, Germany) was used with target-specific primers (§3.3). The qPCR reactions were carried out either in a BIO-RAD 96-well iCycler (BIO-RAD Laboratories, Inc., Hercules, CA, USA) or in a Rotor-Gene cycler (Qiagen). Relative changes of RNA abundance were determined by the $2^{-\Delta\Delta Cq}$ method using the house-keeping genes: glyceraldehyde-3-phosphate dehydrogenase (GAPDH), β-actin (ACTB) or delta-aminolevulinate synthase 1 (ALAS1) for normalization. The relative miR expression levels were normalized to the corresponding expression levels of the small ncRNA RNU6 (RNU6A). The reactions were performed at least in two technical replicates of at least three biological replicates.

4.5 Protein extraction and measurement of protein concentration

For protein extractions, 5×10^5 – 1×10^7 cells were harvested and subsequently washed twice with 5 mL ice cold PBS (300xg, 5 min, 4°C). The resulting cell pellets were resuspended and then transferred into 1.5 mL reaction tubes (Eppendorf Safe-Lock) and again centrifuged (300xg, 5 min, 4°C). After discarding the supernatant, the cell pellets were immediately frozen in liquid nitrogen. Afterwards, they were resuspended in RIPA buffer supplemented with fresh protease and phosphatase inhibitor cocktail (1:100, Thermo Scientific) and sonicated twice (Bandelin HD 2070 Sonoplus equipped with a MS 73 micro needle) with at least five pulses (1 sec pause) and 70% intensity in order to lyse the cells and destroy the DNA. The cell lysate was stored on ice for 5 min and then centrifuged (12000xg, 30 min, 4°C) in order to clear the lysate from residual fragments. The supernatant was transferred into a new sterile 1.5 mL reaction tube. Next, the protein concentration was determined by using the Pierce BCA kit (Thermo Scientific) according to the manufacturer's instructions and measured in an Infinite® 200Pro absorbance microplate reader system (TECAN). The corresponding calibration curves were established using eight defined bovine serum albumin (BSA) standards (ranging from 0 to 2 mg/mL). Aliquots of the lysates were further supplemented with 4x Laemmli buffer containing 10% (v/v) β-mercaptoethanol (AppliChem GmbH, Darmstadt, Deutschland) and heated up for 5 min at 95°C, before they were loaded on 10% sodium dodecyl sulfate–polyacrylamide gel electrophoresis (SDS-PAGE) gels for Western blot analysis.

4.6 Western blot analysis

For Western blot analysis, 25 - 50 µg protein/lane were separated in 10% SDS-PAGE gels. Moreover, each gel carried a prestained protein ladder (Thermo Scientific), which was co-separated as an indicator for the respective molecular weight range. The samples were run at 10 mA/gel for 25 min and then at 20 mA/gel in running buffer. Thereafter, the separated samples were transferred (wet Western blot transfer) in transfer buffer (running buffer + 20% methanol (Sigma-Aldrich)) onto nitrocellulose membranes (Schleicher & Schuell, Munich, Germany) overnight at 100 mA (Trans-Blot® Tank, BIO-RAD, Laboratories, Inc, California, USA) at room temperature (RT). Subsequently, the membranes were separated from the gels and stained with Ponceau S (AppliChem) staining solution (0.2% (w/v) Ponceau S in 3% (w/v) TCA) and washed carefully with water as previously described[318]. After washing, the membranes were blocked for 2 h with 5% BSA (w/v) diluted in TBS-T (0.2 M Tris, 1.4 M NaCl, 0.2% Tween, pH 7.6) supplemented with 10% horse serum on a gentle, orbital gel shaker (Blue Shake 3D, SERVA, Heidelberg, Germany) under constant agitation. Immunodetection was performed using target-specific primary rabbit or mouse antibodies (§ 3.4). Stainings with either anti-GAPDH specific antibody (Ab) (Cell Signaling Technology, Danvers, Massachusetts, USA) or anti-ACTB specific Ab (Sigma) served as loading controls. After the incubation with primary Ab, the membranes were washed trice at RT with TBS-T and stained with suitable anti-rabbit or anti-mouse horseradish peroxidase (HRP) conjugated secondary Ab (DAKO, Hamburg, Germany or Cell Signaling Technology). Membranes were incubated with primary or secondary Ab according to manufacturer's instructions. The resulting chemoluminescense signals were detected using the Pierce Western Blot Signal Enhancer substrate (Thermo Scientific) and recorded with a LAS3000 camera system

(Fuji LAS3000, Fuji GmbH, Düsseldorf). The digitized immunostaining signals were subsequently analysed and quantified using the ImageJ software (NIH, Bethesda, USA). Relative protein expression levels were represented as arbitrary units by setting the peak values of the corresponding GAPDH or ACTB signals to 1.

4.7 Flow cytometric analysis

For flow cytometric analysis, either directly conjugated Ab with a variety of fluorescent labels or unconjugated Ab were employed (§ 3.4) according to the manufacturer's instructions. Flow cytometry analysis was performed as previously described[319]. 2×10^5 cells were harvested by trypsinization, washed twice with PBS (300xg, 5 min, 4°C), incubated with the appropriate volume of the respective Ab for 30 min on ice, washed again twice with PBS (300xg, 5 min, 4°C), before they were analysed by flow cytometry. Dead cells were identified by red-fluorescent propidium iodide (PI) staining, which was added shortly before the measurement. The measurement was carried out either on the LSRFortessa (BD Biosciences, Heidelberg, Germany) or the Navios (Beckman Coulter, Krefeld, Germany) flow cytometer. Subsequently, the obtained data were evaluated with the FACS Diva analysis software (BD Biosciences) or with the Kaluza® flow analysis software (Beckman Coulter), respectively. The data were presented as histograms of the mean fluorescence intensity (MFI) of cellular surface markers or as dot plots.

4.8 CD107 degranulation assays

Tumour cell susceptibility to the Mart-1-specific CTL clone or to NK cells within the stimulated PBMCs was evaluated by the CD107a degranulation assay[320]. Briefly, target cells were co-incubated with effector cells at 37°C. After one hour of incubation, the anti-CD107a Ab (Biolegend, San Diego, California, USA) was added and after additionally 3 h the effector cells were stained with the anti-CD3 and anti-CD8 Ab (Biolegend) for the CTL assays, or with the anti-CD3, anti-CD16 (both from Biolegend) and anti-CD56 Ab (Thermo Scientific) for the NK assays and analysed on the Navios flow cytometer (Beckman Coulter) according to manufacturer's instructions. Effector cells in the absence of any target were used to determine the spontaneous degranulation that was removed from the specific one. For pulsing, tumour cells were incubated for 1 h at 37°C with 1 µg Mart-1 peptide /100000 cells and washed before addition to the T-cells. The data were expressed as percentage of CD107a positive effector cells.

For the CTL assays target cells were co-incubated with effector cells at a 1:1 ratio at 37°C, while for the NK cell assays, the effector: target cell (E:T) ratio was 1:1 with total PBMCs and the cells were co-incubated at 37°C. To test the functionality of the T-cells or the NK cells, incubation with peptide-pulsed versus unpulsed T2 cells was used as positive control for the T-cells and with K562 cells for the NK cells, respectively.

Both of the functional T- and NK cell assays were performed by Dr. Chiara Massa (Institute for Medical Immunology, Martin Luther University Halle-Wittenberg, Halle (Saale), Germany).

4.9 Dual luciferase reporter assay

In order to verify the direct interaction and the binding site of a miR to the 3'-UTR of the mRNA of interest, the dual luciferase (luc) reporter assay[321] was employed. Briefly, the TAP1 3'-UTRs was cloned in the pmiR-Glo Dual-Luciferase miRNA target

expression vector (Promega, Madison, Washington, USA) with the restriction enzymes NheI and SalI (Thermo Scientific) as described in figure 4.1. On day 0, 1×10^4 HEK293T cells were seeded into 96-well plates. After 12-16 h, the cells were co-transfected with 30 nM mimics and 5 ng recombinant pmiR-Glo vectors using Lipofectamin 2000 (Invitrogen). The cells were washed with PBS 48 h post-transfection and lysed in lysis buffer (Promega). Firefly luciferase (FFL) activities were internally normalized by Renilla (RL) activities yielding relative activities (RLU). Commercially available substrate solutions (Promega) were used according to manufacturer's instructions. The FFL and RL activities were determined using the DualGlo reagents (Promega) and the GloMax 96-Microplate luminometer (Promega) kindly provided by Professor Dr. Guido Posern (Institute of Biophysical Chemistry, Martin-Luther-University Halle-Wittenberg, Halle (Saale), Germany) with the Dual-Luciferase® Reporter Assay System (Promega) according to manufacturer's instructions.

To determine the specificity of the interaction between the candidate miRs and TAP1 3'-UTR, the putative binding sites of the candidate miRs were deleted in the luc reporter gene construct. For the deletion of the binding sites of the candidate miRs in the 3'-UTRs, specific primers were designed using to the NEBaseChanger software (https://nebasechanger.neb.com/, NEB) (§ 3.4) and by employing the Q5® Site-Directed Mutagenesis kit (NEB) according to manufacturer's instructions. Mimic negative control (NC) and the empty vector containing the multiple cloning site (MCS) served as negative controls. RLU ratios were normalized to control populations. All reactions were performed in three technical replicates of at least three biological replicates.
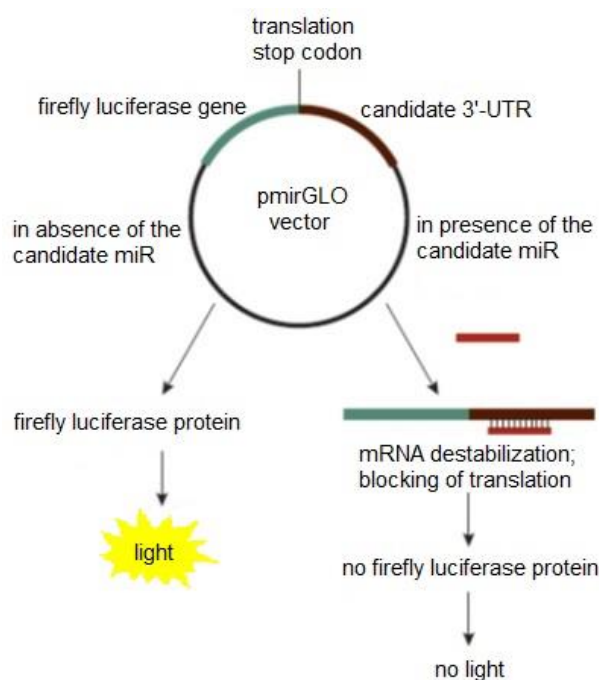
Figure 4.1. Experimental approach of the dual luc reporter assay[321]
The pmirGLO vector is designed to quantitatively evaluate miR activity by the insertion of the 3'-UTR of the candidate mRNA with the miR target sites downstream of the firefly luc gene (FFL). FFL is the primary reporter gene; reduced FFL expression indicates the binding of introduced miRs. The renilla luciferase (RLU) acts as a control reporter for normalization using the Dual-Luciferase® Assay. (edited from "pmirGLO Dual-Luciferase miRNA Target Expression Vector, Promega")

4.10 MiRNA trapping by RNA *in vitro* affinity purification (miTRAP) assay

To enrich specific miRs targeting the 3'-UTRs of the APM components TAP1, TAP2 and TPN respectively, the miTRAP assay was employed[322,323]. Apart from the 3'-UTR, the target sequences can be the 5'-UTR or the coding sequence (CDS). All solutions were prepared with Millipore water (Merck Millipore) and analytical grade reagents.

Sterile plastic ware was used for all the procedures. The following steps were carried out at RT unless indicated otherwise[322].

For efficient immobilization of the bait RNAs on beads, the MS2 tagging technique was used, based on the interaction of the MS2 bacteriophage coat protein and specific RNA stem-loop structures from the phage genome[324]. Therefore, the DNA sequences of the 3'-UTRs of the APM components of interest were cloned upstream of the coding sequence for two MS2 "stem-loop" structures. The recombinant plasmid pcDNA™ 3.1(+) (Invitrogen) with two MS2 loops was kindly provided by Dr. Bianca Busch and Professor Dr. Stefan Hüttelmaier (Institute of Molecular Medicine, Martin-Luther-University Halle-Wittenberg, Halle (Salle), Germany). The PCR components were amplified employing the Q5 DNA polymerase (NEB) and respective oligonucleotides (§ 3.3). The amplified PCR products were extracted from the agarose gels with the NucleoSpin® Gel and PCR Clean-up kit (Macherey-Nagel) according to manufacturers' instructions and incubated overnight with the respective restriction enzymes (NEB). After another purification step using the NucleoSpin® Gel and PCR Clean-up kit (Macherey-Nagel), the insert and vector were ligated into the linear vector using the T4 DNA-Ligase (Promega) according to manufacturers' instructions and the ligation mix was transformed into dam⁻/dcm⁻ cells (NEB) and plasmid DNA was isolated with the NucleoBond® Xtra Midi kit (Macherey-Nagel) for medium scale plasmid preparation. The recombinant plasmids were then *in vitro* transcribed overnight with T7 RiboMAX™ large scale RNA production system (Promega), cleaned with the MEGAclear™ Transcription Clean Up Kit (Invitrogen) according to manufacturers' instructions and used for the enrichment of specific miRs from cell lysates of several melanoma cell lines, showing high mRNA levels but low protein levels for each APM component.

Briefly, amylose resin beads (NEB) were washed and incubated with the fusion protein MS2BP-MBP, blocked with yeast tRNA (Invitrogen) and BSA, and incubated with the bait RNAs or the sequence encoding only the two MS2 loops (MS2, here serving as a negative control) and the cell lysate. For the preparation of the cell lysates, 10×10^6 cells of the selected cell line were harvested, washed three times with PBS and resuspended in 2mL lysis buffer supplemented with fresh protease and phosphatase inhibitor cocktail (1:100, Thermo Scientific). This number of cells is sufficient for one target, the MS2 control, the beads control and the input control. With the exception of cell lysis procedure, all steps were performed at room temperature under constant agitation.

For miR analysis, RNA complexes were eluted twice by incubation with 15 mM maltose and miRs were purified from maltose solution by phenol/chloroform/isoamylalcohol extraction. After incubation with Proteinase K (Promega), 0.5 mL cell lysate was also used for RNA extraction and the sample was applied as an input control. After RNA precipitation, the RNA samples resuspended in water and stored at -80°C and the miR enrichment was further validated by RT-qPCR. Alternatively, the beads were incubated with 25 µL 4x Laemmli buffer at 95°C for 5 min, centrifuged (1000xg, 1 min, RT) and the supernatants were loaded on 10% SDS-PAGE gels, together with 1%, 0.5% and 0.2% of the cell lysate inputs. Western blot analysis follows as described previously in §4.4.

The complete method and its alteration are described in detail in several publications[322,323]. A scheme of the miTRAP procedure is depicted in figure 4.2[322].
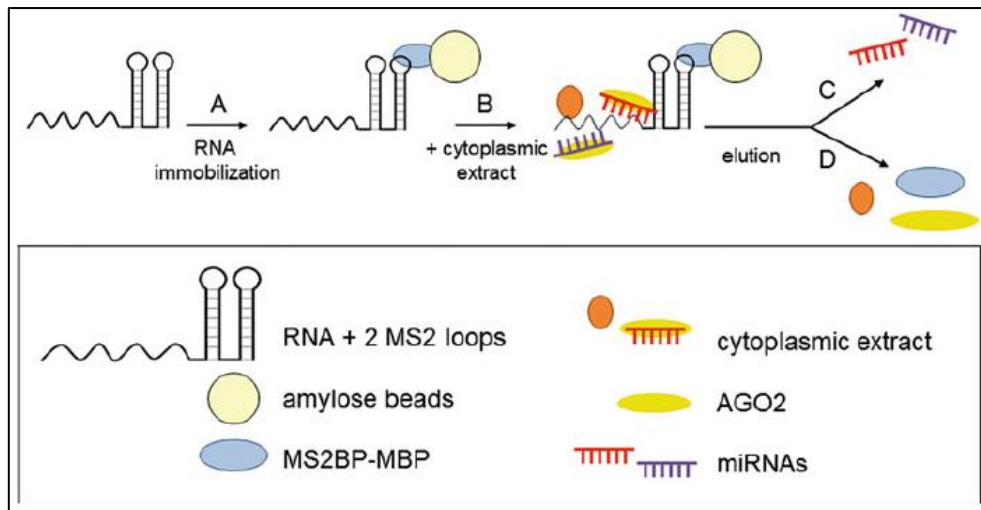
Figure 4.2. Scheme of the miTRAP procedure[322]
(A) The target RNA and 2MS2 stem-loops are immobilized via MS2BP-MBP on amylose beads. (B) The cytoplasmic extract is incubated with the target RNA of interest. (C) RNAs and (D) proteins are separately eluted from the beads for downstream analyses, such as small RNA sequencing, qPCR, and Western blot analyses.

4.11 Small RNA sequencing analysis

Next generation sequencing (NGS) methods have been widely used for the identification of small RNAs of certain species under particular conditions[325], among them also miRs[326], as well as the generation of small RNA differential expression profile between different conditions, such as tumour and healthy samples[327]. Especially the Illumina sequencing technology is extensively employed, since it has the benefits of small sample requirements (low input), high throughput and high accuracy[328].

As previously described in the miTRAP method[322,323], miRs can be separately eluted from the beads for downstream analyses, such as small RNA sequencing. Therefore, in order to identify enriched miRs binding to each construct, miTRAP eluates of TAP1 and TAP2 3'-UTR constructs have been sent for small RNA sequencing to Novogene Co., Ltd (Hong Kong, China) and TPN 3'-UTR constructs to Dr. Andreas Dahl (Deep Sequencing Group, TU Dresden, Germany) together with the MS2 and input controls. After the small RNA library preparation, the sequencing was conducted on an Illumina HiSeq 2500 machine and 50 bp long single-end reads were obtained. Cutadapt[329] and custom perl scripts were used to trim the reverse primers and the unique molecular identifiers (UMI) sequences, respectively. UMIs are molecular tags (4-10bp) that are attached to each transcript prior amplification in order to detect and quantify unique mRNA transcripts[330]. The trimmed UMI sequences were appended to the FastQ header so that they could be used in later steps. Reads that did not contain the adapter or were too short (<18bp) or long (>25bp) after adapter/UMI trimming were discarded. After trimming, the remaining read sequence should contain the miR inserts, visible as a major peak at 21-23 bp in the length distribution. The isolation of the miR fraction was based on size selection and fractions of other non-interesting RNA species, for example rRNA and tRNA, were to be expected and excluded. Reads were further mapped with bowtie1[331] against the human genome hg38 and reads mapping to mRNA exonic loci as well as ncRNA loci - with the exception of miRs - were identified with bedtools[3] and discarded. MiRs were detected and quantified with mirdeep*[332] from the databank mirBase (v21)[213]. The output was a table with counts per miR loci, taking into

account that a miR can be encoded by multiple loci. In this case, reads were equally distributed among the loci.

Different normalization methods are available:

- "counts per million" (cpm): count per miR divided by the total count per sample multiplied by one million
- "transcripts per million" (tpm): count per miR divided by the transcript length and the scaling factor by one million, giving a normalized transcript expression level[333].
- "DESeq2": commonly used in RNA-seq experiments and preferred; the geometric mean between samples is used as normalisation factor for a gene[334].

For determination of the differential expression pattern DESeq2 was used for normalisation[334]. Therefore, the 3'-UTR constructs have been compared with the MS2 and input controls. MiRs were considered as differentially expressed with corrected p-value (q-value) <0.05.

4.12 RNA affinity purification for the detection of RNA-binding proteins

To enrich specific RBPs targeting the 3'-UTRs of the APM components, the RNA affinity purification method for the enrichment of RBPs was employed. The complete detailed method and its alterations are described in detail in several publications[309,335,336], while the workflow is depicted at figure 4.3.
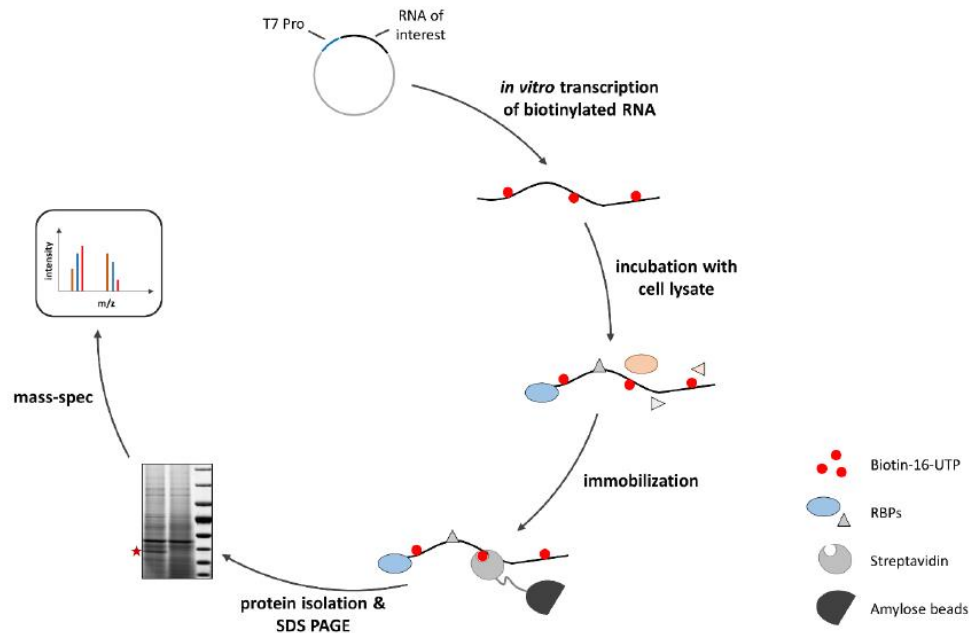
Figure 4.3. Experimental approach of the RNA-AP assay for RBPs[335]

Briefly, the sequences of the respective 3'-UTR of APM components have already been cloned into the recombinant plasmid DNA pcDNA™ 3.1(+) (Invitrogen) with two MS2 loops in order to perform the miTRAP assay (previously described in §4.9). The constructs for the miTRAP (as described previously) can be also used for the identification of RBPs to the respective 3'-UTR constructs. Using these recombinant plasmids as templates, a standard PCR was performed using the Q5 DNA polymerase (NEB) and oligonucleotides (§ 3.3), with the forward primer annealing to the T7 promoter and the reverse primer annealing to the end of the 3'-UTRs. The PCR products were extracted from the agarose gels with the NucleoSpin® Gel and PCR

Clean-up kit (Macharey-Nagel) according to manufacturers' instructions. Since the method is based on the biotin-streptavidin interaction, the RNA synthesis was performed in the presence of biotinylated UTPs (B-UTPs) in a ratio of B-UTP:UTPs (1:20), in order to get approximately 5 to 6 B-UTPs in the transcript sequence. For RNA preparation, the *in vitro* transcription reaction was performed using the RiboMax T7 Large Scale transcription kit (Promega) according to the manufacturer's recommendations. RNA was purified using the MEGAclear™ Transcription Clean Up kit (Invitrogen), according to manufacturer's instructions. Non-biotinylated transcript sequences and sequences with comparable G/C content and length were required for every mRNA of interest as controls for unspecific binding of RBPs. For preparation of the cytoplasmic extract, cell pellets with packed cell volume (pcv) of at least 700 µL were required. The cells were cultured, collected upon trypsinization and washed twice with cold PBS. For the preparation of the cytoplasmic extract, the cell pellets were resuspended in 3 pcv hypotonic buffer and incubated on ice for 20 min (or longer) in order to swell. Using a glass homogenizer, the cell membranes were disrupted with about 50 strokes. Cells were centrifuged (3300xg, 15 min, 4°C) several times until the supernatant was clear. Protein concentration was determined via the BCA assay (Pierce BCA assay kit, Thermo Scientific) as described in §4.5. The cytoplasmic extract was supplemented with 0.11 volumes of 10x cytoplasmic buffer and RNAasin (Promega), before it was stored in -80°C. For every construct 1.5 mg of protein was used.

On day 1, 50 µL Streptavidin-coated agarose beads (GE Healthcare, Chicago, USA) were used per reaction and 200 µL for pre-clearing of the cytoplasmic extract. The beads were washed twice with LS-washing buffer and incubated with blocking buffer for overnight at 4°C on a turning wheel. On day 2, the beads were washed with HS300-washing buffer. The cytoplasmic extract was pre-cleared with the washed beads in order to minimize unspecific binding to the streptavidin coated agarose beads. For RNA coupling, 250 pmol of biotinylated RNA was added together with HS300-washing buffer per sample. RNA coupling and pre-clearing of the cytoplasmic extract were performed overnight at 4°C on a turning wheel. On day 3, the cytoplasmic extract was centrifuged (1500xg, 3 min, 4°C) and collected. The beads were washed four times with HS400-washing buffer at RT. The supernatant of the pre-cleared cytoplasmic extract was incubated with the RNA-coupled beads overnight at 4°C on a turning wheel. On day 4, the beads were washed seven times with HS400-washing buffer on a turning wheel and the proteins were eluted from the beads with 6 M Urea (AppliChem), 0.01% NP-40 (Roche Applied Sciences, Mannheim, Germany), 1 mM DTT (Promega) by shaking at 900 rpm on a thermomixer (Eppendorf) at RT for 1 h. After centrifugation (1500xg, 1 min, 4°C), the supernatant was transferred and the proteins were precipitated overnight in 5 volumes ice cold acetone at -20°C.

After preparation of the samples according to the universal, solid-phase protein preparation (USP3) method[337], the protein samples were directly analysed by mass spectrometry (MS, Core facility for mass spectrometry, Dr. Matt Fuszard, Martin-Luther-University Halle-Wittenberg, Halle (Saale), Germany).

Alternatively, the samples were centrifuged (13000xg, 30min, RT), washed twice with 80% acetone and finally the protein pellets were dissolved and incubated with 2x Laemmli buffer at 95°C for 5 min. For separation of the co-purified proteins, 4-20% gradient SDS-PAGE gels (4-20% Mini- PROTEAN® TGX™ precast protein gel,

SERVA, Heidelberg, Germany) were used and run slowly at 50V in order to improve the resolution of proteins with low molecular weight.

4.13 Colloidal Coomassie staining

The SDS-PAGE gradient gels were then washed twice with deionized water and incubated overnight in a Colloidal Coomassie staining solution (according to Neuhoff and co-authors) on a gentle, orbital gel shaker (Blue Shake 3D, SERVA, Heidelberg, Germany). After staining, the gels were repeatedly washed with deionized water to reduce the background staining and until the bands were clearly visible.

4.14 Protein band picking and sample preparation for mass spectrometry analysis

As recently described in detail[335,338], protein bands of interest were excised semi-manually using a spot picker unit (GelPal spot picker, Genetix) equipped with a 0.6 mm needle. Briefly, the picking procedure consisted of 4 steps: (1) excision of a gel fragment by cutting it out with the needle, (2) placing the gel fragment into a 96-well reaction plate (Intavis) and (3-4) purging the needle twice, prior excising the next gel fragment. Next, the 96-well reaction plate was placed into an automated protein digestion and sample preparation system (DigestPro MSi, Intavis) and further processed as previously described[338]. Protein bands of interest were extracted and identified by MS performed in close collaboration with Dr. Jette Rahn (Institute for Medical Immunology, Martin-Luther-University Halle-Wittenberg, Halle (Saale) Germany).

4.15 Mass spectrometry analysis

Peptide mass fingerprint analyses were performed using a MALDI mass spectrometer (ultrafleXtreme™, Bruker) run in positive reflector mode with an accelerating voltage of 25 kV as previously described in detail[335,338]. Prior each measurement the instrument was externally calibrated and the resulting peptide mass fingerprint datasets were subjected to be fed into the MASCOT search engine (Matrix Science). The spot picking and mass spectrometric analyses were performed in close collaboration with Dr. Jette Rahn (Institute for Medical Immunology, Martin-Luther-University Halle-Wittenberg, Halle (Saale) Germany).

Alternatively, ESI MS analysis was performed by Dr. Matt Fuszard (Mass Spectrometry Core Facility, Martin-Luther-University Halle-Wittenberg, Halle (Saale), Germany). After identification of differentially expressed proteins, the panel of candidate RBPs were validated by downstream assays, such as qPCR, Western blot and flow cytometry analyses.

4.16 Immunohistochemical staining of the paraffin-embedded tissue sections of melanoma patients

Formalin-fixed paraffin-embedded (FFPE) tumour samples were processed and analysed at collaborating institutions in Zurich (Dr. Reinhard Dummer, Institute of Dermatology, University Hospital Zürich, Zürich, Switzerland) and Salzburg (Professor Dr. Peter Koelblinger, Department of Dermatology and Allergology, University Hospital Salzburg, Salzburg, Austria). The studies were performed according to the declaration of Helsinki and approved by the ethical committees of the University Hospital in Zurich (KEK-ZH-No. 647 and 800) as well as of the University Hospital in Salzburg (E-No.

2142). As previously described[339], 4 µm thickness sections were cut from each FFPE tissue block. After deparaffinization in xylene and rehydration in decreasing concentrations of ethanol, tumour sections were boiled for epitope retrieval in pre-heated buffers in a pressure cooker for 40 minutes. Thereafter, sections were cooled for 20 minutes and rinsed with deionized water. If necessary, endogenous peroxidases were blocked with 3% H_2O_2 solution for 10 minutes. Further staining steps were performed using the Dako Autostainer Plus platform (Agilent Technologies Inc., Santa Clara, USA) and have been described elsewhere in detail[339].

Immunohistochemical stainings were evaluated by three independent dermatopathologists. A consensus-based score was derived for every single evaluation. Cell count was estimated by averaging at least ten high powered fields (HPF, 400x magnification) representative of the entire tumour. Expression of TAP1 on tumour cells was graded into four categories (0%, 1-10%, 11-30%, >30%). Slides were scored upon counting positive cells in 3-4 randomly selected high power fields (HPF). For the present study, TAP1high (>30 %) and TAP1low (0-10 %) lesions were processed for RT-qPCR analysis in close collaboration with Diana Handke (Institute for Medical Immunology, Martin-Luther-University Halle-Wittenberg, Halle (Saale) Germany) (Appendix A.10).

4.17 Functional and pathway enrichment analyses

Gene Ontology (GO) analysis was performed using the respective data base (http://www.geneontology.org/) enrichment analysis. Predicted target gene candidates of miRs identified in this study[340] were categorized regarding their functions into biological process (BP), molecular functions (MF), and cellular component (CC) localisation[341]. Particularly for miRs, it provides all GO terms significantly enriched in the predicted target gene candidates of the enriched known as well as novel identified miRs compared to the reference gene background (in this study the MS2 control) as well as the genes corresponding to certain biological functions. The corrected p-value (q-value) of < 0.05 and gene count of ≥ 2 were chosen as a significant threshold[341].

4.18 Survival analysis of clinical data of tumour patients

The transcriptomic profile data from patient samples with various tumours were analysed for the expression of several genes of interest, such as HLA-I molecules, APM components, IGF2BPs as well as a panel of candidate miRs, in correlation with the survival data of the patients (disease-specific overall survival, metastasis-free or progression free survival). For this purpose, the databases "Xena" (https://xenabrowser.net/) and starbase v2.0[342,343] (http://starbase.sysu.edu.cn/) and "R2: microarray analysis and visualization platform" (http://r2.amc.nl) with available TCGA data were used. For the recorded Kaplan-Meier curves, the median cut-off modus of the gene expression was also possible to be correlated with specific molecular, histological and other characteristics of the patients, such as the gender, status (dead or alive) and tumour stages.

In silico analysis was performed using these web tools in order to predict the association of the expression of miRs, RBPs, APM components and HLA-I molecules with the survival of primary and metastatic melanoma patients. The statistical differences in the gene expression values between the patients' groups with 'high' and 'low' mRNA expression levels were evaluated by ANOVA tests implemented in the R2 web tool. The p-values were corrected for multiple testing according to the false

discovery rate (FDR). All cut-off expression levels and their resulting groups were correlated with the patients' survival and used for the generation of the Kaplan-Meier curves, which allowed to classify patients into 'good' and 'bad' prognosis cohorts. Kaplan Meier analysis was performed to estimate the overall survival, the disease specific survival probability, the progression free interval and the distant metastasis free survival probability according to mRNA expression status.

For this reason, the following datasets were chosen:

1. "R2: Tumor Melanoma – Jöhnsson – 214 – custom – ilmnht12v4"[344] dataset, where 214 unique metastatic melanoma patients were included for the analysis. Total RNA was extracted from fresh-frozen melanoma tumours and genome-wide expression profiling was performed using Illlumina Human HT-12V4.0 BeadChip arrays by standard methods and after removal of replicate samples, 214 unique melanoma samples were analysed.

2. "Tumor skin cutaneous melanoma (SKCM) - TCGA – 470" dataset[345-350], where 475 melanoma patients (103 primary and 353 metastatic) were included for the analysis.

3. "Tumor SKCM - TCGA – 375" dataset[351], where 375 melanoma patients (65 primary and 266 metastatic) were included for the analysis.

For determination of the high and low expression of the candidate genes, the cut-off modus "median" divided the patients into two groups containing the same number of patients. The raw p-value significance was calculated for every graph with the respective web database. Correlation of pre-miR expression with the candidate genes was determined with the "R2: Tumor Melanoma – Jöhnsson – 214 – custom – ilmnht12v4" dataset[344]. Pearson's correlation was calculated with the transform 2log setting. The 2log expression ratio was compared and a linear regression was calculated. The gene expression pattern of the candidate molecules was compared with each other and correlated to the clinical parameters. A p-value<0.05 was considered as significant.

4.19 Statistical analysis

Unless it's stated otherwise all the experiments were repeated at least three times with independent biological replicates. The results were presented as mean values with associated standard deviation or standard error of at least three independent experiments (biological replicates). For experiments in 96-well plates, such as the dual luciferase reporter assays, the mean and standard deviation were calculated using three technical replicates of at least three biological replicates. The data were analysed and visualized using Microsoft Excel 2010, Microsoft Power Point 2010 and Microsoft Word 2010 (Microsoft Corporation, Redmond, WA, USA), ImageJ (NIH, Bethesda, Maryland, USA) and GraphPad Prism 8.0.1 (GraphPad Software, LLC, San Diego, USA). For the statistical evaluation, the data were subjected to a two-tailed t-test. Furthermore, the differences between the individual experiments were calculated for their statistical significance. The p-values of $p<0.05$ (*), $p<0.01$ (**), $p<0.001$ (***) or $p<0.0001$ (****) were considered as statistically significant, using the paired or un-paired t-test unless otherwise stated.

5. Results

5.1 Heterogeneous expression of HLA-I APM components in melanoma cell lines

A large panel of melanoma cell lines (n = 42) has been previously analysed for the mRNA and/or protein expression of TAP1, TAP2, TPN, β_2-m and HLA-I HC and/or HLA-I surface expression. An APM score was calculated by adding the expression levels of the 5 APM components upon normalization to their expression levels in melanocytes. The melanoma cell lines were also categorized into three groups: high, intermediate and low expressors based on their APM score or on their HLA-I surface expression in comparison to melanocytes (Fig. 5.1 and 5.2). The range of the intermediate group was computed by adding and subtracting 1.96*standard error to/from the mean value. The value of 1.96 is based on the fact that 95% of the area of a normal (Gaussian) distribution is within 1.96 standard deviations of the mean (95% confidence interval).

At the mRNA level (Fig. 5.1A), a lower, intermediate and higher APM score was detected in 40.38%, 33.33% and 26.19% of the melanoma cell lines when compared to the melanocytes respectively, while at the protein level (Fig. 5.1B), lower, intermediate and higher APM score relative to melanocytes was found in 38.10%, 21.43% and 40.48% of the melanoma cell lines, respectively.
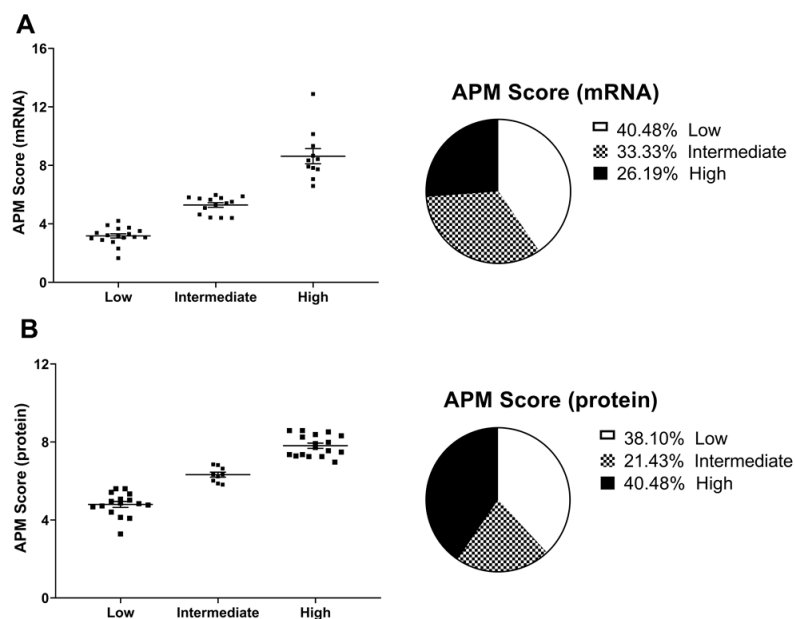
Figure 5.1. Characterization of the expression of APM components in melanoma cell lines
Melanoma cell lines (n=42) have been characterized for the expression of the different HLA-I APM components TAP1, TAP2, TPN, β_2-m and HLA-ABC at the mRNA (A) and protein level (B) by RT-qPCR and Western blot analyses, respectively. An APM score was calculated by adding the expression levels of the 5 APM components upon normalization to melanocytes.

When compared to melanocytes, lower, intermediate and higher HLA-I surface expression was found in 45.24%, 26.19% and 28.57% of melanoma cell lines, respectively (Fig. 5.2). This was accompanied by heterogeneous, but often statistically significant reduced mRNA and/or protein expression levels of APM components and of HLA-I HC in melanoma cell lines.
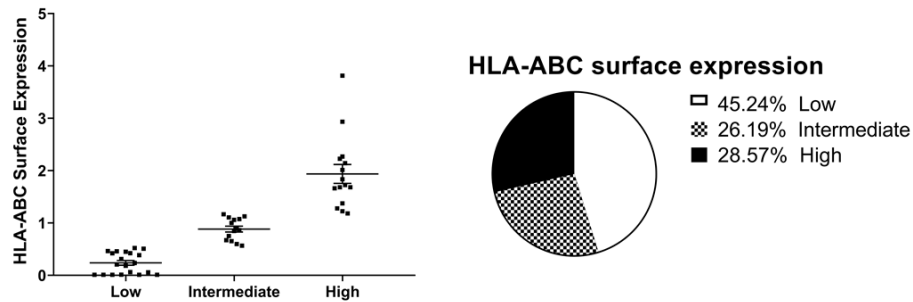
Figure 5.2. Characterization of the HLA-ABC surface expression in melanoma cell lines
Melanoma cell lines (n=42) have been characterized for the surface expression of HLA-ABC by flow cytometry. Shown are the values for each individual cell line *(left)* as well as a pie chart providing the percentage of high, intermediate and low expressors *(right)*.

The melanoma cell lines with mutated HLA-I APM components, such as BUF1195, BUF1280[313,352], BUF1317, BUF526[352], or with a mutation in the IFN-γ signalling pathway, such as COLO857[313,353], were excluded from analysis. The observed impaired expression levels of APM component in the remaining melanoma cell lines was postulated to be mainly caused by deregulation of these molecules[104,313,353], since their expression rates could be upregulated upon IFN-γ stimulation (Fig. 5.3 and 5.4). IFN-γ treatment for 24h or 48 h increased the expression levels of APM components (Fig. 5.3) and HLA-I molecules at the cell surface in comparison to the untreated melanoma cell lines. Interestingly, the increase of HLA-I surface expression after IFN-γ treatment was quite heterogeneous among the melanoma cell lines and was more prominent after 48h IFN-γ treatment with a 1.3fold higher HLA-I surface expression than after 24h of treatment.

Based on the established HLA-I APM expression profiles, three melanoma cell lines namely BUF1379, FM3 and FM81 representing distinct HLA-I APM phenotypes classified as high, intermediate and low expressors, respectively, were selected for further expression and functional analyses.

A
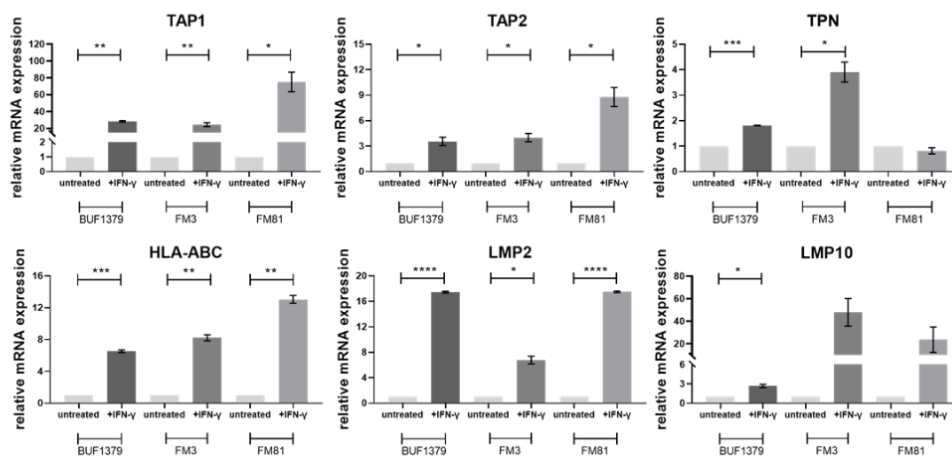
B
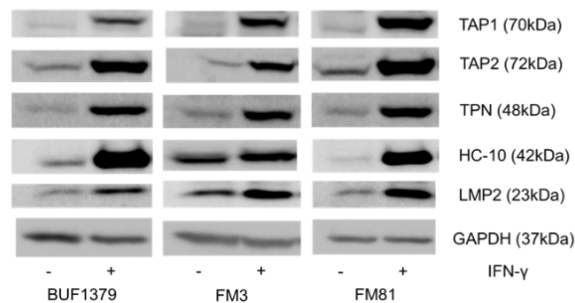
Figure 5.3. Effects of IFN-γ treatment on APM components mRNA and protein expression levels
BUF1379, FM3 and FM81 were left untreated (-) or stimulated (+) with 200 U/mL IFN-γ for 48 h and evaluated (A) by qPCR and (B) by Western blot analyses for the expression of the indicated APM components. Shown are the expression levels upon normalization to the corresponding expression levels of the untreated cells. GAPDH served as loading control. Shown are representative blots out of three biologic replicates.

A

B
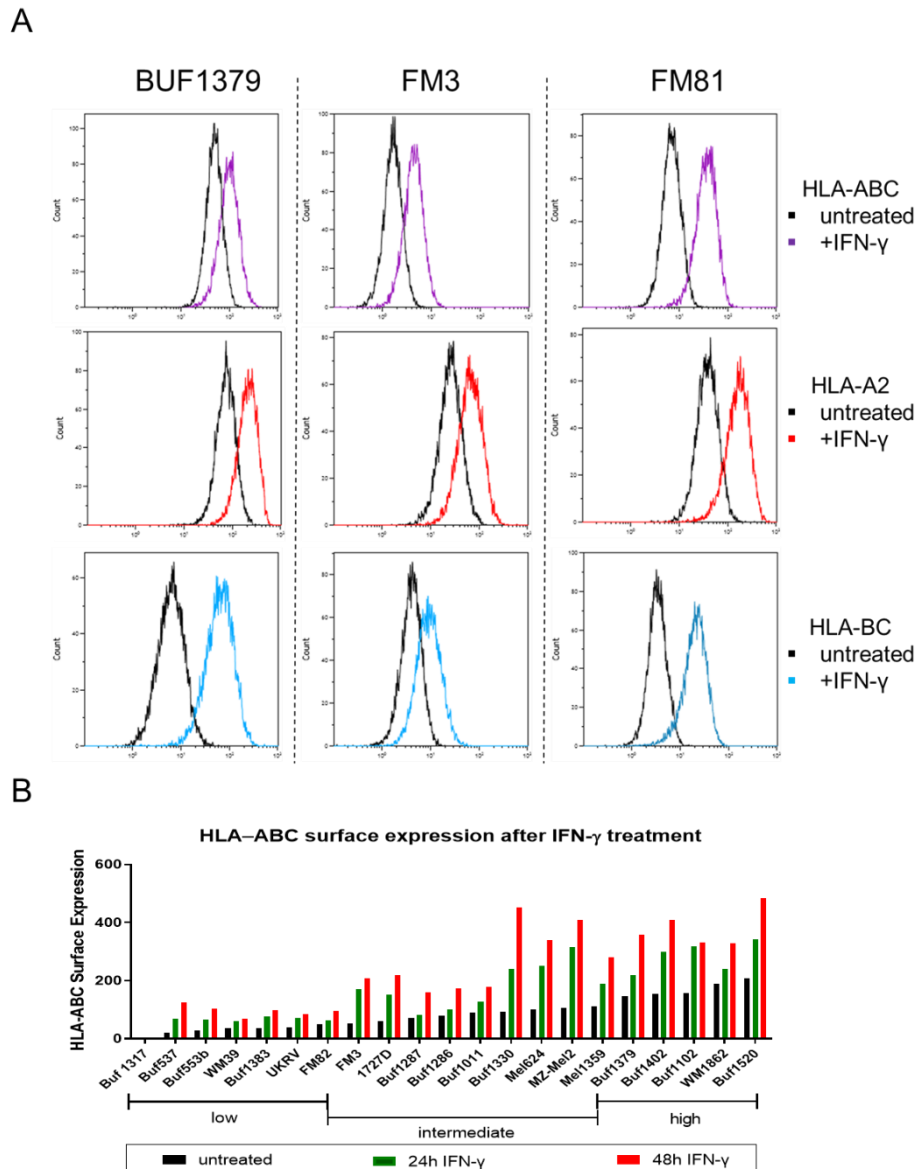
Figure 5.4. Effects of IFN-γ treatment on HLA-I surface expression
(A) BUF1379, FM3 and FM81 either left untreated or stimulated with 200 U/mL IFN-γ for 48 h were also evaluated by flow cytometry for the surface expression of HLA-I molecules by applying the following panel of pan- or allele-specific HLA-I-targeting antibodies, HLA-ABC, HLA-A2 and HLA-BC. Shown are histograms of the untreated (black) and stimulated (coloured) BUF1379, FM3 and FM81 cells. (B) Representative flow cytometry analysis of HLA-ABC surface expression of melanoma cells treated without (black bars)/with IFN-γ for 24 h (green bars) or 48 h (red bars).

For the analysis of the allele specific HLA-I surface expression pattern as well as for the evaluation of the immune response the candidate melanoma cell lines were genotyped for their HLA-I alleles by PCR and flow cytometry analyses. The HLA-ABC phenotype of the selected melanoma cell lines is listed in Table 5.1.

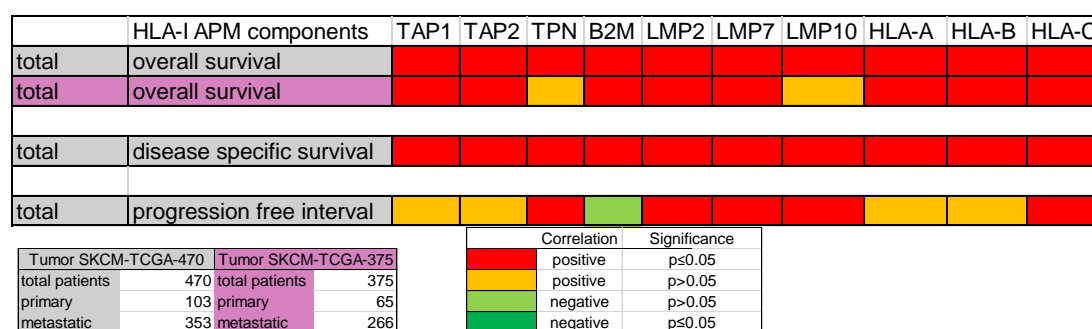**Table 5.1. HLA-ABC phenotype of the selected melanoma cell lines**

Cell line	HLA-A	HLA-B		HLA-C		
BUF1379[354]	02, 03	07, 14	Bw6, Bw6	w7, w8	C1, C1
FM3[312]	02, 02	07, 44	Bw4, Bw6	05, 03	C1, C2
FM81[312]	02, 68	15, 44	Bw6, Bw6	03, 07	C1, C1

5.2 Clinical relevance of APM components and HLA-I molecules with survival of metastatic melanoma patients

Several independent studies reported that the aberrant expression of the HLA-I APM components TAP1, TAP2, TPN and the HLA-I molecules (HLA-A, -B and -C) are directly associated with patients' reduced T-cell response, worse prognosis and reduced survival in several types of cancer, including melanoma. This was *in silico* re-evaluated using the datasets "Tumor SKCM-TCGA-375" with 375 melanoma patients (65 primary and 266 metastatic melanoma patients)[45,355-357] available at the R2 genomics analysis and visualization platform (http://r2.amc.nl) and the "TCGA Skin Cutaneous Melanoma (SKCM)" dataset[358-364] with 470 melanoma patients (103 primary and 353 metastatic melanoma patients) available at the UCSC Xena functional genomics explorer browser (https://xenabrowser.net/) in order to determine the clinical relevance of HLA-I APM components' expression patterns.

A heatmap plot (Fig. 5.5) is depicting the association between the expression of the HLA-I APM components and the survival of melanoma patients. The corresponding Kaplan Meier curves for each HLA-I APM component are available in the Appendix A.4. Particularly, the expression of the HLA-I APM components were directly correlated with the overall survival of melanoma patients.

	HLA-I APM components	TAP1	TAP2	TPN	B2M	LMP2	LMP7	LMP10	HLA-A	HLA-B	HLA-C
total	overall survival	red	red	red	red	red	red	red	red	red	red
total	overall survival	red	red	orange	red	red	red	orange	red	red	red
total	disease specific survival	red	red	red	red	red	red	red	red	red	red
total	progression free interval	orange	orange	red	green	red	red	red	orange	orange	red

Tumor SKCM-TCGA-470		Tumor SKCM-TCGA-375	
total patients	470	total patients	375
primary	103	primary	65
metastatic	353	metastatic	266

	Correlation	Significance
red	positive	p≤0.05
orange	positive	p>0.05
light green	negative	p>0.05
green	negative	p≤0.05

Figure 5.5. Correlation heatmap between the expression pattern of HLA-I APM components and clinical parameters among different groups of melanoma patients
Correlation heatmap between the expression pattern of HLA-I APM components and clinical parameters (overall survival, disease specific survival or progression free interval) as defined across distinct melanoma patient cohorts.

5.3 Identification of immune modulatory miRs by the miTRAP assay in melanoma cell lines

The frequently observed heterogeneous and discordant expression pattern of the various HLA-I APM components suggests a posttranscriptional gene regulation by key players, such as miRs or RBPs. So far, only a few miRs have been described[3,4,365] regulating the expression of TAP1 or TAP2, while none have been published to target TPN. However, several candidate miRs could be identified by screening a variety of online available *in silico* prediction tools, such as miRWalk[366,367], TargetScan[220], miRDB[368], RNA22[369], microrna.org[370] and RNAhybrid[371,372].

In order to identify new candidate immune modulatory miRs (im-miRs) that bind to TAP1, TAP2 or TPN, the miTRAP assay[322,323,373] was performed in cooperation with Dr. Bianca Busch and Prof. Dr. Stefan Hüttelmaier (Institute of Molecular Medicine, Martin-Luther-University Halle-Wittenberg, Halle (Saale), Germany) in the context of the graduate program GRK1591 and combined with small RNA sequencing analysis of the miTRAP eluates.

For this reason, the 3'-UTRs of the three APM components were cloned upstream of the coding sequence of two MS2 stem-loop structures. Yet for TAP2 and TPN, the 3'-UTR had to be splitted into 3 and 2 parts, respectively, due to their size (Table 5.2). Each construct was *in vitro* transcribed and bound to amylose resin beads by using a fusion MS2-maltose binding protein in order to facilitate the specific enrichment of miRs binding to TAP1, TAP2 or TPN 3'-UTR, respectively. As sources for this enrichment strategy served the cell lysates of melanoma cell lines exhibiting high mRNA levels, but low protein levels for the APM component of interest. These included MZ-Mel2 (TAP1 mRNA⁺ and TAP1 protein⁻), Mel1359 (TAP2 mRNA⁺ and TAP2 protein⁻) and MKR (TPN mRNA⁺ and TPN protein⁻) (Table 5.2). A schematic representation of the assay is shown in figure 4.2 (§4.10).

Table 5.2. Summary of the constructs of the APM components' 3'-UTRs analysed with the miTRAP assay

APM components 3'-UTR	Construct(s)	Cell lysate (mRNA+, protein-)
TAP1 (341 bp)	TAP1 3'-UTR (1-341 bp)	MZ-Mel2
TAP2 (3521 bp)	TAP2-1 3'-UTR (22-1094 bp) TAP2-2 3'-UTR (1044-2208 bp) TAP2-3 3'-UTR (2185-3399 bp)	Mel1359
TPN (2037 bp)`	TPN-1 3'-UTR (1-1020 bp) TPN-2 3'-UTR (907-2008 bp)	MKR

Using the melanoma cell lysates and the miTRAP eluates of the *in vitro* transcribed MS2 control RNA and the 3'-UTR of the APM components, the AGO2 protein was detected in the melanoma cell lysates and in the 3'-UTR of the APM components eluates suggesting a putative posttranscriptional regulation of TAP1, TAP2 or TPN expression by miRs[374] (Fig. 5.6). The detection of AGO2 was of particular significance, since it is required for RNA-mediated gene silencing by the RNA-induced silencing complex (RISC)[375].

As expected, no AGO2 signal was detected for the MS2 control or the amylose resin beads loaded with MS2BP-MBP. Additionally, ACTB was employed as a negative control for unspecific binding and MBP served as a positive control for the equal binding of the complex on the amylose beads. The affinity purification of the bait RNA (APM components 3'-UTRs and MS2 controls) was confirmed after detection on a guanidinium thiocyanate denaturing agarose gel.
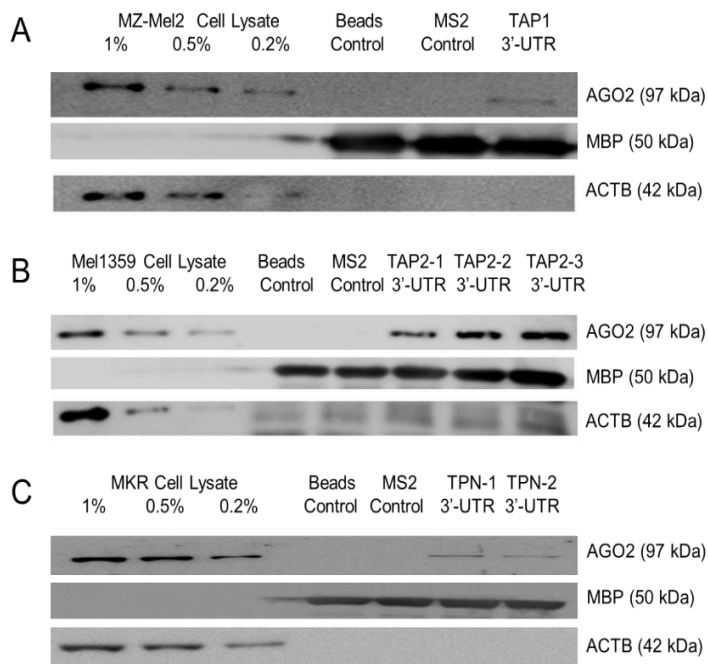
Figure 5.6. Detection of AGO2, MBP and ACTB are shown in the respective miTRAP eluates and input controls
After Western blot analysis of the miTRAP eluates of TAP1 3'-UTR (A), TAP2 3'-UTRs (B) and TPN 3'-UTRs (C) using different melanoma cell lysates, AGO2 was detected in the APM components' 3'-UTRs and input controls, MBP in miTRAP eluates and ACTB in input controls. Different dilutions (1%, 0.5% and 0.2%) of each melanoma cell lysate were used in order to semi-quantify the AGO2 signal in the miTRAP eluates of the APM components of interest.

In order to identify candidate miRs that might specifically target the respective 3'-UTR of the APM components, the miTRAP eluates from two biological replicates and the respective controls were subjected to small RNA sequencing. TAP1 3'-UTR and TAP2 3'-UTR eluates have been sent to Novogene Co., Ltd (Hong Kong, China) and TPN 3'-UTR eluates to Dr. Andreas Dahl (Deep Sequencing Group, TU Dresden, Germany) in order to identify the eluted enriched miRs binding to each construct. The quality control (QC) of the miTRAP eluates sent for small RNA sequencing was compulsory and conducted appropriately by each company, by performing agarose gel electrophoresis as a primary QC and evaluating the sample purity and quantity with Nanodrop (Thermo Fischer), while the determination of the sample integrity was performed with Agilent 2000.

Upon bioinformatics analysis of the small RNA sequencing data, more than 12×10^6 reads were achieved for each construct (Appendix A.6). The small RNA reads were mapped to the genome by bowtie1[331] to analyse their expression and distribution on the genome against human rRNA and tRNA databases. Furthermore, the length distribution analysis was also conducted regarding information on the composition of the small RNA samples, since miRs are usually 21nt - 23nt, siRNAs 24nt and piRNA between 28nt and 30nt long. MiRs were detected and quantified with mirdeep* [376] from mirBase (v21) [377] and represented as counts per miR loci taking into account that a miR can be encoded by multiple loci. For analysis at the miR level, the tpm counts were used representing a normalized transcript expression level[323,339]. Figure 5.7 shows the length distribution histograms of the miTRAP eluates for TAP1 constructs and the respective control eluates. The length distribution diagrams for the other miTRAP eluates are provided in Appendix A.5.
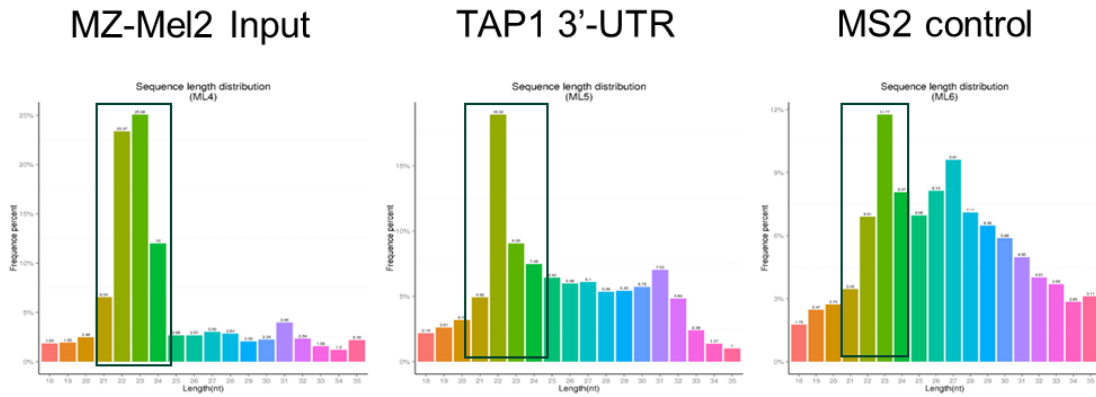
Figure 5.7. The length distribution histograms of the miTRAP eluates for MZ-Mel2 input control, TAP1 3'-UTR and MS2 control

The isolation of the miR fraction was based on size selection and fractions of other RNA species, such as rRNA and tRNA, were excluded. A major peak of 21-23nt was found at the sequence length distribution.

Selective binding of miRs to the target 3'-UTRs was determined relative to MS2 control by calculating the ratio of the respective tpm counts indicating enrichment of the candidate miR as previously described[323,333]. In total, 352 of 2693 (13.07%) miRs determined by miRBase[377] were enriched in the TAP1 3'-UTR eluate when compared to the MS2 control. After bioinformatics analysis of the sequencing data, the strongly enriched miRs were further validated by *in silico* and qPCR analyses when compared to the *in silico* analysis by available online tools (miRWalk[366,367], TargetScan[220], miRDB[368], RNA22[369], microrna.org[370] and RNAhybrid[371,372]), all of the strongly enriched miRs identified via the miTRAP assays were indeed predicted by at least two of the selected tools (Fig. 5.8, Appendix A.7).

A

B

C
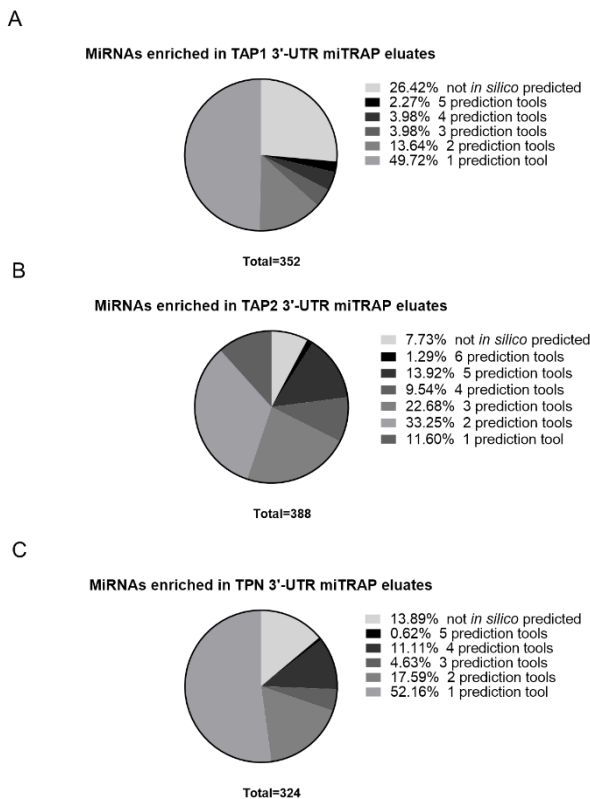
Figure 5.8. Comparison of the percentage of enriched miRs identified targeting TAP1 3'-UTR, TAP2 3'-UTR or TPN 3'-UTR by miTRAP assay with *in silico* predicted miRs
Pie chart depicting the percentage of the enriched miRs identified after miTRAP combined with small RNA sequencing analysis binding to (A) TAP1 3'-UTR, (B) TAP2 3'-UTR or (C) TPN 3'-UTR, which are also *in silico* predicted by indicated number of bioinformatics-based prediction tools.

In order to define the enrichment of miRs, the "miTRAP ratio" was determined by the $2^{-\Delta Cq}$ method reflecting the ratio of miR abundance in the miTRAP eluate versus the input. Dilution factors of the individual fractions were considered. Several candidate miRs were enriched in the miTRAP eluates of each 3'-UTR of APM components in comparison to the MS2 or input controls (Fig. 5.9-5.11).
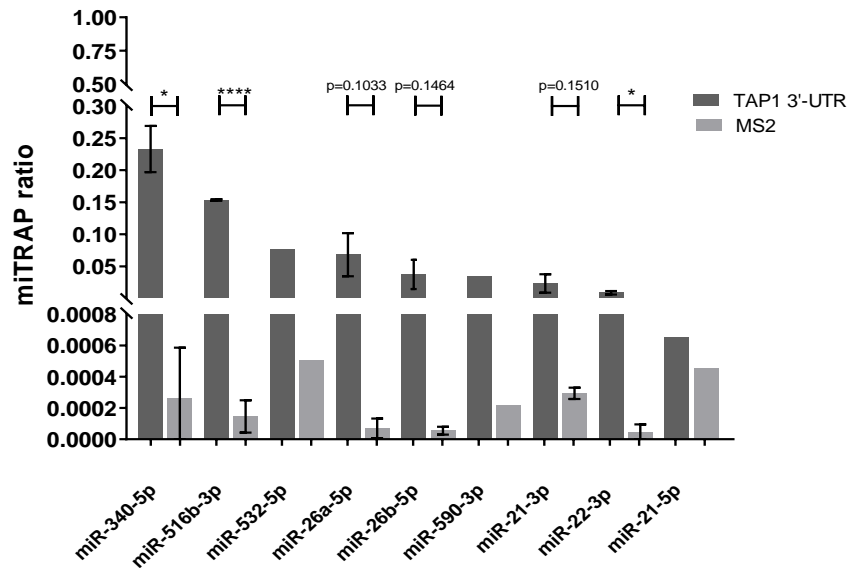
Figure 5.9. Quantification of miRs in miTRAP eluates from MZ-Mel2 cell lysates
Bar graphs showing the miTRAP ratio of several miRs. Given that the input value is 1, the bars show the enrichment of the respective miRs on the MS2 only RNA in comparison to TAP1 3'-UTR RNA. The enrichment of miRs was determined by RT-qPCR and assessed by the "miTRAP ratio" Shown are the normalized mean values ± SE from a minimum of 3 different biological replicates, *p < 0.05, ****p<0.0001 in unpaired t-test.

Concerning the miTRAP eluates targeting TAP1 3'-UTR as a bait, miR-340-5p was strongly enriched, followed by miR-516b-3p, miR-532-5p, miRs of the miR-26 family (miR-26a-5p and miR-26b-5p), miR-590-5p, miR-21-3p and miR-22-3p. Interestingly, miR-346, which is already published to bind to TAP1 3'-UTR[250], was not found enriched in the miTRAP eluates by the small RNA sequencing analysis (Fig. 5.9, Appendix A.7.1). All of the strongly enriched miRs were also predicted by the selected *in silico* prediction tools.
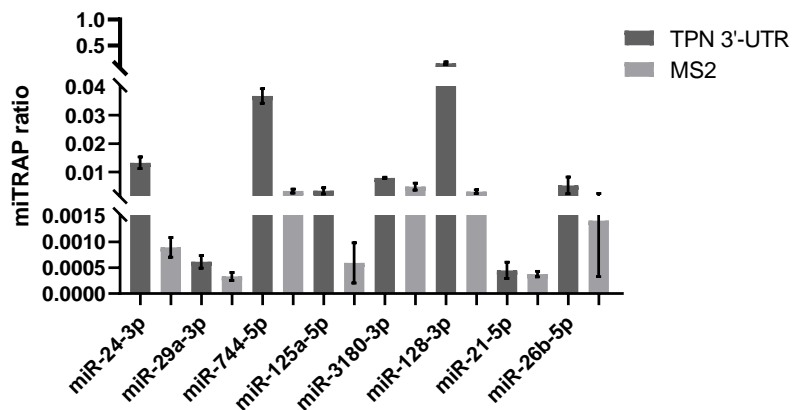
A

B
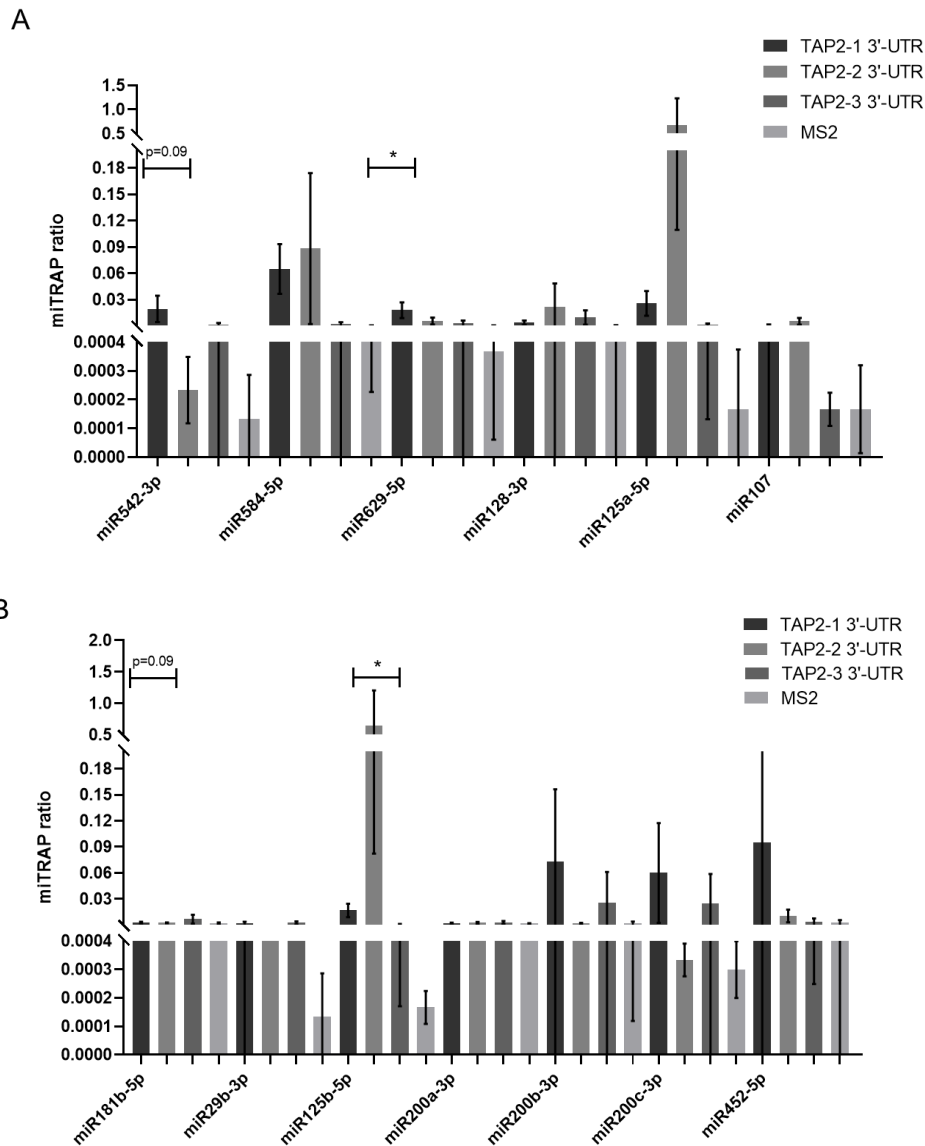
Figure 5.10. Quantification of miRs in miTRAP eluates from Mel1359 cell lysates
(A, B) Bar graphs showing the miTRAP ratio of several miRs. Given that the input value is 1, the bars show the enrichment of the respective miRs on the MS2 only RNA in comparison to the three parts of TAP2 3'-UTR RNA. The enrichment of miRs was determined by RT-qPCR and assessed by the "miTRAP ratio". Shown are the normalized mean values ± SE from a minimum of 3 different biological replicates, *p < 0.05 in unpaired t-test.

Regarding the miTRAP eluates targeting the various TAP2 3'-UTR fragments as baits, several miRs could be either enriched in one, two or all the distinct fragments of the TAP2 3'-UTR. As shown in figure 5.10, miRs of the miR-125 family and two members of the miR-200 family were higher enriched. In particular miR-125a-5p and miR-125b-5p were enriched, followed by miR-452-5p, miR-584-5p, miR-200b-3p, miR-200c-3p and miR-128-3p. MiR-125a-5p is one of the two miRs published to target TAP2 3'-UTR in esophageal adenocarcinoma cells[242] and was found strongly and statistically significantly enriched in the first part of TAP2 3'-UTR (TAP2-1 3'-UTR). Interestingly, miR-1270, the other published miR targeting TAP2 3'-UTR in kidney tissues[264], was not enriched in any of the miTRAP eluates of either the biological replicates sent for small RNA sequencing analysis. All of the strongly enriched miRs were also predicted by the selected *in silico* prediction tools (Fig. 5.10, Appendix A.7.2). The determination

of the candidate miRs targeting TAP2 3'-UTR has been conducted together with the candidate master student Viola Gast.

Figure 5.11. Quantification of miRs in miTRAP eluates from MKR cell lysates
Bar graphs showing the miTRAP ratio of several miRs. Given that the input value is 1, the bars show the enrichment of the respective miRs on the MS2 only RNA in comparison to TAP1 3'-UTR RNA. The enrichment of miRs was determined by RT-qPCR and assessed by the "miTRAP ratio" Although 3 biological replicates are the minimum required for any statistical analysis, shown are the normalized mean values ± SE from 2 biological replicates.

Concerning the miTRAP eluates targeting TPN 3'-UTR as a bait, several miRs were enriched. MiR-128-5p was strongly enriched, followed by miR-744-5p and miR-24-3p. Interestingly, miR-125a-5p was also enriched in miTRAP eluates of TPN 3'-UTRs, but not as strong as in the miTRAP eluates of TAP2 3'-UTRs. All of the strongly enriched miRs were also predicted by the different *in silico* prediction tools (Fig. 5.11, Appendix A.7.3).

Since several miRs were enriched in miTRAP eluates from different APM components, thereby two or more miRs might simultaneously affect the expression of the different APM components. Particularly, miR-26a-5p, miR-26b-5p, miR-22-3p and miR-340-5p were enriched in TAP1 3'-UTR and TPN 3'-UTR miTRAP eluates, while miR-181-5p, miR-128-3p, miR-629-5p, miR-125a-5p and miR-125b-5p in TAP2 3'-UTR and TPN 3'-UTR miTRAP eluates, respectively.

The miTRAP experiments suggest that there might be common regulators, which target the 3'-UTRs of TAP1, TAP2 or TPN and that these candidate miRs might be derived from several miR "families". Therefore, luciferase reporter assays in combination with expression analyses and functional assays for selected miRs were performed.

5.4 Expression of the strongly enriched candidate miRs in melanoma cell lines

Apart from the candidate miRs, enriched in the miTRAP eluates of the TAP1 3'-UTR, two additional candidate miRs were of interest. Based on previous data from our group by analysing RCC patients' samples with microRNA arrays, miR-200a-5p was suggested to target TAP1 3'-UTR. Furthermore, the upregulation of the tumour-suppressive miR-9-5p has already been published to interact indirectly with several HLA-I APM components[249], such as TAP1, β2-m, the proteasome subunits LMP2 and LMP10 as well as classical and non-classical HLA-I molecules such as HLA-B, HLA-C and HLA-F, leading to their upregulation on mRNA level, but the mechanism of

action remains still unclear. Therefore, it was decided to investigate the effects of the overexpression of these two miRs in addition to the enriched candidate miRs targeting the 3'-UTRs of TAP1, TAP2 or TPN in melanoma cell lines.

The expression of several candidate miRs, which were enriched in miTRAP eluates and might target TAP1, TAP2 or TPN 3'-UTRs, was screened in 40 melanoma cell lines and correlated, respectively, with the corresponding TAP1, TAP2 or TPN mRNA expression levels. Some miRs targeting the TAP1 3'-UTR, such as miR-340-5p, miR-26a-5p, and in addition to miR-200a-5p were inversely correlated to TAP1 mRNA expression, whereas miR-9-5p expression levels were correlated with TAP1 mRNA expression (Fig. 5.12).
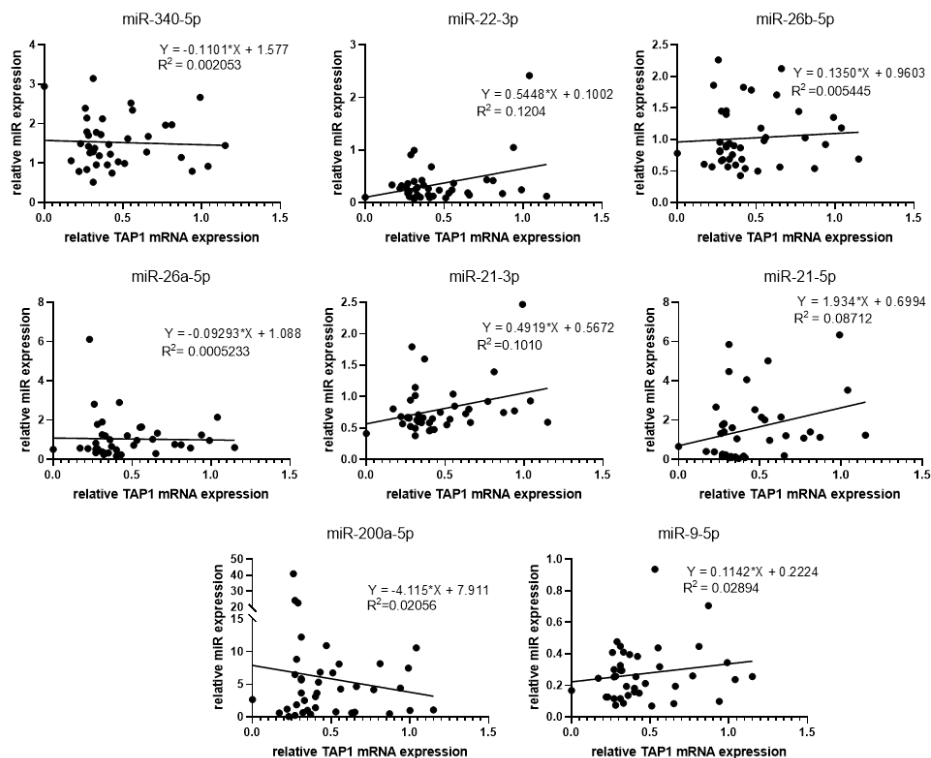
Figure 5.12. Correlation of the expression of enriched miRs in TAP1 3'-UTR miTRAP eluates and the mRNA expression levels of TAP1 in different melanoma cell lines
The different melanoma cell lines were analysed by RT-qPCR for the relative expression of miRs and TAP1. Shown are the expression levels upon normalization to melanocytes as well as the linear regression equation and the R^2 value. Each dot represents a distinct melanoma cell line.

Concerning the miRs targeting TAP2 3'-UTR, miR-200b-3p, miR-200c-3p, miR-452-5p and miR-542-3p showed an inverse correlation with TAP2 mRNA levels in the different melanoma cell lines analysed (Fig. 5.13).
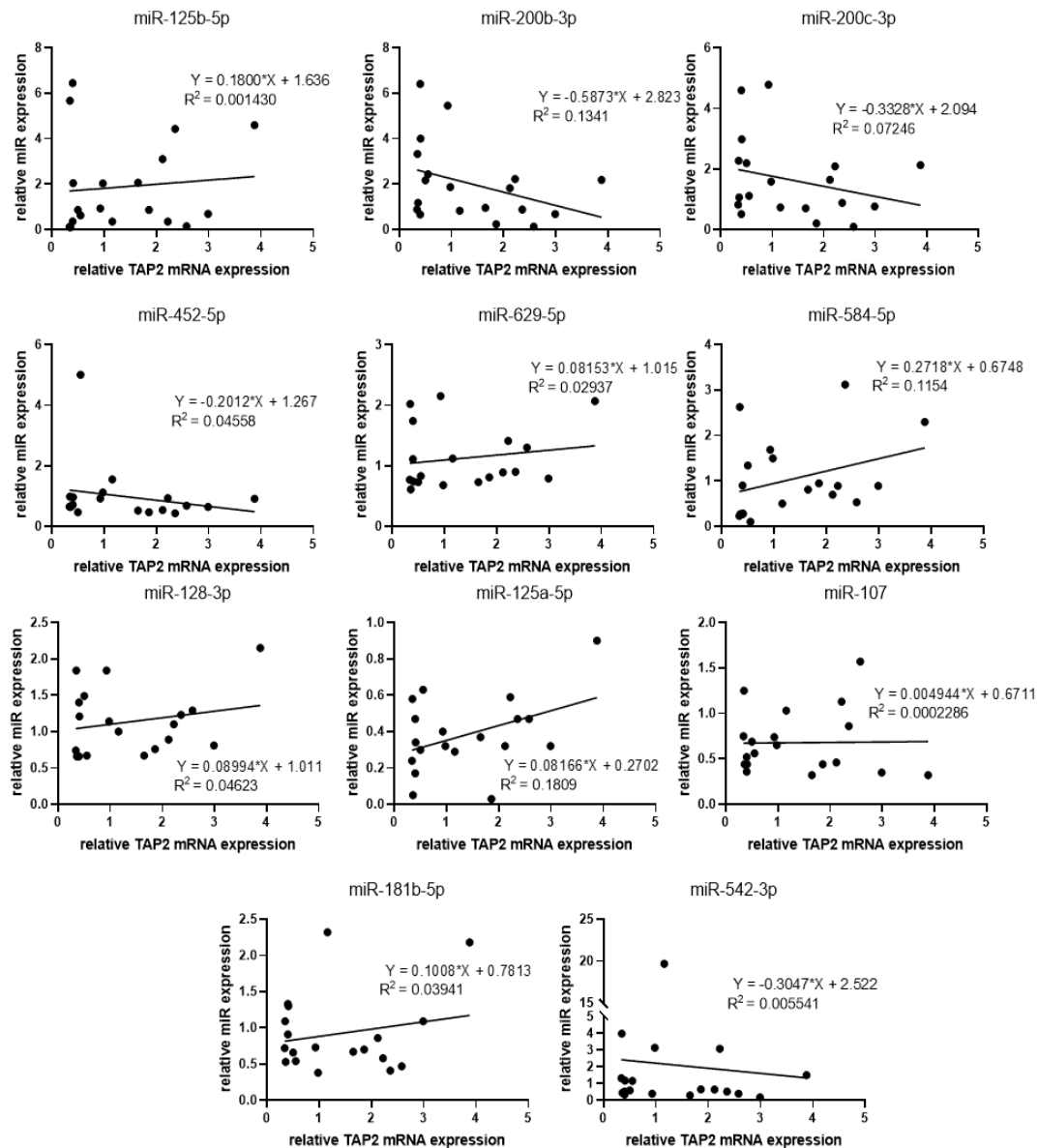
Figure 5.13. Correlation of the expression of enriched miRs in TAP2 3'-UTR miTRAP eluates and the mRNA expression levels of TAP2 in different melanoma cell lines
The different melanoma cell lines were analysed by RT-qPCR for the relative expression of miRs and TAP2. Shown are the expression levels upon normalization to melanocytes as well as the linear regression equation and the R^2 value. Each dot represents a distinct melanoma cell line.

Regarding the miRs targeting TPN 3'-UTR, miR-125a-5p was inversely correlated with TPN mRNA levels among the melanoma cell lines (Fig. 5.14).
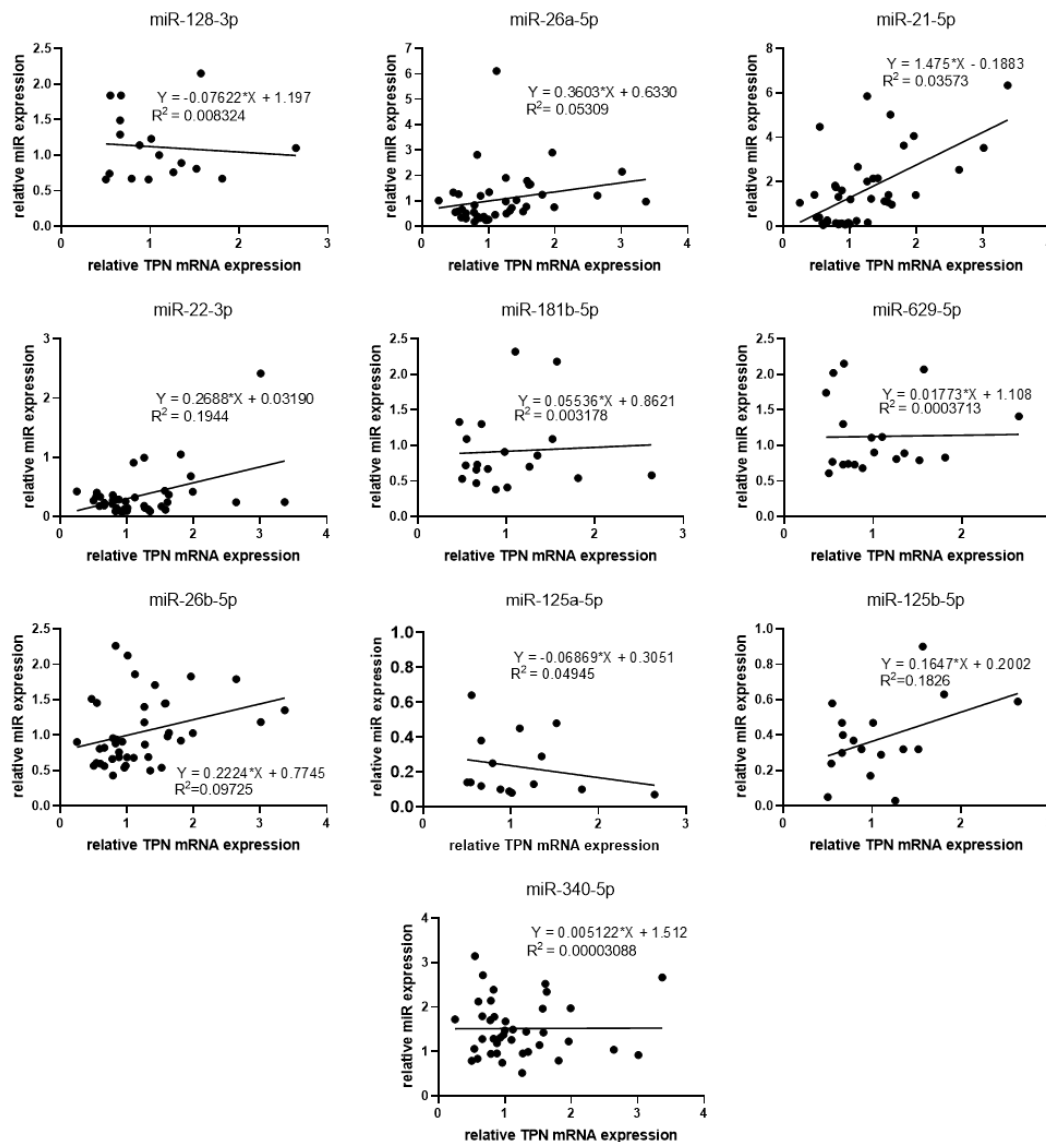
Figure 5.14. Correlation of the expression of enriched miRs in TPN 3'-UTR and the mRNA expression levels of TPN in different melanoma cell lines
The different melanoma cell lines were analysed by RT-qPCR for the relative expression of miRs and TPN. Shown are the expression levels upon normalization to melanocytes as well as the linear regression equation and the R^2 value. Each dot represents a distinct melanoma cell line.

In order to select the candidate miRs, several criteria were applied such as (i) a specific binding site for the respective candidate miRs within the TAP1 3'-UTR should be predicted by at least four out of the six selected bioinformatic tools, (ii) the tpm counts observed in the TAP1 3'-UTR miTRAP eluate should be higher than 1000, while (iii) the tpm counts observed in the MS2 control miTRAP eluate should be less than 100 and (iv) the enrichment ratio should be higher than 50. Additionally, (v) a strong binding affinity of complementary structures between the putative miRs and the target TAP1 3'-UTR calculated as a high free binding energy and (vi) a high "miTRAP ratio", defining

the enrichment of miRs in the miTRAP eluate versus the input and determined by the ΔCq method were taken into consideration[378].

Based on the *in silico* prediction by the selected bioinformatic tools, the small RNA sequencing enrichment, the free binding energy, the "miTRAP ratio", the constitutive abundance in melanoma cell lines assessed by RT-qPCR and the current literature, miR-26b-5p and miR-21-3p as novel candidate miRs targeting the TAP1 3'UTR were selected for further analyses. Therefore, functional assays for miR-26b-5p, miR-21-3p, miR-9-5p and miR-200a-5p were performed.

5.5 Proof of direct interaction of the newly identified regulating miRs with the TAP1 3'-UTR by the dual luciferase reporter assay

From the candidate miRs regulating TAP1 3'-UTR, miR-9-5p, miR-200a-5p, miR-26b-5p and miR-21-3p were of particular interest based on the small RNA sequencing enrichment, the "miTRAP ratio", the constitutive abundance in melanoma cell lines assessed by RT-qPCR, the *in silico* prediction using different bioinformatic tools and current literature. Based on these criteria these miRs were selected for further investigation of their role on the regulation of TAP1, of other APM components and HLA-I surface expression in melanoma cell lines. In addition, miR expression was correlated with TAP1 expression and immune cell infiltration in samples from melanoma patients.

5.5.1 Prediction of the minimum free energy for the candidate miRs and TAP1 3'-UTR by the *in silico* RNAhybrid tool

The RNAhybrid[371,372] tool enables to calculate the binding affinity of complementary structures between the putative miRs and the target mRNA demonstrated as free binding energy (ΔG, kcal/mol). Therefore, for each of the candidate miRs targeting TAP1 3'-UTR, the free binding energy of the respective miR-mRNA interaction was calculated and presented in table 5.3. Lower values of free binding energy can imply stronger binding of the candidate miR to the TAP1 3'-UTR.

Table 5.3. Prediction of the respective calculated minimum free energy (mfe) for each miR and TAP1 3'-UTR by the *in silico* RNAhybrid tool

miR	miR-200a-5p	miR-26b-5p	miR-21-3p
mfe (kcal/mol)	-26.3	-25.4	-20.3

5.5.2 Functional validation of candidate miRs via dual luciferase reporter assays

The direct interaction between miR-200a-5p, miR-26b-5p and miR-21-3p and the TAP1 3'-UTR was validated by the dual luc reporter assay. TAP1 3'-UTR was cloned in the pMir-Glo vector downstream of the firefly luc (FFL) using the restriction enzymes SalI and NheI. After the transient transfection of HEK293T cells with the pMir-Glo vector containing the TAP1 3'-UTR in the presence of the miR-200a-5p, miR-26b-5p or miR-21-3p mimics, the luc activity was significantly decreased upon overexpression of the miR by 25-40% in comparison to the miR mimic negative control (NC) (Fig. 5.15). As expected, the deletion of the predicted binding site for each of the candidate miRs did neither alter the luc activity with the miR mimics nor with the NC.
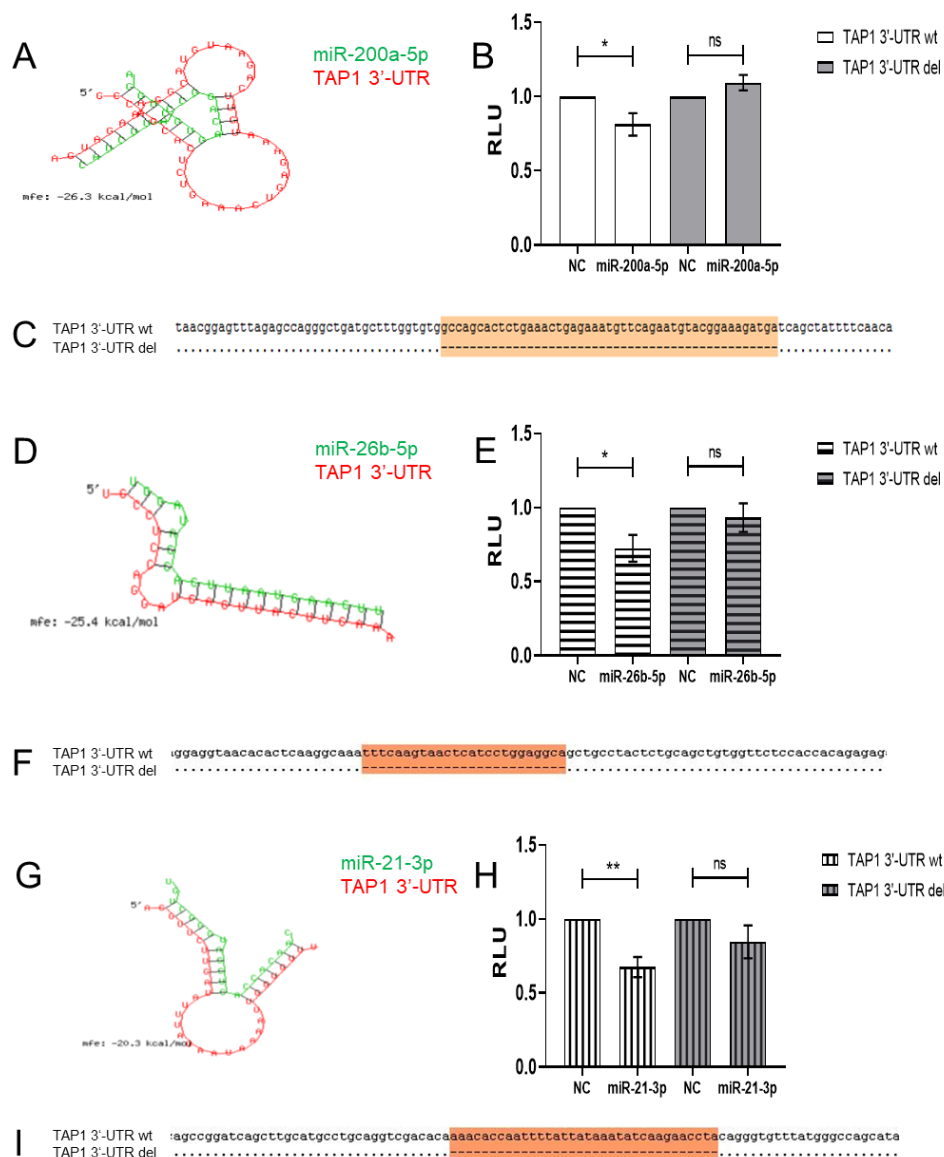
Figure 5.15. Identification of miRs interaction with the TAP1 3'-UTR

(A, D, G) Sequence alignment, secondary structure and minimum free energy (mfe) for predicting the interaction of TAP1 3'-UTR (NM_000593.5, red) and the selected miRs (green) were obtained using the free online data base RNAhybrid. (B, E, H) The dual luc reporter assay was performed with HEK293T cells as described in Materials and Methods. Briefly, HEK293T cells were transiently transfected with the miR-200a-5p, miR-26b-5p, miR-21-3p or miR mimic negative control (NC) together with the plasmid encoding for the Firefly luciferase (FFL) cloned downstream the TAP1 3'-UTR in its wild type form (TAP1 3'-UTR wt) or upon deletion of the predicted binding site for each of the candidate miRs (TAP1 3'-UTR del). FFL activities were internally normalized to Renilla luc activities yielding relative light units (RLU). Shown are the respective mean values ± standard error (SE) from 3 to 6 independent experiments upon their normalization to the miR mimic NC. * p < 0.05, **p<0.01, ns = not significant in un-paired t-test. (C, F, I) Alignment of the various TAP1 3'-UTR wt fragment sequences with their corresponding TAP1 3'-UTR del variants as confirmed by plasmid sequencing. The dots indicate the identical sequences as shown for the wild type sequence, while the orange boxes highlight the deletion of the binding site of the selected miRs.

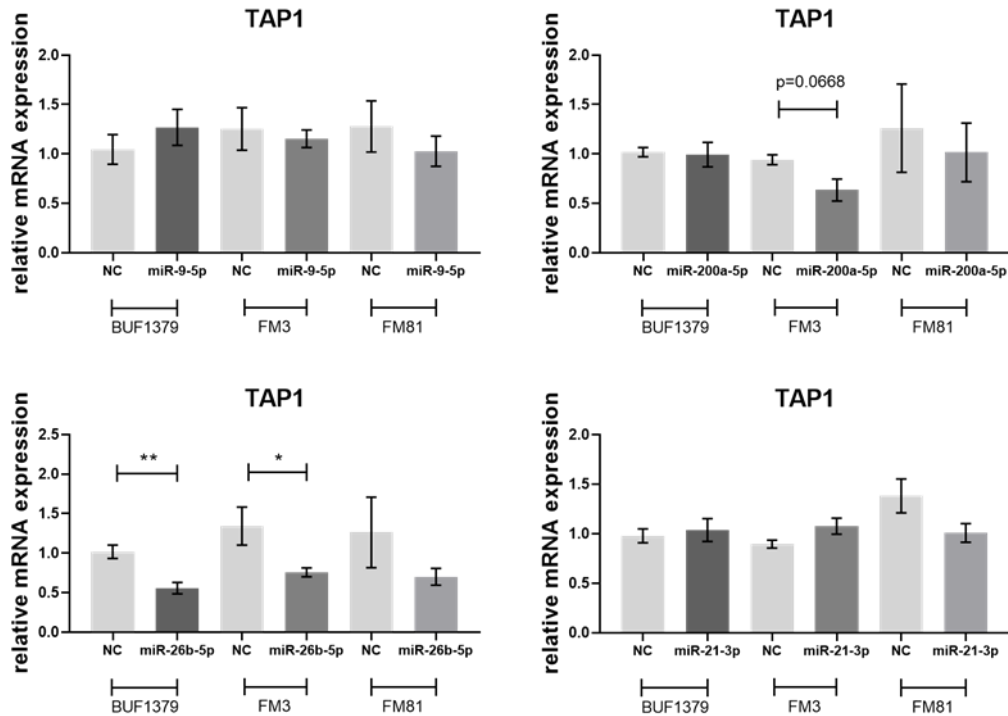## 5.6 Effects of the overexpression of the candidate miRs on HLA-I APM component expression

To further define the effects of selected candidate miRs (miR-9-5p, miR-200a-5p, miR-26b-5p and miR-21-3p), the respective miR mimics or NC with no homology to any known miR or mRNA sequences in mouse, rat or human, were transiently transfected into the three selected melanoma cell lines BUF1379, FM3 and FM81. MiR mimics simulate the natural functions of endogenous miRs and their introduction is able to increase the proportion of the RISC containing that particular miR. All the candidate miRs were endogenously expressed in the selected melanoma cell lines. As shown in figure 5.16, overexpression of the respective miRs was obtained in the selected melanoma cell lines, while cells transfected with the NC showed similar relative expression when compared to parental cells. However, the level of miR overexpression highly varied between the melanoma cell lines analysed. This was in particular the case for miR-21-3p.
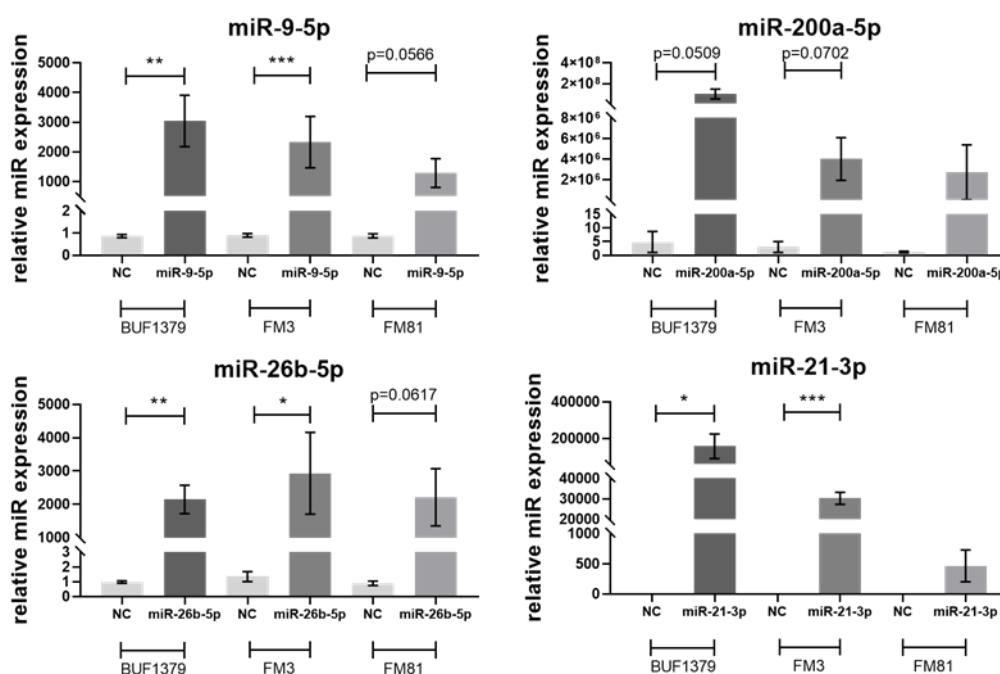
Figure 5.16. Overexpression of the candidate miRs in the three selected melanoma cell lines via miR mimics

BUF1379, FM3 and FM81 melanoma cells were transiently transfected with 30 nM miR mimic negative control (NC) or miR mimic. After 48 h miR overexpression was determined by RT-qPCR. The relative expression levels of the selected miRs were determined by RT-qPCR analysis and they were normalized to the corresponding expression levels of the small ncRNA RNU6 (RNU6A).The cellular levels of the candidate miRs were upregulated, although the fold of the overexpression depended also on the endogenous miR levels in each melanoma cell line. Shown are the normalized mean values ± SE from a minimum of 3 different biological replicates, *p<0.05, **p<0.01, ***p<0.001 in unpaired t-test.

In the next step, the effect of miR overexpression on the expression of TAP1 was determined. Whereas the overexpression of miR-200a-5p and miR-26b-5p in BUF1379 and FM3 cells reduced the targeted TAP1 mRNA levels by more than 30%, the overexpression of miR-9-5p and miR-21-3p had no statistically relevant influence on the corresponding TAP1 mRNA expression levels (Fig. 5.17).

Figure 5.17. Effects of the overexpression of the candidate miRs on the corresponding TAP1 mRNA expression levels

BUF1379, FM3 and FM81 melanoma cells were transiently transfected with 30 nM miR mimic negative control (NC) or miR mimic. After 48 h the mRNA expression levels of TAP1 were determined by RT-qPCR. Particularly, the relative TAP1 mRNA expression was significantly decreased upon overexpression of miR-26b-5p by more than 35% in comparison to the miR mimic negative control (NC) in BUF1379 and FM3 cell lines. Shown are the normalized mean values ± SE from a minimum of 3 different biological replicates, *p<0.05, **p<0.01 in unpaired t-test.

The overexpression of the miRs did not affect the mRNA expression pattern of the other HLA-I APM components, such as TAP2 (Fig. 5.18A), TPN (Fig. 5.18B) and HLA–ABC (Fig. 5.18C), underlining the specific effect of these candidate miRs on the regulation of TAP1 expression levels.
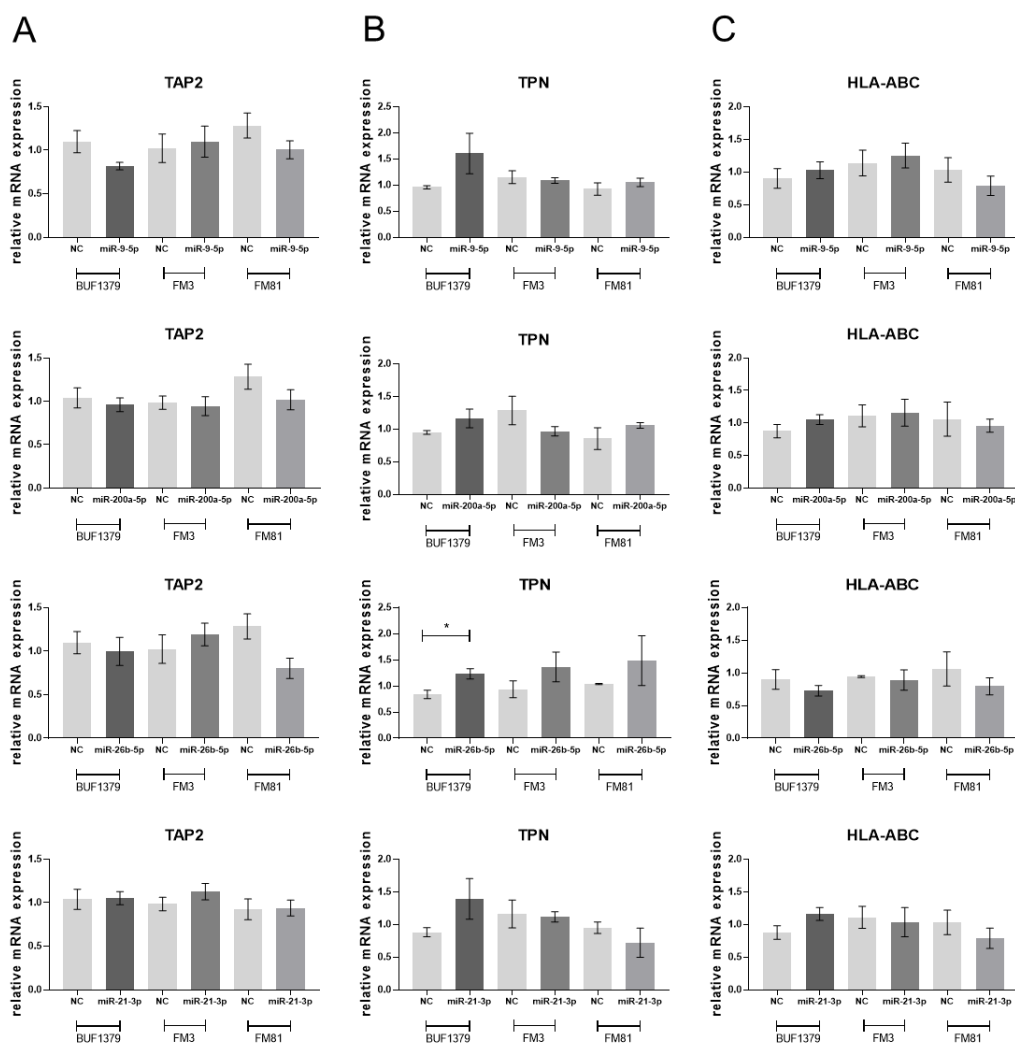
Figure 5.18. Effects of the overexpression of the candidate miRs on the mRNA expression pattern of other HLA-I APM components

BUF1379, FM3 and FM81 melanoma cells were transiently transfected with 30 nM miR mimic negative control (NC) or miR mimic, respectively. After 48 h the mRNA expression levels of TAP2 (A, *left*), TPN (B, *centre*) and HLA-ABC (C, *right*) were determined by RT-qPCR. Shown are the normalized mean values ± SE from a minimum of 3 different biological replicates.

For Western blot analyses, melanoma cells only cultured in the transfection reagent named "control" served as an additional control to the NC. Overexpression of miR-200a-5p in BUF1379 and FM3 cells caused a 40% downregulation of TAP1 protein levels compared to that of the NC or control samples (Fig. 5.19). In contrast, overexpression of miR-9-5p increased the protein levels of TAP1 by 65% in BUF1379 cells (Fig. 5.19). Overexpression of miR-26b-5p in BUF1379 and FM3 cells decreased the TAP1 protein levels by approximately 30% when compared to controls (Fig. 5.19), while miR-21-3p overexpression resulted in 25% decreased TAP1 protein levels in BUF1379 and FM3 transfectants compared to controls samples (Fig. 5.19). The protein expression of other APM components, such as TAP2, TPN and LMP2, was not affected by the overexpression of these miRs.
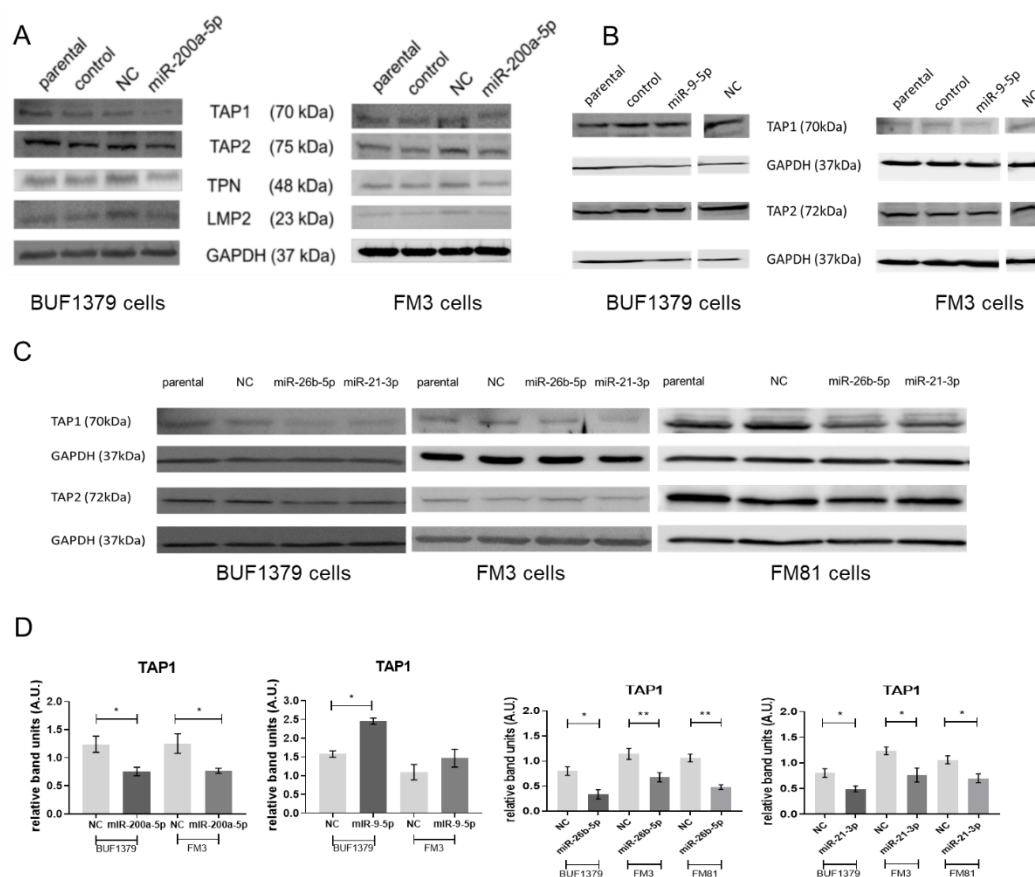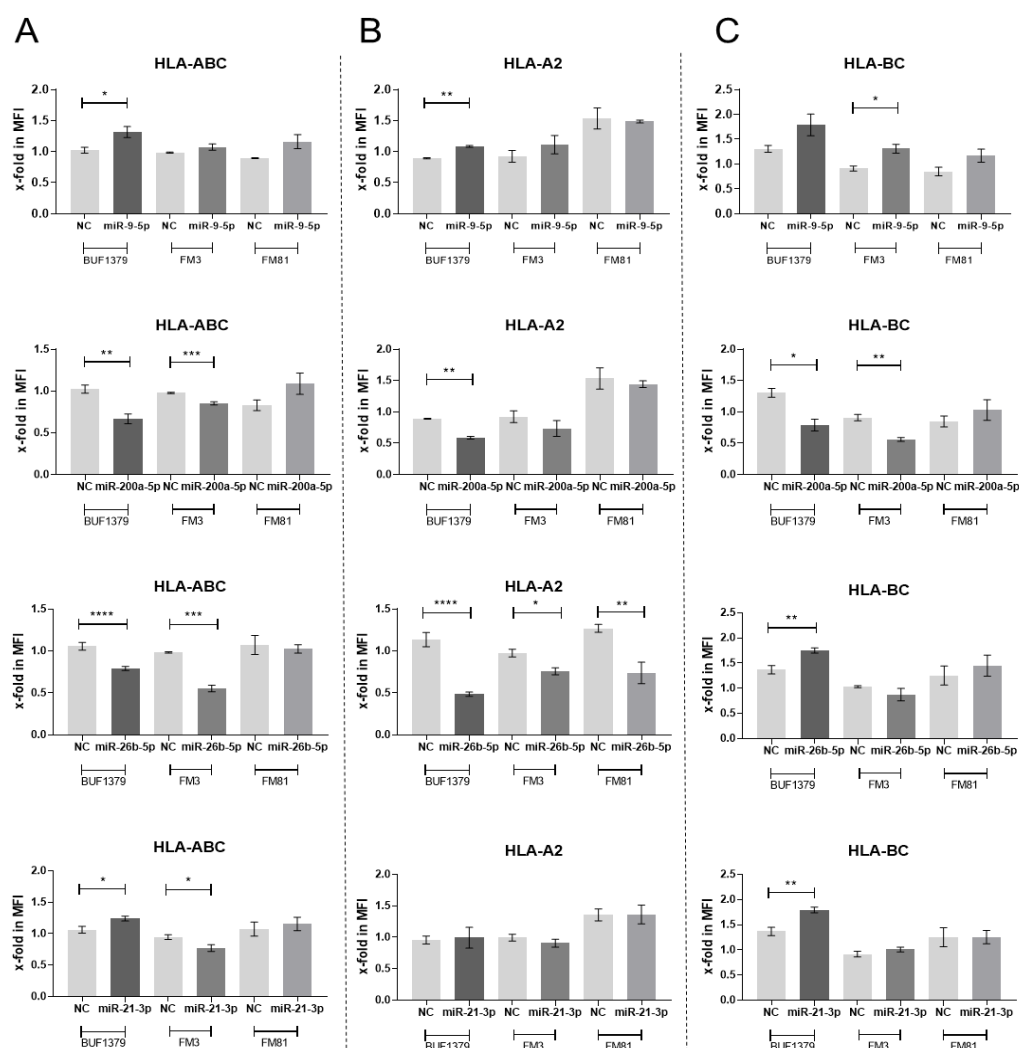
Figure 5.19. Effects of the overexpression of the candidate miRs on the protein expression pattern of APM components and quantification of the effect of the overexpression of the candidate miRs on TAP1 protein expression

The effects on the protein expression pattern of APM components in response to the indicated miR transfection in the model melanoma cell lines was evaluated by Western blot analyses as respectively shown in (A-C). Shown are representative Western blots. The corresponding quantification of the Western blot results is shown in (D), where the relative band intensity (A.U., arbitrary units) of transfectants was calculated in comparison to the respective parental melanoma cells and normalized to the respective GAPDH signals. Shown are the normalized mean values ± SE from a minimum of 3 different biological replicates, $^*p < 0.05$, $^{**}p < 0.01$ in un-paired t-test.

The downregulation of TAP1 was accompanied by a decrease of HLA-I surface expression particularly of HLA-ABC and HLA-BC by 30-50% in the miR-200a-5p transfectants and of HLA-ABC and HLA-A2 by 20-25% and 35-50%, respectively, in the miR-26b-5p transfectants (Fig. 5.20). In the miR-9-5p transfectants, HLA-ABC surface expression was indirectly increased by more than 20% in BUF1379 cells (Fig. 5.20) and in the miR-21-3p transfectants HLA-ABC and HLA-BC surface expression were increased by 20% in the same cell line, probably due to an indirect mechanism. HLA-BC surface expression was also increased by 20% in miR-26b-5p transfected BUF1379 cells. The surface expression levels of control transfectants (NC) were comparable to that of parental samples.

Figure 5.20. Effects of the overexpression of the candidate miRs on HLA-I surface expression pattern

The HLA-I surface expression levels were evaluated by flow cytometry using different HLA-I specific antibodies (A: HLA-ABC, B: HLA-A2 and C: HLA-BC). Shown are the normalized mean values ± SE from a minimum of 3 different biological replicates, *p < 0.05, **p < 0.01, ***p < 0.001, ****p<0.0001 in un-paired t-test.

5.7 Correlation between the miR-mediated downregulation of TAP1 protein expression and its effect on the recognition by NK or T-cells

Since the overexpression of miR-200a-5p, miR-26b-5p and miR-21-3p resulted in suppression of TAP1 mRNA and/or protein expression and deregulation of HLA-I surface expression, their effect was evaluated on the recognition of the melanoma transfectants by NK or T-cells.

5.7.1 Effect of the miR-200a-5p-mediated downregulation of TAP1 protein expression on the recognition by NK cells

To evaluate the functional relevance of miR-200a-5p- and miR-21-3p-induced suppression of TAP1 and consequently of HLA-I surface expression, NK cell-mediated recognition was determined performing the CD107a degranulation assays[320,379]. Due to the previously described comparable effects observed in the model cell lines

BUF1379 and FM3 in response to transfections with the miR-200a-5p, the NK-cell assays were performed with FM3 cells. Higher levels of CD107a positive NK cells were found in response to FM3 cells overexpressing the miR-200a-5p when compared to the corresponding NC transfectants (Fig. 5.21). This might be due to the miR-200a-5p-mediated silencing of TAP1 expression followed by a reduced HLA-I surface expression. No effect was observed in FM3 cells overexpressing the miR-21-3p in comparison to the corresponding NC transfectants. The NK cell-sensitive erythroleukemic cell line K562 served as positive control in these functional assays.
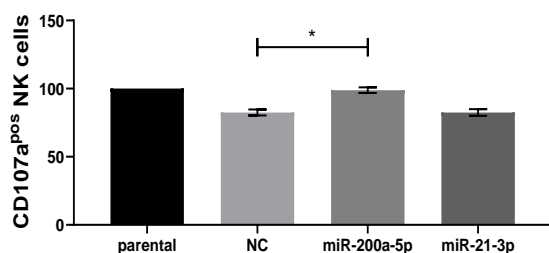
Figure 5.21. Increased recognition of miR-200a-5p overexpressing FM3 melanoma cells by NK cells
NK cells from healthy donors were co-incubated with FM3 cells, either left untreated (parental), transfected with the negative control (NC), miR-200a-5p, miR-21-3p mimics or with K562 cells (PC). After 4 h the percentage of CD107a expressing NK cells was determined by flow cytometry. Shown are the normalized mean values ± SE from 3 independent experiments, *p < 0.05 in paired t-test.

5.7.2 Correlation of the miR26b-5p-mediated downregulation of TAP1 with decreased T-cell recognition

To assess the functional relevance of miR-26b-5p- and miR-21-3p-induced suppression of TAP1 and the reduced HLA-I surface expression, the MART-1^{+} BUF1379 miR transfectants were cocultured with CD8^{+} T-cells specific for the HLA-A2 restricted MelanA/Mart-1 epitope. The miR-26b-5p-mediated downregulation of TAP1 accompanied by reduced HLA-A2 surface antigens decreased T-cell recognition of unpulsed tumour cells. Melanoma cells transfected with the miR-26b-5p, but not with the miR-21-3p mimics had a reduced T-cell recognition(Fig. 5.22A). Upon pulsing with the MART1-peptide, the surface HLA-A2 molecule of the FM3 cells was saturated with exogenous MART-1 peptide and the T-cells recognized the pulsed miR-26b-5p transfectants comparable to the corresponding NC transfectants, implying an aberrant function of the antigen processing components, such as TAP1, and not of the expression of the HLA-A2 molecules (Fig. 5.22B).
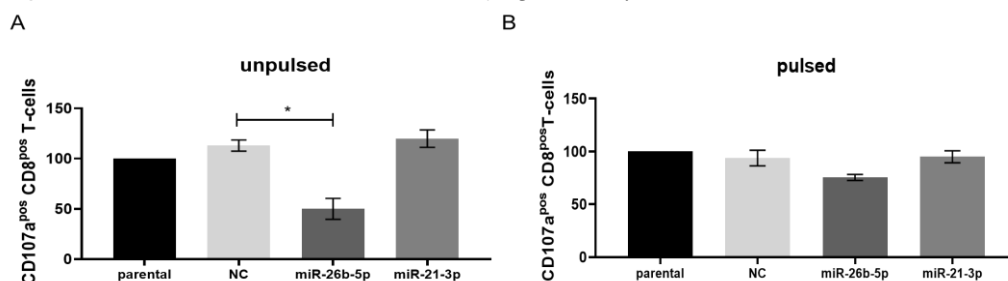

Figure 5.22. Effects of miR mimics on unpulsed and pulsed BUF1379 cells by antigen-specific CD8+ T-cells
MelanA/MART1-specific CD8+ T cells were incubated for 4 hrs with (A) unpulsed or (B) MART1-peptide pulsed BUF1379 cells either transfected with the negative control (NC) or with the indicated miR mimics and subsequently evaluated for degranulation. Shown are the changes in CD107a positive cells from 3 independent experiments, *p < 0.05 in paired t-test.

5.8 Effects of the miR-26b-5p- or miR-21-3p-mediated inhibition on theTAP1 expression and HLA-I surface expression pattern

To evaluate the specific effects of the miR-26b-5p and miR-21-3p in regard to the modulation of TAP1 expression rates, miR inhibitors and a control inhibitor (NC inhibitor) were transiently transfected into BUF1379 and FM3 cells. MiR Inhibitors are chemically modified ssRNAs, which specifically bind and inhibit endogenous miR function after transient transfection into cells. The miR expression levels were significantly reduced in the BUF1379 and FM3 transfectants, while cells transfected with the NC inhibitors showed a comparable relative expression pattern to parental cells, since it is a sequence with no homology to any known mammalian gene (Fig. 5.23A). Thus, miR inhibitors efficiently downregulated the endogenous miR expression in BUF1379 and FM3 cells. Inhibition of miR-26b-5p and miR-21-3p increased by more than 25% TAP1 mRNA levels in FM3 cells (Fig. 5.23B).
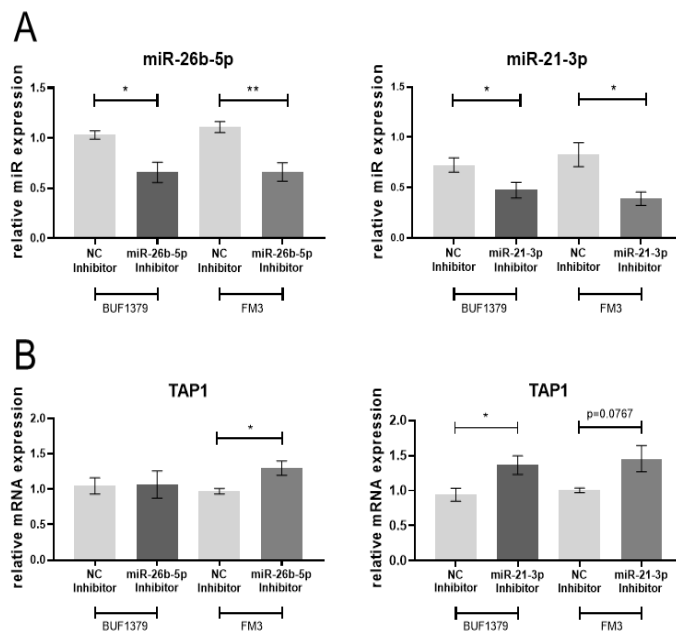
Figure 5.23. Effect of miRs inhibition on miRs and TAP1 mRNA expression in melanoma cell lines
BUF1379 and FM3 melanoma cells were transiently transfected with 100 nM negative control inhibitor (NC Inhibitor) or miR inhibitors (miR-26b-5p Inhibitor (*left*) or miR-21-3p Inhibitor (*right*)). (A) After 48 h the inhibition of miR endogenous expression levels as well as (B) the TAP1 mRNA expression levels were determined by RT-qPCR. Shown are the normalized mean values ± SE from a minimum of 3 different biological replicates and one representative Western blot, *p < 0.05, **p < 0.01 in un-paired t-test.

This increase of TAP1 mRNA levels was accompanied by a comparable increase of TAP1 protein levels (Fig.5.24A and B) and an increased HLA-I surface expression in both melanoma cell lines (Fig. 5.24C). The inhibition of miR-26b-5p or miR-21-3p in BUF1379 and FM3 cells increased HLA-A2 surface antigens (Figure 5.24D), while HLA-BC surface expression remained unchanged (Fig. 5.24E).
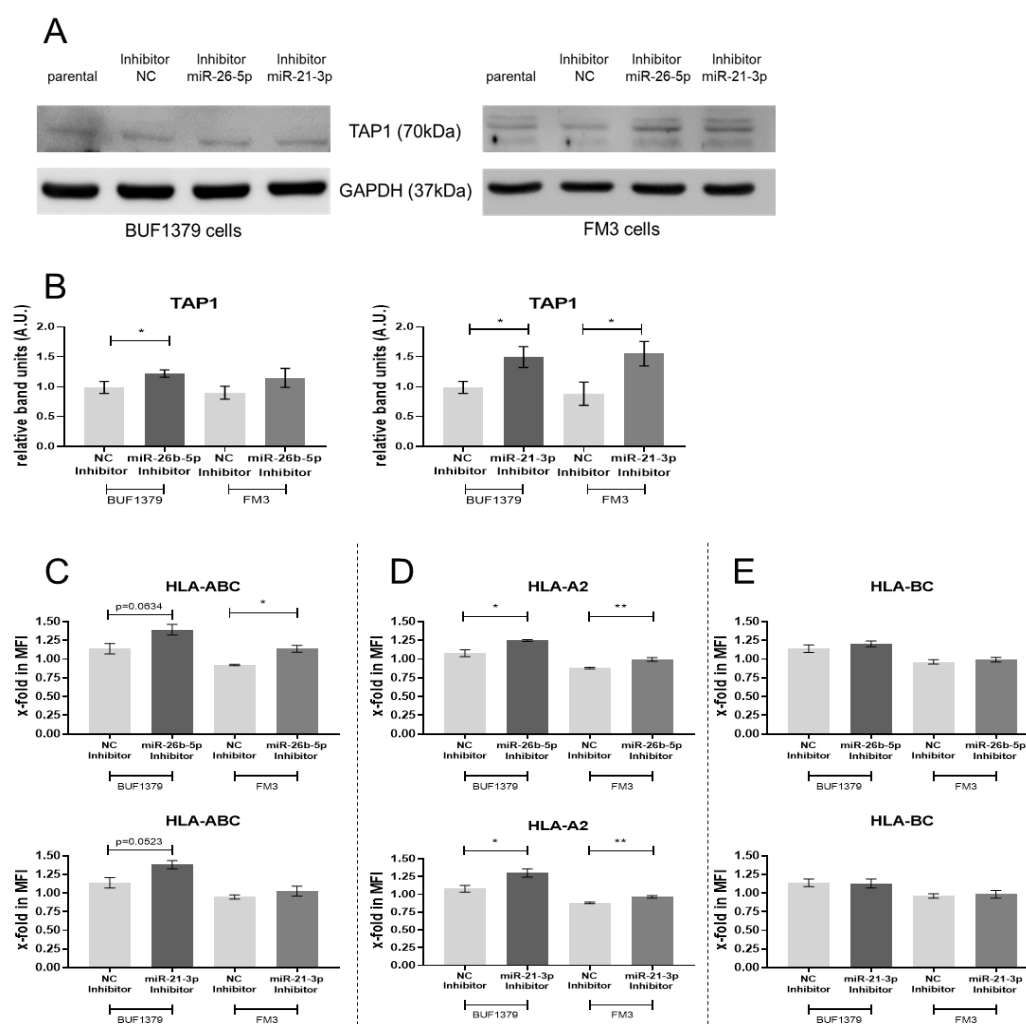
Figure 5.24. Effects of specific miR inhibitors on the TAP1 protein and HLA-I surface expression levels in melanoma cell lines

BUF1379 and FM3 melanoma cells were transiently transfected with 100 nM negative control inhibitor (NC Inhibitor) or specific miR inhibitors (miR-26b-5p Inhibitor or miR-21-3p Inhibitor). After 48 h of the respective transfections the corresponding protein expression levels were evaluated by Western blot analyses (A and B) or flow cytometry (C-E). Shown are representative Western blots. For quantification of Western blot results, the relative band intensity (A.U., arbitrary units) of transfectants was calculated in comparison to the respective parental melanoma cells and normalized to the GAPDH signals. Shown are the normalized mean values ± SE from a minimum of 3 different biological replicates, *$p < 0.05$, **$p < 0.01$ in un-paired t-test).

5.9 Correlations between miRs expression pattern and corresponding TAP1 expression levels as well as immune cell infiltration in primary melanoma tissues

In order to determine the clinical relevance of the expression of TAP1 relevant miRs and the role of TAP1 expression on the tumour microenvironment, TAP1 expression levels were first analysed on melanoma lesions. The TAP1 expression levels on tumour cells were determined by immunohistochemistry and analysed by the pathologists based on a common scoring system categorizing the frequency of TAP1+ tumour cells within the FFPE samples of 0%, 1-10%, 11-30%, >30% graded into the four categories 0, 1, 2 and 3, respectively. For the present study, TAP1^{high} (>30 %, n=16) and TAP1^{low} (0-10 %, n=10) lesions were processed. The same melanoma samples were also analysed regarding their immune cell infiltration, in particular for the

presence of CD8+, CD4+, FOXP3+, CD163+, CD123+, CD68+ and CD11+ immune cells, using immunohistochemistry (IHC). Each of these markers represent a group of immune cells, CD8+ for CTLs, CD4+ for T_H cells, CD11+ and CD68+ for NK, T-cells, monocytes, CD11+ for pDCs and CD163+ for monocytes and macrophages. Although TAP1 expression is primarily relevant for the presentation of antigenic peptides via HLA-I molecules to CD8+ T-cells, the knowledge about the presence of other immune cells contributes to a better understanding of the immune cell infiltration of primary tumours. The TAP1 expression levels were correlated with the frequency of immune cells defined by these markers. The TAP1 expression levels were positively correlated with CD8+ and CD163+ expression levels (Fig. 5.25B and Fig. 5.26B).
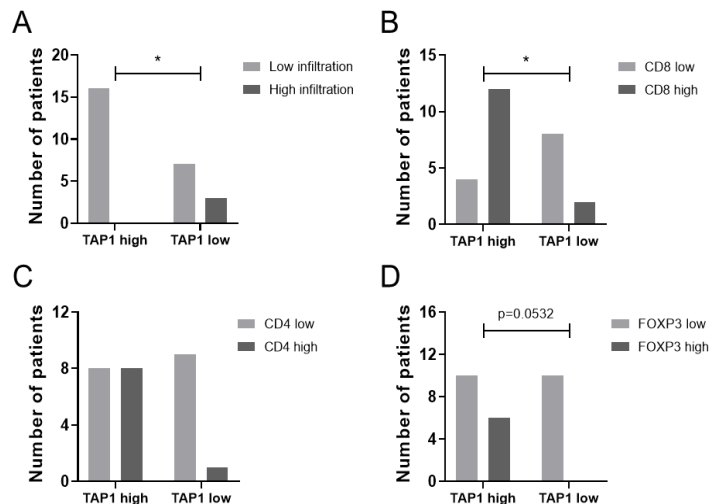
Figure 5.25. Correlation between TAP1 expression levels and immune cell infiltration in primary melanoma tissue sections
The immunological status of the 26 human FFPE melanoma tissue sections was characterised for (A) the total immune cell infiltration rates and the presence of (B) CD8+ cells, (C) CD4+ cells and (D) FOXP3+ cells via immunohistochemistry, *p < 0.05 in Fisher's exact test.
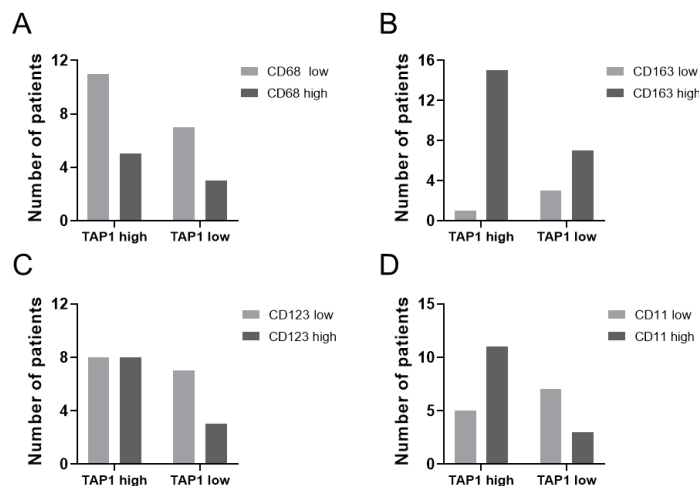
Figure 5.26. Correlation between TAP1 expression levels and immune cell infiltration in primary melanoma tissue sections (continue)
The immunological status of the 26 human FFPE melanoma tissue sections was characterised for the presence of (A) CD68+ cells, (B) CD163+ cells, (C) CD123+ cells and (D) CD11+ cells via immunohistochemistry.

After demonstrating a correlation of TAP1 expression levels with the immune cell infiltration, the expression levels of the candidate miRs miR-200a-5p, miR-26b-5p and miR-21-3p were assessed by RT-qPCR analyses in 26 FFPE tissue sections from human primary melanoma patients scored as TAP1low (n=10) and TAP1high (n=16). MiR-200a-5p expression was statistically significant inversely correlated with the TAP1 score (Fig. 5.27A) thereby supporting the *in vitro* data established in the experimental model cell line systems. In contrast, no obvious correlations were detectable for miR-26b-5p (Fig. 5.27B). However, at least an inverse trend was observed between miR-21-3p and TAP1 score (Fig. 5.27C).
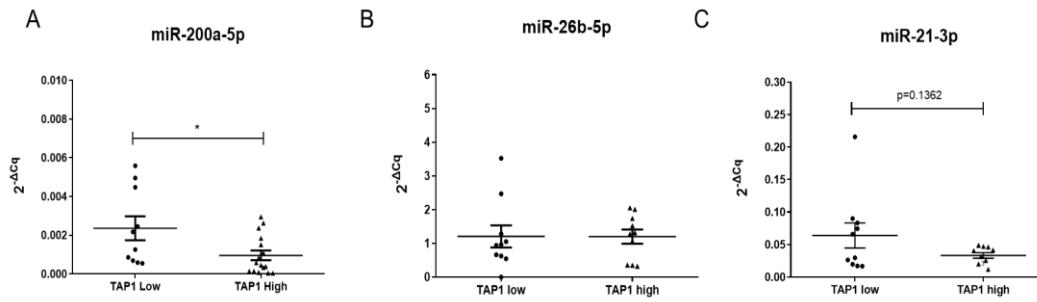
Figure 5.27. Inverse correlations between miR-200a-5p and miR-21-3p expression levels andTAP1 levels in tissue sections as well as the survival probability of melanoma patients
Paraffin-embedded tissue sections from primary melanoma patients were analysed to define the expression levels of the miRs, miR-200a-5p, miR-26b-5p or miR-21-3p by RT-qPCR and in addition scored regarding their TAP1 expression levels as high or low based on immunohistochemical stainings. Correlations between TAP1 high and TAP1 low melanoma lesions and the selected miRs are shown in (A) for miR-200a-5p, in (B) for miR-26b-5p and in (C) for miR-21-3p expression, *p < 0.05 in paired t-test.

By taking into account that the immune cell infiltration of the very same melanoma samples was previously also analysed for the presence of CD8$^+$ T-cells by IHC; it was possible to correlate the respective TAP1 and CD8$^+$ scores with the corresponding miRs expression pattern. As shown in figure 5.28, the TAP1 expression scores were directly correlated with the frequency of CD8$^+$ immune cells with TAP1^{low} / TAP1^{high} melanoma lesions exhibiting low/high frequency of CD8$^+$ T-cells. Furthermore, a direct link exists between the low TAP1 score with CD8$^+$ T-cell infiltration, but high miR-200a-5p, miR-26b-5p and miR-21-3p expression levels and *vice versa*.
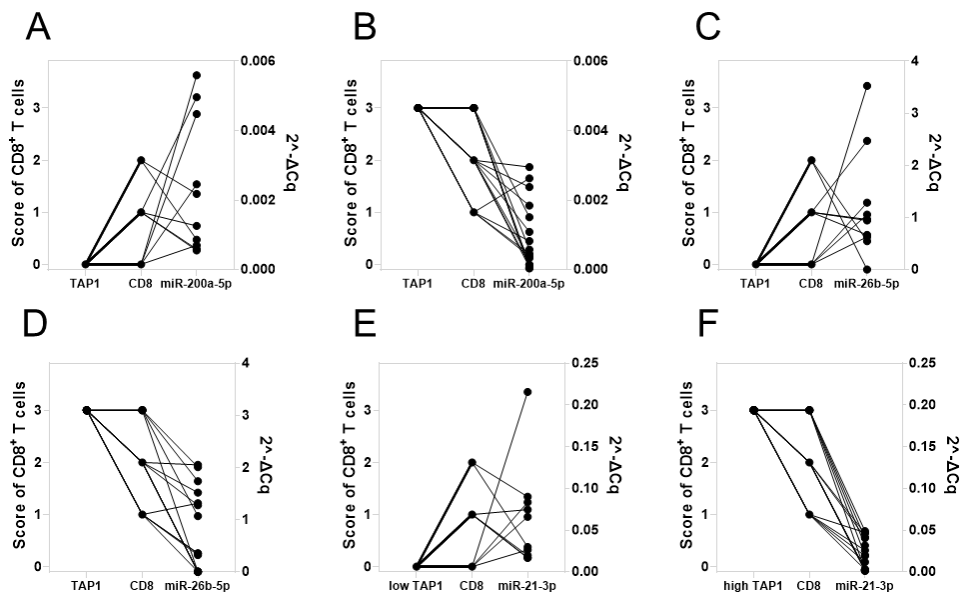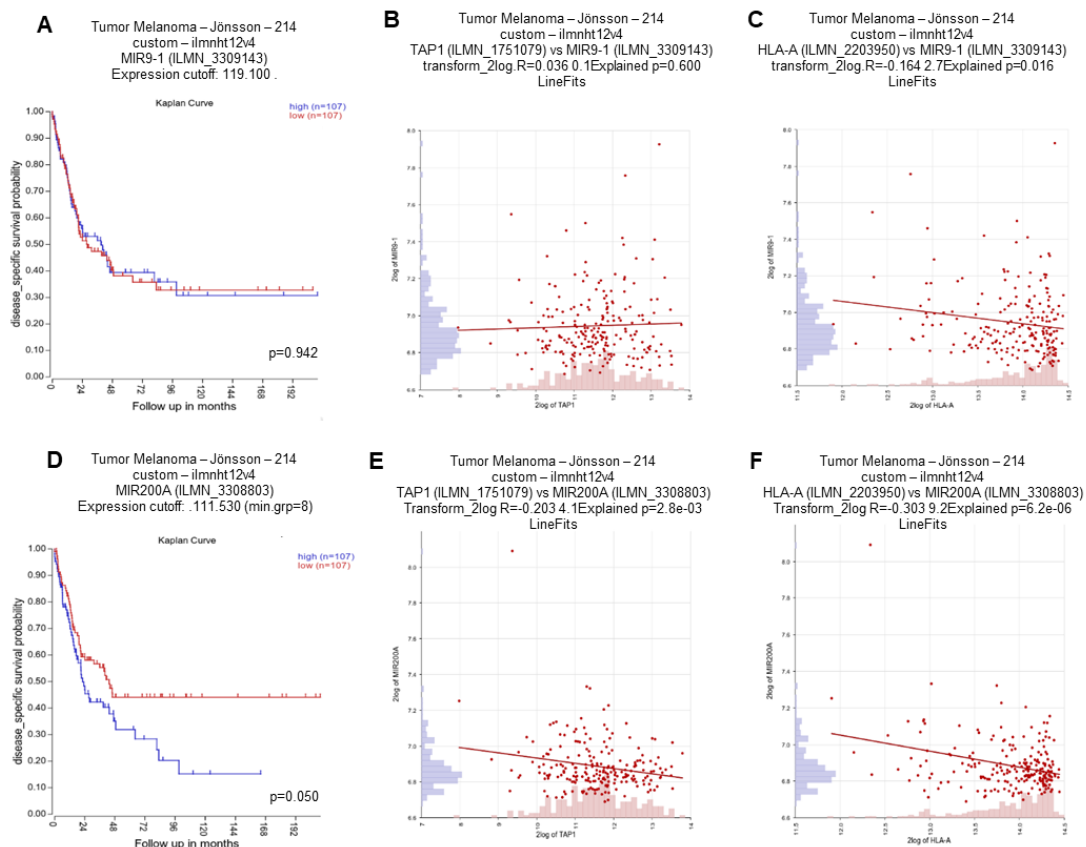

Figure 5.28. Correlations between miR-expression pattern and TAP1 expression levels or CD8$^+$ infiltration rates in melanoma tissue sections
Paraffin-embedded tissue sections from primary melanoma patients were analysed to define the expression levels of the miRs, miR-200a-5p, miR-26b-5p or miR-21-3p by RT-qPCR and in addition scored regarding their TAP1 expression levels as high or low based on immunohistochemical staining. An overview of the correlations between TAP1, CD8$^+$ score (*left y-axis*) and miR-200a-5p expression (*right y-axis*) for each individual patient among the TAP1 low and TAP1 high group is provided (A and B). Respective graphs are provided for miR-26b-5p (C and D) and miR-21-3p (E and F).

5.10 Associations of the expression pattern of the candidate miRs with clinical parameters and in particular with the survival of melanoma patients

Based on the *in silico*, *in vitro* and *in vivo* data established so far there is clear evidence that some of the newly identified candidate miRs such as miR-9-5p, miR-200a-5p, miR-26b-5p and miR-21-3p are capable to modulate the TAP1 expression rates in melanoma cells. Thus, it was of interest to define if the expression of these candidate miRs was correlated with the disease specific survival probability of metastatic melanoma patients and with the expression pattern of TAP1 and HLA-A in such patient cohorts. To address this issue, the "R2: Tumor Melanoma – Jöhnsson – 214 – custom – ilmnht12v4" dataset[344] was employed. Upon bioinformatics analysis of the data from 214 patients, higher miR-200a expression rates were significantly associated with a worse disease specific survival probability of patients with metastatic melanoma (Fig. 5.29D). Furthermore, the miR-200a expression pattern was inversely correlated not only to the expression rates of TAP1, but also to HLA-A antigens (Fig. 5.29E and F). MiR-9 was negatively correlated with the HLA-A expression (p=0.016), but not with the TAP1 expression (p=0.600) (Fig. 5.29A-C).

Figure 5.29. Correlation between miR-9-5p and miR-200a-5p expression patterns with survival probability, TAP1 or HLA-A expression levels in melanoma patients
The "R2: Tumor Melanoma – Jöhnsson – 214 – custom – ilmnht12v4" dataset was used to evaluate the correlations between miRs expression profiles and patients' disease specific survival probability by Kaplan Meier estimation curve (A, D) as well as with TAP1 (B, E) and HLA-A expression (C, F). The raw p-values were based on log-rank tests and calculated for every graph with the web database.

For the miR-26b and miR-21 expression patterns, negative trends were either detected for TAP1 or for HLA-A expression, respectively (Fig. 5.30A-F).
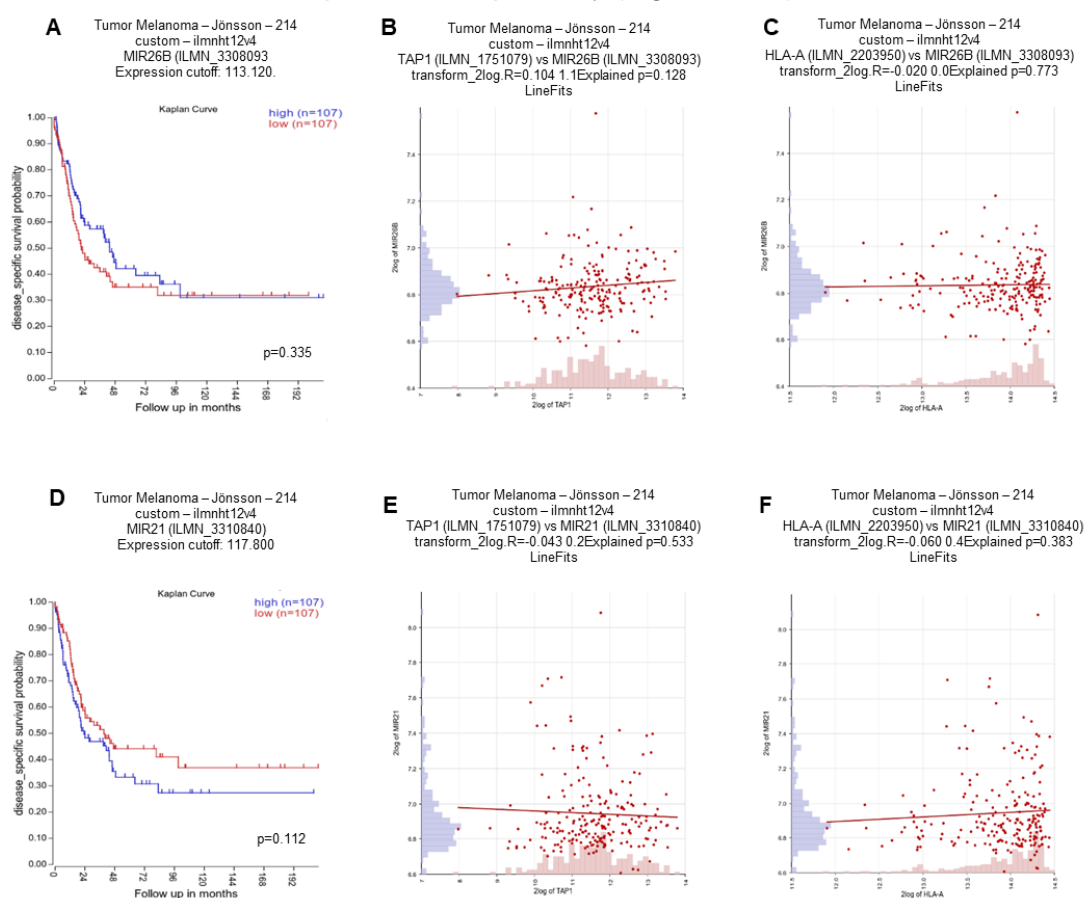
Figure 5.30. Correlation between miR-26b-5p and miR-21-3p expression patterns with survival probability, TAP1 or HLA-A expression levels in melanoma patients
The "R2: Tumor Melanoma – Jöhnsson – 214 – custom – ilmnht12v4" dataset was used to evaluate the correlation between miRs expression and patients' disease specific survival probability by Kaplan Meier estimation curve (A, D) as well as with TAP1 (B, E) and HLA-A expression (C, F). The raw p-values were based on log-rank tests and calculated for every graph with the web database.

5.11 Identification of immune modulatory RBPs by RNA-AP assays in melanoma cell lines

Since miRs may not solely participate in the posttranscriptional regulation of HLA-I APM components, it is assumed that RNA binding proteins (RBPs) might also be substantially involved in the posttranscriptional control. So far, several RBPs have been documented to regulate the expression of HLA-I molecules[305-307,309], but no RBPs have been reported to regulate the expression of any APM component[3]. Therefore, a RNA affinity purification (RNA-AP) assay for the enrichment of RBPs[309,335,336] was employed in order to identify candidate RBPs, which might be able to modulate the expression levels of TAP1 or TPN by binding to the respective 3'-UTRs, respectively. A scheme of the assay is shown in Fig. 4.3 (§4.10). The 3'-UTRs of TAP1 and TPN genes were generated using specific primers (§ 3.3) and the recombinant plasmids constructed for the miTRAP assay[322,323,373], described in §4.9 and §5.3 served as template. Each construct was *in vitro* transcribed in the presence of biotinylated UTRs (B-UTPs) and bound to streptavidin beads to facilitate the specific enrichment of RBPs

binding to the TAP1 or TPN 3'-UTR, respectively. Non-biotinylated transcript sequences and sequences with comparable length and guanine/cytosine (G/C) content were used as controls for unspecific binding of RBPs. The HLA-G 3'-UTR served as a control for TAP1 3'-UTR and the TGFBR2 3'-UTR and HLA-G CDS served as controls for the TPN-1 and TPN-2 3'-UTR, respectively. Cell lysates of the MKR (TAP1 mRNA$^+$ and TAP1 protein$^+$) and MZ-Mel2 (TPN mRNA$^+$ and TPN protein$^+$) cell lines were employed for the enrichment of RBPs targeting TAP1 and TPN 3'-UTRs (Table 5.4).

Table 5.4. Summary of the APM components 3'-UTRs analysed with RNA-AP assay for RBPs identification

Construct	Control construct	Cell lysate	MALDI TOF MS analysis (Dr. Jette Rahn)	ESI MS analysis (Dr. Matt Fuszard)	Validation
TAP1 3'-UTR	HLA-G 3'-UTR	MKR	Yes	No	No
TPN-1 3'-UTR	TGFBR2 3'-UTR	MZ-Mel2	Yes	Yes	Yes
TPN-2 3'-UTR	HLA-G CDS		Yes	Yes	Yes

Protein samples were separated on gradient SDS-PAGE gels as described in §4.12-15 before gels were stained in Colloid Coomassie Blue. In figure 5.31, a representative SDS-PAGE gradient gel stained with Colloidal Coomassie Blue staining is provided.
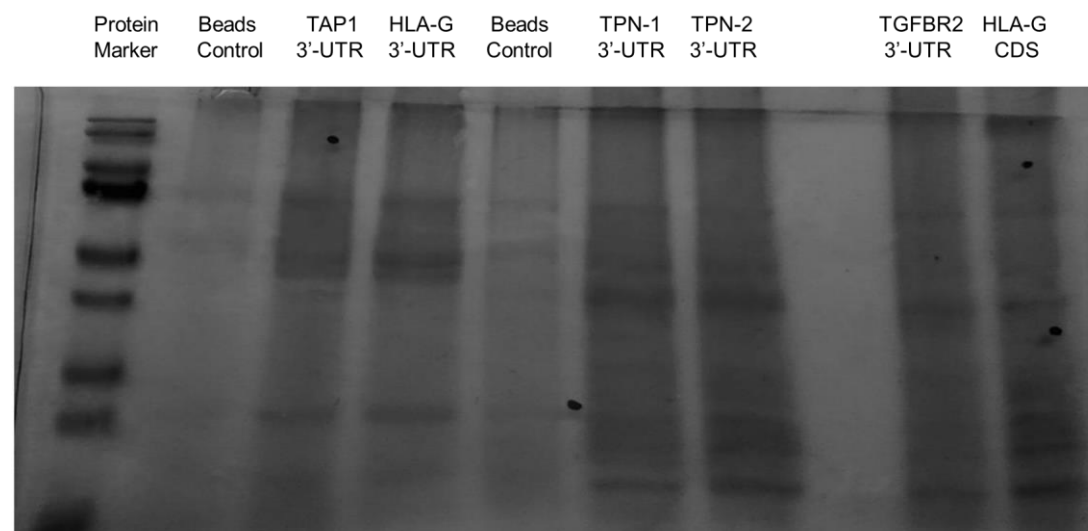
Figure 5.31. Representative SDS-PAGE gel of co-purified proteins
Colloidal Coomassie Blue stained SDS-PAGE gel of co-purified proteins. The dots indicate the picked protein bands for mass spectrometry, which are clearly present in target samples (TAP1 3'-UTR, TPN-1 or TPN-2 3'-UTR), but not in the corresponding control samples (HLA-G 3'-UTR, TGFBR2 3'-UTR or, HLA-G CDS).

Distinct protein bands were picked and subjected to MALDI-TOF MS followed by bioinformatics analysis. The MALDI-TOF MS analyses and database searches of the respective spectra (using the MASCOT search engine (Matrix Science) were performed by Dr. Jette Rahn. Using this approach, the Y-box-binding proteins 1

(YBOX1) and 3 (YBOX3) were identified as enriched in the TAP1 3'-UTR targeting eluate, whereas in the TPN 3'-UTR targeting eluates the 60S ribosomal protein L13 (RPL13), the insulin-like growth factor 2 mRNA binding protein 1 (IGF2BP1) and the heterogenous ribonucleoprotein C (HNRNPC) were successfully identified as enriched.

In addition, the eluates of two biological replicates targeting the TPN 3'-UTR (provided as two separate constructs as previously described for the corresponding miTRAP assays) together with the respective control samples were sent for ESI MS analysis to Dr. Matt Fuszard (Mass Spectrometry Core Facility, Martin Luther University Halle-Wittenberg, Halle (Saale), Germany). These eluates were generated with the cell lysates of the MZ-Mel2 melanoma cell line.

After bioinformatics analysis of the MS data, the RBPs, which had a number of spectra ≥ 3 and were not identified in the control eluates, were selected and further validated by *in silico* analyses, qPCR, flow cytometry and Western blot. A list of candidate RBPs binding to TPN 3'-UTR using MZ-Mel2 cell lysate is cited in Table 5.5.

Table 5.5. List of the candidate, enriched RBPs targeting TPN 3'-UTR

| Description	# of spectra (1st)	# of spectra (2nd)	Part of TPN 3'-UTR	*In silico* predicted (*)
Q9BUJ2 / HNRL1 Heterogeneous nuclear ribonucleoprotein U-like protein 1 (**HNRNPUL1**)	12	11	1st+2nd	
O00425 / IF2B3 Insulin-like growth factor 2 mRNA-binding protein 3 (**IGF2BP3**)	12	7	1st+2nd	yes
Q15717 / ELAV1 HUMAN ELAV-like protein 1 (**ELAVL**1)	10		1st	
O75569 / PRKRA Interferon-inducible double-stranded RNA-dependent protein kinase activator A (**PRKRA**)	9		1st	
O43175 / SERA D-3-phosphoglycerate dehydrogenase (**PHGDH**)	9	6	1st+2nd	
P11586 / C1TC C-1-tetrahydrofolate synthase, cytoplasmic (**MTHFD1**)	8		1st	
P50454 / SERPH Serpin H1 (**SERPINH1**)	6	3	1st+2nd	yes
Q08211 / DHX9 ATP-dependent RNA helicase A (**DHX9**)	5		1st	yes
P02511 / CRYAB Alpha-crystallin B chain (**CRYAB)**	4	3	1st+2nd	
P04792 / HSPB1 Heat shock protein beta-1 (**HSPB1**)	9		2nd	
Q96DH6 / MSI2H RNA-binding protein Musashi homolog 2 (**MSI2**)	4		2nd	
Q92616 / GCN1 eIF-2-alpha kinase activator GCN1 (**GCN1**)	4		2nd	
P49327 / FAS Fatty acid synthase (**FASN**)	4		2nd	yes
P52597 / HNRPF Heterogeneous nuclear ribonucleoprotein F (**HNRNPF**)	4		2nd	yes

*The *in silico* prediction analysis was performed using the bioinformatic tool starBase v2.0.

Several of the strongly enriched candidate RBPs were also predicted by the *in silico* prediction tool starBase v2.0[342,343] (http://starbase.sysu.edu.cn/starbase2/index.php) (Table 5.5) supporting their role as putative regulators of TPN.

From the panel of successfully identified 3'-UTR-binding RBP candidates, the putative targets IGF2BP1 and IGF2BP3 were selected for further validation experiments in the respective melanoma cell lines.

## 5.12   Expression of the enriched candidate RBPs in melanoma cell lines

The two selected candidate RBPs IGF2BP1 and IGF2BP3 have not only been defined as specifically enriched in the eluates using TPN 3'-UTRs as baits, but they were also *in silico* predicted by the online available bioinformatic tool starBase v2.0[342,343]. The presence of IGF2BP1 and IGF2BP3 was also verified by Western blot analyses in miTRAP eluates of TPN 3'-UTRs using the cell lysates of the MKR melanoma cell line (Fig. 5.32). In this context, the successful detection of the RBPs IGF2BP1 (Fig. 5.32A) and IGF2BP3 (Fig. 5.32B) specifically in the MZ-Mel2 cell lysate and TPN 3'-UTR baits strongly supports the specific binding of these candidate RBPs proteins to the TPN 3'-UTR.
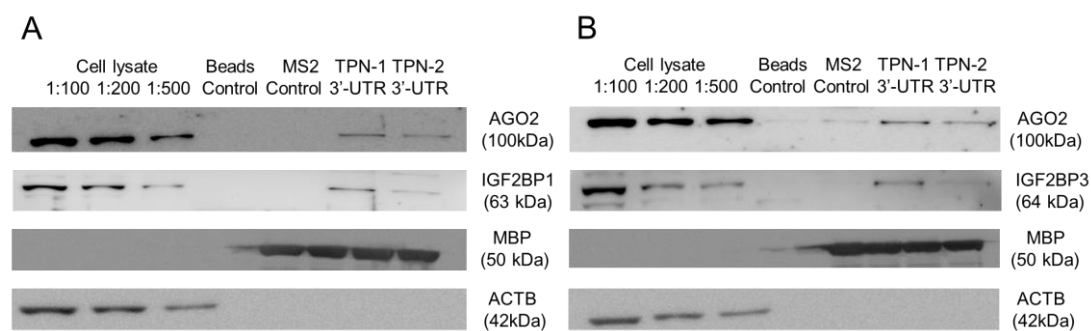
Figure 5.32. Identification of IGF2BP1 and IGF2BP3 in miTRAP eluates
Western blot analyses of the miTRAP eluates of TPN 3'-UTRs using MKR cell lysates reveal that next to AGO2 (A) IGF2BP1 and (B) IGF2BP3 were detectable in the TPN 3'-UTR specific eluates as well as in the input controls. ACTB was employed as a negative control for unspecific binding, while MBP served as a positive control for the equal binding of the complex on the amylose beads. Shown are representative Western blots.

The expression pattern of IGF2BP1 and IGF2BP3 were further screened in 40 melanoma cell lines and correlated with TPN mRNA expression levels. Interestingly, the majority of the melanoma cell lines expressed more than 1000-fold higher IGF2BP1 mRNA levels relative to melanocytes (32/40, 80%).Furthermore, an inverse correlation was observed between IGF2BP1 and the relative TPN mRNA expression levels (Fig. 5.33A). In addition, the majority of the melanoma cell lines expressed 4-fold higher IGF2BP3 mRNA levels than melanocytes (30/40, 75%) and an inverse correlation was also observed between the IGF2BP3 and the corresponding TPN mRNA expression levels (Fig. 5.33B).
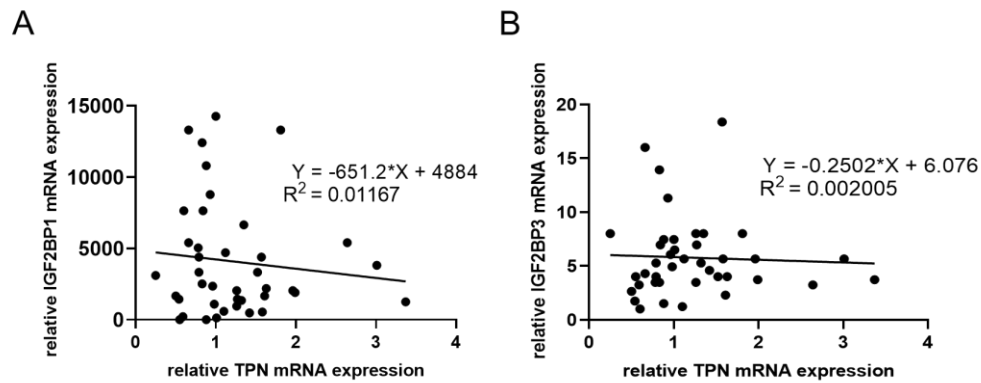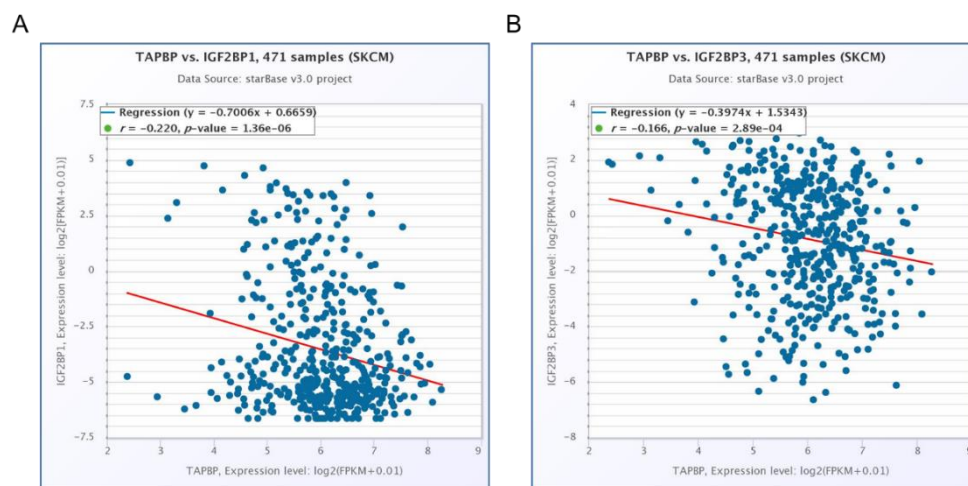
Figure 5.33. Correlation between the mRNA expression levels of IGF2BP1 or IGF2BP3 and the mRNA expression levels of TPN in different melanoma cell lines
The different melanoma cell lines were analysed by RT-qPCR for the expression of (A) IGF2BP1 or (B) IGF2BP3 and TPN. Shown are the expression levels upon normalization to melanocytes as well as the linear regression equation and the R^2 value. Each dot represents a distinct melanoma cell line.

5.13 Correlation between the mRNA expression levels of enriched candidate RBPs and TPN as well as the survival rates of melanoma patients

Since *in silico* as well as *in vitro* interaction demonstrated an enrichment of the candidate RBPs IGF2BP1 or IGF2BP3 with TPN, the expression of these RBPs was correlated to the mRNA expression levels of TPN and the clinical parameters (overall survival, disease specific survival or progression free interval) of primary and / or metastatic melanoma patients.

For *in silico* correlation of the mRNA expression levels of IGF2BP1 or IGF2BP3 with TPN, the "SKCM Cancer" dataset[358-364] was used, which is available at the starbase v2.0 web tool (http://starbase.sysu.edu.cn/)[380,381]. Interestingly, the mRNA expression levels of IGF2BP1 or IGF2BP3 were inversely correlated with the mRNA expression levels of TPN (Fig. 5.34). These data are comparable to the correlation between mRNA expression levels of IGF2BP1 or IGF2BP3 and the mRNA expression levels of TPN in the different melanoma cell lines, as described in §5.12 (Fig. 5.33).

Figure 5.34. Correlation of between TPN and IGF2BP1 or IGF2BP3 mRNA expression levels in melanoma patients
The mRNA expression levels of TPN and (A) IGF2BP1 or (B) IGF2BP3 were correlated by using the starbase v2.0 web tool[380,381] and the "SKCM Cancer" dataset[358-364] comprised of 471 individual melanoma patients. The raw p-values were based on log-rank tests and calculated for every graph with this web tool (http://starbase.sysu.edu.cn/).

In silico analyses were also performed using the "UCSC Xena Functional Genomics Explorer" (https://xenabrowser.net/) and "R2: microarray analysis and visualization platform" (http://r2.amc.nl) in order to predict the correlation of candidate and already known RBPs with the survival of melanoma patients.

A heatmap plot (Fig. 5.35) demonstrates the association of the expression of IGF2BP1 or IGF2BP3 with the clinical parameters (overall survival, disease specific survival or progression free interval) of melanoma patients. The Kaplan Meier curves for each RBP are available in the Appendix (A.4). Particularly, the IGF2BP3 expression levels were directly correlated with disease specific survival probability of metastatic melanoma patients and inversely correlated with the disease specific survival and the progression free survival interval of primary melanoma patients. In the same group of primary melanoma patients, the IGF2BP1 expression levels were inversely correlated with the overall survival of these patients.

	RBPs	IGF2BP1	IGF2BP3
total patients	overall survival		
total patients	overall survival		
total patients	disease specific survival		
total patients	progression free interval		

Tumor SKCM-TCGA-470		Tumor SKCM-TCGA-375	
total patients	470	total	375
primary	103	primary	65
metastatic	353	metastatic	266

|	Correlation	Significance
	positive	p≤0.05
	positive	p>0.05
	negative	p<0.05
	negative	p≤0.05

Figure 5.35. Correlation heatmap between the expression pattern of RBPs and clinical parameters among different groups of melanoma patients
Correlation heatmap between the expression levels of IGF2BP1 or IGF2BP3 and clinical parameters of melanoma patients (overall survival, disease specific survival or progression free interval) as defined across distinct melanoma patient cohorts from various datasets.

5.14 Effect of the deregulation of the RBPs IGF2BP1 and IGF2BP3 on the expression pattern of HLA-I APM components

To further analyse the effect of the candidate RBPs (IGF2BP1 and IGF2BP3), the respective recombinant plasmids (pMSCV PIG IMP-1 short[382] or pDESTmycIGF2BP3[383]) and siRNAs with the empty vector (EF-pLink2, kindly provided by Professor Dr. Guido Posern (Institute of Biophysical Chemistry, Martin-Luther-University Halle-Wittenberg, Halle (Saale), Germany)) or siRNA negative control (NC) were transiently transfected into our three model melanoma cell lines BUF1379, MZ-Mel2 and FM3.

Upon siRNA transfection, the constitutive expression of IGF2BP1 and IGF2BP3 was reduced by more than 60% and 40% at the mRNA and protein level, respectively, while cells transfected with the siRNA NC showed a comparable relative expression pattern to parental cells (Fig. 5.36).
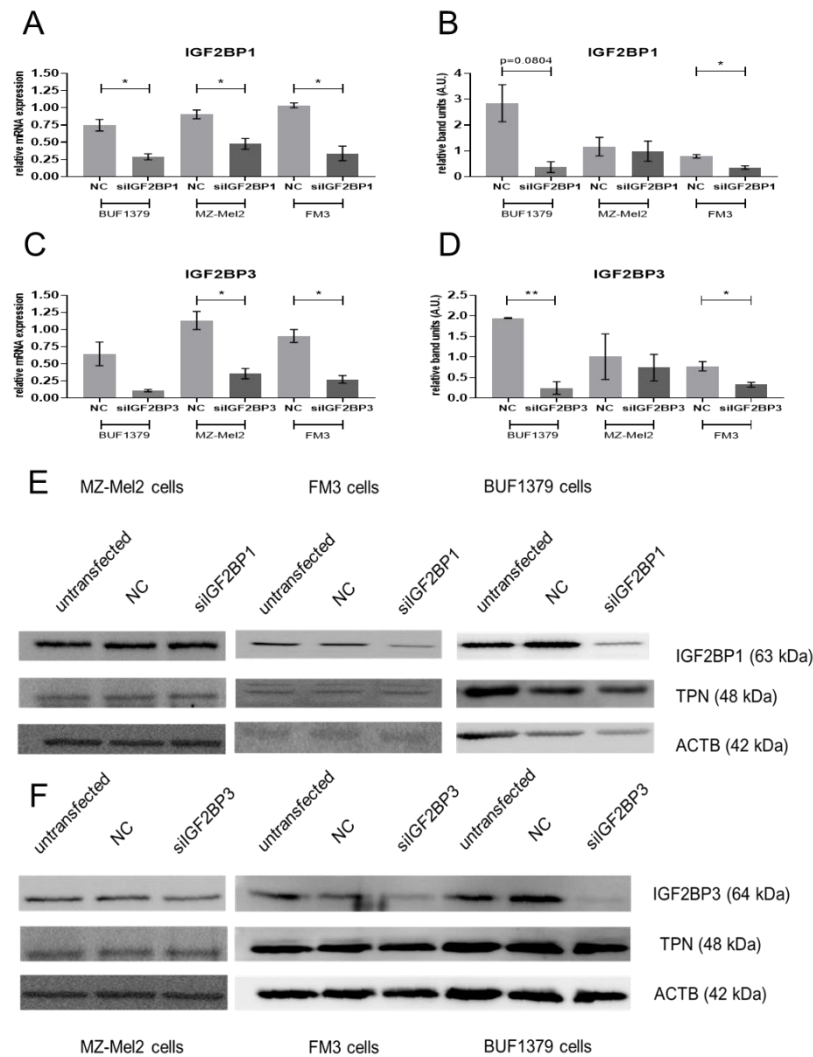
Figures 5.36. Verification of the intended knock down of IGF2BP1 or IGF2BP3 at the mRNA and protein expression levels

BUF1379, MZ-Mel2 and FM3 melanoma cells were either left untreated (untransfected) or transiently transfected either with 2 ng/mL siRNA of the respective targeting siRNA or the siRNA negative control (NC). After 48 h the mRNA expression levels of the genes indicated were determined by RT-qPCR (A and C) and were normalized to the corresponding expression levels of GAPDH and ACTB. The corresponding protein expression patterns were evaluated by Western blot analyses (E and F). To further quantify the Western blot results (B and D), the relative band intensity (A.U., arbitrary units) of the transfectants was measured and compared to the respective parental melanoma cells to define their ratios thereby normalizing to the co-detected GAPDH signals. Shown are the normalized mean values ± SE from a minimum of 3 different biological replicates and representative Western blots, *p < 0.05, **p < 0.01 in un-paired t-test. (siIGF2BP1= knock down of IGF2BP1 via siRNAs, siIGF2BP3= knock down of IGF2BP3 via siRNAs)

Upon plasmid transfection, the expression of each RBP in the selected melanoma cell lines was increased by more than 20-fold at the mRNA and 2-fold at the protein level, respectively, while cells transfected with the NC showed a comparable expression pattern to their parental cells (Fig. 5.37), with the exception of the expression of IGF2BP1 in BUF1379 transfected cells, in which no significant increase was found at the protein level.
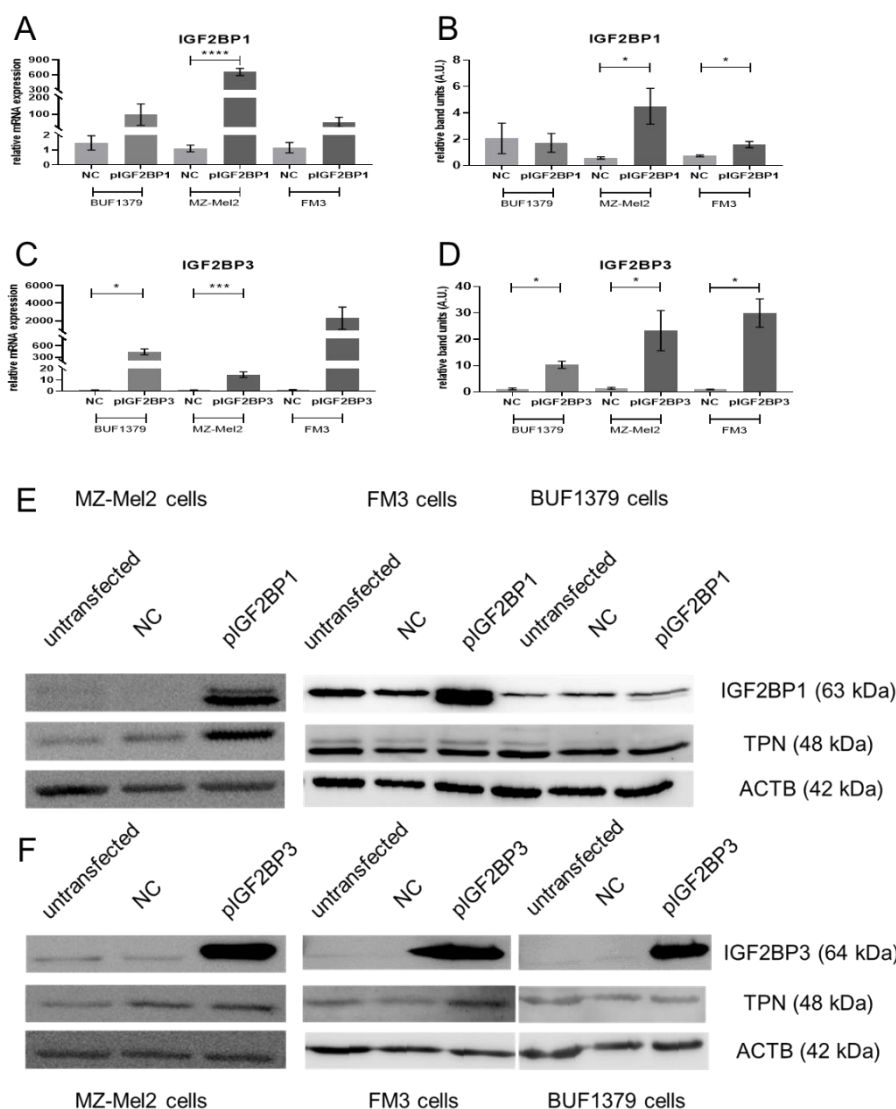
Figure 5.37. Overexpression of IGF2BP1 or IGF2BP3 and its effect on TPN expression
BUF1379, MZ-Mel2 and FM3 melanoma cells were either left untreated (untransfected) or transiently transfected either with 2 µg/mL recombinant plasmid encoding for IGF2BP1 or IGF2BP3 or the negative control (NC). After 48 h the mRNA expression levels of the indicated genes were determined by RT-qPCR (A and C) and were normalized to the corresponding expression levels of GAPDH and ACTB of the parental cells. The corresponding protein expression patterns were evaluated by Western blot analyses (E and F). To further quantify the Western blot results (B and D), the relative band intensity (A.U., arbitrary units) of the transfectants was measured and compared to the respective parental melanoma cells and normalized to the co-detected GAPDH expression. Shown are the normalized mean values ± SE from a minimum of 3 different biological replicates and representative Western blots, *p < 0.05, ***p < 0.001, ****p < 0.0001 in un-paired t-test. (pIGF2BP1= overexpression of IGF2BP1 via recombinant plasmid, pIGF2BP3= overexpression of IGF2BP3 via recombinant plasmid)

Altered expression levels of the IGF2BP1 and IGF2BP3 mediated either by the respective plasmids or siRNAs had relevant, but not statistically significant influence on the corresponding TPN mRNA and protein expression levels (Fig. 5.37, 5.38).
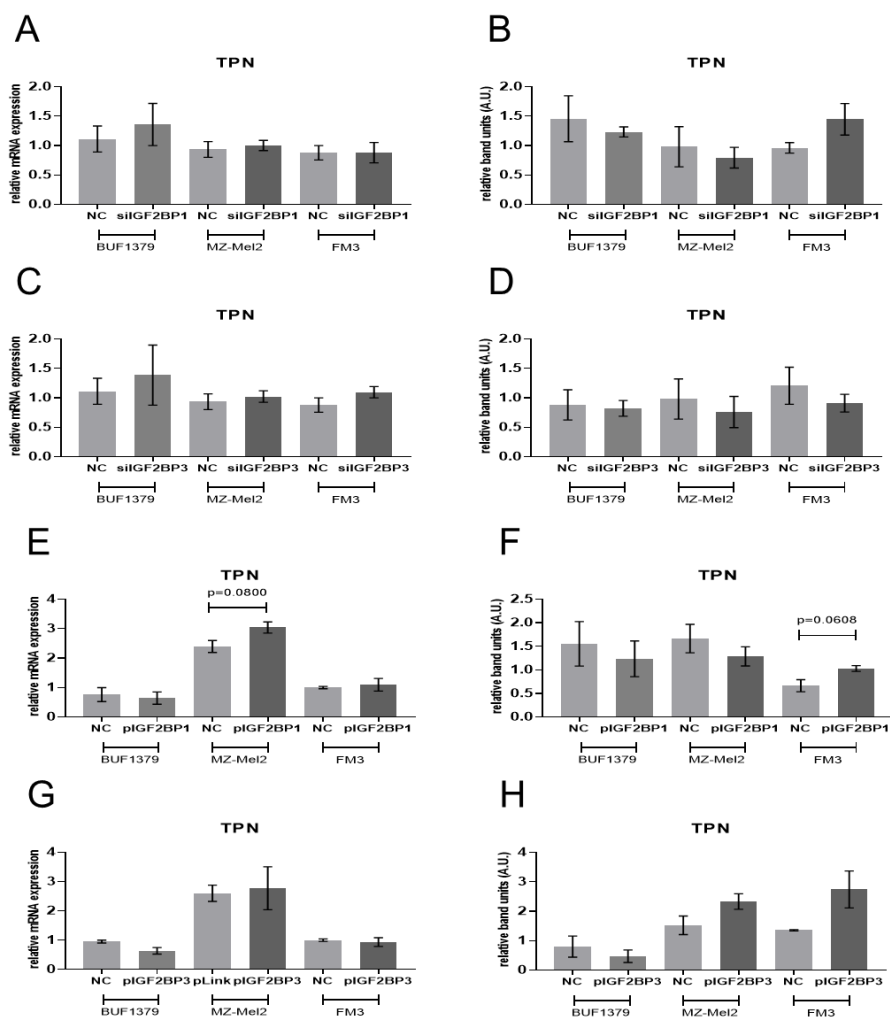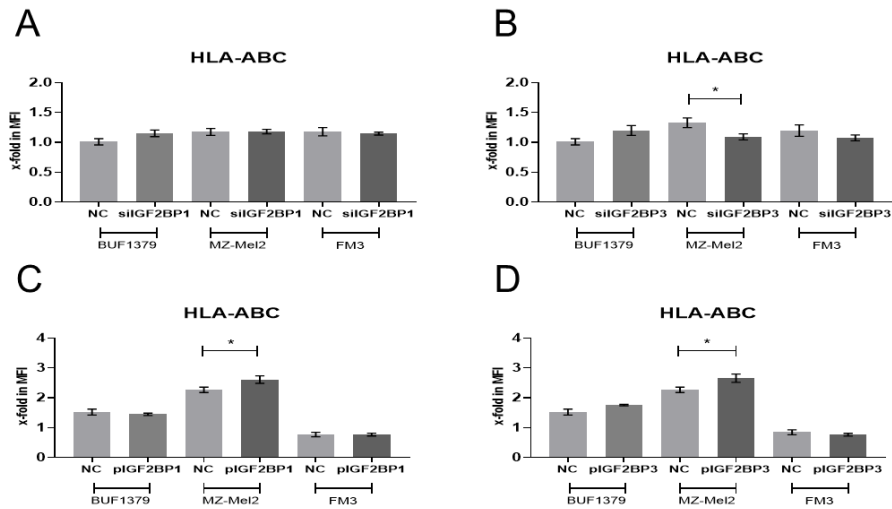
Figure 5.38. Effect of the deregulation of IGF2BPs on TPN mRNA and protein levels
BUF1379, MZ-Mel2 and FM3 melanoma cells were either transiently transfected with 2 ng/mL siRNA of the respective targeting siRNA or the siRNA negative control (NC) or with 2µg/mL recombinant plasmid for the IGF2BP1 or IGF2BP3 or the negative control (NC). After 48 h the mRNA expression levels of TPN were determined by RT-qPCR (A and C, E and G) and were normalized to the corresponding expression levels of GAPDH and ACTB. The corresponding protein expression levels were evaluated by Western blot analyses (Fig. 5.37E and F). To further quantify the Western blot results (B, D, F and H), the relative band intensity (A.U., arbitrary units) of the transfectants was determined and compared to the respective parental melanoma cells to define their rations thereby normalizing to co-detected GAPDH expression. Shown are the normalized mean values ± SE from a minimum of 3 different biological replicates and representative Western blots. (siIGF2BP1= knock down of IGF2BP1 via siRNAs, siIGF2BP3= knock down of IGF2BP3 via siRNAs, pIGF2BP1= overexpression of IGF2BP1 via recombinant plasmid, pIGF2BP3= overexpression of IGF2BP3 via recombinant plasmid)

Apart from the deregulation of TPN upon the aberrant expression of IGF2BP1 and IGF2BP3, the surface expression levels of HLA-I were determined by flow cytometry analyses, Interestingly, concerning the classical HLA-I surface expression levels, the overexpression of IGF2BP1 or IGF2BP3 through the respective recombinant plasmids increased by 25% the HLA-ABC surface expression of the transfectants compared to the NC (Fig. 5.39C and D), while knock down of IGF2BP3 expression decreased the HLA-ABC surface expression levels in MZ-Mel2 cells by 15% (Fig. 5.39B).

Figure 5.39. Effect of deregulation of IGF2BP1 and IGF2BP3 on HLA-I surface expression
The HLA-ABC surface expression levels were evaluated by flow cytometry. Shown are the normalized mean values ± SE from a minimum of 3 different biological replicates, *p < 0.05 in un-paired t-test. (siIGF2BP1= knock down of IGF2BP1 via siRNAs, siIGF2BP3= knock down of IGF2BP3 via siRNAs, pIGF2BP1= overexpression of IGF2BP1 via recombinant plasmid, pIGF2BP3= overexpression of IGF2BP3 via recombinant plasmid)

5.15 Identification of deregulated proteins upon knock down or overexpression of IGF2BP1 or IGF2BP3 in FM3 melanoma cells

Two biological replicates of FM3 cells either transfected with siRNA or recombinant plasmids encoding for IGF2BP1 or IGF2BP3 together with the respective control samples (the siRNA NC and the empty vector) and untransfected samples were sent for ESI MS analysis to Dr. Matt Fuszard (Mass Spectrometry Core Facility, Martin-Luther-University Halle-Wittenberg, Halle (Saale), Germany).

Upon the MS analysis, the proteins, which were identified in the FM3 transfectants, but not in the control samples and were statistically significantly deregulated 1.5fold, were further employed for *in silico* and expression analyses (Fig. 5.40 and 5.41).
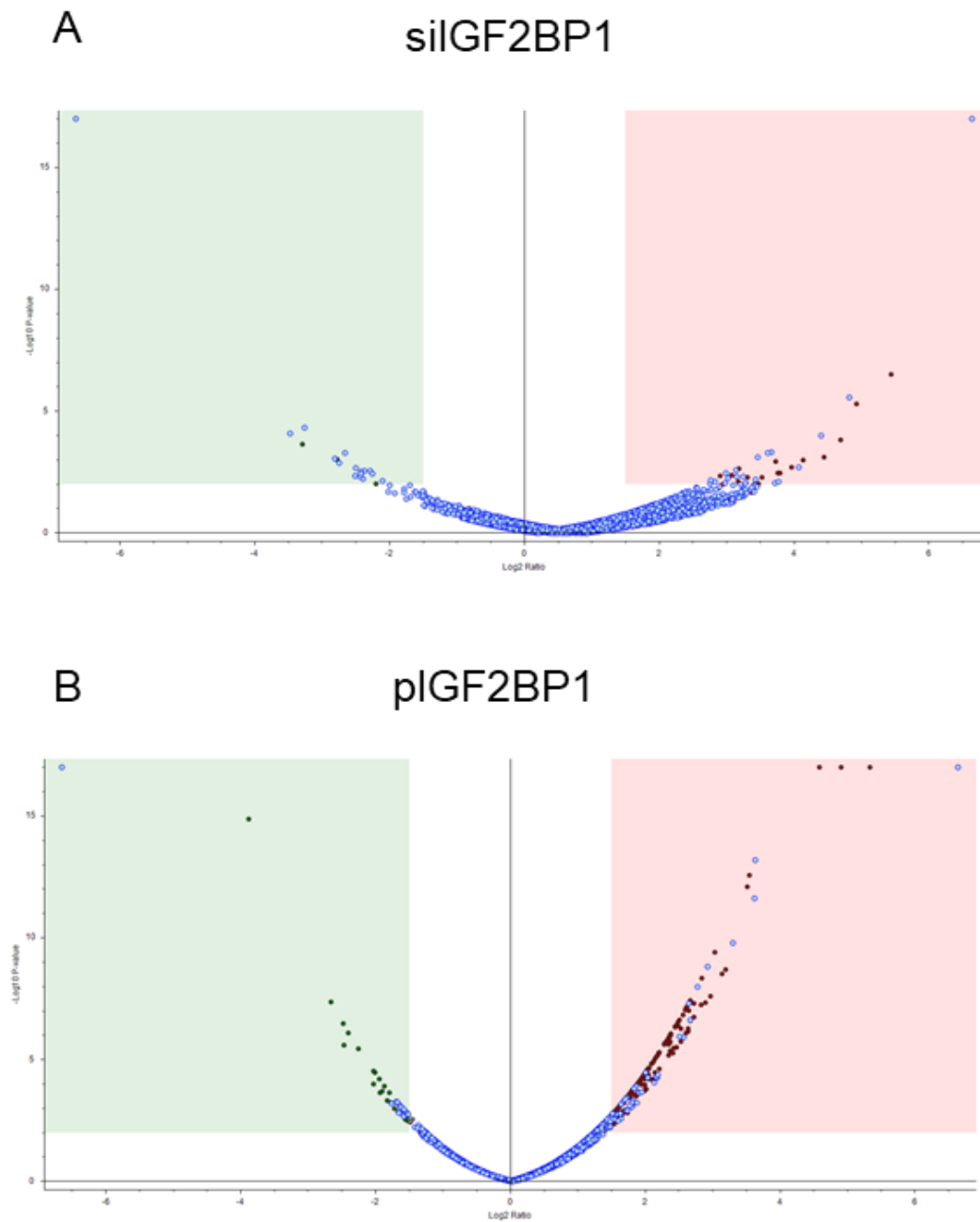
Figure 5.40. Volcano plots depicting the distribution pattern of the overall protein profiles upon knock down or overexpression of IGF2BP1

Upon knock down with siRNAs (A) or overexpression (B) with recombinant plasmids encoding for IGF2BP1, several proteins were deregulated. After exclusion of the proteins, which were deregulated also in the control samples (green and red dots), those which were either upregulated or downregulated by a factor of at least 1.5fold and in addition fulfilled q-values criteria (corrected p-values) ≤ 0.01, were subjected to further *in silico* and expression profiling analyses. (siIGF2BP1= knock down of IGF2BP1 via siRNAs, pIGF2BP1= overexpression of IGF2BP1 via recombinant plasmid)
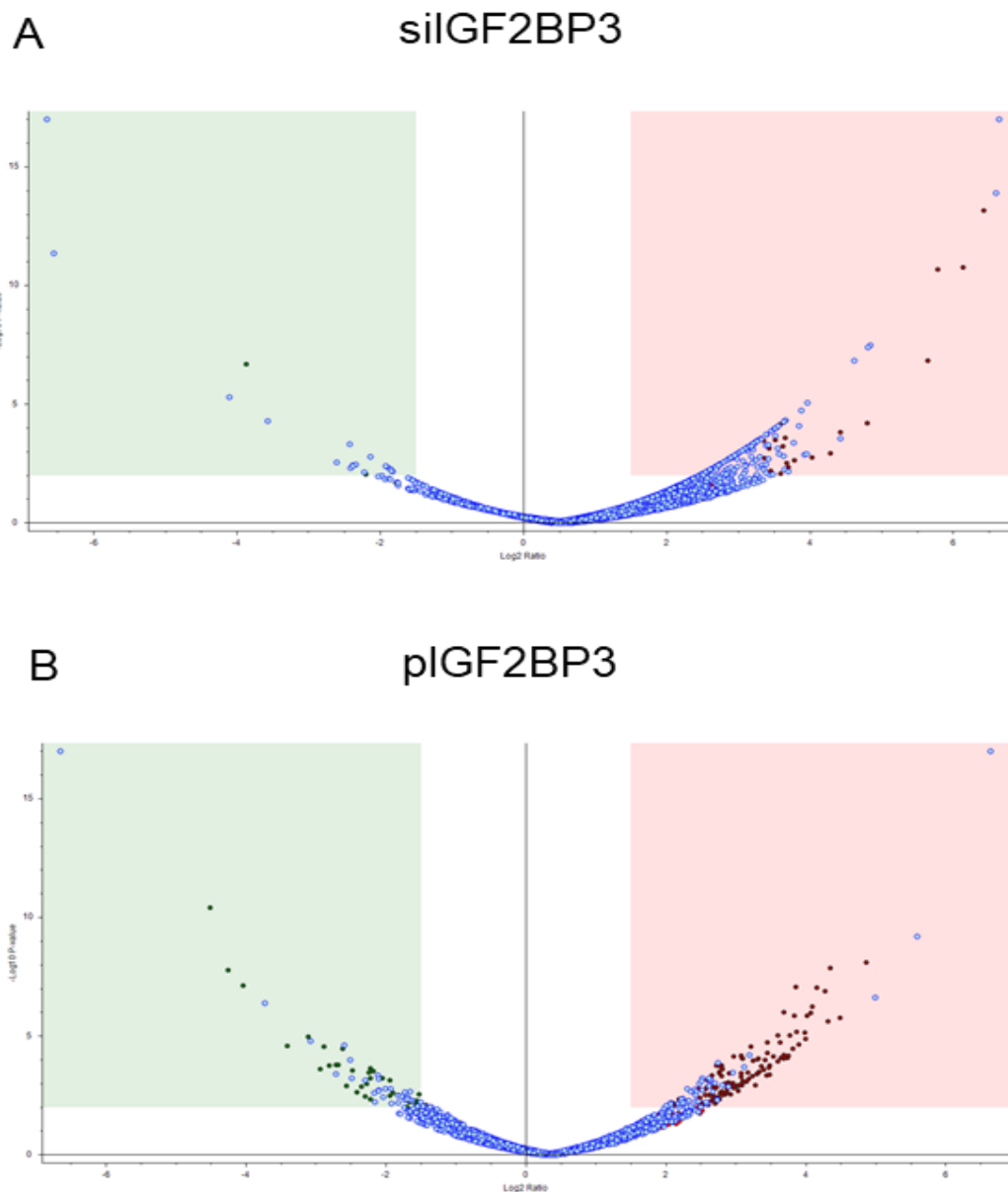
Figure 5.41. Volcano plots depicting the distribution pattern of the overall protein profiles upon knock down or overexpression of IGF2BP3

Upon knock down with siRNAs (A) or overexpression (B) with recombinant plasmids encoding for IGF2BP3, several proteins were deregulated. After exclusion of the proteins, which were deregulated also in the control samples (green and red dots), those which were either upregulated or downregulated by a factor of at least 1.5fold and in addition fulfilled q-values criteria (corrected p-values) ≤ 0.01, were subjected to further *in silico* and expression profiling analysis. (siIGF2BP3= knock down of IGF2BP3 via siRNAs, pIGF2BP3= overexpression of IGF2BP3 via recombinant plasmid)

Upon proteomic profiling, proteins were defined as upregulated or downregulated in response to the modulation of the IGF2BP1 or IGF2BP3 expression levels and were summarised in Table 5.6.

Table 5.6. Differentially expressed proteins upon overexpression or knock down of IGF2BP1 or IGF2BP3

🟩 Downregulated
🟥 Upregulated

Table 5.6.1. Differentially expressed proteins upon knock down of IGF2BP1

	Accession	Description	Gene Symbol	Abundance Ratio: NC siRNA / parental	Abundance Ratio: siIGF2BP1 / parental	Abundance Ratio Adj. P-Value: siIGF2BP1 / NC siRNA
🟩	Q86WR7	Proline and serine-rich protein 2	PROSER2	2,033	0,143	0,007016
🟩	Q9NZI8	Insulin-like growth factor 2 mRNA-binding protein 1	IGF2BP1	1,644	1,311	0,988643
🟥	Q9UHY7	Enolase-phosphatase E1	ENOPH1	4,011	21,152	0,000846
🟥	Q8NFF5	FAD synthase	FLAD1	3,434	13,689	0,060653
🟥	P97526	Neurofibromin 1	Nf1	3,72	12,246	0,004171
🟥	Q9Y6K1	DNA (cytosine-5)-methyltransferase 3A	DNMT3A	2,983	11,03	0,006272

Table 5.6.2. Differentially expressed proteins upon overexpression of IGF2BP1

	Accession	Description	Gene Symbol	Abundance Ratio: NC plasmid / parental	Abundance Ratio: pIGF2BP1 / parental	Abundance Ratio Adj. P-Value: pIGF2BP1 / parental
🟩	P30040	Endoplasmic reticulum resident protein 29	ERP29	0,492	0,332	0,008184
🟩	Q07352	mRNA decay activator protein ZFP36L1	ZFP36L1	0,552	0,319	0,012041
🟥	Q96P63	Serpin B12	SERPINB12	0,982	12,407	7,36E-13
🟥	Q5T749	Keratinocyte proline-rich protein	KPRP	1,092	7,63	1,66E-08
🟥	Q08554	Desmocollin-1	DSC1	0,459	6,261	5,24E-07
🟥	P23490	Loricrin	LOR	0,507	6,388	2,43E-06
🟥	Q9NZT1	Calmodulin-like protein 5	CALML5	0,418	3,662	0,001098
🟥	Q9NZI8	Insulin-like growth factor 2 mRNA-binding protein 1	IGF2BP1	1,228	3,224	0,004099

Table 5.6.3. Differentially expressed proteins upon knock down of IGF2BP3

	Accession	Description	Gene Symbol	Abundance Ratio: NC siRNA / parental	Abundance Ratio: siIGF2BP3 / parental	Abundance Ratio Adj. P-Value: siIGF2BP3 / parental
🟩	Q9HCN4	GPN-loop GTPase 1	GPN1	1,338	0,011	3,36E-11
🟩	Q86WR7	Proline and serine-rich protein 2	PROSER2	2,033	0,058	3,87E-05
🟩	Q8IYQ7	Threonine synthase-like 1	THNSL1	0,419	0,164	0,019691
🟩	Q9NSK0	Kinesin light chain 4	KLC4	0,825	0,193	0,025285
🟩	Q9BYJ9	YTH domain-containing family protein 1	YTHDF1	1,154	0,193	0,02641
🟥	Q9P1F3	Costars family protein ABRACL	ABRACL	3,828	28,67	2,57E-07
🟥	Q8NBF2	NHL repeat-containing protein 2	NHLRC2	3,722	28,004	3,26E-07
🟥	Q9NZT1	Calmodulin-like protein 5	CALML5	1,492	24,654	1,15E-06
🟥	Q9Y6K1	DNA (cytosine-5)-methyltransferase 3A	DNMT3A	2,983	21,486	0,002142
🟥	O43681	ATPase ASNA1	ASNA1	3,176	15,678	6,78E-05

Table 5.6.4. Differentially expressed proteins upon overexpression of IGF2BP3

	Accession	Description	Gene Symbol	Abundance Ratio: NC plasmid / parental	Abundance Ratio: pIGF2BP3 / parental	Abundance Ratio Adj. P-Value: pIGF2BP3 / parental
🟩	Q96G46	tRNA-dihydrouridine(47) synthase [NAD(P)(+)]-like	DUS3L	0,473	0,075	3,64E-06
🟩	Q6PIU2	Neutral cholesterol ester hydrolase 1	NCEH1		0,119	0,000143
🟩	Q9BSF4	Mitochondrial import inner membrane translocase sub	TIMM29	0,383	0,166	0,000209
🟩	P14927	Cytochrome b-c1 complex subunit 7	UQCRB	0,593	0,176	0,000835
🟩	P30040	Endoplasmic reticulum resident protein 29	ERP29	0,492	0,179	0,004811
🟩	Q02818	Nucleobindin-1	NUCB1	0,404	0,232	0,014475
🟩	Q15293	Reticulocalbin-1	RCN1	0,368	0,25	0,012285
🟥	P04279	Semenogelin-1	SEMG1	2,197	31,938	2,14E-06
🟥	Q9BYR9	Keratin-associated protein 2-4	KRTAP2-4	0,839	9,175	0,000522
🟥	Q9UHQ4	B-cell receptor-associated protein 29	BCAP29	2,437	8,725	0,001606
🟥	Q96IX5	ATP synthase membrane subunit DAPIT, mitochondri	USMG5	2,507	7,771	0,002828
🟥	P28370	Probable global transcription activator SNF2L1	SMARCA1	0,705	7,024	0,009115

Although the validation of the deregulated genes on mRNA level is still an ongoing process, preliminary and representative results are depicted in figure 5.42.
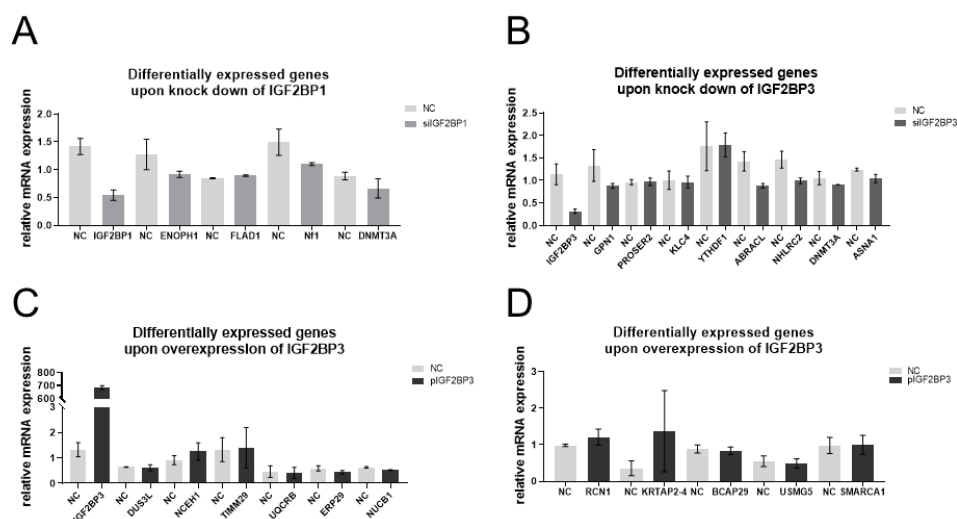
Figure 5.42. Effect of the deregulation of IGF2BPs on the mRNA levels of selected downstream targets

FM3 melanoma cells were either transiently transfected with 2 ng/mL siRNA of the respective targeting siRNA or the siRNA negative control (NC) or with 2µg/mL recombinant plasmid for the IGF2BP3 or the negative control (NC). After 48 h the mRNA expression levels were determined by RT-qPCR and were normalized to the corresponding expression levels of GAPDH and ACTB of the parental cells. Although 3 biological replicates are the minimum required for any statistical analysis, shown are the normalized mean values ± SE from 2 biological replicates. (siIGF2BP1= knock down of IGF2BP1 via siRNAs, siIGF2BP3= knock down of IGF2BP3 via siRNAs, pIGF2BP3= overexpression of IGF2BP3 via recombinant plasmid)

Each group of deregulated proteins was subjected to computational analysis using the STRING database[384] of known and predicted protein-protein interactions. The interactions included direct (physical) and indirect (functional) associations, deriving from computational prediction and from interactions aggregated from other (primary) databases[385] (Appendix A.8).

Functional enrichment analysis of the deregulated proteins has been also performed with the STRING database. The database presents and groups statistical enrichment observations for a number of pathways and functional subsystems based on the submitted deregulated proteins for every condition (for the current study, overexpression or knock down of IGF2BP1 or IGF2BP3).

Data from the GO analysis of the deregulated protein candidates from the knock down or overexpression of IGF2BPs are illustrating a categorization into biologic process, molecular function and cellular components. The KEGG pathway analysis strengthens the assumption that the identified, differentially expressed proteins are involved in multiples mechanisms in melanoma.

6. Discussion

6.1 Heterogeneous expression of HLA-I APM components in tumours

It is generally accepted that tumour could evade immune response by aberrant expression of classical and non-classical HLA-I molecules, which are frequently early events during carcinogenesis[386]. Such abnormalities have clinical significance[387] since they are often correlated with disease progression, disease aggressiveness, poor patient survival[357] and/or limited response to immunotherapy[388]. Indeed, in regard to the latter tumours with acquired classical HLA-I resistance mechanisms to ICP inhibitor therapy or adoptive T-cell transfer have acquired genetic deficiencies or downregulation of APM components resulting in the loss or reduced expression of HLA-I surface antigens[389].

Primary tumours are mostly composed of homogeneous HLA-I positive cancer cells[390]. Nevertheless, primary tumours may start to alterate their HLA-I expression pattern and the decrease of HLA-I expression can be defined as a mandatory step during their transformation process[386,391] (Fig. 6.1). The frequency of this phenomenon ranges from 4% to 95% as reported in the literature[392-395], thereby varying depending on the given tumour type, differentiation status, as well as proliferative capacity[357,395,396]. The frequently observed alterations in regard to the surface expression and/or function of HLA-I antigens equip the neoplastic cells with mechanisms to escape immune surveillance[355,393,397-401]. The malignant transformation process of cells is often associated with alterations in their gene expression pattern [386]. The underlying molecular mechanisms are either mediated by structural alterations or by deregulation(s) of HLA-I APM components at the epigenetic, transcriptional, posttranscriptional and/or posttranslational level[355,357].
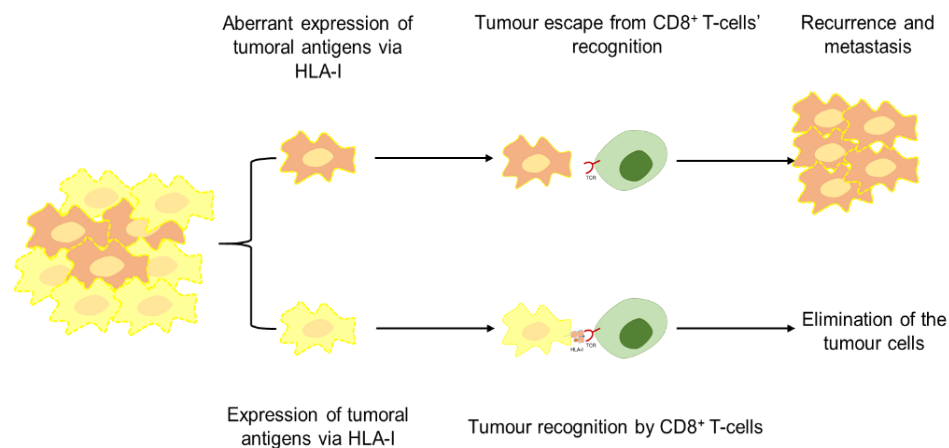
Figure 6.1. Tumour immune escape mediated by aberrant HLA-I surface expression during tumour progression
Primary tumours can consist of heterogeneous populations of cells giving rise to different cell clones undergoing immune selection. Tumour cells with normal HLA-I expression are subjected to CTL response and destruction, but new variants thereof aberrantly expressing HLA-I APM components resulting in decreased surface expression of HLA-I molecules might be spared giving rise to metastasis formation and/or recurrence.

As tumour cells, and particularly melanoma cells, are immunogenic, they can acquire a plethora of molecular mechanisms, like the deregulation of HLA-I surface expression,

in order to avoid destruction by CTLs[402]. CTLs require interaction with HLA-I molecules to recognize tumour antigens processed and presented as small peptides by the APM. Particularly, the APM components TAP1, TAP2 and TPN are crucial components for this process[161]. Downregulation of classical HLA-I molecules prevents tumour recognition and rejection by CTLs, while overexpression of non-classical HLA-I molecules disable immune cells involved in their elimination (including T- and B-cells, DCs, macrophages and NK cells)[402]. Interestingly, high expression levels of major APM components including TAP1 and HLA-I loci were directly associated with a better outcome of most cancer patients including skin cutaneous melanoma, with the exception of brain tumours, uveal melanoma and thymoma[378].

There are multiple molecular mechanisms which can contribute to the generation of phenotypes displaying altered HLA-I surface expression levels[396]. Inactivating mutations within the human HLA-I HC and β2-m genes/coding regions have been mainly described in melanoma and CRC, but at a low frequency[403], while mutations in APM components, such as TAP1, TAP2, TPN, LMP2, LMP7 and LMP10, occur even less frequently in melanoma, lung and cervical cancer[355]. Cai *et al.* analysed the expression of HLA-I APM components in several types of cancer. TAP1 and TAP2 have been defined as dysregulated in at least 40% of all the tumours analysed except for orbital melanoma, breast and ovarian cancers.

Although highly variable, loss of heterozygosity (LOH) in chromosome 6p21.3 and 15q12 (LOH-6 and LOH-15, respectively), which include parts of the HLA and the β2-m loci[386,404], respectively, are the most widespread LOH phenotypes, resulting not only in the given HLA-I haplotype loss but as a consequence in the presentation of a less diverse HLA/peptide repertoire on the tumour cell surface[405]. LOH for HLA and β2-m have been described in glioblastoma, laryngeal carcinoma, bladder carcinoma colorectal cancer and melanoma with a frequency of at least 16%[403,406-409]. LOH-15 was associated with shorter patients' survival in melanoma[406], but no causal mechanism has been as yet defined. In some tumours (melanoma, MSI-H colorectal carcinoma and bladder cancer) this chromosomal instability is not only a frequent and early event, but can be later in addition associated with other abnormalities, such as HLA-I transcriptional downregulation or β2-m mutations, altogether leading to a HLA-I loss[404,410,411]. In contrast to other epithelial tumours, a low frequency of HLA haplotype LOH-6 (6.6%) was observed in clear cell RCC[412].

Downregulation of the TAP expression level was more frequently observed in metastatic than in primary melanoma lesions or in nevi. Moreover, synchronous downregulations of TAP1, TAP2, and HLA-I were observed in 58% of primary and 52% of metastatic melanoma lesions[413]. Concerning the proteasome subunits, LMP2 was less frequently expressed than LMP7 in primary and metastatic melanoma lesions[413]. TAP1, in particular, was characterised as an independent prognostic factor for melanoma metastases[414]. Downregulation of TAP and HLA-I surface expression associates with primary melanoma lesion thickness, advanced stage of disease, reduced time to disease progression and reduced survival[134,413]. Additionally, reduced mRNA and/or protein expression levels of various APM components were described for a large series of melanoma cell lines and lesions and subsequently correlated with an increased tumour grading[415,416] thereby independently supporting the concept that the deregulation of HLA-I APM components has a significant impact on the outcome of melanoma patients.

Depending on the tumour microenvironment, the underlying molecular mechanism and the ability to eventually rescue HLA-I expression by cytokine treatments, the different molecular mechanisms responsible for HLA-I alterations can be classified in reversible ("soft") and irreversible ("hard") alterations[417]. If the molecular alteration is reversible by cytokine treatment (''soft'' lesion), the HLA-I expression level, and as a consequence the specific T-cell–mediated recognition/response will be restored. Thus, such a "soft" lesion will likely regress in response to treatment. However, if the molecular defect is structural (''hard'' lesion), the HLA-I expression will remain at a low level, the escape mechanism will prevail and the primary tumour or the metastatic lesion will further progress[417]. Consequently, immunotherapy building on CD8^{+} T-cells will be ineffective in patients harbouring HLA-I deficient or negative cancer cells[418]. In metastatic melanoma patients, regression of metastasis after immunotherapy was associated with the expression of HLA-I APM components and IFN-regulated genes (HLA-I HC, β2-m, HLA-A, B, and C)[419], underlining the importance of monitoring the levels of HLA-I expression in order to define reversible versus non-reversible alterations in metastases that will further determine the progression or regression after immunotherapy[419].

Moreover, the deregulation of the expression of HLA-I APM components could also occur at the epigenetic, transcriptional and/or posttranscriptional levels[355,357,420] providing tumours cells with additional mechanisms to limit immune responses, thereby resulting in tumour growth, metastasis formation and evasion from host immune attacks.

Thus, the concepts of posttranscriptional regulation mechanisms of HLA-I APM components mediated either by miRs and/or RBPs were analysed in this thesis, in particular since discordant mRNA and protein expression pattern of APM components, including TAP1, TAP2, TPN, and HLA-I surface expression has been frequently described in tumours of distinct origin, including the panel of extensively analysed human melanoma cell lines (§5.1 Heterogeneous expression of HLA-I APM components in melanoma cell lines).

6.2 Posttranscriptional regulation of HLA-I APM components mediated by miRs
This study suggests that the expression of HLA-I APM components in melanoma cell lines and tumour lesions of melanoma patients might be at least in part controlled by several miRs resulting in a deregulation of surface expression levels of HLA-I molecules. The latter is often linked with an aberrant immune recognition and a reduced survival of melanoma patients (Fig. 6.2).
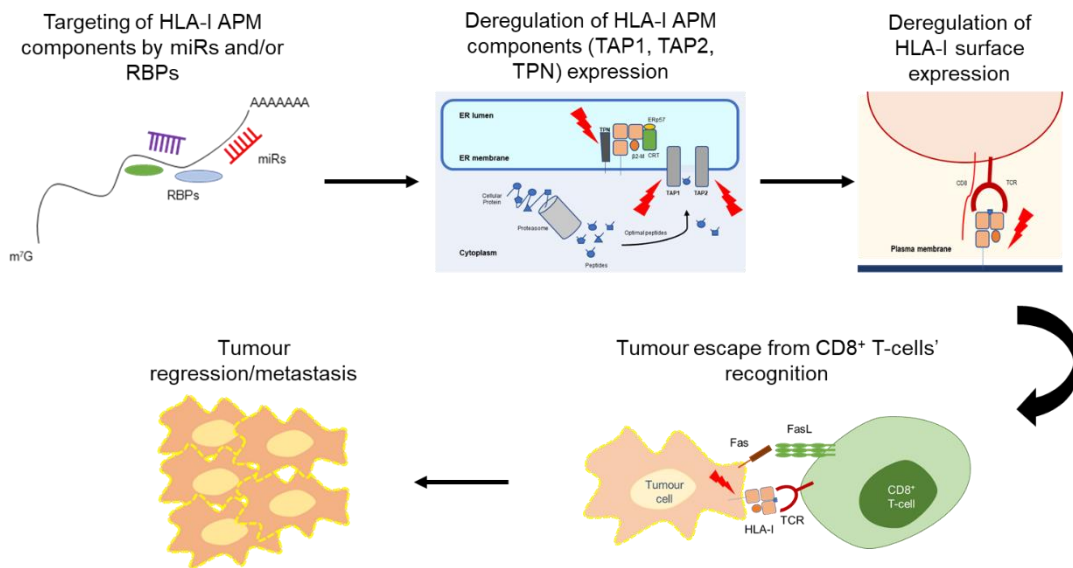
Figure 6.2. Schematic representation of the suggested model of this study
Upon posttranscriptional regulation of key HLA-I APM components (such as TAP1, TAP2 and TPN) by miRs, such as miR-200a-5p, miR-26b-5p and miR-21-3p, or RBPs like IGF2BP1 and IGF2BP3, the expression of these components can be deregulated, resulting in aberrant HLA-I surface expression. CD8^{+} T-cells may not be able to detect and destroy the deregulated tumour cells, which will escape the immune destruction and be able to lead to tumour regression and metastasis.

Amongst the various candidate miRs targeting the TAP1 3'-UTR, in particular the miR-200a-5p is of interest. The miR-200 family includes 5 members (miR-200a, miR-200b, miR-200c, miR-141 and miR-429) located at two different genomic clusters: the first cluster consists of miR-200a, miR-200b and miR-429 on chromosome 1 and the second of miR-200c and miR-141 on chromosome 12[421,422]. Under physiological conditions, the miR-200 family is involved in establishing an epithelial cell barrier[423,424], but is also known for its role in cancer metastasis by inhibiting the epithelial mesenchymal transition (EMT) process [425]. Three members of the family: miR-200a, miR-200b and miR-429 were previously defined as upregulated in breast cancer, ovarian cancer and melanoma as determined via high-resolution arrays based on comparative genomic hybridization[426]. Particularly miR-200a-5p overexpression has recently been found in several types of cancer, such as NSCLC[427], ovarian cancer[428], papillary thyroid carcinoma[429] and heart disease[430,431], but as yet neither linked to modulations of the expression levels of APM components nor of HLA-I molecules. MiR-200a-5p has also been reported to play important role in the innate immune response of zebrafish larvae against bacterial invasion during *Vibrio parahaemolyticus* (Vp13) infection, since dre-miR-200a-5p was among the miRs that could participate in the innate immune response by regulating the blood and lymphatic system, haematopoiesis, energy metabolism, cell migration and communication, protein synthesis, signal transduction, and the transmission of neural signals[424].

In the current study it was shown that miR-200a-5p can directly regulate the expression level of TAP1 thereby subsequently modulating the HLA-I surface expression levels in melanoma cells. MiR-200a-5p was initially found by *in silico* prediction to bind to the TAP1 3'-UTR. This predicted binding was indeed confirmed in the course of this thesis by the dual luc reporter assay and the calculation of the free binding energy. The relative expression level of miR-200a-5p in 40 melanoma cell lines was inversely

correlated with the relative TAP1 mRNA expression levels, supporting the predicted mechanism. Moreover, a specific effect of miR-200a-5p overexpression on TAP1 protein expression level, but not at the TAP1 mRNA level, was detected in two melanoma cell lines. In general, miRs direct the RISC complex to downregulate its target expression either by mRNA degradation and/or by translational repression[205,432-434]. Although often typically mild[435,436], the most relevant readout of the miR regulatory effects are at the protein level[432]. It is, however, shown in both zebrafish and fruit fly that the translational inhibition is the favoured mechanism of miR-mediated gene silencing[437]. Upon overexpression of miR-200a-5p with mimics, a specific downregulation of TAP1 mRNA and protein levels was observed resulting in a downregulation of HLA-I surface molecules that could be detected with the pan-specific anti-HLA-ABC antibody. Since in particular HLA-BC expression was affected by this miR, possible HLA allele specific (TAP-dependent) functional consequences of TAP1 downregulation could be suggested. Interestingly, this might depend on the HLA-I surface expression levels of melanoma cells, since miR-200a-5p affects the HLA-I expression level of the HLA-I high and medium, respectively, expressing cell line BUF1379 and FM3, but not of the HLA-I low expressing cell line FM81. Furthermore, the miR-200a-5p-mediated reduced HLA-BC expression level was accompanied by an increased number of CD107a positive NK cells upon co-culture with miR-200a-5p expression melanoma cells. No effect of miR-200a-5p overexpression was detected on other APM components supporting the specific binding of miR-200a-5p to the TAP1 3'-UTR.

In order to also verify the role of the miR-200a-5p *in vivo*, its expression was correlated with the corresponding TAP1 protein expression levels along with the immune cell infiltrates (thereby mainly focussing on CD8+ T-cell infiltrates). For this reason, FFPE tumour samples were processed and analysed by immunohistochemistry. By comparing ulcerated and non-ulcerated primary tumours, the pattern and composition of the cellular immune cell infiltrates were analysed (i.e. concerning T-lymphocytes, macrophages and dendritic cells) as well as presentation of tumour antigens (TAP1). The expression pattern of various markers specifically identifying tumour-infiltrating lymphocytes (CD3, CD4 and CD8), macrophages (CD11 and CD163) and dendritic cells (CD123) were evaluated semi-quantitatively and graded into four categories (0%, 1-10%, 11-30%, >30%) by three independent investigators[339,354]. Concerning the characteristics of the patients' population, the median age at first melanoma diagnosis was 64.0 and the median Breslow thickness was ranged from 0.8 mm to 17 mm. It has been previously shown that alterations in the APM components could influence the efficacy of adjuvant immunotherapy in ulcerated primary melanomas, as the downregulation of TAP1 and TAP2 in primary melanomas have been proposed as prognostic factors for metastasis formation[414]. IFN-α has been reported to upregulate TAP1 expression levels in PMBCs of treated patients as well as in murine blood and tumour tissue in this context[438]. However, Koeblinger *et al.* could neither reveal differences in TAP1 expression between ulcerated and non-ulcerated tumours from 112 patients, nor confirm the value of TAP1 expression as a predictive marker of recurrence[339].

The expression of TAP1 and the CD3, CD4, CD8, CD11, CD163, CD123 molecules was evaluated by pathologists and RNA was extracted for miR analysis from 26 patients from the lowest and highest categories. MiR-200a-5p levels were inversely correlated with the detectable TAP1 protein levels. High levels of miR-200a-5p were

detected in patients with low levels of TAP1 supporting the hypothesis that miR-200a-5p can modulate the expression of TAP1 at the posttranscriptional level. Interestingly, the densities of the corresponding immune cell infiltrates, such as CD8^{+} cells as determined by immunohistochemistry were also inversely correlated with the miR-200a-5p expression levels thereby further supporting its role as an immune modulatory miR.

To identify new miRs regulating TAP1 expression, the miTRAP assay was employed[322,323,439,440]. Functional miRs are necessarily associated with one of the four human Argonaute proteins (AGO1-4) to form the RISC complex[322]. Since the majority of miRs is incorporated into AGO2[441], Western blot-based detection of co-purified AGO2 in miTRAP eluates indirectly indicates the presence of miRs[322]. Therefore, the detection of AGO2 in the miTRAP eluates of TAP1 3'-UTR was a first qualitative sign indicated that miRs can bind to TAP1 3'-UTR[374]. After small RNA next generation sequencing analysis at Novogene (Hong Kong), a group of 352 out of 2693 (13.07%) mature miRs determined by miRBase[213] were enriched in the two biological replicates of the TAP1 3'-UTR eluates when compared to the MS2 control, using cell lysate from the MZ-Mel2 melanoma cell line (TAP1 mRNA[+] and TAP1 protein[-]). Some of the strongly enriched miRs were miR-340-5p, miR-532-5p, miR-516b-3p, miR-26a-5p, miR-26b-5p, miR-590-3p, miR-21-3p and miR-22-3p, all of which were *in silico* predicted at least from 2 of the selected prediction tools (Appendix A.7) and they have been already published to regulate cancer progression.

Among the strongly enriched miRs in TAP1 3'-UTR eluates, two candidate miRs attracted particular interest: miR-26b-5p and miR-21-3p. Their enrichment was further confirmed in the TAP1 3'-UTR eluates by RT-qPCR. MiR-26b-5p belongs to the miR-26 family, while miR-21-3p to miR-21, respectively. MiR-21-3p was strongly enriched particularly in miTRAP eluates of TAP1 3'-UTR, while miR-26b-5p was also enriched in miTRAP eluates of TPN 3'-UTR using cell lysate from the MKR melanoma cell line (TPN mRNA[+] and TPN protein[-]), but it is *in silico* predicted to bind to the TAP1 3'-UTR by more bioinformatics tools than to TPN 3'-UTR. Both of these candidate miRs are newly identified to target TAP1 3'-UTR, since none of them was ever published to target TAP1, TPN or any of the other HLA-I APM components[3,4].

The miR-26 family has been reported to play diverse roles in regulating key aspects of cellular growth, development, and activation[442]. The human and mouse miR-26 family include 3 members (miR-26a-1, miR-26a-2 and miR-26b). The predicted hairpin precursor sequence of miR-26a-1, miR-26a-2 and miR-26b are localized on chromosomes 3, 12 and 2, respectively. The mature miRs for miR-26a-1 and miR-26a-2 have almost the same sequence which differ by two nucleotides from the mature miR-26b sequence[442]. Interestingly, miR-26b is a negative regulator of the NF-kB pathway, which is important for the expression of many immune modulatory molecules including cytokines and APM components[443]. The role of miR-26b-5p in cancer and its targets in a range of cell types is summarized in table A.9.1.

Regarding miR-21-3p, pri-miR-21 is located in the 3'-UTR of the vacuole membrane protein 1 (VMP1) gene at chromosome 17 (17q23.2)[444]. The hairpin pre-miR-21 is further processed by RNase III complex, generating miR-21–5p (the guide strand) and miR-21–3p (the passenger strand)[445]. MiR-21-5p is one of the most analysed miRs, which has been overexpressed in any type of solid tumour. It may participate in the process of melanoma occurrence, development, and metastasis[446-448] and particularly its expression was correlated with Breslow thickness and advanced clinical stage and

inversely correlated with 5-year disease-free or overall survival of patients with cutaneous melanoma[449]. Interestingly, it is already suggested to be potentially used as an anticancer agent for the treatment of melanoma[450]. Researchers have started to show interest also on miR-21-3p[451], reporting its role in cutaneous melanoma[452], ovarian cancer[453,454], laryngeal[455] or esophageal squamous cell carcinoma[456], breast cancer[457], colorectal carcinogenesis[458] and as exosomal miR in RCC[459]. Nevertheless, both the guide and the passenger strands have been identified to target equal numbers of genes and that both could suppress the expression of their target genes[445]. The role of miR-21-3p in cancer and its targets in a range of cell types is summarized in table A.9.2.

In the current study, miR-26b-5p and miR-21-3p have been *in silico* predicted by selected bioinformatics tools and, using the RNAhybrid prediction tool, the binding affinity of complementary structures was calculated between the putative miRs and the target TAP1 3'-UTR demonstrated a high free binding energy of -25.4 kcal/mol for miR-26b-5p and -20.3 kcal/mol for miR-21-3p, suggesting a high probability of interaction for both candidate miRs. After further validation by qPCR in comparison to the MS2 and input controls their binding to the TAP1 3'-UTR was further confirmed by dual luc reporter assays.

Upon overexpression of miR-26b-5p with mimics, a specific downregulation of the corresponding TAP1 mRNA and protein levels by more than 30% were observed in the melanoma transfectants resulting in a downregulation of HLA-I-molecules that could be detected with the pan-specific anti-HLA-ABC antibody. Since in particular the HLA-A2 expression levels were affected in response to miR-26b-5p overexpression, possible even HLA allele specific (yet still TAP-dependent) functional consequences of TAP1 downregulation could be suggested. Furthermore, the miR-26b-5p-mediated reduced HLA-A2 expression was accompanied by a decreased number of CD107a positive MART T-cells upon coculture with miR-26b-5p expression melanoma cells. Upon overexpression of miR-21-3p with mimics, a downregulation by approximately 25% was observed at TAP1 protein expression in two melanoma cell lines, but not at the TAP1 mRNA level. Interestingly, its overexpression resulted in an upregulation of HLA-ABC and HLA-BC surface expression in BUF1379 cell line. No effect of miR-26b-5p or miR-21-3p overexpression was detected on other APM components suggesting a TAP1-specific effect. Upon inhibition of the miRs expression with inhibitors, TAP1 mRNA and protein levels were increased in both melanoma cell lines, which was accompanied by an increased HLA-ABC and HLA-A2 surface expression.

In order to verify the role of the miR-26b-5p and miR-21-3p *in vivo*, their relative levels were correlated with TAP1 protein expression and immune cell infiltration (mainly with CD8 T-cells infiltration) following the same procedure as was previously described in detail for miR-200a-5p. An inverse trend was observed when high levels of miR-21-3p were found in patients with low levels of TAP1, supporting our hypothesis about posttranscriptional regulation of TAP1 by miR-21-3p. The levels CD8$^+$ cells determined by immunohistochemistry analysis, were also inversely correlated with the levels of miR-21-3p supporting its immune modulatory role.

Concerning miR-9-5p, it was one of the few miRs already published to regulate TAP1, although its mode of action may be indirect since its mimic-based overexpression in NPC exerted a broad effect to many well-known IFN inducible genes. Upon its overexpression, TAP1, β2-m, proteasome subunits (e.g. PSMB8, PSMB10), classical (e.g. HLA-B, HLA-C) and non-classical HLA class I molecules (e.g. HLA-F) were

upregulated at the mRNA level[249], but the mechanism of action remains still unclear. The human and mouse miR-9 family include 3 members (miR-9-1, miR-9-2 and miR-9-3). The predicted hairpin precursor sequence of miR-9-1, miR-9-2 and miR-9-3 are localized on the chromosomes 1 (1q22), 5 (5q14.3) and 15 (15q26.1), respectively. The hairpin pre-miR-9 is further processed by RNase III complex, generating miR-9–5p (the guide strand) and miR-9–3p (the passenger strand). The mature miR-9-5p has the same sequence independently from its precursor.

Apart from its role in NPC, miR-9-5p was reported to have a suppressive role in malignant melanoma, since it was downregulated in metastatic[460] and malignant melanoma tumours[461,462]. The role of miR-9-5p in cancer and a selection of its targets in a range of cell types is summarized in table A.9.3.

Interestingly, a positive correlation was observed between the relative expression of miR-9-5p and TAP1 mRNA expression levels upon analysing 40 in-house melanoma cell lines, supporting the implying indirect mechanism shown in NPC[249]. Moreover, miR-9-5p was not found by the screening of the available *in silico* prediction tools as a candidate which might to bind to the TAP1 3'-UTR, which was further confirmed by its absence in the list of the enriched miRs in TAP1 3'-UTR miTRAP eluates provided by the sequencing company Novogene. For this reason, its binding to TAP1 3'-UTR was not tested by the dual luc reporter assay. However, upon significant overexpression of miR-9-5p with mimics into all three model melanoma cell lines (BUF1379, FM3 and FM81), upregulations of TAP1 and TPN mRNA expression levels were observed in BUF1379 tranfectants, but also the corresponding TAP1 protein expression levels were defined as increased in BUF1379 and FM3 cell lines, respectively. Finally, its overexpression subsequently led to significant upregulation of HLA-ABC surface expression in BUF1379 and HLA-BC in FM3 cells, and not only on mRNA level as it was published for NPC[249].

6.3 Posttranscriptional regulation of HLA-I APM components mediated by RBPs

Key players of the posttranscriptional gene regulation are not only miRs but also RBPs, which can also modulate the expression level of their targets by binding to their mRNA 3'-UTRs[463]. By binding to their target transcripts RBPs form ribonucleoprotein complexes which can posttranscriptionally affect the biogenesis, stability, function, transport and cellular localization of the respective mRNA[266]. This study proposes that the expression of HLA-I APM components in melanoma cell lines can be also regulated by RPBs, thereby resulting in a deregulation of the HLA-I surface expression pattern, which is often inversely linked to the survival of melanoma patients. In order to define potential RBP candidates, which might be able to modulate the expression pattern of APM components a variation of the previously described miTRAP approach was successfully applied. These RNA-AP assays differ from the basic miTRAP assays by rather focussing on the elution of proteins from such ribonucleoprotein complexes instead of eluting the bound miRs. Thus, this approach was implemented to identify potential candidate RBPs targeting either the TAP1 or the TPN 3'-UTRs (Fig. 6.2).

RBPs have been recently identified targeting HLA-I molecules and their altered expression has been shown to contribute to the immune escape of tumour cells[4]. Amongst the panel of already published RBPs regulating HLA-I molecules, the association of HLA-A with members of the muscle excess (MEX)-3 RNA-binding protein family is currently the best analysed RNP complex in this context[305,306]. Interestingly, a strong correlation of MEX-3B with the resistance to cancer

immunotherapy was observed in metastatic melanoma. MEX-3B was identified as a top candidate that decreased the susceptibility of melanoma cells to be targeted by T-cells. This was mediated by the binding of MEX-3B to the HLA-A 3'-UTR, thereby resulting in a destabilization of the targeted HLA-A transcript levels and as a consequence to decreased HLA-A surface expression levels in tumour cells. Interestingly, analyses of anti-PD-1-treated melanoma patient tumour samples suggested that higher MEX-3B expression levels were associated with the occurrence of resistance to PD-1 blockade[305]. Another member of this family, MEX-3C, was reported to regulate even allotype-specifically the expression level of HLA-A by binding to the HLA-A2 3'-UTR mRNA and subsequently inducing its degradation[306].

Moreover, the synaptotagmin binding cytoplasmic RNA interacting protein (SYNCRIP) has been reported to regulate at the posttranscriptional level the protein expression pattern of HLA-A by triggering alternative polyadenylation signals (PAS)[307]. Upon downregulation of SYNCRIP by siRNA a selective increase of the surface expression level of an HLA-A allotype that used primarily the long 3'-UTR was observed, whereas the allotype expressing the shorter form, which differs in length by about 100 bp, remained unaffected[307]. Recently, the heterogeneous nuclear ribonucleoprotein R (HNRNPR) was identified as the first positive posttranscriptional regulator for MHC-I molecules. It was documented to bind to the 3'-UTR of classical (HLA-A, HLA-B, HLA-C) and non-classical (HLA-G) MHC-I molecules to enhance their stability and expression pattern and to modulate the cytotoxic activity of NK cells. Consequently, the knockdown of HNRNPR reduced the expression level of specific HLA-C subtypes and therefore increased killing by NK cells[259]. However, the specific binding site of HNRNPR or putative interaction partner(s) remain currently unknown. Regarding TAP1 and TPN, no regulation by RBPs has been reported until now, emphasizing the need of further research in order to reveal the significance of their posttranscriptional regulation mediated by RBPs. Tables 1.2 and 1.3 (§ 1.5 Posttranscriptional regulation of gene expression) lists known interactions of miRs and RBPs with HLA-I molecules and APM components.

By performing RNA affinity purification assays, candidate RBPs were for the first time successfully identified, which either bind to the 3'-UTRs of TAP1 or TPN and thus are likely involved in controlling the expression levels of these APM components. As a consequence, these RBPs might modulate the HLA-I surface expression level and the recognition of the tumour cells by the immune cells. For identification of RBPs binding to the TAP1 3'-UTR, the RNA-APs were performed using cell lysates from MKR melanoma cells (TAP1 mRNA+, TAP1 protein+). After separation of the co-purified proteins, protein bands were picked and the sample were prepared for the MALDI-TOF MS analysis but, except the Y box binding protein 1 (YBOX1) and YBOX3, no other proteins have been specifically identified binding to TAP1 3'-UTR in comparison to HLA-G 3'-UTR, which served as a control for unspecific binding of RBPs, despite the fact that several RBPs have been *in silico* predicted to bind to TAP1 3'-UTR and correlated with several types of tumour, including cutaneous melanoma, using the starbase v2.0 prediction tool[342,343].

Concerning the RBPs targeting the TPN 3'-UTR, the eluates together with the respective control samples were sent for MS analysis at the core facility for MS (Dr. Matt Fuszard, Martin-Luther-University Halle-Wittenberg). The RNP complexes were herefore established using cell lysates of the MZ-Mel2 melanoma cell line (TPN mRNA+, TPN protein+). The valid, specific for TPN 3'-UTR identified RBPs should have

had a number of spectra ≥ 3 and shouldn't have been identified in the controls' eluates (TGFBR2 3'-UTR and HLA-G CDS). Interestingly, after analysis of the MS data (Table 5.5), more candidate RBPs were enriched in the eluate of TPN-1 3'-UTR (1-1020nt) (55.21%) than in the TPN-2 3'-UTR (907-2008nt) (44.79%) suggesting a possible preference for binding at the first part of TPN 3'-UTR. Upon *in silico* analysis, several of the strongly enriched candidate RBPs were also predicted using the prediction tool starBase v2.0[342,343]. Among the enriched candidate RBPs targeting TPN 3'-UTR, the insulin growth factor 2 binding protein family (IGF2BP) was of particular interest.

Insulin-like growth factor (IGF) 2 is a member of the insulin family of polypeptide growth factors which regulate both cell development and cell growth[464,465]. Its expression is tightly controlled during development by epigenetic, transcriptional and translational regulation mechanisms[465,466]. It is also modulated posttranslationally by RBPs by binding to IGF2 transcripts thereby mediating their localization, stability, and translation[266,271]. These proteins include the IGF2BPs protein family, consisting of IGF2BP1, IGF2BP2 and IGF2BP3[467]. They have a conserved domain structure including two N-terminal RNA recognition motifs (RRM) and four C-terminal hnRNP K homology (KH) domains[468], which recognize and bind to m^6A-mRNAs, conferring IGF2BPs the affinity towards RNA and the regulation capacity of multiple target transcripts[271]. *In vitro* studies revealed that IGF2BPs serve as posttranscriptional fine-tuners modulating the expression of genes implicated in the control of tumour cell proliferation, survival, resistance to chemotherapy, the expression of oncogenic factors (KRAS[469], c-MYC[470-472] and MDR1[472]) and metastasis formation[473]. Despite their high degree of similarity and their high abundancies during embryogenesis[467], only IGF2BP2 is ubiquitously expressed in adult mouse tissues, while in cancer cells, either *de novo* synthesis or at least an upregulation of IGF2BP1 and IGF2BP3 have been described so far thereby defining these two family members as bona fide oncofetal proteins[468]. Consistently, the upregulated expression levels of IGF2BP1 and IGF2BP3 have been reported for various human cancers[468,473-476], such as breast, colon, skin and lung adenocarcinoma[477] and correlate with poor overall prognosis and increased metastasis formation.

IGF2BP1 is located on chromosome 17q21.32 and two transcript variants encoding different isoforms (with short and long 3'-UTR) have been found for this gene. The expression of the shorter mRNA isoform of IGF2BP1 has been reported to lead to far more oncogenic transformation than the expression of the full-length variant/isoform[478]. It was initially identified as a protein which is involved in the stabilization of MYC trancripts[470], by preventing their degradation and resulting in the promotion of tumour cell proliferation and survival in various cancer types. It controlled also the subcellular sorting of ACTB transcripts in primary fibroblasts and neurons by binding to the ACTB 3'-UTR[479] and, later, to enhance neurite outgrowth and axonal guidance[480]. However, although it has been traditionally regarded as an oncogene and potential therapeutic target for cancers, a few studies have also demonstrated its tumour-suppressive role. Thus, the details about the apparently contradictory functions of IGF2BP1 remain as yet unclear[474]. Interestingly, a modulation of interconnectivity between IGF2BP1 and its targeted mRNAs or ncRNAs has been observed in HCC, where miR-625[481], miR-9[482], miR-1275[483] and miR-196b[484] targeted IGF2BP1 and further affected HCC development, while in cervical cancer miR-124-3p inhibited cell growth and metastasis formation by targeting IGF2BP1[485]. Particularly in melanoma, the expression of IGF2BP1 was upregulated[486,487], affecting several downstream proto-oncogenes and

oncogenic signaling pathways that mediate tumour development, survival, and drug resistance[487]. In metastatic melanoma, IGF2BP1 expression was observed to confer a resistance to chemotherapeutic agents, whereas its inhibition or knockdown enhanced the effects of chemotherapy and reduced tumourigenic characteristics[487]. Moreover, IGF2BP1 knockdown was reduced the expression levels of c-MYC, contributing to the suppression of NF-kB activity and of anchorage-independent growth of melanoma cells and their proliferation, as well as inducing apoptosis[488]. Thus, it is strongly suggested as a potential reduce-chemoresistance target for melanoma.

IGF2BP2 is located on chromosome 3q27.2. Alternative splicing and promoter usage results in multiple transcript variants[467]. Most notably, it was correlated with an elevated risk of type two diabetes[489] and identified as a modulator of the mTOR signalling pathway[490]. Several target mRNAs have been reported to be regulated by IGF2BP2 in a variety of diseases and disorders such as diabetes and cancer[491,492].

IGF2BP3 is located on chromosome 7p15.3 and was initially identified due to its high abundance in pancreatic cancer tissue[493]. Interestingly, based on current publications, it appears to be the mainly expressed family member in human cancer[494]. It has been significantly higher expressed in metastatic melanomas than in primary cutaneous melanoma, while none of the benign nevi and dysplastic nevi expressed IGF2BP3. Thus, IGF2BP3 may be useful diagnostically as a marker to differentiate melanoma from benign, dysplastic or Spitz nevi[495]. Various studies reported upregulated expression of IGF2BP3 in keratoacanthomas, SCC of the skin[496], melanoma[495,497-499], merkel cell carcinoma and ovarian cancer[500]. As observed for various other solid cancers, a higher incidence of IGF2BP3 expression was also observed in invasive SCC of the skin[496] as well as in metastatic melanoma[495,498]. Notably, it was revealed that the expression of IGF2BP1 and/or IGF2BP3 in metastatic melanoma could be increased due to chromosomal gain[499]. In agreement with this findings, highly expressed IGF2BP1 enhanced the migratory potential and a mesenchymal-like cell phenotype in melanoma-derived tumour cells[501]. Recently, silencing of cerebellar degeneration-related 1 antisense (CDR1as), a regulator of miR-7, was reported to be associated with melanoma progression, by promoting invasion as demonstrated *in vitro* and metastasis formation as demonstrated *in vivo* via a miR-7-independent but IGF2BP3-mediated mechanism[502].

Based on the aforementioned publications, IGF2BP1 and IGF2BP3 have been presented in many cases as potent posttranscriptional oncogenes, enhancing tumour growth, drug-resistance and metastasis formation. It has been also mentioned that the paralogue-detection techniques have been neglected by several studies and the use of paralogue-specific antibodies and transgenic mouse models was strongly recommended in order to explore their putative synergistic action *in vivo* and their potential as cancer biomarkers[473]. For these reasons, it was quite motivating to examine the role of IGF2BPs in regard to its potency to mediate the posttranscriptional regulation of the TPN expression level and subsequently its impact on the deregulation of the HLA-I surface expression pattern.

Upon qPCR analysis, the mRNA levels of IGF2BP1 or IGF2BP3 and TPN were evaluated in 40 melanoma cell lines normalized to melanocytes. As it was also mentioned before[473,474,488,494-496], IGF2BP3 has been strongly higher expressed in the majority of the metastatic melanoma cell lines in comparison to the mRNA levels in melanocytes. In the case of IGF2BP1, the difference in mRNA expression was even stronger between the melanoma cell lines and the melanocytes. Moreover, it was also

possible to verify the *in silico* predicted negative correlation between the mRNA levels of the two IGF2BPs and TPN in the melanoma cell lines.

Upon *in silico* prediction analysis using the bioinformatics tool starBase v2.0[342,343], IGF2BP1 and IGF2BP3 have been predicted to bind to TPN in several types of tumours, such as breast cancer, ovarian cancer and SKCM. Interestingly, a statistically significant negative correlation between the expression levels of IGF2BP1 or IGF2BP3 and TPN was observed in SKCM, implying a potential immune modulatory role of these RPBs. In order to analyse the clinical relevance of the candidate RBPs with the survival of melanoma patients, the databases "Xena" (https://xenabrowser.net/) and "R2: microarray analysis and visualization platform" (http://r2.amc.nl) were selected. In the "R2: Tumour Melanoma – Jöhnsson – 214 – custom – ilmnht12v4" dataset, higher IGF2BP3 mRNA transcript levels were statistically significant correlated with higher disease specific survival probability, while in primary melanoma patients IGF2BP1 expression was negatively correlated with overall survival and IGF2BP3 with disease specific survival and free survival interval, respectively, suggesting a possible role of these oncogenic RBPs in melanoma development, as it is already discussed[473,474].

Upon overexpressing or knocking down of the candidate RBPs by performing expression assays (qPCR, Western blot and flow cytometry analyses), none of the candidates affected significantly the expression levels of TPN, although they did deregulate HLA-I surface expression levels in MZ-Mel2 cell line. Interestingly, the MZ-Mel2 transfectants overexpressing IGF2BP3 showed increased HLA-I surface expression in comparison to the control transfectants, while the MZ-Mel2 transfectants with siRNAs against IGF2BP3 expressed lower HLA-I on their surface compared to the control transfectants. Moreover, overexpression of IGF2BP1 resulted in upregulation of HLA-I surface expression in MZ-Mel2 cells, but no significant effect was observed upon its knock down. The observed deregulation of HLA-I surface expression can suggest the regulation of HLA-I and/or other members of the APM directly or indirectly by the IGF2BPs. Since until now no interactions were documented between RBPs and APM components, the identification of novel RBPs potentially regulating TAP1 or TPN at the posttranscriptional level can be of great importance.

In response to the defined deregulation of either IGF2BP1 or IGF2BP3, several proteins were successfully identified as being specifically and statistically significant differentially expressed after MS analysis. Each group of these differentially expressed proteins was subjected to computational analysis using the STRING database and a number of pathways and functional subsystems were retrieved thereby depending both on the given target as well as its expression modulation (IGF2BP1 or IGF2BP3, overexpression or knock down transfectants) (Appendix A9). Data from the GO and the KEGG pathway analyses strengthen the assumption that the identified, dysregulated proteins are involved in multiples pathways in melanoma, such as "miRNAs in cancer" (upon knock down of IGF2BP1, $p=0.0297$), "proteasome and metabolomic pathways" (upon knock down of IGF2BP3, $p=0.00027$ and $p=0.0052$, respectively), "oxidative phosphorylation" (upon overexpression of IGF2BP3) and others.

Apart from identifying new candidate miRs or RBPs regulating the TAP or TPN, it would be also quite interesting to validate the combinational effect of enriched miRs and RBPs bound to TAP1, TAP2 or TPN 3'-UTR. Hence, it should be further studied to reveal its significance.

In conclusion, the pivotal role of TAP within the adaptive immune system predestines it as a target for infectious diseases and malignant disorders, such as BLS I and cancer, respectively. For this reason, the development of therapies or drugs requires a detailed comprehension of structure and function of this ABC transporter and other member of the MHC-I assembly, such as TPN. Better understanding of the TAP and TPN structure and regulation will crucially affect the development of therapies or novel drugs, design of inhibitors or vaccination strategies against such diseases.

7. Summary

Tumours are characterised by an aberrant cell proliferation rate along with the potential to invade or spread to other parts of the body. Melanoma is acknowledged as one of the most immunogenic types of human tumours. "Avoiding immune destruction" is a key hallmark of cancer cells which can be accomplished via several immune escape mechanisms limiting their recognition and destruction by either CD8$^+$ T- or NK cells. Such tumour-mediated escape mechanisms can be associated with structural alterations, epigenetic modulations, loss of heterozygosity as well as posttranscriptional or posttranslational regulation mechanisms of genes associated with the HLA-I APM thereby limiting the HLA-I surface expression levels.

In regard to the HLA-I APM, in particular the TAP subunits TAP1 and TAP2 along with the chaperone TPN are functionally critical components for the binding of peptide fragments, since TAP stabilizes the HC/β2-m heterodimers and TPN facilitates the peptide loading onto empty HLA-I molecules. However, in addition to the presentation of such antigenic peptide ligands in combination with classical HLA-I molecules to CD8$^+$ T-cells, presentation of non-classical HLA-I molecules mediating inhibitory stimuli to NK cells can be involved in limiting cellular immune responses.

In the context of the current thesis, the aspects of posttranscriptional regulations of HLA-I APM components by miRs and RBPs were analysed in more detail, since a heterogeneous and discordant mRNA and protein expression pattern of several HLA-I APM components, including TAP1, TAP2, TPN next to the HLA-I surface expression rate has been frequently described in tumours of distinct origin, including several in-house extensively characterized human melanoma cell lines. Thus, it was of great interest to define miRs and RBPs which can affect the expression of such immune regulatory molecules in tumour and immune cells, thereby leading to the escape of tumour cells from the immune surveillance or at least lowering their immune response capacity.

Based on the successful identification of novel miRs and RPBs by performing high throughput analyses in combination with the miTRAP and RNA-AP assays, respectively the focus was set on defining posttranscriptional regulators of TAP1, TAP2 or TPN, targeting the respective 3'-UTRs. Moreover, the specific binding of the candidate miRs miR-200a-5p, miR-26b-5p and miR-21-3p to the TAP1 3'-UTR have been successfully confirmed via dual luciferase reporter assays.

In addition, the expression rates of selected candidate miRs were not only correlated with the corresponding protein expression rates in a panel of model cell lines but also in a series of primary melanoma lesions along with their associations with relevant clinical parameters. Furthermore, their impact in regard to the susceptibility to undergo lysis be either CD8+ T- or NK cells were assessed.

The presented data show that miR-mediated modulations of APM components can be associated with altered immune recognition pattern thereby having an impact on overall survival rates of melanoma patients. Thus, miR-200a-5p, miR-26-5p and miR-21-3p, together with miR-9-5p might be worth to be considered as potential future candidate biomarkers or eventually even could be further developed towards novel therapeutic targets for melanoma patients.

Aside from these miR targets also a set of candidate RBPs was successfully identified which bind to either the 3'-UTRs of TAP1 or TPN, respectively. Amongst them, the roles of the candidate RBPs IGF2BP1 and IGF2BP3 have been characterized in more

detail. Next to their impact on the modulation of the expression rates of the targeted APM components and on overall HLA-I surface expression levels. For IGF2BP transfectants comparative proteomic profilings versus respective controls resulted even in the successful identification of differentially expressed proteins which could further linked to functional networks, thereby implying that the dysregulation of these RBPs might be worthy to be addressed in further studies.

Taken together, by the identification of these novel immune modulatory miRs and RBPs targeting TAP1, TAP2 or TPN, this study underlines the importance of the initially proposed posttranscriptional control mechanisms for HLA-I APM components and their likely role in contributing at least to some extent to the frequently observed immune escape promoting tumour growth. These molecules might thus be used as novel predictive markers or even as targets for future combinatorial cancer immunotherapy approaches.

Zusammenfassung

Tumore zeichnen sich durch eine aberrante Zellproliferationsrate sowie die Fähigkeit aus, in andere Körperteile einzudringen oder sich auszubreiten. Das Melanom gilt als einer der immunogensten Tumore. Die Vermeidung der Zerstörung durch Immunzellen ist ein Schlüsselmerkmal von Krebszellen, das über mehrere *immune escape* Mechanismen erreicht werden kann, die ihre Erkennung und Zerstörung durch CD8$^+$ T- oder NK-Zellen einschränken. Solche tumorvermittelten Fluchtmechanismen können mit strukturellen Veränderungen, epigenetischen Modulationen, Verlust der Heterozygotie sowie posttranskriptionellen oder posttranslationalen Regulationsmechanismen assoziiert sein, die mit dem HLA-I-APM assoziiert sind, wodurch die HLA-I-Oberflächenexpressionsniveaus begrenzt werden.

In Bezug auf das HLA-I-APM sind insbesondere die TAP-Untereinheiten TAP1 und TAP2 zusammen mit dem Chaperon TPN funktionell kritische Komponenten für die Bindung von Peptidfragmenten, da TAP die HC / β2-m-Heterodimere stabilisiert und TPN die Peptidbeladung auf leere HLA-I-Moleküle erleichtert. Zusätzlich zur Präsentation solcher antigener Peptidligenden in Kombination mit klassischen HLA-I-Molekülen gegenüber CD8$^+$-T-Zellen kann die Präsentation nicht klassischer HLA-I-Moleküle, die inhibitorische Stimuli gegenüber NK-Zellen vermitteln, an der Begrenzung der zellulären Immunantworten beteiligt sein.

Im Rahmen der vorliegenden Arbeit wurden die Aspekte der posttranskriptionellen Regulation von HLA-I-APM-Komponenten durch miRs und RBPs analysiert, da ein heterogenes und nicht übereinstimmendes mRNA- und Proteinexpressionsmuster bei mehreren HLA-I-APM-Komponenten, einschließlich der TAP1-, TAP2-, TPN- und HLA-I-Oberflächenexpressionsrate häufig bei Tumoren beschrieben wurde. Daher war es von großem Interesse, miRs und RBPs zu definieren, die die Expression solcher Immunregulationsmoleküle in Tumor- und Immunzellen beeinflussen können, wodurch Tumorzellen aus der Immunüberwachung entkommen oder ihre Immunantwortkapazität verringern.

Basierend auf der erfolgreichen Identifizierung neuartiger miRs und RPBs durch die Durchführung von Hochdurchsatzanalysen in Kombination mit den miTRAP- und RNA-AP-Assays wurde der Schwerpunkt auf die Definition posttranskriptionaler Regulatoren von TAP1, TAP2 oder TPN gelegt, die auf die jeweiligen 3'-UTRs abzielen. Darüber hinaus wurde die spezifische Bindung der Kandidaten-miRs miR-200a-5p, miR-26b-5p und miR-21-3p an die TAP1 3'-UTR erfolgreich über Dual-Luciferase-Reporter-Assays bestätigt.

Darüber hinaus korrelierten die Expressionsraten ausgewählter miRs-Kandidaten nicht nur mit den entsprechenden Proteinexpressionsraten in einer Vielzahl von Modellzelllinien, sondern auch in einer Reihe von primären Melanomläsionen sowie deren Assoziation mit relevanten klinischen Parametern. Darüber hinaus wurde ihre Auswirkung auf die Anfälligkeit für eine Lyse von entweder CD8$^+$ T- oder NK-Zellen bewertet.

Die präsentierten Daten zeigen, dass miR-vermittelte Modulationen von APM-Komponenten mit einem veränderten Immunerkennungsmuster assoziiert sein können, wodurch sich dies auf die Gesamtüberlebensrate von Melanompatienten auswirkt. Daher könnten miR-200a-5p, miR-26-5p und miR-21-3p zusammen mit miR-9-5p als potenzielle zukünftige Kandidaten für Biomarker in Betracht gezogen oder

möglicherweise sogar in Richtung neuartiger therapeutischer Ziele für Melanompatienten weiterentwickelt werden.

Abgesehen von diesen miR-Zielstrukturen wurden auch eine Reihe von Kandidaten-RBPs erfolgreich identifiziert, die an die 3'-UTRs von TAP1 bzw. TPN binden. Unter diesen wurde die Rolle der Kandidaten-RBPs IGF2BP1 und IGF2BP3 detaillierter charakterisiert. Neben ihrem Einfluss auf die Modulation der Expressionsraten der Ziel-APM-Komponenten veränderten sie ebenfalls das HLA-I-Oberflächenexpressionsniveau. Für IGF2BP-Transfektanten führten vergleichende proteomische Profilierungen gegenüber den jeweiligen Kontrollen sogar zur erfolgreichen Identifizierung differentiell exprimierter Proteine, die weiter mit funktionellen Netzwerken verknüpft sein könnten, was impliziert, dass die Deregulation dieser RBPs in weiteren Studien behandelt werden könnte.

Zusammengenommen unterstreicht diese Studie durch die Identifizierung dieser neuartigen immunmodulierenden miRs und RBPs, die auf TAP1, TAP2 oder TPN abzielen, die Bedeutung der ursprünglich vorgeschlagenen posttranskriptionellen Kontrollmechanismen für HLA-I-APM-Komponenten und ihre wahrscheinliche Rolle, zumindest teilweise für die häufig beobachtete Immunflucht beizutragen, die das Tumorwachstum fördert. Diese Moleküle könnten daher als neuartige prädiktive Marker oder sogar als Ziele für zukünftige kombinatorische Krebsimmuntherapieansätze verwendet werden.

8. Outlook

Immunotherapies have emerged as highly promising approaches to treat cancer patients with a variety of tumour types but their clinical efficacy is still rather limited so that currently only a small number of cancer patients truly benefit from such treatment regimens. Despite the initial enthusiasm, particularly due to some early success rates in melanoma patients, a lot of melanoma patients still do not respond to treatments with checkpoint inhibitors. Therefore, novel therapeutical approaches are critically needed in order to further improve the efficacy of antitumoral immunotherapies. Recently gained insights into the roles of miRs and RBPs in regard to the development and progress of diseases, particularly in cancer, have turned these posttranscriptional regulators into attractive tools and/or targets for novel, improved biomarkers or even therapeutic approaches.

Understanding the tumour/immune interface at the cellular and molecular level and selecting appropriate patients for a specific immunotherapeutic agent or more likely combinatory therapy strategies depends on the optimization of biomarker identification as well as patient stratification strategies to further improve the response rates of cancer immunotherapies, which in addition might need to be tailored to the individual patient's disease status.

In this study, possible immune modulatory roles for a panel of miRs, including miR-200a-5p, miR-26b-5p and miR-21-3p were described for the first time in the context of melanoma. These miRs were shown to specifically target the 3'-UTR of the TAP1 gene, resulting in a downregulation of the TAP1 protein expression level and consequently in reduced HLA-I surface expression levels in a group of melanoma model cell lines, thereby causing an aberrant recognition by immune cells, such as CD8+ T-cells or NK cells. These initially with melanoma model cell lines established profiling data were subsequently further supported by the observed correlations of the miRs and the corresponding TAP1 protein expression levels, the immune cell infiltration rates of primary melanoma lesions as well as with the overall survival rates of metastatic melanoma patients. Therefore, the clinical relevance of these newly identified candidate miRs should be further evaluated, particularly in trials, in which treatment options are determined based on the expression pattern of the HLA-I APM components , since they have the potential to not only serve as novel biomarkers for the selection/response prediction of melanoma patients but might be even further developed into novel therapeutic targets for melanoma patients thereby contributing to further improvement of immunotherapy-based treatment modalities.

Apart from the already identified and analysed miRs and RBPs, the combination of RNA affinity purification assays (such as miTRAP and RNA affinity purification assay for RBPs) with high-throughput analyses (such as small RNA sequencing and MS analyses, respectively) can give rise to further extend the identification of novel candidate miRs and RBPs, targeting not only TAP1, TAP2 and TPN, but also other immune modulatory molecules, like the classical and non-classical HLA-I molecules, and immune checkpoint molecules, such as PD-1, CTLA-4, TIM-3 and LAG-3.

The current surge in availability of genomic and proteomic data on numerous human tumour entities will certainly aid in the identification of key miRs and RBPs potentially serving as prognostic and/or predictive tumour markers and novel drug targets. Several preclinical miR-targeting therapeutics have already reached the clinical development phase. However, very strict and careful evaluations of toxicity data and

concerning the envisioned target engagements will be necessary to avoid early failures during clinical trials.
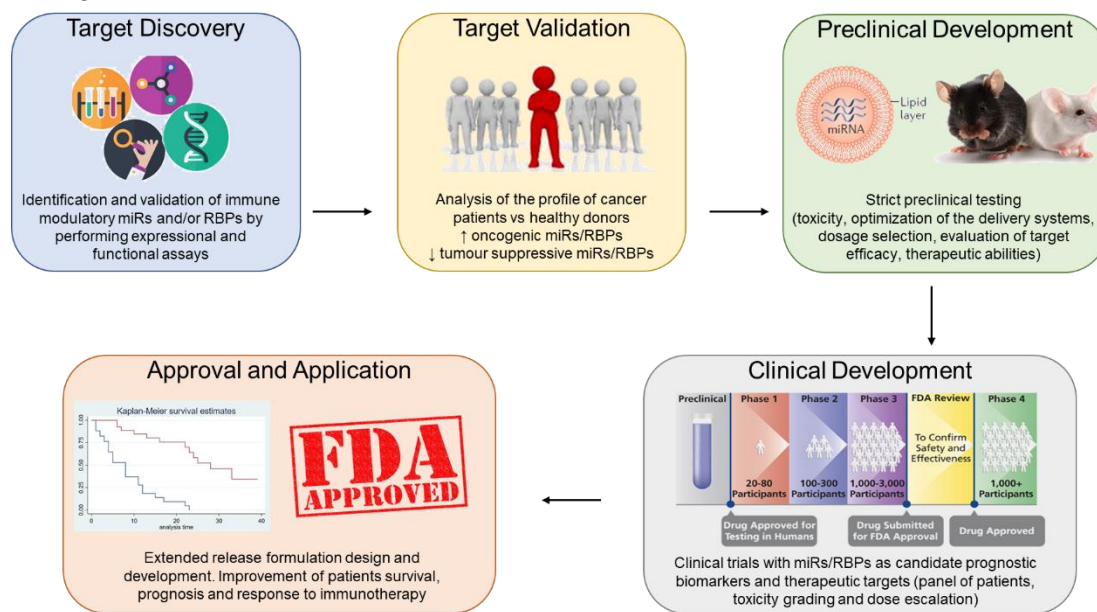
Figure 8.1. Summary of the key steps in the development of miR- and/or RBPs- therapeutics
After identification and characterization of candidate immune modulatory miRs and/or RBPs, their expression shall be validated in samples derived from healthy donors or tumour patients. Strict preclinical studies shall then be conducted, followed by the execution of clinical trials until the molecules can be approved by the FDA and used into the clinics.

9. References

1   Mukherji, B. Immunology of melanoma. *Clinics in dermatology* **31**, 156-165, doi:10.1016/j.clindermatol.2012.08.017 (2013).

2   Hanahan, D. & Weinberg, R. A. Hallmarks of cancer: the next generation. *Cell* **144**, 646-674, doi:10.1016/j.cell.2011.02.013 (2011).

3   Friedrich, M. *et al.* Tumor-induced escape mechanisms and their association with resistance to checkpoint inhibitor therapy. *Cancer immunology, immunotherapy : CII*, doi:10.1007/s00262-019-02373-1 (2019).

4   Eichmuller, S. B., Osen, W., Mandelboim, O. & Seliger, B. Immune Modulatory microRNAs Involved in Tumor Attack and Tumor Immune Escape. *Journal of the National Cancer Institute* **109**, doi:10.1093/jnci/djx034 (2017).

5   Bray, F. *et al.* Global cancer statistics 2018: GLOBOCAN estimates of incidence and mortality worldwide for 36 cancers in 185 countries. *CA: a cancer journal for clinicians* **68**, 394-424, doi:10.3322/caac.21492 (2018).

6   Siegel, R. L., Miller, K. D. & Jemal, A. Cancer statistics, 2019. *CA: a cancer journal for clinicians* **69**, 7-34, doi:10.3322/caac.21551 (2019).

7   Azoury, S. C. & Lange, J. R. Epidemiology, Risk Factors, Prevention, and Early Detection of Melanoma. *Surgical Clinics of North America* **94**, 945-962, doi:https://doi.org/10.1016/j.suc.2014.07.013 (2014).

8   Stewart, B. & Kleihues, P. World Cancer Report. *IARCPress* (2003).

9   Board, P. D. Q. A. T. E. in *PDQ Cancer Information Summaries*   (National Cancer Institute (US), 2002).

10   Dummer, R. & Flaherty, K. T. Resistance patterns with tyrosine kinase inhibitors in melanoma: new insights. *Current Opinion in Oncology* **24**, 150-154, doi:10.1097/CCO.0b013e32834fca92 (2012).

11   Balch, C. M. *et al.* Final version of the American Joint Committee on Cancer staging system for cutaneous melanoma. *Journal of clinical oncology : official journal of the American Society of Clinical Oncology* **19**, 3635-3648, doi:10.1200/jco.2001.19.16.3635 (2001).

12   Lowe, J. B., Hurst, E., Moley, J. F. & Cornelius, L. A. Sentinel lymph node biopsy in patients with thin melanoma. *Archives of dermatology* **139**, 617-621, doi:10.1001/archderm.139.5.617 (2003).

13   Risucci, D. A., Tortolani, A. J. & Ward, R. J. Ratings of surgical residents by self, supervisors and peers. *Surgery, gynecology & obstetrics* **169**, 519-526 (1989).

14   Saldanha, G. *et al.* Breslow Density Is a Novel Prognostic Feature That Adds Value to Melanoma Staging. *The American journal of surgical pathology* **42**, 715-725, doi:10.1097/pas.0000000000001034 (2018).

15   Morton, D. L. *et al.* Sentinel-Node Biopsy or Nodal Observation in Melanoma. *New England Journal of Medicine* **355**, 1307-1317, doi:10.1056/NEJMoa060992 (2006).

16   Mohtar, J., Abdullah, Z. & Zaaba, S. *Review on Melanoma Skin Cancer Treatment by Cold Atmospheric Plasma*. (2018).

17   Sepideh Mohammadi, M. *et al.* Cancer detection based on electrical impedance spectroscopy: A clinical study. *Journal of Electrical Bioimpedance* **9**, 17-23, doi:https://doi.org/10.2478/joeb-2018-0004 (2018).

18   Rastrelli, M., Tropea, S., Rossi, C. R. & Alaibac, M. Melanoma: epidemiology, risk factors, pathogenesis, diagnosis and classification. *In vivo (Athens, Greece)* **28**, 1005-1011 (2014).

19   Greene, M. H. The genetics of hereditary melanoma and nevi. 1998 update. *Cancer* **86**, 2464-2477, doi:10.1002/(sici)1097-0142(19991201)86:11+<2464::aid-cncr3>3.0.co;2-f (1999).

20   Colombino, M. *et al.* BRAF/NRAS mutation frequencies among primary tumors and metastases in patients with melanoma. *Journal of clinical oncology : official journal of the American Society of Clinical Oncology* **30**, 2522-2529, doi:10.1200/jco.2011.41.2452 (2012).

21   Spathis, A. *et al.* BRAF Mutation Status in Primary, Recurrent, and Metastatic Malignant Melanoma and Its Relation to Histopathological Parameters. *Dermatol Pract Concept* **9**, 54-62, doi:10.5826/dpc.0901a13 (2019).

22   Sullivan, R. J. & Flaherty, K. MAP kinase signaling and inhibition in melanoma. *Oncogene* **32**, 2373-2379, doi:10.1038/onc.2012.345 (2013).

23   Rossi, M. *et al.* Familial Melanoma: Diagnostic and Management Implications. *Dermatol Pract Concept* **9**, 10-16, doi:10.5826/dpc.0901a03 (2019).

24   Muñoz-Couselo, E., Adelantado, E. Z., Ortiz, C., García, J. S. & Perez-Garcia, J. NRAS-mutant melanoma: current challenges and future prospect. *OncoTargets and therapy* **10**, 3941-3947, doi:10.2147/OTT.S117121 (2017).

25   Box, N. F., Vukmer, T. O. & Terzian, T. Targeting p53 in melanoma. *Pigment cell & melanoma research* **27**, 8-10, doi:10.1111/pcmr.12180 (2014).

26   Fernandes, M. *et al.* Acral Lentiginous Melanomas Harbour Intratumor Heterogeneity in BRAF Exon 15, With Mutations Distinct From V600E/V600K. *The American Journal of Dermatopathology* **41**, 733-740, doi:10.1097/dad.0000000000001418 (2019).

27   Yan, J. *et al.* Analysis of NRAS gain in 657 patients with melanoma and evaluation of its sensitivity to a MEK inhibitor. *European Journal of Cancer* **89**, 90-101, doi:https://doi.org/10.1016/j.ejca.2017.11.011 (2018).

28   Cirenajwis, H. *et al.* NF1-mutated melanoma tumors harbor distinct clinical and biological characteristics. *Mol Oncol* **11**, 438-451, doi:10.1002/1878-0261.12050 (2017).

29   Hintzsche, J. D. *et al.* Whole-exome sequencing identifies recurrent SF3B1 R625 mutation and comutation of NF1 and KIT in mucosal melanoma. *Melanoma research* **27**, 189-199, doi:10.1097/cmr.0000000000000345 (2017).

30   Hayward, N. K. *et al.* Whole-genome landscapes of major melanoma subtypes. *Nature* **545**, 175-180, doi:10.1038/nature22071 (2017).

31   Willmore-Payne, C., Holden, J. A., Tripp, S. & Layfield, L. J. Human malignant melanoma: detection of BRAF- and c-kit-activating mutations by high-resolution amplicon melting analysis. *Human pathology* **36**, 486-493, doi:10.1016/j.humpath.2005.03.015 (2005).

32   Mirshafiey, A., Ghalamfarsa, G., Asghari, B. & Azizi, G. Receptor Tyrosine Kinase and Tyrosine Kinase Inhibitors: New Hope for Success in Multiple Sclerosis Therapy. *Innov Clin Neurosci* **11**, 23-36 (2014).

33   Nazarian, R. *et al.* Melanomas acquire resistance to B-RAF(V600E) inhibition by RTK or N-RAS upregulation. *Nature* **468**, 973-977, doi:10.1038/nature09626 (2010).

34   Wagle, N. *et al.* Dissecting therapeutic resistance to RAF inhibition in melanoma by tumor genomic profiling. *Journal of clinical oncology : official journal of the American Society of Clinical Oncology* **29**, 3085-3096, doi:10.1200/jco.2010.33.2312 (2011).

35   Johannessen, C. M. *et al.* COT drives resistance to RAF inhibition through MAP kinase pathway reactivation. *Nature* **468**, 968-972, doi:10.1038/nature09627 (2010).

36   Villanueva, J. *et al.* Acquired resistance to BRAF inhibitors mediated by a RAF kinase switch in melanoma can be overcome by cotargeting MEK and IGF-1R/PI3K. *Cancer cell* **18**, 683-695, doi:10.1016/j.ccr.2010.11.023 (2010).

37   Hanahan, D. & Weinberg, R. A. The hallmarks of cancer. *Cell* **100**, 57-70, doi:10.1016/s0092-8674(00)81683-9 (2000).

38   Ko, J. S. The Immunology of Melanoma. *Clinics in laboratory medicine* **37**, 449-471, doi:10.1016/j.cll.2017.06.001 (2017).

39   Passarelli, A., Mannavola, F., Stucci, L. S., Tucci, M. & Silvestris, F. Immune system and melanoma biology: a balance between immunosurveillance and immune escape. *Oncotarget* **8**, 106132-106142, doi:10.18632/oncotarget.22190 (2017).

40   Dunn, G. P., Old, L. J. & Schreiber, R. D. The three Es of cancer immunoediting. *Annual review of immunology* **22**, 329-360, doi:10.1146/annurev.immunol.22.012703.104803 (2004).

41   Schreiber, R. D., Old, L. J. & Smyth, M. J. Cancer immunoediting: integrating immunity's roles in cancer suppression and promotion. *Science (New York, N.Y.)* **331**, 1565-1570, doi:10.1126/science.1203486 (2011).

42   Nakano, O. *et al.* Proliferative activity of intratumoral CD8(+) T-lymphocytes as a prognostic factor in human renal cell carcinoma: clinicopathologic demonstration of antitumor immunity. *Cancer research* **61**, 5132-5136 (2001).

43   Papac, R. J. Spontaneous regression of cancer. *Cancer treatment reviews* **22**, 395-423, doi:10.1016/s0305-7372(96)90023-7 (1996).

44   Drake, C. G., Lipson, E. J. & Brahmer, J. R. Breathing new life into immunotherapy: review of melanoma, lung and kidney cancer. *Nature reviews. Clinical oncology* **11**, 24-37, doi:10.1038/nrclinonc.2013.208 (2014).

45   Galluzzi, L. *et al.* Classification of current anticancer immunotherapies. *Oncotarget* **5**, 12472-12508, doi:10.18632/oncotarget.2998 (2014).

46   Mellman, I., Coukos, G. & Dranoff, G. Cancer immunotherapy comes of age. *Nature* **480**, 480-489, doi:10.1038/nature10673 (2011).

47   Lesterhuis, W. J., Haanen, J. B. & Punt, C. J. Cancer immunotherapy--revisited. *Nature reviews. Drug discovery* **10**, 591-600, doi:10.1038/nrd3500 (2011).

48   Restifo, N. P., Dudley, M. E. & Rosenberg, S. A. Adoptive immunotherapy for cancer: harnessing the T cell response. *Nature reviews. Immunology* **12**, 269-281, doi:10.1038/nri3191 (2012).

49   Emens, L. A. *et al.* Cancer immunotherapy: Opportunities and challenges in the rapidly evolving clinical landscape. *European journal of cancer (Oxford, England : 1990)* **81**, 116-129, doi:10.1016/j.ejca.2017.01.035 (2017).

50   Haanen, J. B. & Robert, C. Immune Checkpoint Inhibitors. *Progress in tumor research* **42**, 55-66, doi:10.1159/000437178 (2015).

51   Abbas Abul K., Lichtman Andrew H. & Shiv, P. *Basic Immunology, Functions and disorders of the Immune System.* (Elsevier, 2016).

52   Imler, J. L. & Hoffmann, J. A. Toll receptors in innate immunity. *Trends in cell biology* **11**, 304-311 (2001).

53   Vivier, E. *et al.* Innate or adaptive immunity? The example of natural killer cells. *Science (New York, N.Y.)* **331**, 44-49, doi:10.1126/science.1198687 (2011).

54   Natoli, G. & Ostuni, R. Adaptation and memory in immune responses. *Nature immunology* **20**, 783-792, doi:10.1038/s41590-019-0399-9 (2019).

55   Janeway, C. A., Jr. & Medzhitov, R. Innate immune recognition. *Annual review of immunology* **20**, 197-216, doi:10.1146/annurev.immunol.20.083001.084359 (2002).

56   Mogensen, T. H. Pathogen recognition and inflammatory signaling in innate immune defenses. *Clin Microbiol Rev* **22**, 240-273, doi:10.1128/CMR.00046-08 (2009).

57   Maverakis, E. *et al.* Glycans in the immune system and The Altered Glycan Theory of Autoimmunity: a critical review. *Journal of autoimmunity* **57**, 1-13, doi:10.1016/j.jaut.2014.12.002 (2015).

58   Jensen, S. & Thomsen, A. R. Sensing of RNA viruses: a review of innate immune receptors involved in recognizing RNA virus invasion. *J Virol* **86**, 2900-2910, doi:10.1128/JVI.05738-11 (2012).

59   Cooper, M. D. & Alder, M. N. The evolution of adaptive immune systems. *Cell* **124**, 815-822, doi:10.1016/j.cell.2006.02.001 (2006).

60   Alberts B, J. A., Lewis J, et al. *Molecular Biology of the Cell.* 4th edition edn, Vol. Lymphocytes and the Cellular Basis of Adaptive Immunity (Garland Science, 2002).

61   Burnet, F. M. S. *The clonal selection theory of acquired immunity.* (Vanderbilt University Press, 1959).

62   Parkin, J. & Cohen, B. An overview of the immune system. *Lancet (London, England)* **357**, 1777-1789, doi:10.1016/s0140-6736(00)04904-7 (2001).

63   Sedwick, C. The education of Mr. T. *PLoS biology* **4**, e117-e117, doi:10.1371/journal.pbio.0040117 (2006).

64   Tsukishiro, T., Donnenberg, A. D. & Whiteside, T. L. Rapid turnover of the CD8(+)CD28(-) T-cell subset of effector cells in the circulation of patients with head and neck cancer. *Cancer immunology, immunotherapy : CII* **52**, 599-607, doi:10.1007/s00262-003-0395-6 (2003).

65   Arosa, F. A. CD8+CD28- T cells: certainties and uncertainties of a prevalent human T-cell subset. *Immunology and cell biology* **80**, 1-13, doi:10.1046/j.1440-1711.2002.01057.x (2002).

66   Huse, M. Mechanical forces in the immune system. *Nature reviews. Immunology* **17**, 679-690, doi:10.1038/nri.2017.74 (2017).

67   Boesteanu, A. C. & Katsikis, P. D. Memory T cells need CD28 costimulation to remember. *Seminars in immunology* **21**, 69-77, doi:10.1016/j.smim.2009.02.005 (2009).

68   Brenchley, J. M. *et al.* Expression of CD57 defines replicative senescence and antigen-induced apoptotic death of CD8+ T cells. *Blood* **101**, 2711-2720, doi:10.1182/blood-2002-07-2103 (2003).

69   Kaech, S. M., Wherry, E. J. & Ahmed, R. Effector and memory T-cell differentiation: implications for vaccine development. *Nature reviews. Immunology* **2**, 251-262, doi:10.1038/nri778 (2002).

70   Strioga, M., Pasukoniene, V. & Characiejus, D. CD8+ CD28- and CD8+ CD57+ T cells and their role in health and disease. *Immunology* **134**, 17-32, doi:10.1111/j.1365-2567.2011.03470.x (2011).

71   Bots, M. & Medema, J. P. Granzymes at a glance. *Journal of cell science* **119**, 5011-5014, doi:10.1242/jcs.03239 (2006).

72   Oshimi, Y., Oda, S., Honda, Y., Nagata, S. & Miyazaki, S. Involvement of Fas ligand and Fas-mediated pathway in the cytotoxicity of human natural killer cells. *Journal of immunology (Baltimore, Md. : 1950)* **157**, 2909-2915 (1996).

73   Strasser, A., Jost, P. J. & Nagata, S. The many roles of FAS receptor signaling in the immune system. *Immunity* **30**, 180-192, doi:10.1016/j.immuni.2009.01.001 (2009).

74   C Janeway, P Travers & M Walport, e. a. *Immunobiology: The Immune System in Health and Disease.* . 5th edition edn, Vol. The major histocompatibility complex and its functions (2001).

75   Herberman, R. B., Nunn, M. E. & Lavrin, D. H. Natural cytotoxic reactivity of mouse lymphoid cells against syngeneic acid allogeneic tumors. I. Distribution of reactivity and specificity. *International journal of cancer* **16**, 216-229, doi:10.1002/ijc.2910160204 (1975).

76   Kiessling, R., Klein, E. & Wigzell, H. "Natural" killer cells in the mouse. I. Cytotoxic cells with specificity for mouse Moloney leukemia cells. Specificity and distribution according to genotype. *European journal of immunology* **5**, 112-117, doi:10.1002/eji.1830050208 (1975).

77   Eidenschenk, C. *et al.* A novel primary immunodeficiency with specific natural-killer cell deficiency maps to the centromeric region of chromosome 8. *Am J Hum Genet* **78**, 721-727, doi:10.1086/503269 (2006).

78   Lee, S. H., Miyagi, T. & Biron, C. A. Keeping NK cells in highly regulated antiviral warfare. *Trends in immunology* **28**, 252-259, doi:10.1016/j.it.2007.04.001 (2007).

79   Smyth, M. J., Hayakawa, Y., Takeda, K. & Yagita, H. New aspects of natural-killer-cell surveillance and therapy of cancer. *Nature reviews. Cancer* **2**, 850-861, doi:10.1038/nrc928 (2002).

80   Vivier, E., Nunes, J. A. & Vely, F. Natural killer cell signaling pathways. *Science (New York, N.Y.)* **306**, 1517-1519, doi:10.1126/science.1103478 (2004).

81   Bryceson, Y. T., March, M. E., Ljunggren, H.-G. & Long, E. O. Activation, coactivation, and costimulation of resting human natural killer cells. *Immunol Rev* **214**, 73-91, doi:10.1111/j.1600-065X.2006.00457.x (2006).

82   Littera, R. *et al.* KIR and their HLA Class I ligands: Two more pieces towards completing the puzzle of chronic rejection and graft loss in kidney transplantation. *PloS one* **12**, e0180831-e0180831, doi:10.1371/journal.pone.0180831 (2017).

83   Orr, M. T. & Lanier, L. L. Natural killer cell education and tolerance. *Cell* **142**, 847-856, doi:10.1016/j.cell.2010.08.031 (2010).

84   Raulet, D. H., Vance, R. E. & McMahon, C. W. Regulation of the natural killer cell receptor repertoire. *Annual review of immunology* **19**, 291-330, doi:10.1146/annurev.immunol.19.1.291 (2001).

85   Raulet, D. H. & Guerra, N. Oncogenic stress sensed by the immune system: role of natural killer cell receptors. *Nature reviews. Immunology* **9**, 568-580, doi:10.1038/nri2604 (2009).

86   Kruse, P. H., Matta, J., Ugolini, S. & Vivier, E. Natural cytotoxicity receptors and their ligands. *Immunology and cell biology* **92**, 221-229, doi:10.1038/icb.2013.98 (2014).

87   Barrow, A. D., Martin, C. J. & Colonna, M. The Natural Cytotoxicity Receptors in Health and Disease. *Frontiers in immunology* **10**, doi:10.3389/fimmu.2019.00909 (2019).

88   Anfossi, N. *et al.* Human NK cell education by inhibitory receptors for MHC class I. *Immunity* **25**, 331-342, doi:10.1016/j.immuni.2006.06.013 (2006).

89   Malmberg, K.-J., Sohlberg, E., Goodridge, J. P. & Ljunggren, H.-G. Immune selection during tumor checkpoint inhibition therapy paves way for NK-cell "missing self" recognition. *Immunogenetics* **69**, 547-556, doi:10.1007/s00251-017-1011-9 (2017).

90   Karre, K., Ljunggren, H. G., Piontek, G. & Kiessling, R. Selective rejection of H-2-deficient lymphoma variants suggests alternative immune defence strategy. *Nature* **319**, 675-678, doi:10.1038/319675a0 (1986).

91   Kawahara, M., York, I. A., Hearn, A., Farfan, D. & Rock, K. L. Analysis of the Role of Tripeptidyl Peptidase II in MHC Class I Antigen Presentation In Vivo. *The Journal of Immunology* **183**, 6069, doi:10.4049/jimmunol.0803564 (2009).

92   Morvan, M. G. & Lanier, L. L. NK cells and cancer: you can teach innate cells new tricks. *Nature reviews. Cancer* **16**, 7-19, doi:10.1038/nrc.2015.5 (2016).

93   Shin, M. H. *et al.* NK Cell-Based Immunotherapies in Cancer. *Immune Netw* **20**, e14-e14, doi:10.4110/in.2020.20.e14 (2020).

94   Roche, P. A. & Furuta, K. The ins and outs of MHC class II-mediated antigen processing and presentation. *Nature reviews. Immunology* **15**, 203-216, doi:10.1038/nri3818 (2015).

95   Joffre, O. P., Segura, E., Savina, A. & Amigorena, S. Cross-presentation by dendritic cells. *Nature reviews. Immunology* **12**, 557-569, doi:10.1038/nri3254 (2012).

96   Gruen, J. R. & Weissman, S. M. Human MHC class III and IV genes and disease associations. *Frontiers in bioscience : a journal and virtual library* **6**, D960-972, doi:10.2741/gruen (2001).

97   Payne, R. & Hackel, E. Inheritance of human leukocyte antigens. *Am J Hum Genet* **13**, 306-319 (1961).

98   Halenius, A., Gerke, C. & Hengel, H. Classical and non-classical MHC I molecule manipulation by human cytomegalovirus: so many targets—but how many arrows in the quiver? *Cellular & Molecular Immunology* **12**, 139-153, doi:10.1038/cmi.2014.105 (2015).

99   Wieczorek, M. *et al.* Major Histocompatibility Complex (MHC) Class I and MHC Class II Proteins: Conformational Plasticity in Antigen Presentation. *Frontiers in immunology* **8**, 292-292, doi:10.3389/fimmu.2017.00292 (2017).

100   Burrows, S. R., Rossjohn, J. & McCluskey, J. Have we cut ourselves too short in mapping CTL epitopes? *Trends in immunology* **27**, 11-16, doi:10.1016/j.it.2005.11.001 (2006).

101   Toh, H. *et al.* Changes at the floor of the peptide-binding groove induce a strong preference for proline at position 3 of the bound peptide: molecular dynamics simulations of HLA-A*0217. *Biopolymers* **54**, 318-327, doi:10.1002/1097-0282(20001015)54:5<318::aid-bip30>3.0.co;2-t (2000).

102   Hulpke, S. & Tampe, R. The MHC I loading complex: a multitasking machinery in adaptive immunity. *Trends in biochemical sciences* **38**, 412-420, doi:10.1016/j.tibs.2013.06.003 (2013).

103   Giorda, E. *et al.* The Antigen Processing Machinery of Class I Human Leukocyte Antigens. *Cancer research* **63**, 4119 (2003).

104   Seliger, B., Ruiz-Cabello, F. & Garrido, F. IFN inducibility of major histocompatibility antigens in tumors. *Advances in cancer research* **101**, 249-276, doi:10.1016/s0065-230x(08)00407-7 (2008).

105   Abele, R. & Tampé, R. Peptide trafficking and translocation across membranes in cellular signaling and self-defense strategies. *Current Opinion in Cell Biology* **21**, 508-515, doi:https://doi.org/10.1016/j.ceb.2009.04.008 (2009).

106   Urlinger, S., Kuchler, K., Meyer, T. H., Uebel, S. & Tampé, R. Intracellular Location, Complex Formation, and Function of the Transporter Associated with Antigen Processing in Yeast. *European Journal of Biochemistry* **245**, 266-272, doi:10.1111/j.1432-1033.1997.00266.x (1997).

107   Lehnert, E. & Tampé, R. Structure and Dynamics of Antigenic Peptides in Complex with TAP. *Frontiers in immunology* **8**, 10-10, doi:10.3389/fimmu.2017.00010 (2017).

108   Bodmer, J. G. *et al.* Nomenclature for factors of the HLA system, 1991. WHO Nomenclature Committee for factors of the HLA system. *Tissue antigens* **39**, 161-173, doi:10.1111/j.1399-0039.1992.tb01932.x (1992).

109   Ortmann, B. *et al.* A critical role for tapasin in the assembly and function of multimeric MHC class I-TAP complexes. *Science (New York, N.Y.)* **277**, 1306-1309, doi:10.1126/science.277.5330.1306 (1997).

110   Eggensperger, S. & Tampe, R. The transporter associated with antigen processing: a key player in adaptive immunity. *Biological chemistry* **396**, 1059-1072, doi:10.1515/hsz-2014-0320 (2015).

111   Kelly, A. & Trowsdale, J. Genetics of antigen processing and presentation. *Immunogenetics* **71**, 161-170, doi:10.1007/s00251-018-1082-2 (2019).

112   Marchler-Bauer, A. *et al.* CDD/SPARCLE: functional classification of proteins via subfamily domain architectures. *Nucleic acids research* **45**, D200-d203, doi:10.1093/nar/gkw1129 (2017).

113   Benkő, S., Kovács, E. G., Hezel, F. & Kufer, T. A. NLRC5 Functions beyond MHC I Regulation-What Do We Know So Far? *Frontiers in immunology* **8**, 150-150, doi:10.3389/fimmu.2017.00150 (2017).

114   Staehli, F. *et al.* NLRC5 deficiency selectively impairs MHC class I- dependent lymphocyte killing by cytotoxic T cells. *Journal of immunology (Baltimore, Md. : 1950)* **188**, 3820-3828, doi:10.4049/jimmunol.1102671 (2012).

115   Seliger, B., Ruiz-Cabello, F. & Garrido, F. IFN inducibility of major histocompatibility antigens in tumors. *Advances in cancer research* **101**, 249-276, doi:10.1016/S0065-230X(08)00407-7 (2008).

116   Goldberg, A. L., Cascio, P., Saric, T. & Rock, K. L. The importance of the proteasome and subsequent proteolytic steps in the generation of antigenic peptides. *Molecular immunology* **39**, 147-164, doi:10.1016/s0161-5890(02)00098-6 (2002).

117   Cerruti, F. *et al.* Enhanced expression of interferon-gamma-induced antigen-processing machinery components in a spontaneously occurring cancer. *Neoplasia* **9**, 960-969, doi:10.1593/neo.07649 (2007).

118   Ferrington, D. A. & Gregerson, D. S. Immunoproteasomes: structure, function, and antigen presentation. *Prog Mol Biol Transl Sci* **109**, 75-112, doi:10.1016/B978-0-12-397863-9.00003-1 (2012).

119   Seliger, B. & Ferrone, S. HLA Class I Antigen Processing Machinery Defects in Cancer Cells-Frequency, Functional Significance, and Clinical Relevance with Special Emphasis on Their Role in T Cell-Based Immunotherapy of Malignant Disease. *Methods in molecular biology (Clifton, N.J.)* **2055**, 325-350, doi:10.1007/978-1-4939-9773-2_15 (2020).

120   Griffin, T. A. *et al.* Immunoproteasome assembly: cooperative incorporation of interferon gamma (IFN-gamma)-inducible subunits. *J Exp Med* **187**, 97-104, doi:10.1084/jem.187.1.97 (1998).

121   Garstka, M. A. *et al.* The first step of peptide selection in antigen presentation by MHC class I molecules. *Proceedings of the National Academy of Sciences* **112**, 1505, doi:10.1073/pnas.1416543112 (2015).

122   Rammensee, H.-G., Friede, T. & Stevanović, S. MHC ligands and peptide motifs: first listing. *Immunogenetics* **41**, 178-228, doi:10.1007/BF00172063 (1995).

123   Goldberg, A. L. Functions of the proteasome: the lysis at the end of the tunnel. *Science (New York, N.Y.)* **268**, 522-523, doi:10.1126/science.7725095 (1995).

124   Kloetzel, P. M. The proteasome and MHC class I antigen processing. *Biochimica et biophysica acta* **1695**, 225-233, doi:10.1016/j.bbamcr.2004.10.004 (2004).

125   Rechsteiner, M., Hoffman, L. & Dubiel, W. The multicatalytic and 26 S proteases. *The Journal of biological chemistry* **268**, 6065-6068 (1993).

126   Voges, D., Zwickl, P. & Baumeister, W. The 26S proteasome: a molecular machine designed for controlled proteolysis. *Annu Rev Biochem* **68**, 1015-1068, doi:10.1146/annurev.biochem.68.1.1015 (1999).

127   Hill, C. P., Masters, E. I. & Whitby, F. G. The 11S regulators of 20S proteasome activity. *Current topics in microbiology and immunology* **268**, 73-89, doi:10.1007/978-3-642-59414-4_4 (2002).

128   Ustrell, V., Hoffman, L., Pratt, G. & Rechsteiner, M. PA200, a nuclear proteasome activator involved in DNA repair. *The EMBO journal* **21**, 3516-3525, doi:10.1093/emboj/cdf333 (2002).

129   McCutchen-Maloney, S. L. *et al.* cDNA cloning, expression, and functional characterization of PI31, a proline-rich inhibitor of the proteasome. *The Journal of biological chemistry* **275**, 18557-18565, doi:10.1074/jbc.M001697200 (2000).

130   Budenholzer, L., Cheng, C. L., Li, Y. & Hochstrasser, M. Proteasome Structure and Assembly. *Journal of molecular biology* **429**, 3500-3524, doi:10.1016/j.jmb.2017.05.027 (2017).

131   Finley, D., Chen, X. & Walters, K. J. Gates, Channels, and Switches: Elements of the Proteasome Machine. *Trends in biochemical sciences* **41**, 77-93, doi:10.1016/j.tibs.2015.10.009 (2016).

132   Bard, J. A. M. *et al.* Structure and Function of the 26S Proteasome. *Annu Rev Biochem* **87**, 697-724, doi:10.1146/annurev-biochem-062917-011931 (2018).

133   Glickman, M. H. & Ciechanover, A. The ubiquitin-proteasome proteolytic pathway: destruction for the sake of construction. *Physiological reviews* **82**, 373-428, doi:10.1152/physrev.00027.2001 (2002).

134   Leone, P. *et al.* MHC class I antigen processing and presenting machinery: organization, function, and defects in tumor cells. *J Natl Cancer Inst* **105**, 1172-1187, doi:10.1093/jnci/djt184 (2013).

135   Hammer, G. E., Kanaseki, T. & Shastri, N. The final touches make perfect the peptide-MHC class I repertoire. *Immunity* **26**, 397-406, doi:10.1016/j.immuni.2007.04.003 (2007).

136   Seliger, B., Ritz, U. & Ferrone, S. Molecular mechanisms of HLA class I antigen abnormalities following viral infection and transformation. *International journal of cancer* **118**, 129-138, doi:10.1002/ijc.21312 (2006).

137   Toes, R. E. *et al.* Discrete cleavage motifs of constitutive and immunoproteasomes revealed by quantitative analysis of cleavage products. *J Exp Med* **194**, 1-12, doi:10.1084/jem.194.1.1 (2001).

138   Roelse, J., Gromme, M., Momburg, F., Hammerling, G. & Neefjes, J. Trimming of TAP-translocated peptides in the endoplasmic reticulum and in the cytosol during recycling. *J Exp Med* **180**, 1591-1597, doi:10.1084/jem.180.5.1591 (1994).

139   Chang, S. C., Momburg, F., Bhutani, N. & Goldberg, A. L. The ER aminopeptidase, ERAP1, trims precursors to lengths of MHC class I peptides by a "molecular ruler" mechanism. *Proceedings of the National Academy of Sciences of the United States of America* **102**, 17107-17112, doi:10.1073/pnas.0500721102 (2005).

140   Hammer, G. E., Gonzalez, F., James, E., Nolla, H. & Shastri, N. In the absence of aminopeptidase ERAAP, MHC class I molecules present many unstable and highly immunogenic peptides. *Nature immunology* **8**, 101-108, doi:10.1038/ni1409 (2007).

141   Saveanu, L. *et al.* Concerted peptide trimming by human ERAP1 and ERAP2 aminopeptidase complexes in the endoplasmic reticulum. *Nature immunology* **6**, 689-697, doi:10.1038/ni1208 (2005).

142   Admon, A. ERAP1 shapes just part of the immunopeptidome. *Human immunology* **80**, 296-301, doi:10.1016/j.humimm.2019.03.004 (2019).

143   Koopmann, J. O. *et al.* Export of antigenic peptides from the endoplasmic reticulum intersects with retrograde protein translocation through the Sec61p channel. *Immunity* **13**, 117-127, doi:10.1016/s1074-7613(00)00013-3 (2000).

144   Reits, E. *et al.* Peptide Diffusion, Protection, and Degradation in Nuclear and Cytoplasmic Compartments before Antigen Presentation by MHC Class I. *Immunity* **18**, 97-108, doi:https://doi.org/10.1016/S1074-7613(02)00511-3 (2003).

145   Zehner, M. *et al.* The Translocon Protein Sec61 Mediates Antigen Transport from Endosomes in the Cytosol for Cross-Presentation to CD8+ T Cells. *Immunity* **42**, 850-863, doi:https://doi.org/10.1016/j.immuni.2015.04.008 (2015).

146   Schmitt, L. & Tampe, R. Structure and mechanism of ABC transporters. *Current opinion in structural biology* **12**, 754-760 (2002).

147   Verweij, M. C. *et al.* Viral Inhibition of the Transporter Associated with Antigen Processing (TAP): A Striking Example of Functional Convergent Evolution. *PLoS pathogens* **11**, e1004743, doi:10.1371/journal.ppat.1004743 (2015).

148   Hulpke, S. *et al.* Direct evidence that the N-terminal extensions of the TAP complex act as autonomous interaction scaffolds for the assembly of the MHC I peptide-loading complex. *Cellular and molecular life sciences : CMLS* **69**, 3317-3327, doi:10.1007/s00018-012-1005-6 (2012).

149   Koch, J., Guntrum, R., Heintke, S., Kyritsis, C. & Tampé, R. Functional dissection of the transmembrane domains of the transporter associated with antigen processing (TAP). *The Journal of biological chemistry* **279**, 10142-10147, doi:10.1074/jbc.M312816200 (2004).

150   Koch, J., Guntrum, R. & Tampé, R. The first N-terminal transmembrane helix of each subunit of the antigenic peptide transporter TAP is essential for independent tapasin binding. *FEBS letters* **580**, 4091-4096, doi:10.1016/j.febslet.2006.06.053 (2006).

151   Plewnia, G., Schulze, K., Hunte, C., Tampé, R. & Koch, J. Modulation of the antigenic peptide transporter TAP by recombinant antibodies binding to the last five residues of TAP1. *Journal of molecular biology* **369**, 95-107, doi:10.1016/j.jmb.2007.02.102 (2007).

152   Arora, S., Lapinski, P. E. & Raghavan, M. Use of chimeric proteins to investigate the role of transporter associated with antigen processing (TAP) structural domains in peptide binding and translocation. *Proceedings of the National Academy of Sciences of the United States of America* **98**, 7241-7246, doi:10.1073/pnas.131132198 (2001).

153   Higgins, C. F. & Linton, K. J. The ATP switch model for ABC transporters. *Nature structural & molecular biology* **11**, 918-926, doi:10.1038/nsmb836 (2004).

154   Parcej, D. & Tampe, R. ABC proteins in antigen translocation and viral inhibition. *Nature chemical biology* **6**, 572-580, doi:10.1038/nchembio.410 (2010).

155   Uebel, S. *et al.* Requirements for peptide binding to the human transporter associated with antigen processing revealed by peptide scans and complex peptide libraries. *The Journal of biological chemistry* **270**, 18512-18516, doi:10.1074/jbc.270.31.18512 (1995).

156   Momburg, F. & Hammerling, G. J. Generation and TAP-mediated transport of peptides for major histocompatibility complex class I molecules. *Advances in immunology* **68**, 191-256 (1998).

157   Momburg, F., Roelse, J., Hammerling, G. J. & Neefjes, J. J. Peptide size selection by the major histocompatibility complex-encoded peptide transporter. *J Exp Med* **179**, 1613-1623, doi:10.1084/jem.179.5.1613 (1994).

158   Lautscham, G., Rickinson, A. & Blake, N. TAP-independent antigen presentation on MHC class I molecules: lessons from Epstein–Barr virus. *Microbes and Infection* **5**, 291-299, doi:https://doi.org/10.1016/S1286-4579(03)00031-5 (2003).

159   Zimmer, J. *et al.* Clinical and immunological aspects of HLA class I deficiency. *QJM : monthly journal of the Association of Physicians* **98**, 719-727, doi:10.1093/qjmed/hci112 (2005).

160   Praest, P., Liaci, A. M., Förster, F. & Wiertz, E. New insights into the structure of the MHC class I peptide-loading complex and mechanisms of TAP inhibition by viral immune evasion proteins. *Molecular immunology* **113**, 103-114, doi:10.1016/j.molimm.2018.03.020 (2019).

161   Elliott, T. & Williams, A. The optimization of peptide cargo bound to MHC class I molecules by the peptide-loading complex. *Immunol Rev* **207**, 89-99, doi:10.1111/j.0105-2896.2005.00311.x (2005).

162   Diedrich, G., Bangia, N., Pan, M. & Cresswell, P. A role for calnexin in the assembly of the MHC class I loading complex in the endoplasmic reticulum. *Journal of immunology (Baltimore, Md. : 1950)* **166**, 1703-1709, doi:10.4049/jimmunol.166.3.1703 (2001).

163   Hughes, E. A. & Cresswell, P. The thiol oxidoreductase ERp57 is a component of the MHC class I peptide-loading complex. *Current biology : CB* **8**, 709-712, doi:10.1016/s0960-9822(98)70278-7 (1998).

164   Morrice, N. A. & Powis, S. J. A role for the thiol-dependent reductase ERp57 in the assembly of MHC class I molecules. *Current biology : CB* **8**, 713-716, doi:10.1016/s0960-9822(98)70279-9 (1998).

165   Sadasivan, B., Lehner, P. J., Ortmann, B., Spies, T. & Cresswell, P. Roles for calreticulin and a novel glycoprotein, tapasin, in the interaction of MHC class I molecules with TAP. *Immunity* **5**, 103-114, doi:10.1016/s1074-7613(00)80487-2 (1996).

166   Blees, A. *et al.* Structure of the human MHC-I peptide-loading complex. *Nature* **551**, 525-528, doi:10.1038/nature24627 (2017).

167   Degen, E., Cohen-Doyle, M. F. & Williams, D. B. Efficient dissociation of the p88 chaperone from major histocompatibility complex class I molecules requires both beta 2-microglobulin and peptide. *J Exp Med* **175**, 1653-1661, doi:10.1084/jem.175.6.1653 (1992).

168   Hulpke, S., Baldauf, C. & Tampé, R. Molecular architecture of the MHC I peptide-loading complex: one tapasin molecule is essential and sufficient for antigen processing. *FASEB journal : official publication of the Federation of American Societies for Experimental Biology* **26**, 5071-5080, doi:10.1096/fj.12-217489 (2012).

169   Oliver, J. D., Roderick, H. L., Llewellyn, D. H. & High, S. ERp57 functions as a subunit of specific complexes formed with the ER lectins calreticulin and calnexin. *Molecular biology of the cell* **10**, 2573-2582, doi:10.1091/mbc.10.8.2573 (1999).

170   Cunningham, B. A., Wang, J. L., Berggard, I. & Peterson, P. A. The complete amino acid sequence of beta 2-microglobulin. *Biochemistry* **12**, 4811-4822, doi:10.1021/bi00748a001 (1973).

171   Raghavan, M., Del Cid, N., Rizvi, S. M. & Peters, L. R. MHC class I assembly: out and about. *Trends in immunology* **29**, 436-443, doi:10.1016/j.it.2008.06.004 (2008).

172   Williams, A., Peh, C. A. & Elliott, T. The cell biology of MHC class I antigen presentation. *Tissue antigens* **59**, 3-17, doi:10.1034/j.1399-0039.2002.590103.x (2002).

173   Park, B., Lee, S., Kim, E. & Ahn, K. A single polymorphic residue within the peptide-binding cleft of MHC class I molecules determines spectrum of tapasin dependence. *Journal of immunology (Baltimore, Md. : 1950)* **170**, 961-968, doi:10.4049/jimmunol.170.2.961 (2003).

174   Garstka, M. *et al.* Tapasin dependence of major histocompatibility complex class I molecules correlates with their conformational flexibility. *FASEB journal : official publication of the Federation of American Societies for Experimental Biology* **25**, 3989-3998, doi:10.1096/fj.11-190249 (2011).

175   Blees, A. *et al.* Structure of the human MHC-I peptide-loading complex. *Nature* **551**, 525-528, doi:10.1038/nature24627 (2017).

176   Natarajan, K. *et al.* The Role of Molecular Flexibility in Antigen Presentation and T Cell Receptor-Mediated Signaling. *Frontiers in immunology* **9**, 1657-1657, doi:10.3389/fimmu.2018.01657 (2018).

177   Neerincx, A. & Boyle, L. H. Properties of the tapasin homologue TAPBPR. *Current opinion in immunology* **46**, 97-102, doi:10.1016/j.coi.2017.04.008 (2017).

178   Paroutis, P., Touret, N. & Grinstein, S. The pH of the Secretory Pathway: Measurement, Determinants, and Regulation. *Physiology* **19**, 207-215, doi:10.1152/physiol.00005.2004 (2004).

179   Jensen, L. F., Hansen, M. M., Mensberg, K. L. & Loeschcke, V. Spatially and temporally fluctuating selection at non-MHC immune genes: evidence from TAP polymorphism in populations of brown trout (Salmo trutta, L.). *Heredity* **100**, 79-91, doi:10.1038/sj.hdy.6801067 (2008).

180   Rock, K. L., Reits, E. & Neefjes, J. Present Yourself! By MHC Class I and MHC Class II Molecules. *Trends in immunology* **37**, 724-737, doi:10.1016/j.it.2016.08.010 (2016).

181   Cavallo, F., De Giovanni, C., Nanni, P., Forni, G. & Lollini, P.-L. 2011: the immune hallmarks of cancer. *Cancer immunology, immunotherapy : CII* **60**, 319-326, doi:10.1007/s00262-010-0968-0 (2011).

182   Giraldo, N. A., Becht, E., Vano, Y., Sautes-Fridman, C. & Fridman, W. H. The immune response in cancer: from immunology to pathology to immunotherapy. *Virchows Arch* **467**, 127-135, doi:10.1007/s00428-015-1787-7 (2015).

183   Wu, A. A., Drake, V., Huang, H. S., Chiu, S. & Zheng, L. Reprogramming the tumor microenvironment: tumor-induced immunosuppressive factors paralyze T cells. *Oncoimmunology* **4**, e1016700, doi:10.1080/2162402X.2015.1016700 (2015).

184   Spranger, S. Mechanisms of tumor escape in the context of the T-cell-inflamed and the non-T-cell-inflamed tumor microenvironment. *Int Immunol* **28**, 383-391, doi:10.1093/intimm/dxw014 (2016).

185   Yaacoub, K., Pedeux, R., Tarte, K. & Guillaudeux, T. Role of the tumor microenvironment in regulating apoptosis and cancer progression. *Cancer Lett* **378**, 150-159, doi:10.1016/j.canlet.2016.05.012 (2016).

186   Dragomir, M., Chen, B., Fu, X. & Calin, G. A. Key questions about the checkpoint blockade-are microRNAs an answer? *Cancer biology & medicine* **15**, 103-115, doi:10.20892/j.issn.2095-3941.2018.0006 (2018).

187   Garrido, F., Ruiz-Cabello, F. & Aptsiauri, N. Rejection versus escape: the tumor MHC dilemma. *Cancer immunology, immunotherapy : CII* **66**, 259-271, doi:10.1007/s00262-016-1947-x (2017).

188   Malyshev, I. Y., Kuznetsova, L. V. & Mardente, S. Cancer immunotherapy through the prism of adaptation: Will Achilles catch the tortoise? *Medical Hypotheses* **137**, 109545, doi:https://doi.org/10.1016/j.mehy.2019.109545 (2020).

189   Niemann, J. *et al.* Molecular retargeting of antibodies converts immune defense against oncolytic viruses into cancer immunotherapy. *Nature Communications* **10**, 3236, doi:10.1038/s41467-019-11137-5 (2019).

190   Pikor, L. A., Bell, J. C. & Diallo, J.-S. Oncolytic Viruses: Exploiting Cancer's Deal with the Devil. *Trends in Cancer* **1**, 266-277, doi:10.1016/j.trecan.2015.10.004 (2015).

191   Zehir, A. *et al.* Mutational landscape of metastatic cancer revealed from prospective clinical sequencing of 10,000 patients. *Nat Med* **23**, 703-713, doi:10.1038/nm.4333 (2017).

192   Seliger, B. Immune modulatory microRNAs as a novel mechanism to revert immune escape of tumors. *Cytokine & growth factor reviews* **36**, 49-56, doi:10.1016/j.cytogfr.2017.07.001 (2017).

193   Bonaventura, P. *et al.* Cold Tumors: A Therapeutic Challenge for Immunotherapy. *Frontiers in immunology* **10**, 168-168, doi:10.3389/fimmu.2019.00168 (2019).

194   Hombach, S. & Kretz, M. Non-coding RNAs: Classification, Biology and Functioning. *Advances in experimental medicine and biology* **937**, 3-17, doi:10.1007/978-3-319-42059-2_1 (2016).

195   Rué, P. & Martinez Arias, A. Cell dynamics and gene expression control in tissue homeostasis and development. *Mol Syst Biol* **11**, 792-792, doi:10.15252/msb.20145549 (2015).

196   Mata, J., Marguerat, S. & Bahler, J. Post-transcriptional control of gene expression: a genome-wide perspective. *Trends in biochemical sciences* **30**, 506-514, doi:10.1016/j.tibs.2005.07.005 (2005).

197   Franks, A., Airoldi, E. & Slavov, N. Post-transcriptional regulation across human tissues. *PLoS Comput Biol* **13**, e1005535-e1005535, doi:10.1371/journal.pcbi.1005535 (2017).

198   Gerstberger, S., Hafner, M. & Tuschl, T. A census of human RNA-binding proteins. *Nature reviews. Genetics* **15**, 829-845, doi:10.1038/nrg3813 (2014).

199   Dahariya, S. *et al.* Long non-coding RNA: Classification, biogenesis and functions in blood cells. *Molecular immunology* **112**, 82-92, doi:10.1016/j.molimm.2019.04.011 (2019).

200   Alvarez-Dominguez, J. R., Knoll, M., Gromatzky, A. A. & Lodish, H. F. The Super-Enhancer-Derived alncRNA-EC7/Bloodlinc Potentiates Red Blood Cell Development in trans. *Cell reports* **19**, 2503-2514, doi:https://doi.org/10.1016/j.celrep.2017.05.082 (2017).

201   Lim, L. P., Glasner, M. E., Yekta, S., Burge, C. B. & Bartel, D. P. Vertebrate microRNA genes. *Science (New York, N.Y.)* **299**, 1540, doi:10.1126/science.1080372 (2003).

202   Reinhart, B. J., Weinstein, E. G., Rhoades, M. W., Bartel, B. & Bartel, D. P. MicroRNAs in plants. *Genes & development* **16**, 1616-1626, doi:10.1101/gad.1004402 (2002).

203   Fabian, M. R., Sonenberg, N. & Filipowicz, W. Regulation of mRNA Translation and Stability by microRNAs. *Annual Review of Biochemistry* **79**, 351-379, doi:10.1146/annurev-biochem-060308-103103 (2010).

204   Bartel, D. P. MicroRNAs: target recognition and regulatory functions. *Cell* **136**, 215-233, doi:10.1016/j.cell.2009.01.002 (2009).

205   Bartel, D. P. MicroRNAs: genomics, biogenesis, mechanism, and function. *Cell* **116**, 281-297, doi:10.1016/s0092-8674(04)00045-5 (2004).

206   Vasudevan, S. Posttranscriptional upregulation by microRNAs. *Wiley interdisciplinary reviews. RNA* **3**, 311-330, doi:10.1002/wrna.121 (2012).

207   Kim, D. H., Saetrom, P., Snøve, O., Jr. & Rossi, J. J. MicroRNA-directed transcriptional gene silencing in mammalian cells. *Proceedings of the National Academy of Sciences of the United States of America* **105**, 16230-16235, doi:10.1073/pnas.0808830105 (2008).

208   O'Brien, J., Hayder, H., Zayed, Y. & Peng, C. Overview of MicroRNA Biogenesis, Mechanisms of Actions, and Circulation. *Front Endocrinol (Lausanne)* **9**, doi:10.3389/fendo.2018.00402 (2018).

209   Ma, F. *et al.* MicroRNA-466l upregulates IL-10 expression in TLR-triggered macrophages by antagonizing RNA-binding protein tristetraprolin-mediated IL-10 mRNA degradation. *Journal of immunology (Baltimore, Md. : 1950)* **184**, 6053-6059, doi:10.4049/jimmunol.0902308 (2010).

210   Castellano, L. & Stebbing, J. Deep sequencing of small RNAs identifies canonical and non-canonical miRNA and endogenous siRNAs in mammalian somatic tissues. *Nucleic acids research* **41**, 3339-3351, doi:10.1093/nar/gks1474 (2013).

211   Lee, R. C., Feinbaum, R. L. & Ambros, V. The C. elegans heterochronic gene lin-4 encodes small RNAs with antisense complementarity to lin-14. *Cell* **75**, 843-854, doi:10.1016/0092-8674(93)90529-y (1993).

212   Abdelfattah, A. M., Park, C. & Choi, M. Y. Update on non-canonical microRNAs. *Biomolecular concepts* **5**, 275-287, doi:10.1515/bmc-2014-0012 (2014).

213   Kozomara, A., Birgaoanu, M. & Griffiths-Jones, S. miRBase: from microRNA sequences to function. *Nucleic acids research* **47**, D155-D162, doi:10.1093/nar/gky1141 (2018).

214   Burroughs, A. M. *et al.* Deep-sequencing of human Argonaute-associated small RNAs provides insight into miRNA sorting and reveals Argonaute association with RNA fragments of diverse origin. *RNA biology* **8**, 158-177, doi:10.4161/rna.8.1.14300 (2011).

215   Ni, W.-J. & Leng, X.-M. Dynamic miRNA–mRNA paradigms: New faces of miRNAs. *Biochemistry and Biophysics Reports* **4**, 337-341, doi:https://doi.org/10.1016/j.bbrep.2015.10.011 (2015).

216   Lewis, B. P., Shih, I. h., Jones-Rhoades, M. W., Bartel, D. P. & Burge, C. B. Prediction of Mammalian MicroRNA Targets. *Cell* **115**, 787-798, doi:10.1016/S0092-8674(03)01018-3 (2003).

217   Krek, A. *et al.* Combinatorial microRNA target predictions. *Nature Genetics* **37**, 495-500, doi:10.1038/ng1536 (2005).

218   Lewis, B. P., Burge, C. B. & Bartel, D. P. Conserved seed pairing, often flanked by adenosines, indicates that thousands of human genes are microRNA targets. *Cell* **120**, 15-20, doi:10.1016/j.cell.2004.12.035 (2005).

219   Brennecke, J., Stark, A., Russell, R. B. & Cohen, S. M. Principles of microRNA-target recognition. *PLoS biology* **3**, e85, doi:10.1371/journal.pbio.0030085 (2005).

220   Agarwal, V., Bell, G. W., Nam, J.-W. & Bartel, D. P. Predicting effective microRNA target sites in mammalian mRNAs. *eLife* **4**, e05005, doi:10.7554/eLife.05005 (2015).

221   Oulas, A. *et al.* in *RNA Bioinformatics* (ed Ernesto Picardi) 207-229 (Springer New York, 2015).

222   Felekkis, K., Touvana, E., Stefanou, C. & Deltas, C. microRNAs: a newly described class of encoded molecules that play a role in health and disease. *Hippokratia* **14**, 236-240 (2010).

223   Han, J. *et al.* The Drosha-DGCR8 complex in primary microRNA processing. *Genes & development* **18**, 3016-3027, doi:10.1101/gad.1262504 (2004).

224   Yi, R., Qin, Y., Macara, I. G. & Cullen, B. R. Exportin-5 mediates the nuclear export of pre-microRNAs and short hairpin RNAs. *Genes & development* **17**, 3011-3016, doi:10.1101/gad.1158803 (2003).

225   O'Brien, J., Hayder, H., Zayed, Y. & Peng, C. Overview of MicroRNA Biogenesis, Mechanisms of Actions, and Circulation. *Front Endocrinol (Lausanne)* **9**, 402-402, doi:10.3389/fendo.2018.00402 (2018).

226   Ketting, R. F. *et al.* Dicer functions in RNA interference and in synthesis of small RNA involved in developmental timing in C. elegans. *Genes & development* **15**, 2654-2659, doi:10.1101/gad.927801 (2001).

227   Khvorova, A., Reynolds, A. & Jayasena, S. D. Functional siRNAs and miRNAs Exhibit Strand Bias. *Cell* **115**, 209-216, doi:https://doi.org/10.1016/S0092-8674(03)00801-8 (2003).

228   Kim, V. N., Han, J. & Siomi, M. C. Biogenesis of small RNAs in animals. *Nature reviews. Molecular cell biology* **10**, 126-139, doi:10.1038/nrm2632 (2009).

229   Krol, J., Loedige, I. & Filipowicz, W. The widespread regulation of microRNA biogenesis, function and decay. *Nature reviews. Genetics* **11**, 597-610, doi:10.1038/nrg2843 (2010).

230 Huntzinger, E. *et al.* The interactions of GW182 proteins with PABP and deadenylases are required for both translational repression and degradation of miRNA targets. *Nucleic acids research* **41**, 978-994, doi:10.1093/nar/gks1078 (2013).

231 Afonso-Grunz, F. & Müller, S. Principles of miRNA–mRNA interactions: beyond sequence complementarity. *Cellular and Molecular Life Sciences* **72**, 3127-3141, doi:10.1007/s00018-015-1922-2 (2015).

232 Okamura, K., Liu, N. & Lai, E. C. Distinct mechanisms for microRNA strand selection by Drosophila Argonautes. *Mol Cell* **36**, 431-444, doi:10.1016/j.molcel.2009.09.027 (2009).

233 Esteller, M. Non-coding RNAs in human disease. *Nature reviews. Genetics* **12**, 861-874, doi:10.1038/nrg3074 (2011).

234 Romano, G., Veneziano, D., Acunzo, M. & Croce, C. M. Small non-coding RNA and cancer. *Carcinogenesis* **38**, 485-491, doi:10.1093/carcin/bgx026 (2017).

235 Lin, S. & Gregory, R. I. MicroRNA biogenesis pathways in cancer. *Nature reviews. Cancer* **15**, 321-333, doi:10.1038/nrc3932 (2015).

236 Long, H. *et al.* Dysregulation of microRNAs in autoimmune diseases: Pathogenesis, biomarkers and potential therapeutic targets. *Cancer letters* **428**, 90-103, doi:10.1016/j.canlet.2018.04.016 (2018).

237 Liu, N. & Olson, E. N. MicroRNA regulatory networks in cardiovascular development. *Developmental cell* **18**, 510-525, doi:10.1016/j.devcel.2010.03.010 (2010).

238 De Hert, M., Detraux, J. & Vancampfort, D. The intriguing relationship between coronary heart disease and mental disorders. *Dialogues Clin Neurosci* **20**, 31-40 (2018).

239 Nana-Sinkam, S. P. & Croce, C. M. MicroRNA regulation of tumorigenesis, cancer progression and interpatient heterogeneity: towards clinical use. *Genome biology* **15**, 445, doi:10.1186/s13059-014-0445-8 (2014).

240 Jiang, C., Chen, X., Alattar, M., Wei, J. & Liu, H. MicroRNAs in tumorigenesis, metastasis, diagnosis and prognosis of gastric cancer. *Cancer gene therapy* **22**, 291-301, doi:10.1038/cgt.2015.19 (2015).

241 Kulkarni, S. *et al.* Differential microRNA regulation of HLA-C expression and its association with HIV control. *Nature* **472**, 495-498, doi:10.1038/nature09914 (2011).

242 Mari, L. *et al.* microRNA 125a Regulates MHC-I Expression on Esophageal Adenocarcinoma Cells, Associated With Suppression of Antitumor Immune Response and Poor Outcomes of Patients. *Gastroenterology* **155**, 784-798, doi:10.1053/j.gastro.2018.06.030 (2018).

243 Friedrich, M. *et al.* The role of the miR-148/-152 family in physiology and disease. *European journal of immunology* **47**, 2026-2038, doi:10.1002/eji.201747132 (2017).

244 Zhao, S. *et al.* MicroRNA-148a inhibits the proliferation and promotes the paclitaxel-induced apoptosis of ovarian cancer cells by targeting PDIA3. *Mol Med Rep* **12**, 3923-3929, doi:10.3892/mmr.2015.3826 (2015).

245 Tan, Z. *et al.* Allele-specific targeting of microRNAs to HLA-G and risk of asthma. *Am J Hum Genet* **81**, 829-834, doi:10.1086/521200 (2007).

246 Zhu, X. M. *et al.* Overexpression of miR-152 leads to reduced expression of human leukocyte antigen-G and increased natural killer cell mediated cytolysis in JEG-3 cells. *Am J Obstet Gynecol* **202**, 592 e591-597, doi:10.1016/j.ajog.2010.03.002 (2010).

247 Jasinski-Bergner, S. *et al.* Clinical relevance of miR-mediated HLA-G regulation and the associated immune cell infiltration in renal cell carcinoma. *Oncoimmunology* **4**, e1008805, doi:10.1080/2162402x.2015.1008805 (2015).

248 Wang, Y. *et al.* MicroRNA-152 regulates immune response via targeting B7-H1 in gastric carcinoma. *Oncotarget* **8**, 28125-28134, doi:10.18632/oncotarget.15924 (2017).

249 Gao, F. *et al.* miR-9 modulates the expression of interferon-regulated genes and MHC class I molecules in human nasopharyngeal carcinoma cells. *Biochemical and biophysical research communications* **431**, 610-616, doi:10.1016/j.bbrc.2012.12.097 (2013).

250 Bartoszewski, R. *et al.* The unfolded protein response (UPR)-activated transcription factor X-box-binding protein 1 (XBP1) induces microRNA-346 expression that targets the human antigen peptide transporter 1 (TAP1) mRNA and governs immune regulatory genes. *The Journal of biological chemistry* **286**, 41862-41870, doi:10.1074/jbc.M111.304956 (2011).

251 Albanese, M. *et al.* Epstein-Barr virus microRNAs reduce immune surveillance by virus-specific CD8+ T cells. *Proceedings of the National Academy of Sciences of the United States of America* **113**, E6467-e6475, doi:10.1073/pnas.1605884113 (2016).

252 Kim, S. *et al.* Human cytomegalovirus microRNA miR-US4-1 inhibits CD8(+) T cell responses by targeting the aminopeptidase ERAP1. *Nature immunology* **12**, 984-991, doi:10.1038/ni.2097 (2011).

253 Belmont, P. J., Chen, W. J., Thuerauf, D. J. & Glembotski, C. C. Regulation of microRNA expression in the heart by the ATF6 branch of the ER stress response. *Journal of molecular and cellular cardiology* **52**, 1176-1182, doi:10.1016/j.yjmcc.2012.01.017 (2012).

254 Colangelo, T. *et al.* Proteomic screening identifies calreticulin as a miR-27a direct target repressing MHC class I cell surface exposure in colorectal cancer. *Cell death & disease* **7**, e2120, doi:10.1038/cddis.2016.28 (2016).

255 Hisaoka, M., Matsuyama, A. & Nakamoto, M. Aberrant calreticulin expression is involved in the dedifferentiation of dedifferentiated liposarcoma. *The American journal of pathology* **180**, 2076-2083, doi:10.1016/j.ajpath.2012.01.042 (2012).

256 Liu, Y. *et al.* Altered expression profiles of microRNAs in a stable hepatitis B virus-expressing cell line. *Chinese medical journal* **122**, 10-14 (2009).

257 Nachmani, D. *et al.* MicroRNA editing facilitates immune elimination of HCMV infected cells. *PLoS pathogens* **10**, e1003963, doi:10.1371/journal.ppat.1003963 (2014).

258 Zhu, X. M. *et al.* Overexpression of miR-152 leads to reduced expression of human leukocyte antigen-G and increased natural killer cell mediated cytolysis in JEG-3 cells. *American journal of obstetrics and gynecology* **202**, 592.e591-597, doi:10.1016/j.ajog.2010.03.002 (2010).

259 Jasinski-Bergner, S. *et al.* Identification of novel microRNAs regulating HLA-G expression and investigating their clinical relevance in renal cell carcinoma. *Oncotarget* **7**, 26866-26878, doi:10.18632/oncotarget.8567 (2016).

260   Song, B. *et al.* Long non-coding RNA HOTAIR promotes HLA-G expression via inhibiting miR-152 in gastric cancer cells. *Biochemical and biophysical research communications* **464**, 807-813, doi:https://doi.org/10.1016/j.bbrc.2015.07.040 (2015).

261   Sun, J. *et al.* Long non-coding RNA HOTAIR modulates HLA-G expression by absorbing miR-148a in human cervical cancer. *International journal of oncology* **49**, 943-952, doi:10.3892/ijo.2016.3589 (2016).

262   Friedrich, M., Vaxevanis, C. K., Biehl, K., Mueller, A. & Seliger, B. Targeting the coding sequence: opposing roles in regulating classical and non-classical MHC class I molecules by miR-16 and miR-744. *Journal for immunotherapy of cancer* **8**, doi:10.1136/jitc-2019-000396 (2020).

263   Yin, P. *et al.* MiR-451 suppresses cell proliferation and metastasis in A549 lung cancer cells. *Molecular biotechnology* **57**, 1-11, doi:10.1007/s12033-014-9796-3 (2015).

264   Knox, B. *et al.* A functional SNP in the 3'-UTR of TAP2 gene interacts with microRNA hsa-miR-1270 to suppress the gene expression. *Environmental and molecular mutagenesis* **59**, 134-143, doi:10.1002/em.22159 (2018).

265   Anders, G. *et al.* doRiNA: a database of RNA interactions in post-transcriptional regulation. *Nucleic acids research* **40**, D180-D186, doi:10.1093/nar/gkr1007 (2011).

266   Glisovic, T., Bachorik, J. L., Yong, J. & Dreyfuss, G. RNA-binding proteins and post-transcriptional gene regulation. *FEBS letters* **582**, 1977-1986, doi:10.1016/j.febslet.2008.03.004 (2008).

267   Idler, R. K. & Yan, W. Control of messenger RNA fate by RNA-binding proteins: an emphasis on mammalian spermatogenesis. *Journal of andrology* **33**, 309-337, doi:10.2164/jandrol.111.014167 (2012).

268   Sutherland, J., Siddall, N., Hime, G. & McLaughlin, E. RNA binding proteins in spermatogenesis: an in depth focus on the Musashi family. *Asian Journal of Andrology* **17**, 529-536, doi:10.4103/1008-682x.151397 (2015).

269   Turner, M. & Díaz-Muñoz, M. D. RNA-binding proteins control gene expression and cell fate in the immune system. *Nature immunology* **19**, 120-129, doi:10.1038/s41590-017-0028-4 (2018).

270   Hentze, M. W., Castello, A., Schwarzl, T. & Preiss, T. A brave new world of RNA-binding proteins. *Nature Reviews Molecular Cell Biology* **19**, 327, doi:10.1038/nrm.2017.130 https://www.nature.com/articles/nrm.2017.130#supplementary-information (2018).

271   Lunde, B. M., Moore, C. & Varani, G. RNA-binding proteins: modular design for efficient function. *Nature reviews. Molecular cell biology* **8**, 479-490, doi:10.1038/nrm2178 (2007).

272   Clery, A., Blatter, M. & Allain, F. H. RNA recognition motifs: boring? Not quite. *Current opinion in structural biology* **18**, 290-298, doi:10.1016/j.sbi.2008.04.002 (2008).

273   Linder, P. & Jankowsky, E. From unwinding to clamping - the DEAD box RNA helicase family. *Nature reviews. Molecular cell biology* **12**, 505-516, doi:10.1038/nrm3154 (2011).

274   Wang, X., McLachlan, J., Zamore, P. D. & Hall, T. M. Modular recognition of RNA by a human pumilio-homology domain. *Cell* **110**, 501-512, doi:10.1016/s0092-8674(02)00873-5 (2002).

275   Neelamraju, Y., Hashemikhabir, S. & Janga, S. C. The human RBPome: from genes and proteins to human disease. *Journal of proteomics* **127**, 61-70, doi:10.1016/j.jprot.2015.04.031 (2015).

276   Sanchez de Groot, N. *et al.* RNA structure drives interaction with proteins. *Nature Communications* **10**, 3246, doi:10.1038/s41467-019-10923-5 (2019).

277   Matera, A. G., Terns, R. M. & Terns, M. P. Non-coding RNAs: lessons from the small nuclear and small nucleolar RNAs. *Nature reviews. Molecular cell biology* **8**, 209-220, doi:10.1038/nrm2124 (2007).

278   Dreyfuss, G., Kim, V. N. & Kataoka, N. Messenger-RNA-binding proteins and the messages they carry. *Nature reviews. Molecular cell biology* **3**, 195-205, doi:10.1038/nrm760 (2002).

279   Vos, P. D., Leedman, P. J., Filipovska, A. & Rackham, O. Modulation of miRNA function by natural and synthetic RNA-binding proteins in cancer. *Cellular and molecular life sciences : CMLS* **76**, 3745-3752, doi:10.1007/s00018-019-03163-9 (2019).

280   Treiber, T. *et al.* A Compendium of RNA-Binding Proteins that Regulate MicroRNA Biogenesis. *Mol Cell* **66**, 270-284.e213, doi:10.1016/j.molcel.2017.03.014 (2017).

281   Connerty, P., Ahadi, A. & Hutvagner, G. RNA Binding Proteins in the miRNA Pathway. *International journal of molecular sciences* **17**, doi:10.3390/ijms17010031 (2015).

282   Nguyen, T. A. *et al.* Functional Anatomy of the Human Microprocessor. *Cell* **161**, 1374-1387, doi:10.1016/j.cell.2015.05.010 (2015).

283   Lee, Y. *et al.* The role of PACT in the RNA silencing pathway. *The EMBO journal* **25**, 522-532, doi:10.1038/sj.emboj.7600942 (2006).

284   Grishok, A. *et al.* Genes and Mechanisms Related to RNA Interference Regulate Expression of the Small Temporal RNAs that Control C. elegans Developmental Timing. *Cell* **106**, 23-34, doi:10.1016/S0092-8674(01)00431-7 (2001).

285   Eulalio, A., Huntzinger, E. & Izaurralde, E. GW182 interaction with Argonaute is essential for miRNA-mediated translational repression and mRNA decay. *Nature structural & molecular biology* **15**, 346-353, doi:10.1038/nsmb.1405 (2008).

286   Kedde, M. & Agami, R. Interplay between microRNAs and RNA-binding proteins determines developmental processes. *Cell Cycle* **7**, 899-903, doi:10.4161/cc.7.7.5644 (2008).

287   Kedde, M. *et al.* A Pumilio-induced RNA structure switch in p27-3' UTR controls miR-221 and miR-222 accessibility. *Nature cell biology* **12**, 1014-1020, doi:10.1038/ncb2105 (2010).

288   Miles, W. O., Tschop, K., Herr, A., Ji, J. Y. & Dyson, N. J. Pumilio facilitates miRNA regulation of the E2F3 oncogene. *Genes & development* **26**, 356-368, doi:10.1101/gad.182568.111 (2012).

289   Bai, Y. *et al.* Overexpression of DICER1 induced by the upregulation of GATA1 contributes to the proliferation and apoptosis of leukemia cells. *International journal of oncology* **42**, 1317-1324, doi:10.3892/ijo.2013.1831 (2013).

290   Zhu, D. X. *et al.* Downregulated Dicer expression predicts poor prognosis in chronic lymphocytic leukemia. *Cancer science* **103**, 875-881, doi:10.1111/j.1349-7006.2012.02234.x (2012).

291   Kitagawa, N. *et al.* Downregulation of the microRNA biogenesis components and its association with poor prognosis in hepatocellular carcinoma. *Cancer science* **104**, 543-551, doi:10.1111/cas.12126 (2013).

292   Srikantan, S., Tominaga, K. & Gorospe, M. Functional interplay between RNA-binding protein HuR and microRNAs. *Curr Protein Pept Sci* **13**, 372-379 (2012).

293   Loffreda, A., Rigamonti, A., Barabino, S. M. L. & Lenzken, S. C. RNA-Binding Proteins in the Regulation of miRNA Activity: A Focus on Neuronal Functions. *Biomolecules* **5**, 2363-2387, doi:10.3390/biom5042363 (2015).

294   Melamed, Z. e. *et al.* Alternative Splicing Regulates Biogenesis of miRNAs Located across Exon-Intron Junctions. *Molecular cell* **50**, doi:10.1016/j.molcel.2013.05.007 (2013).

295   Ciafrè, S. A. & Galardi, S. microRNAs and RNA-binding proteins. *RNA biology* **10**, 934-942, doi:10.4161/rna.24641 (2013).

296   van Kouwenhove, M., Kedde, M. & Agami, R. MicroRNA regulation by RNA-binding proteins and its implications for cancer. *Nature reviews. Cancer* **11**, 644-656, doi:10.1038/nrc3107 (2011).

297   Brinegar, A. E. & Cooper, T. A. Roles for RNA-binding proteins in development and disease. *Brain research* **1647**, 1-8, doi:10.1016/j.brainres.2016.02.050 (2016).

298   Mitchell, S. F. & Parker, R. Principles and properties of eukaryotic mRNPs. *Mol Cell* **54**, 547-558, doi:10.1016/j.molcel.2014.04.033 (2014).

299   Turner, M., Galloway, A. & Vigorito, E. Noncoding RNA and its associated proteins as regulatory elements of the immune system. *Nature immunology* **15**, 484-491, doi:10.1038/ni.2887 (2014).

300   Schmiedel, D. *et al.* The RNA binding protein IMP3 facilitates tumor immune escape by downregulating the stress-induced ligands ULPB2 and MICB. *eLife* **5**, e13426, doi:10.7554/eLife.13426 (2016).

301   Vantourout, P. *et al.* Immunological visibility: posttranscriptional regulation of human NKG2D ligands by the EGF receptor pathway. *Science translational medicine* **6**, 231ra249, doi:10.1126/scitranslmed.3007579 (2014).

302   Sahu, A., Singhal, U. & Chinnaiyan, A. M. Long noncoding RNAs in cancer: from function to translation. *Trends Cancer* **1**, 93-109, doi:10.1016/j.trecan.2015.08.010 (2015).

303   Pereira, B., Billaud, M. & Almeida, R. RNA-Binding Proteins in Cancer: Old Players and New Actors. *Trends in Cancer* **3**, 506-528, doi:10.1016/j.trecan.2017.05.003 (2017).

304   Hong, S. RNA Binding Protein as an Emerging Therapeutic Target for Cancer Prevention and Treatment. *J Cancer Prev* **22**, 203-210, doi:10.15430/JCP.2017.22.4.203 (2017).

305   Huang, L. *et al.* The RNA-binding Protein MEX3B Mediates Resistance to Cancer Immunotherapy by Downregulating HLA-A Expression. *Clin Cancer Res* **24**, 3366-3376, doi:10.1158/1078-0432.CCR-17-2483 (2018).

306   Cano, F. *et al.* The RNA-binding E3 ubiquitin ligase MEX-3C links ubiquitination with MHC-I mRNA degradation. *The EMBO journal* **31**, 3596-3606, doi:10.1038/emboj.2012.218 (2012).

307   Kulkarni, S. *et al.* Posttranscriptional Regulation of HLA-A Protein Expression by Alternative Polyadenylation Signals Involving the RNA-Binding Protein Syncrip. *Journal of immunology (Baltimore, Md. : 1950)* **199**, 3892-3899, doi:10.4049/jimmunol.1700697 (2017).

308   Sahlberg, A. S., Ruuska, M., Granfors, K. & Penttinen, M. A. Altered regulation of ELAVL1/HuR in HLA-B27-expressing U937 monocytic cells. *PloS one* **8**, e70377, doi:10.1371/journal.pone.0070377 (2013).

309   Reches, A. *et al.* HNRNPR Regulates the Expression of Classical and Nonclassical MHC Class I Proteins. *Journal of immunology (Baltimore, Md. : 1950)* **196**, 4967-4976, doi:10.4049/jimmunol.1501550 (2016).

310   Kulkarni, S. *et al.* Genetic interplay between HLA-C and MIR148A in HIV control and Crohn disease. *Proceedings of the National Academy of Sciences of the United States of America* **110**, 20705-20710, doi:10.1073/pnas.1312237110 (2013).

311   Bignell, G. R. *et al.* Signatures of mutation and selection in the cancer genome. *Nature* **463**, 893-898, doi:10.1038/nature08768 (2010).

312   Pawelec, G. & Marsh, S. G. ESTDAB: a collection of immunologically characterised melanoma cell lines and searchable databank. *Cancer immunology, immunotherapy : CII* **55**, 623-627, doi:10.1007/s00262-005-0117-3 (2006).

313   Wulfanger, J. *et al.* Heterogeneous expression and functional relevance of the ubiquitin carboxyl-terminal hydrolase L1 in melanoma. *International journal of cancer* **133**, 2522-2532, doi:10.1002/ijc.28278 (2013).

314   Salter, R. D. & Cresswell, P. Impaired assembly and transport of HLA-A and -B antigens in a mutant TxB cell hybrid. *EMBO J* **5**, 943-949 (1986).

315   Bossi, G. *et al.* Examining the presentation of tumor-associated antigens on peptide-pulsed T2 cells. *Oncoimmunology* **2**, e26840-e26840, doi:10.4161/onci.26840 (2013).

316   Varkonyi-Gasic, E., Wu, R., Wood, M., Walton, E. F. & Hellens, R. P. Protocol: a highly sensitive RT-PCR method for detection and quantification of microRNAs. *Plant methods* **3**, 12, doi:10.1186/1746-4811-3-12 (2007).

317   Kramer, M. F. Stem-loop RT-qPCR for miRNAs. *Current protocols in molecular biology* **Chapter 15**, Unit 15.10, doi:10.1002/0471142727.mb1510s95 (2011).

318   Bukur, J., Herrmann, F., Handke, D., Recktenwald, C. & Seliger, B. Identification of E2F1 as an important transcription factor for the regulation of tapasin expression. *The Journal of biological chemistry* **285**, 30419-30426, doi:10.1074/jbc.M109.094284 (2010).

319   Steven, A. *et al.* HER-2/neu mediates oncogenic transformation via altered CREB expression and function. *Molecular cancer research : MCR* **11**, 1462-1477, doi:10.1158/1541-7786.mcr-13-0125 (2013).

320   Lorenzo-Herrero, S., Sordo-Bahamonde, C., Gonzalez, S. & Lopez-Soto, A. CD107a Degranulation Assay to Evaluate Immune Cell Antitumor Activity. *Methods in molecular biology (Clifton, N.J.)* **1884**, 119-130, doi:10.1007/978-1-4939-8885-3_7 (2019).

321   Zeng, Y. & Cullen, B. R. Sequence requirements for micro RNA processing and function in human cells. *RNA (New York, N.Y.)* **9**, 112-123, doi:10.1261/rna.2780503 (2003).

322   Tretbar, U. S., Friedrich, M., Lazaridou, M. F. & Seliger, B. Identification of Immune Modulatory miRNAs by miRNA Enrichment via RNA Affinity Purification. *Methods in molecular biology (Clifton, N.J.)* **1913**, 81-101, doi:10.1007/978-1-4939-8979-9_6 (2019).

323   Braun, J., Misiak, D., Busch, B., Krohn, K. & Huttelmaier, S. Rapid identification of regulatory microRNAs by miTRAP (miRNA trapping by RNA in vitro affinity purification). *Nucleic acids research* **42**, e66, doi:10.1093/nar/gku127 (2014).

324 Johansson, H. E., Liljas, L. & Uhlenbeck, O. C. RNA Recognition by the MS2 Phage Coat Protein. *Seminars in Virology* **8**, 176-185, doi:https://doi.org/10.1006/smvy.1997.0120 (1997).

325 Kukurba, K. R. & Montgomery, S. B. RNA Sequencing and Analysis. *Cold Spring Harb Protoc* **2015**, 951-969, doi:10.1101/pdb.top084970 (2015).

326 Backes, C. *et al.* Prioritizing and selecting likely novel miRNAs from NGS data. *Nucleic acids research* **44**, e53-e53, doi:10.1093/nar/gkv1335 (2016).

327 Liu, J., Jennings, S. F., Tong, W. & Hong, H. Next generation sequencing for profiling expression of miRNAs: technical progress and applications in drug development. *J Biomed Sci Eng* **4**, 666-676, doi:10.4236/jbise.2011.410083 (2011).

328 Giraldez, M. D. *et al.* Comprehensive multi-center assessment of small RNA-seq methods for quantitative miRNA profiling. *Nature biotechnology* **36**, 746-757, doi:10.1038/nbt.4183 (2018).

329 Martin, M. Cutadapt removes adapter sequences from high-throughput sequencing reads. *2011* **17**, 3, doi:10.14806/ej.17.1.200 (2011).

330 Islam, S. *et al.* Quantitative single-cell RNA-seq with unique molecular identifiers. *Nature methods* **11**, 163-166, doi:10.1038/nmeth.2772 (2014).

331 Langmead, B., Trapnell, C., Pop, M. & Salzberg, S. L. Ultrafast and memory-efficient alignment of short DNA sequences to the human genome. *Genome biology* **10**, R25, doi:10.1186/gb-2009-10-3-r25 (2009).

332 An, J., Lai, J., Lehman, M. L. & Nelson, C. C. miRDeep*: an integrated application tool for miRNA identification from RNA sequencing data. *Nucleic acids research* **41**, 727-737, doi:10.1093/nar/gks1187 (2012).

333 Zhou, L. *et al.* Integrated profiling of microRNAs and mRNAs: microRNAs located on Xq27.3 associate with clear cell renal cell carcinoma. *PloS one* **5**, e15224, doi:10.1371/journal.pone.0015224 (2010).

334 Love, M. I., Huber, W. & Anders, S. Moderated estimation of fold change and dispersion for RNA-seq data with DESeq2. *Genome biology* **15**, 550, doi:10.1186/s13059-014-0550-8 (2014).

335 Friedrich, M. *et al.*   (2019).

336 Hammerle, M. *et al.* Posttranscriptional destabilization of the liver-specific long noncoding RNA HULC by the IGF2 mRNA-binding protein 1 (IGF2BP1). *Hepatology (Baltimore, Md.)* **58**, 1703-1712, doi:10.1002/hep.26537 (2013).

337 Dagley, L. F., Infusini, G., Larsen, R. H., Sandow, J. J. & Webb, A. I. Universal Solid-Phase Protein Preparation (USP(3)) for Bottom-up and Top-down Proteomics. *Journal of proteome research* **18**, 2915-2924, doi:10.1021/acs.jproteome.9b00217 (2019).

338 Rahn, J. *et al.* Altered protein expression pattern in colon tissue of mice upon supplementation with distinct selenium compounds. *Proteomics* **17**, doi:10.1002/pmic.201600486 (2017).

339 Koelblinger, P. *et al.* Increased tumour cell PD-L1 expression, macrophage and dendritic cell infiltration characterise the tumour microenvironment of ulcerated primary melanomas. *Journal of the European Academy of Dermatology and Venereology : JEADV* **33**, 667-675, doi:10.1111/jdv.15302 (2019).

340 Young, M. D., Wakefield, M. J., Smyth, G. K. & Oshlack, A. Gene ontology analysis for RNA-seq: accounting for selection bias. *Genome Biol* **11**, R14, doi:10.1186/gb-2010-11-2-r14 (2010).

341 Wei, L., He, F., Zhang, W., Chen, W. & Yu, B. Bioinformatics analysis of microarray data to reveal the pathogenesis of diffuse intrinsic pontine glioma. *Biological research* **51**, 26, doi:10.1186/s40659-018-0175-6 (2018).

342 Li, J.-H., Liu, S., Zhou, H., Qu, L.-H. & Yang, J.-H. starBase v2.0: decoding miRNA-ceRNA, miRNA-ncRNA and protein–RNA interaction networks from large-scale CLIP-Seq data. *Nucleic acids research* **42**, D92-D97, doi:10.1093/nar/gkt1248 (2013).

343 Yang, J.-H. *et al.* starBase: a database for exploring microRNA–mRNA interaction maps from Argonaute CLIP-Seq and Degradome-Seq data. *Nucleic acids research* **39**, D202-D209, doi:10.1093/nar/gkq1056 (2010).

344 Cirenajwis, H. *et al.* Molecular stratification of metastatic melanoma using gene expression profiling: Prediction of survival outcome and benefit from molecular targeted therapy. *Oncotarget* **6**, 12297-12309, doi:10.18632/oncotarget.3655 (2015).

345 Ellrott, K. *et al.* Scalable Open Science Approach for Mutation Calling of Tumor Exomes Using Multiple Genomic Pipelines. *Cell systems* **6**, 271-281.e277, doi:10.1016/j.cels.2018.03.002 (2018).

346 Gao, Q. *et al.* Driver Fusions and Their Implications in the Development and Treatment of Human Cancers. *Cell reports* **23**, 227-238.e223, doi:10.1016/j.celrep.2018.03.050 (2018).

347 Hoadley, K. A. *et al.* Cell-of-Origin Patterns Dominate the Molecular Classification of 10,000 Tumors from 33 Types of Cancer. *Cell* **173**, 291-304.e296, doi:10.1016/j.cell.2018.03.022 (2018).

348 Liu, J. *et al.* An Integrated TCGA Pan-Cancer Clinical Data Resource to Drive High-Quality Survival Outcome Analytics. *Cell* **173**, 400-416.e411, doi:10.1016/j.cell.2018.02.052 (2018).

349 Sanchez-Vega, F. *et al.* Oncogenic Signaling Pathways in The Cancer Genome Atlas. *Cell* **173**, 321-337.e310, doi:10.1016/j.cell.2018.03.035 (2018).

350 Taylor, A. M. *et al.* Genomic and Functional Approaches to Understanding Cancer Aneuploidy. *Cancer cell* **33**, 676-689.e673, doi:10.1016/j.ccell.2018.03.007 (2018).

351 Akbani, R. *et al.* Genomic Classification of Cutaneous Melanoma. *Cell* **161**, 1681-1696, doi:https://doi.org/10.1016/j.cell.2015.05.044 (2015).

352 Cormier, J. N. *et al.* Natural variation of the expression of HLA and endogenous antigen modulates CTL recognition in an in vitro melanoma model. *International journal of cancer* **80**, 781-790, doi:10.1002/(sici)1097-0215(19990301)80:5<781::aid-ijc24>3.0.co;2-a (1999).

353 Respa, A. *et al.* Association of IFN-gamma signal transduction defects with impaired HLA class I antigen processing in melanoma cell lines. *Clinical cancer research : an official journal of the American Association for Cancer Research* **17**, 2668-2678, doi:10.1158/1078-0432.ccr-10-2114 (2011).

354 Lazaridou, M.-F. *et al.* Identification of miR-200a-5p targeting the peptide transporter TAP1 and its association with the clinical outcome of melanoma patients. *Oncoimmunology* **9**, 1774323, doi:10.1080/2162402X.2020.1774323 (2020).

355 Bukur, J., Jasinski, S. & Seliger, B. The role of classical and non-classical HLA class I antigens in human tumors. *Seminars in cancer biology* **22**, 350-358, doi:10.1016/j.semcancer.2012.03.003 (2012).

356   Qin, Z. *et al.* Increased tumorigenicity, but unchanged immunogenicity, of transporter for antigen presentation 1-deficient tumors. *Cancer research* **62**, 2856-2860 (2002).

357   Seliger, B. The link between MHC class I abnormalities of tumors, oncogenes, tumor suppressor genes, and transcription factors. *Journal of immunotoxicology* **11**, 308-310, doi:10.3109/1547691x.2013.875084 (2014).

358   Guan, J., Gupta, R. & Filipp, F. V. Cancer systems biology of TCGA SKCM: efficient detection of genomic drivers in melanoma. *Sci Rep* **5**, 7857, doi:10.1038/srep07857 (2015).

359   Ellrott, K. *et al.* Scalable Open Science Approach for Mutation Calling of Tumor Exomes Using Multiple Genomic Pipelines. *Cell Syst* **6**, 271-281 e277, doi:10.1016/j.cels.2018.03.002 (2018).

360   Gao, Q. *et al.* Driver Fusions and Their Implications in the Development and Treatment of Human Cancers. *Cell Rep* **23**, 227-238 e223, doi:10.1016/j.celrep.2018.03.050 (2018).

361   Hoadley, K. A. *et al.* Cell-of-Origin Patterns Dominate the Molecular Classification of 10,000 Tumors from 33 Types of Cancer. *Cell* **173**, 291-304 e296, doi:10.1016/j.cell.2018.03.022 (2018).

362   Liu, J. *et al.* An Integrated TCGA Pan-Cancer Clinical Data Resource to Drive High-Quality Survival Outcome Analytics. *Cell* **173**, 400-416 e411, doi:10.1016/j.cell.2018.02.052 (2018).

363   Sanchez-Vega, F. *et al.* Oncogenic Signaling Pathways in The Cancer Genome Atlas. *Cell* **173**, 321-337 e310, doi:10.1016/j.cell.2018.03.035 (2018).

364   Taylor, A. M. *et al.* Genomic and Functional Approaches to Understanding Cancer Aneuploidy. *Cancer Cell* **33**, 676-689 e673, doi:10.1016/j.ccell.2018.03.007 (2018).

365   Seliger B. , M. A. a. F. D. The Role of Immune Modulatory MicroRNAs in Tumors. *INTEC*, doi:10.5772/61805 (2016).

366   Dweep, H., Sticht, C., Pandey, P. & Gretz, N. miRWalk--database: prediction of possible miRNA binding sites by "walking" the genes of three genomes. *Journal of biomedical informatics* **44**, 839-847, doi:10.1016/j.jbi.2011.05.002 (2011).

367   Dweep, H. & Gretz, N. miRWalk2.0: a comprehensive atlas of microRNA-target interactions. *Nature methods* **12**, 697, doi:10.1038/nmeth.3485 (2015).

368   Wong, N. & Wang, X. miRDB: an online resource for microRNA target prediction and functional annotations. *Nucleic acids research* **43**, D146-D152, doi:10.1093/nar/gku1104 (2014).

369   Miranda, K. C. *et al.* A pattern-based method for the identification of MicroRNA binding sites and their corresponding heteroduplexes. *Cell* **126**, 1203-1217, doi:10.1016/j.cell.2006.07.031 (2006).

370   Betel, D., Wilson, M., Gabow, A., Marks, D. S. & Sander, C. The microRNA.org resource: targets and expression. *Nucleic acids research* **36**, D149-D153, doi:10.1093/nar/gkm995 (2008).

371   Rehmsmeier, M., Steffen, P., Hochsmann, M. & Giegerich, R. Fast and effective prediction of microRNA/target duplexes. *RNA (New York, N.Y.)* **10**, 1507-1517, doi:10.1261/rna.5248604 (2004).

372   Krüger, J. & Rehmsmeier, M. RNAhybrid: microRNA target prediction easy, fast and flexible. *Nucleic acids research* **34**, W451-W454, doi:10.1093/nar/gkl243 (2006).

373   Jasinski-Bergner, S. *et al.*   (2019).

374   Hannon, G. J. RNA interference. *Nature* **418**, 244-251, doi:10.1038/418244a (2002).

375   Meister, G. *et al.* Human Argonaute2 mediates RNA cleavage targeted by miRNAs and siRNAs. *Mol Cell* **15**, 185-197, doi:10.1016/j.molcel.2004.07.007 (2004).

376   An, J., Lai, J., Lehman, M. L. & Nelson, C. C. miRDeep*: an integrated application tool for miRNA identification from RNA sequencing data. *Nucleic Acids Res* **41**, 727-737, doi:10.1093/nar/gks1187 (2013).

377   Kozomara, A., Birgaoanu, M. & Griffiths-Jones, S. miRBase: from microRNA sequences to function. *Nucleic Acids Res* **47**, D155-D162, doi:10.1093/nar/gky1141 (2019).

378   Lazaridou, M. F. *et al.* Identification of microRNAs Targeting the Transporter Associated with Antigen Processing TAP1 in Melanoma. *Journal of clinical medicine* **9**, doi:10.3390/jcm9092690 (2020).

379   Alter, G., Malenfant, J. M. & Altfeld, M. CD107a as a functional marker for the identification of natural killer cell activity. *Journal of immunological methods* **294**, 15-22, doi:10.1016/j.jim.2004.08.008 (2004).

380   Li, J. H., Liu, S., Zhou, H., Qu, L. H. & Yang, J. H. starBase v2.0: decoding miRNA-ceRNA, miRNA-ncRNA and protein-RNA interaction networks from large-scale CLIP-Seq data. *Nucleic Acids Res* **42**, D92-97, doi:10.1093/nar/gkt1248 (2014).

381   Yang, J. H. *et al.* starBase: a database for exploring microRNA-mRNA interaction maps from Argonaute CLIP-Seq and Degradome-Seq data. *Nucleic Acids Res* **39**, D202-209, doi:10.1093/nar/gkq1056 (2011).

382   Mayr, C. & Bartel, D. P. Widespread shortening of 3'UTRs by alternative cleavage and polyadenylation activates oncogenes in cancer cells. *Cell* **138**, 673-684, doi:10.1016/j.cell.2009.06.016 (2009).

383   Landthaler, M. *et al.* Molecular characterization of human Argonaute-containing ribonucleoprotein complexes and their bound target mRNAs. *RNA (New York, N.Y.)* **14**, 2580-2596, doi:10.1261/rna.1351608 (2008).

384   Snel, B., Lehmann, G., Bork, P. & Huynen, M. A. STRING: a web-server to retrieve and display the repeatedly occurring neighbourhood of a gene. *Nucleic acids research* **28**, 3442-3444, doi:10.1093/nar/28.18.3442 (2000).

385   Szklarczyk, D. *et al.* STRING v11: protein-protein association networks with increased coverage, supporting functional discovery in genome-wide experimental datasets. *Nucleic acids research* **47**, D607-d613, doi:10.1093/nar/gky1131 (2019).

386   Rodriguez, J. A. HLA-mediated tumor escape mechanisms that may impair immunotherapy clinical outcomes via T-cell activation. *Oncology letters* **14**, 4415-4427, doi:10.3892/ol.2017.6784 (2017).

387   Cai, L. *et al.* Defective HLA class I antigen processing machinery in cancer. *Cancer immunology, immunotherapy : CII* **67**, 999-1009, doi:10.1007/s00262-018-2131-2 (2018).

388   Mendez, R. *et al.* HLA and melanoma: multiple alterations in HLA class I and II expression in human melanoma cell lines from ESTDAB cell bank. *Cancer immunology, immunotherapy : CII* **58**, 1507-1515, doi:10.1007/s00262-009-0701-z (2009).

389   Gettinger, S. *et al.* Impaired HLA Class I Antigen Processing and Presentation as a Mechanism of Acquired Resistance to Immune Checkpoint Inhibitors in Lung Cancer. *Cancer discovery* **7**, 1420-1435, doi:10.1158/2159-8290.cd-17-0593 (2017).

390   Garrido, F. & Aptsiauri, N. Cancer immune escape: MHC expression in primary tumours versus metastases. *Immunology* **158**, 255-266, doi:10.1111/imm.13114 (2019).

391   Garrido, F., Aptsiauri, N., Doorduijn, E. M., Garcia Lora, A. M. & van Hall, T. The urgent need to recover MHC class I in cancers for effective immunotherapy. *Current opinion in immunology* **39**, 44-51, doi:10.1016/j.coi.2015.12.007 (2016).

392   Garrido, F. *et al.* Natural history of HLA expression during tumour development. *Immunology today* **14**, 491-499, doi:https://doi.org/10.1016/0167-5699(93)90264-L (1993).

393   Garrido, F. *et al.* Implications for immunosurveillance of altered HLA class I phenotypes in human tumours. *Immunology today* **18**, 89-95 (1997).

394   Koopman, L. A., Corver, W. E., van der Slik, A. R., Giphart, M. J. & Fleuren, G. J. Multiple Genetic Alterations Cause Frequent and Heterogeneous Human Histocompatibility Leukocyte Antigen Class I Loss in Cervical Cancer. *The Journal of Experimental Medicine* **191**, 961, doi:10.1084/jem.191.6.961 (2000).

395   Hicklin, D. J., Marincola, F. M. & Ferrone, S. HLA class I antigen downregulation in human cancers: T-cell immunotherapy revives an old story. *Molecular medicine today* **5**, 178-186, doi:10.1016/s1357-4310(99)01451-3 (1999).

396   Seliger, B., Maeurer, M. J. & Ferrone, S. Antigen-processing machinery breakdown and tumor growth. *Immunology today* **21**, 455-464, doi:10.1016/s0167-5699(00)01692-3 (2000).

397   Marincola, F. M., Jaffee, E. M., Hicklin, D. J. & Ferrone, S. Escape of human solid tumors from T-cell recognition: molecular mechanisms and functional significance. *Advances in immunology* **74**, 181-273 (2000).

398   Campoli, M., Chang, C. C. & Ferrone, S. HLA class I antigen loss, tumor immune escape and immune selection. *Vaccine* **20 Suppl 4**, A40-45, doi:10.1016/s0264-410x(02)00386-9 (2002).

399   Chang, C. C., Campoli, M. & Ferrone, S. Classical and nonclassical HLA class I antigen and NK Cell-activating ligand changes in malignant cells: current challenges and future directions. *Advances in cancer research* **93**, 189-234, doi:10.1016/s0065-230x(05)93006-6 (2005).

400   Aptsiauri, N. *et al.* Role of altered expression of HLA class I molecules in cancer progression. *Advances in experimental medicine and biology* **601**, 123-131, doi:10.1007/978-0-387-72005-0_13 (2007).

401   Aptsiauri, N. *et al.* Regressing and progressing metastatic lesions: resistance to immunotherapy is predetermined by irreversible HLA class I antigen alterations. *Cancer immunology, immunotherapy : CII* **57**, 1727-1733, doi:10.1007/s00262-008-0532-3 (2008).

402   Ferns, D. M. *et al.* Classical and non-classical HLA class I aberrations in primary cervical squamous- and adenocarcinomas and paired lymph node metastases. *Journal for immunotherapy of cancer* **4**, 78, doi:10.1186/s40425-016-0184-3 (2016).

403   Maleno, I. *et al.* Frequent loss of heterozygosity in the beta2-microglobulin region of chromosome 15 in primary human tumors. *Immunogenetics* **63**, 65-71, doi:10.1007/s00251-010-0494-4 (2011).

404   Faber, H. E., Kucherlapati, R. S., Poulik, M. D., Ruddle, F. H. & Smithies, O. beta2-microglobulin locus on human chromosome 15. *Somatic cell genetics* **2**, 141-153 (1976).

405   Aptsiauri, N., Ruiz-Cabello, F. & Garrido, F. The transition from HLA-I positive to HLA-I negative primary tumors: the road to escape from T-cell responses. *Current opinion in immunology* **51**, 123-132, doi:10.1016/j.coi.2018.03.006 (2018).

406   Sade-Feldman, M. *et al.* Resistance to checkpoint blockade therapy through inactivation of antigen presentation. *Nature Communications* **8**, 1136, doi:10.1038/s41467-017-01062-w (2017).

407   Maleno, I., Lopez-Nevot, M. A., Cabrera, T., Salinero, J. & Garrido, F. Multiple mechanisms generate HLA class I altered phenotypes in laryngeal carcinomas: high frequency of HLA haplotype loss associated with loss of heterozygosity in chromosome region 6p21. *Cancer immunology, immunotherapy : CII* **51**, 389-396, doi:10.1007/s00262-002-0296-0 (2002).

408   Maleno, I. *et al.* Distribution of HLA class I altered phenotypes in colorectal carcinomas: high frequency of HLA haplotype loss associated with loss of heterozygosity in chromosome region 6p21. *Immunogenetics* **56**, 244-253, doi:10.1007/s00251-004-0692-z (2004).

409   Maleno, I. *et al.* LOH at 6p21.3 region and HLA class I altered phenotypes in bladder carcinomas. *Immunogenetics* **58**, 503-510, doi:10.1007/s00251-006-0111-8 (2006).

410   McGranahan, N. *et al.* Allele-Specific HLA Loss and Immune Escape in Lung Cancer Evolution. *Cell* **171**, 1259-1271.e1211, doi:10.1016/j.cell.2017.10.001 (2017).

411   Pereira, C. *et al.* Genomic Profiling of Patient-Derived Xenografts for Lung Cancer Identifies B2M Inactivation Impairing Immunorecognition. *Clinical Cancer Research*, doi:10.1158/1078-0432.CCR-16-1946 (2016).

412   Maleno, I., Nevot, M. A. L., Seliger, B. & Garrido, F. Low frequency of HLA haplotype loss associated with loss of heterozygocity in chromosome region 6p21 in clear renal cell carcinomas. *International journal of cancer* **109**, 636-638, doi:10.1002/ijc.20000 (2004).

413   Kageshita, T., Hirai, S., Ono, T., Hicklin, D. J. & Ferrone, S. Down-regulation of HLA class I antigen-processing molecules in malignant melanoma: association with disease progression. *The American journal of pathology* **154**, 745-754, doi:10.1016/s0002-9440(10)65321-7 (1999).

414   Kamarashev, J. *et al.* TAP1 down-regulation in primary melanoma lesions: an independent marker of poor prognosis. *International journal of cancer* **95**, 23-28, doi:10.1002/1097-0215(20010120)95:1<23::aid-ijc1004>3.0.co;2-4 (2001).

415   Meyer, S. *et al.* Role of signal transduction and microRNAs on the immunogenicity of melanoma cells. *Journal of Translational Medicine* **13**, K15, doi:10.1186/1479-5876-13-s1-k15 (2015).

416   Guennoun, A. *et al.* Harnessing the immune system for the treatment of melanoma: current status and future prospects. *Expert review of clinical immunology* **12**, 879-893, doi:10.1080/1744666x.2016.1176529 (2016).

417   Garrido, F., Cabrera, T. & Aptsiauri, N. "Hard" and "soft" lesions underlying the HLA class I alterations in cancer cells: implications for immunotherapy. *International journal of cancer* **127**, 249-256, doi:10.1002/ijc.25270 (2010).

418   thor Straten, P. & Garrido, F. Targetless T cells in cancer immunotherapy. *Journal for immunotherapy of cancer* **4**, 23, doi:10.1186/s40425-016-0127-z (2016).

419   Carretero, R. *et al.* Regression of melanoma metastases after immunotherapy is associated with activation of antigen presentation and interferon-mediated rejection genes. *International journal of cancer* **131**, 387-395, doi:10.1002/ijc.26471 (2012).

420   Seliger, B. Novel insights into the molecular mechanisms of HLA class I abnormalities. *Cancer immunology, immunotherapy : CII* **61**, 249-254, doi:10.1007/s00262-011-1153-9 (2012).

421   Lee, J. S. *et al.* Prognostic Role of the MicroRNA-200 Family in Various Carcinomas: A Systematic Review and Meta-Analysis. *BioMed research international* **2017**, 1928021, doi:10.1155/2017/1928021 (2017).

422   Senfter, D., Madlener, S., Krupitza, G. & Mader, R. M. The microRNA-200 family: still much to discover. *Biomolecular concepts* **7**, 311-319, doi:10.1515/bmc-2016-0020 (2016).

423   Yi, R. *et al.* Morphogenesis in skin is governed by discrete sets of differentially expressed microRNAs. *Nature Genetics* **38**, 356-362, doi:10.1038/ng1744 (2006).

424   Ji, C. *et al.* Transcriptomic analysis of microRNAs-mRNAs regulating innate immune response of zebrafish larvae against Vibrio parahaemolyticus infection. *Fish & shellfish immunology* **91**, 333-342, doi:10.1016/j.fsi.2019.05.050 (2019).

425   Elson-Schwab, I., Lorentzen, A. & Marshall, C. J. MicroRNA-200 family members differentially regulate morphological plasticity and mode of melanoma cell invasion. *PloS one* **5**, doi:10.1371/journal.pone.0013176 (2010).

426   Zhang, L. *et al.* microRNAs exhibit high frequency genomic alterations in human cancer. *Proceedings of the National Academy of Sciences of the United States of America* **103**, 9136-9141, doi:10.1073/pnas.0508889103 (2006).

427   Xie, K. *et al.* Genetic variants in regulatory regions of microRNAs are associated with lung cancer risk. *Oncotarget* **7**, 47966-47974, doi:10.18632/oncotarget.10299 (2016).

428   Wang, Y. *et al.* FOXD1 is targeted by miR-30a-5p and miR-200a-5p and suppresses the proliferation of human ovarian carcinoma cells by promoting p21 expression in a p53-independent manner. *International journal of oncology* **52**, 2130-2142, doi:10.3892/ijo.2018.4359 (2018).

429   Wang, X. *et al.* A potential biomarker hsa-miR-200a-5p distinguishing between benign thyroid tumors with papillary hyperplasia and papillary thyroid carcinoma. *PloS one* **13**, e0200290, doi:10.1371/journal.pone.0200290 (2018).

430   Yang, T. *et al.* miR-200a-5p regulates myocardial necroptosis induced by Se deficiency via targeting RNF11. *Redox biology* **15**, 159-169, doi:10.1016/j.redox.2017.11.025 (2018).

431   Yang, T., Liu, T., Cao, C. & Xu, S. miR-200a-5p augments cardiomyocyte hypertrophy induced by glucose metabolism disorder via the regulation of selenoproteins. *Journal of cellular physiology* **234**, 4095-4103, doi:10.1002/jcp.27206 (2019).

432   Baek, D. *et al.* The impact of microRNAs on protein output. *Nature* **455**, 64-71, doi:10.1038/nature07242 (2008).

433   Stavast, C. J. & Erkeland, S. J. The Non-Canonical Aspects of MicroRNAs: Many Roads to Gene Regulation. *Cells* **8**, doi:10.3390/cells8111465 (2019).

434   Seo, J., Jin, D., Choi, C. H. & Lee, H. Integration of MicroRNA, mRNA, and Protein Expression Data for the Identification of Cancer-Related MicroRNAs. *PloS one* **12**, e0168412, doi:10.1371/journal.pone.0168412 (2017).

435   van Rooij, E. & Olson, E. N. MicroRNA therapeutics for cardiovascular disease: opportunities and obstacles. *Nature Reviews Drug Discovery* **11**, 860-872, doi:10.1038/nrd3864 (2012).

436   Selbach, M. *et al.* Widespread changes in protein synthesis induced by microRNAs. *Nature* **455**, 58-63, doi:10.1038/nature07228 (2008).

437   Hu, W. & Coller, J. What comes first: translational repression or mRNA degradation? The deepening mystery of microRNA function. *Cell Research* **22**, 1322-1324, doi:10.1038/cr.2012.80 (2012).

438   Heise, R. *et al.* Interferon Alpha Signalling and Its Relevance for the Upregulatory Effect of Transporter Proteins Associated with Antigen Processing (TAP) in Patients with Malignant Melanoma. *PloS one* **11**, e0146325, doi:10.1371/journal.pone.0146325 (2016).

439   Jasinski-Bergner, S. *et al.* An altered miTRAP method for miRNA affinity purification with its pros and cons. *Methods in enzymology* **636**, 323-337, doi:10.1016/bs.mie.2019.05.016 (2020).

440   Yoon, J. H., Srikantan, S. & Gorospe, M. MS2-TRAP (MS2-tagged RNA affinity purification): tagging RNA to identify associated miRNAs. *Methods (San Diego, Calif.)* **58**, 81-87, doi:10.1016/j.ymeth.2012.07.004 (2012).

441   Wang, D. *et al.* Quantitative functions of Argonaute proteins in mammalian development. *Genes & development* **26**, 693-704, doi:10.1101/gad.182758.111 (2012).

442   Icli, B., Dorbala, P. & Feinberg, M. W. An emerging role for the miR-26 family in cardiovascular disease. *Trends in cardiovascular medicine* **24**, 241-248, doi:10.1016/j.tcm.2014.06.003 (2014).

443   Li, H., Wang, Y. & Song, Y. MicroRNA-26b inhibits the immune response to Mycobacterium tuberculosis (M.tb) infection in THP-1 cells via targeting TGFβ-activated kinase-1 (TAK1), a promoter of the NF-κB pathway. *International journal of clinical and experimental pathology* **11**, 1218-1227 (2018).

444   Volinia, S. *et al.* A microRNA expression signature of human solid tumors defines cancer gene targets. *Proceedings of the National Academy of Sciences of the United States of America* **103**, 2257-2261, doi:10.1073/pnas.0510565103 (2006).

445   Ro, S., Park, C., Young, D., Sanders, K. M. & Yan, W. Tissue-dependent paired expression of miRNAs. *Nucleic acids research* **35**, 5944-5953, doi:10.1093/nar/gkm641 (2007).

446   Melnik, B. C. MiR-21: an environmental driver of malignant melanoma? *Journal of Translational Medicine* **13**, 202, doi:10.1186/s12967-015-0570-5 (2015).

447   Mo, H. *et al.* Expression and predictive value of miR-489 and miR-21 in melanoma metastasis. *World J Clin Cases* **7**, 2930-2941, doi:10.12998/wjcc.v7.i19.2930 (2019).

448   Wandler, A. *et al.* Quantification of microRNA-21 and microRNA-125b in melanoma tissue. *Melanoma research* **27**, 417-428, doi:10.1097/cmr.0000000000000374 (2017).

449   Jiang, L. *et al.* The status of microRNA-21 expression and its clinical significance in human cutaneous malignant melanoma. *Acta histochemica* **114**, 582-588, doi:10.1016/j.acthis.2011.11.001 (2012).

450   Javanmard, S. H. *et al.* Therapeutic inhibition of microRNA-21 (miR21) using locked-nucleic acid (LNA)-anti-miR and its effects on the biological behaviors of melanoma cancer cells in preclinical studies. *Cancer cell international* **20**, 384, doi:10.1186/s12935-020-01394-6 (2020).

451   Jiao, W. *et al.* Different miR-21-3p isoforms and their different features in colorectal cancer. *International journal of cancer* **141**, 2103-2111, doi:10.1002/ijc.30902 (2017).

452   Babapoor, S. *et al.* Identification of microRNAs associated with invasive and aggressive phenotype in cutaneous melanoma by next-generation sequencing. *Laboratory investigation; a journal of technical methods and pathology* **97**, 636-648, doi:10.1038/labinvest.2017.5 (2017).

453   Pink, R. C. *et al.* The passenger strand, miR-21-3p, plays a role in mediating cisplatin resistance in ovarian cancer cells. *Gynecologic oncology* **137**, 143-151, doi:10.1016/j.ygyno.2014.12.042 (2015).

454   Baez-Vega, P. M. *et al.* Targeting miR-21-3p inhibits proliferation and invasion of ovarian cancer cells. *Oncotarget* **7**, 36321-36337, doi:10.18632/oncotarget.9216 (2016).

455   Cybula, M. *et al.* New miRNA expression abnormalities in laryngeal squamous cell carcinoma. *Cancer biomarkers : section A of Disease markers* **16**, 559-568, doi:10.3233/cbm-160598 (2016).

456   Gao, Z. *et al.* Identification of Cancer Stem Cell Molecular Markers and Effects of hsa-miR-21-3p on Stemness in Esophageal Squamous Cell Carcinoma. *Cancers* **11**, doi:10.3390/cancers11040518 (2019).

457   Yu, X. *et al.* Identification and Validation of Circulating MicroRNA Signatures for Breast Cancer Early Detection Based on Large Scale Tissue-Derived Data. *Journal of breast cancer* **21**, 363-370, doi:10.4048/jbc.2018.21.e56 (2018).

458   Proenca, M. A. *et al.* Relationship between Fusobacterium nucleatum, inflammatory mediators and microRNAs in colorectal carcinogenesis. *World journal of gastroenterology* **24**, 5351-5365, doi:10.3748/wjg.v24.i47.5351 (2018).

459   Butz, H. *et al.* Exosomal MicroRNAs Are Diagnostic Biomarkers and Can Mediate Cell-Cell Communication in Renal Cell Carcinoma. *European urology focus* **2**, 210-218, doi:10.1016/j.euf.2015.11.006 (2016).

460   Liu, S. *et al.* MicroRNA-9 up-regulates E-cadherin through inhibition of NF-kappaB1-Snail1 pathway in melanoma. *The Journal of pathology* **226**, 61-72, doi:10.1002/path.2964 (2012).

461   Xu, D., Chen, X., He, Q. & Luo, C. MicroRNA-9 suppresses the growth, migration, and invasion of malignant melanoma cells via targeting NRP1. *OncoTargets and therapy* **9**, 7047-7057, doi:10.2147/ott.s107235 (2016).

462   Bu, P. *et al.* MicroRNA-9 inhibits the proliferation and migration of malignant melanoma cells via targeting sirituin 1. *Experimental and therapeutic medicine* **14**, 931-938, doi:10.3892/etm.2017.4595 (2017).

463   Szostak, E. & Gebauer, F. Translational control by 3′-UTR-binding proteins. *Briefings in Functional Genomics* **12**, 58-65, doi:10.1093/bfgp/els056 (2012).

464   Wozniak, M., Dus-Szachniewicz, K. & Ziolkowski, P. Insulin-Like Growth Factor-2 Is Induced Following 5-Aminolevulinic Acid-Mediated Photodynamic Therapy in SW620 Human Colon Cancer Cell Line. *International journal of molecular sciences* **16**, 23615-23629, doi:10.3390/ijms161023615 (2015).

465   Bergman, D., Halje, M., Nordin, M. & Engstrom, W. Insulin-like growth factor 2 in development and disease: a mini-review. *Gerontology* **59**, 240-249, doi:10.1159/000343995 (2013).

466   Sasaki, H., Ishihara, K. & Kato, R. Mechanisms of Igf2/H19 imprinting: DNA methylation, chromatin and long-distance gene regulation. *Journal of biochemistry* **127**, 711-715, doi:10.1093/oxfordjournals.jbchem.a022661 (2000).

467   Nielsen, J. *et al.* A Family of Insulin-Like Growth Factor II mRNA-Binding Proteins Represses Translation in Late Development. *Molecular and Cellular Biology* **19**, 1262, doi:10.1128/MCB.19.2.1262 (1999).

468   Bell, J. L. *et al.* Insulin-like growth factor 2 mRNA-binding proteins (IGF2BPs): post-transcriptional drivers of cancer progression? *Cellular and Molecular Life Sciences* **70**, 2657-2675, doi:10.1007/s00018-012-1186-z (2013).

469   Mongroo, P. S. *et al.* IMP-1 displays cross-talk with K-Ras and modulates colon cancer cell survival through the novel proapoptotic protein CYFIP2. *Cancer research* **71**, 2172-2182, doi:10.1158/0008-5472.can-10-3295 (2011).

470   Bernstein, P. L., Herrick, D. J., Prokipcak, R. D. & Ross, J. Control of c-myc mRNA half-life in vitro by a protein capable of binding to a coding region stability determinant. *Genes & development* **6**, 642-654, doi:10.1101/gad.6.4.642 (1992).

471   Weidensdorfer, D. *et al.* Control of c-myc mRNA stability by IGF2BP1-associated cytoplasmic RNPs. *RNA (New York, N.Y.)* **15**, 104-115, doi:10.1261/rna.1175909 (2009).

472   Sparanese, D. & Lee, C. H. CRD-BP shields c-myc and MDR-1 RNA from endonucleolytic attack by a mammalian endoribonuclease. *Nucleic acids research* **35**, 1209-1221, doi:10.1093/nar/gkl1148 (2007).

473   Lederer, M., Bley, N., Schleifer, C. & Huttelmaier, S. The role of the oncofetal IGF2 mRNA-binding protein 3 (IGF2BP3) in cancer. *Seminars in cancer biology* **29**, 3-12, doi:10.1016/j.semcancer.2014.07.006 (2014).

474   Huang, X. *et al.* Insulin-like growth factor 2 mRNA-binding protein 1 (IGF2BP1) in cancer. *Journal of hematology & oncology* **11**, 88, doi:10.1186/s13045-018-0628-y (2018).

475   Cao, J. *et al.* HLA Class I Antigen Expression in Conjunctival Melanoma Is Not Associated With PD-L1/PD-1 Status. *Investigative ophthalmology & visual science* **59**, 1005-1015, doi:10.1167/iovs.17-23209 (2018).

476   Degrauwe, N., Suva, M. L., Janiszewska, M., Riggi, N. & Stamenkovic, I. IMPs: an RNA-binding protein family that provides a link between stem cell maintenance in normal development and cancer. *Genes & development* **30**, 2459-2474, doi:10.1101/gad.287540.116 (2016).

477   Rosenfeld, Y. B. *et al.* VICKZ1 enhances tumor progression and metastasis in lung adenocarcinomas in mice. *Oncogene* **38**, 4169-4181, doi:10.1038/s41388-019-0715-8 (2019).

478   Mayr, C. & Bartel, D. P. Widespread Shortening of 3′UTRs by Alternative Cleavage and Polyadenylation Activates Oncogenes in Cancer Cells. *Cell* **138**, 673-684, doi:https://doi.org/10.1016/j.cell.2009.06.016 (2009).

479   Ross, A. F., Oleynikov, Y., Kislauskis, E. H., Taneja, K. L. & Singer, R. H. Characterization of a beta-actin mRNA zipcode-binding protein. *Molecular and Cellular Biology* **17**, 2158, doi:10.1128/MCB.17.4.2158 (1997).

480   Hüttelmaier, S. *et al.* Spatial regulation of β-actin translation by Src-dependent phosphorylation of ZBP1. *Nature* **438**, 512-515, doi:10.1038/nature04115 (2005).

481   Jiang, T. *et al.* MicroRNA-98-5p Inhibits Cell Proliferation and Induces Cell Apoptosis in Hepatocellular Carcinoma via Targeting IGF2BP1. *Oncology research* **25**, 1117-1127, doi:10.3727/096504016x14821952695683 (2017).

482   Zhang, J. *et al.* Comprehensive profiling of novel microRNA-9 targets and a tumor suppressor role of microRNA-9 via targeting IGF2BP1 in hepatocellular carcinoma. *Oncotarget* **6**, 42040-42052, doi:10.18632/oncotarget.5969 (2015).

483   Fawzy, I. O. *et al.* miR-1275: A single microRNA that targets the three IGF2-mRNA-binding proteins hindering tumor growth in hepatocellular carcinoma. *FEBS letters* **589**, 2257-2265, doi:10.1016/j.febslet.2015.06.038 (2015).

484   Rebucci, M. *et al.* miRNA-196b inhibits cell proliferation and induces apoptosis in HepG2 cells by targeting IGF2BP1. *Molecular cancer* **14**, 79, doi:10.1186/s12943-015-0349-6 (2015).

485   Wang, P., Zhang, L., Zhang, J. & Xu, G. MicroRNA-124-3p inhibits cell growth and metastasis in cervical cancer by targeting IGF2BP1. *Experimental and therapeutic medicine* **15**, 1385-1393, doi:10.3892/etm.2017.5528 (2018).

486   Fortis, S. P. *et al.* Potential Prognostic Molecular Signatures in a Preclinical Model of Melanoma. *Anticancer research* **37**, 143-148, doi:10.21873/anticanres.11299 (2017).

487   Kim, T. *et al.* Targeting insulin-like growth factor 2 mRNA-binding protein 1 (IGF2BP1) in metastatic melanoma to increase efficacy of BRAF(V600E) inhibitors. *Molecular carcinogenesis* **57**, 678-683, doi:10.1002/mc.22786 (2018).

488   Elcheva, I., Tarapore, R. S., Bhatia, N. & Spiegelman, V. S. Overexpression of mRNA-binding protein CRD-BP in malignant melanomas. *Oncogene* **27**, 5069-5074, doi:10.1038/onc.2008.141 (2008).

489   Jan, C., Astrid, M. K., Thomas v, O. H. & Finn, C. N. IGF2 mRNA-binding protein 2: biological function and putative role in type 2 diabetes. *Journal of Molecular Endocrinology* **43**, 187-195, doi:10.1677/JME-09-0016 (2009).

490   Dai, N. *et al.* mTOR phosphorylates IMP2 to promote IGF2 mRNA translation by internal ribosomal entry. *Genes & development* **25**, 1159-1172, doi:10.1101/gad.2042311 (2011).

491   Christiansen, J., Kolte, A. M., Hansen, T. & Nielsen, F. C. IGF2 mRNA-binding protein 2: biological function and putative role in type 2 diabetes. *J Mol Endocrinol* **43**, 187-195, doi:10.1677/jme-09-0016 (2009).

492   Cao, J., Mu, Q. & Huang, H. The Roles of Insulin-Like Growth Factor 2 mRNA-Binding Protein 2 in Cancer and Cancer Stem Cells. *Stem cells international* **2018**, 4217259, doi:10.1155/2018/4217259 (2018).

493   Müeller-Pillasch, F. *et al.* Cloning of a gene highly overexpressed in cancer coding for a novel KH-domain containing protein. *Oncogene* **14**, 2729-2733, doi:10.1038/sj.onc.1201110 (1997).

494   Findeis-Hosey, J. J. & Xu, H. The use of insulin like-growth factor II messenger RNA binding protein-3 in diagnostic pathology. *Human pathology* **42**, 303-314, doi:10.1016/j.humpath.2010.06.003 (2011).

495   Pryor, J. G. *et al.* IMP-3 is a novel progression marker in malignant melanoma. *Modern Pathology* **21**, 431-437, doi:10.1038/modpathol.3801016 (2008).

496   Soddu, S. *et al.* IMP-3 expression in keratoacanthomas and squamous cell carcinomas of the skin: an immunohistochemical study. *European journal of histochemistry : EJH* **57**, e6, doi:10.4081/ejh.2013.e6 (2013).

497   Yu, L., Xu, H., Wasco, M. J., Bourne, P. A. & Ma, L. IMP-3 expression in melanocytic lesions. *Journal of Cutaneous Pathology* **37**, 316-322, doi:10.1111/j.1600-0560.2009.01428.x (2010).

498   Mentrikoski, M. J. *et al.* Diagnostic utility of IMP3 in segregating metastatic melanoma from benign nevi in lymph nodes. *Modern Pathology* **22**, 1582, doi:10.1038/modpathol.2009.128 (2009).

499   Kabbarah, O. *et al.* Integrative Genome Comparison of Primary and Metastatic Melanomas. *PloS one* **5**, e10770, doi:10.1371/journal.pone.0010770 (2010).

500   Liu, H. *et al.* Overexpression of IGF2BP3 as a Potential Oncogene in Ovarian Clear Cell Carcinoma. *Frontiers in oncology* **9**, 1570, doi:10.3389/fonc.2019.01570 (2019).

501   Zirkel, A., Lederer, M., Stöhr, N., Pazaitis, N. & Hüttelmaier, S. IGF2BP1 promotes mesenchymal cell properties and migration of tumor-derived cells by enhancing the expression of LEF1 and SNAI2 (SLUG). *Nucleic acids research* **41**, 6618-6636, doi:10.1093/nar/gkt410 (2013).

502   Hanniford, D. *et al.* Epigenetic Silencing of CDR1as Drives IGF2BP3-Mediated Melanoma Invasion and Metastasis. *Cancer cell* **37**, 55-70.e15, doi:10.1016/j.ccell.2019.12.007 (2020).

503   Kozubek, J. *et al.* In-depth characterization of microRNA transcriptome in melanoma. *PloS one* **8**, e72699, doi:10.1371/journal.pone.0072699 (2013).

504   Wei, C.-Y. *et al.* TRIM44 activates the AKT/mTOR signal pathway to induce melanoma progression by stabilizing TLR4. *Journal of Experimental & Clinical Cancer Research* **38**, 137, doi:10.1186/s13046-019-1138-7 (2019).

505   Li, M., Long, C., Yang, G., Luo, Y. & Du, H. MiR-26b inhibits melanoma cell proliferation and enhances apoptosis by suppressing TRAF5-mediated MAPK activation. *Biochemical and biophysical research communications* **471**, 361-367, doi:10.1016/j.bbrc.2016.02.021 (2016).

506   Gasque Schoof, C. R., Izzotti, A., Jasiulionis, M. G. & Vasques Ldos, R. The Roles of miR-26, miR-29, and miR-203 in the Silencing of the Epigenetic Machinery during Melanocyte Transformation. *BioMed research international* **2015**, 634749, doi:10.1155/2015/634749 (2015).

507   Wang, Y. *et al.* Twist1-related miR-26b-5p suppresses epithelial-mesenchymal transition, migration and invasion by targeting SMAD1 in hepatocellular carcinoma. *Oncotarget* **7** (2016).

508   Wang, Y. *et al.* Regulation of proliferation, angiogenesis and apoptosis in hepatocellular carcinoma by miR-26b-5p. *Tumor Biology* **37**, 10965-10979, doi:10.1007/s13277-016-4964-7 (2016).

509   Khosla, R. *et al.* miR-26b-5p helps in EpCAM+cancer stem cells maintenance via HSC71/HSPA8 and augments malignant features in HCC. *Liver international : official journal of the International Association for the Study of the Liver* **39**, 1692-1703, doi:10.1111/liv.14188 (2019).

510   Fan, F. *et al.* MicroRNA-26b-5p regulates cell proliferation, invasion and metastasis in human intrahepatic cholangiocarcinoma by targeting S100A7. *Oncology letters* **15**, 386-392, doi:10.3892/ol.2017.7331 (2018).

511   Miyamoto, K. *et al.* Tumour-suppressive miRNA-26a-5p and miR-26b-5p inhibit cell aggressiveness by regulating PLOD2 in bladder cancer. *Br J Cancer* **115**, 354-363, doi:10.1038/bjc.2016.179 (2016).

512   Suárez-Arriaga, M. C. *et al.* A proposed method for the relative quantification of levels of circulating microRNAs in the plasma of gastric cancer patients. *Oncology letters* **13**, 3109-3117, doi:10.3892/ol.2017.5816 (2017).

513   Jia, C. M., Tian, Y. Y., Quan, L. N., Jiang, L. & Liu, A. C. miR-26b-5p suppresses proliferation and promotes apoptosis in multiple myeloma cells by targeting JAG1. *Pathology, research and practice* **214**, 1388-1394, doi:10.1016/j.prp.2018.07.025 (2018).

514   Wilke, C. M. *et al.* Expression of miRNA-26b-5p and its target TRPS1 is associated with radiation exposure in post-Chernobyl breast cancer. *International journal of cancer* **142**, 573-583, doi:10.1002/ijc.31072 (2018).

515   Wu, T. *et al.* Huaier suppresses proliferation and induces apoptosis in human pulmonary cancer cells via upregulation of miR-26b-5p. *FEBS letters* **588**, 2107-2114, doi:10.1016/j.febslet.2014.04.044 (2014).

516   Zhou, A. *et al.* miR-26b-5p Inhibits the Proliferation, Migration and Invasion of Human Papillary Thyroid Cancer in a beta-Catenin-Dependent Manner. *OncoTargets and therapy* **13**, 1593-1603, doi:10.2147/ott.s236319 (2020).

517   Zhou, A. *et al.* Inhibitory effects of miR26b5p on thyroid cancer. *Mol Med Rep* **20**, 1196-1202, doi:10.3892/mmr.2019.10315 (2019).

518   Lekchnov, E. A. *et al.* Searching for the Novel Specific Predictors of Prostate Cancer in Urine: The Analysis of 84 miRNA Expression. *International journal of molecular sciences* **19**, doi:10.3390/ijms19124088 (2018).

519   Zhang, R., Niu, Z., Pei, H. & Peng, Z. Long noncoding RNA LINC00657 induced by SP1 contributes to the non-small cell lung cancer progression through targeting miR-26b-5p/COMMD8 axis. *Journal of cellular physiology* **235**, 3340-3349, doi:10.1002/jcp.29222 (2020).

520   Cochetti, G. *et al.* Different levels of serum microRNAs in prostate cancer and benign prostatic hyperplasia: evaluation of potential diagnostic and prognostic role. *OncoTargets and therapy* **9**, 7545-7553, doi:10.2147/ott.s119027 (2016).

521   McFall, T. *et al.* Progesterone receptor A promotes invasiveness and metastasis of luminal breast cancer by suppressing regulation of critical microRNAs by estrogen. *The Journal of biological chemistry* **293**, 1163-1177, doi:10.1074/jbc.M117.812438 (2018).

522   Wu, K. *et al.* miRNA26a5p and miR26b5p inhibit the proliferation of bladder cancer cells by regulating PDCD10. *Oncology reports* **40**, 3523-3532, doi:10.3892/or.2018.6734 (2018).

523   Andrew, A. S. *et al.* MicroRNA Dysregulation and Non-Muscle-Invasive Bladder Cancer Prognosis. *Cancer epidemiology, biomarkers & prevention : a publication of the American Association for Cancer Research, cosponsored by the American Society of Preventive Oncology* **28**, 782-788, doi:10.1158/1055-9965.epi-18-0884 (2019).

524   Beckers, A. *et al.* MYCN-driven regulatory mechanisms controlling LIN28B in neuroblastoma. *Cancer letters* **366**, 123-132, doi:10.1016/j.canlet.2015.06.015 (2015).

525   Xie, L. *et al.* Identification of the miRNA-mRNA regulatory network of small cell osteosarcoma based on RNA-seq. *Oncotarget* **8**, 42525-42536, doi:10.18632/oncotarget.17208 (2017).

526   Namkung, J. *et al.* Molecular subtypes of pancreatic cancer based on miRNA expression profiles have independent prognostic value. *Journal of gastroenterology and hepatology* **31**, 1160-1167, doi:10.1111/jgh.13253 (2016).

527   Shaikh, I. *et al.* Differential gene expression analysis of HNSCC tumors deciphered tobacco dependent and independent molecular signatures. *Oncotarget* **10**, 6168-6183, doi:10.18632/oncotarget.27249 (2019).

528   Cui, X. W., Qian, Z. L., Li, C. & Cui, S. C. Identification of miRNA and mRNA expression profiles by PCR microarray in hepatitis B virusassociated hepatocellular carcinoma. *Mol Med Rep* **18**, 5123-5132, doi:10.3892/mmr.2018.9516 (2018).

529   Wach, S. *et al.* RNA Sequencing of Collecting Duct Renal Cell Carcinoma Suggests an Interaction between miRNA and Target Genes and a Predominance of Deregulated Solute Carrier Genes. *Cancers* **12**, doi:10.3390/cancers12010064 (2019).

530   Vicchio, T. M. *et al.* MicroRNAs expression in pituitary tumors: differences related to functional status, pathological features, and clinical behavior. *Journal of endocrinological investigation*, doi:10.1007/s40618-019-01178-4 (2020).

531   Tolle, A. *et al.* Identification of microRNAs in blood and urine as tumour markers for the detection of urinary bladder cancer. *Oncology reports* **30**, 1949-1956, doi:10.3892/or.2013.2621 (2013).

532   Xia, M., Duan, M. L., Tong, J. H. & Xu, J. G. MiR-26b suppresses tumor cell proliferation, migration and invasion by directly targeting COX-2 in lung cancer. *European review for medical and pharmacological sciences* **19**, 4728-4737 (2015).

533   Wu, N. *et al.* Role of microRNA-26b in glioma development and its mediated regulation on EphA2. *PloS one* **6**, e16264, doi:10.1371/journal.pone.0016264 (2011).

534   Shen, G. *et al.* MicroRNA-26b inhibits epithelial-mesenchymal transition in hepatocellular carcinoma by targeting USP9X. *BMC cancer* **14**, 393, doi:10.1186/1471-2407-14-393 (2014).

535   Li, D., Wei, Y., Wang, D., Gao, H. & Liu, K. MicroRNA-26b suppresses the metastasis of non-small cell lung cancer by targeting MIEN1 via NF-kappaB/MMP-9/VEGF pathways. *Biochemical and biophysical research communications* **472**, 465-470, doi:10.1016/j.bbrc.2016.01.163 (2016).

536   John Clotaire, D. Z. *et al.* MiR-26b inhibits autophagy by targeting ULK2 in prostate cancer cells. *Biochemical and biophysical research communications* **472**, 194-200, doi:10.1016/j.bbrc.2016.02.093 (2016).

537   Kikulska, A. *et al.* Coordinated expression and genetic polymorphisms in Grainyhead-like genes in human non-melanoma skin cancers. *BMC cancer* **18**, 23, doi:10.1186/s12885-017-3943-8 (2018).

538   Wu, X., Ding, M. & Lin, J. Three-microRNA expression signature predicts survival in triple-negative breast cancer. *Oncology letters* **19**, 301-308, doi:10.3892/ol.2019.11118 (2020).

539   Hou, N. *et al.* Inhibition of microRNA-21-3p suppresses proliferation as well as invasion and induces apoptosis by targeting RNA-binding protein with multiple splicing through Smad4/extra cellular signal-regulated protein kinase signalling pathway in human colorectal cancer HCT116 cells. *Clinical and experimental pharmacology & physiology* **45**, 729-741, doi:10.1111/1440-1681.12931 (2018).

540   Morales-Prieto, D. M. *et al.* Identification of miRNAs and associated pathways regulated by Leukemia Inhibitory Factor in trophoblastic cell lines. *Placenta* **88**, 20-27, doi:10.1016/j.placenta.2019.09.005 (2019).

541   Lo, T. F., Tsai, W. C. & Chen, S. T. MicroRNA-21-3p, a berberine-induced miRNA, directly down-regulates human methionine adenosyltransferases 2A and 2B and inhibits hepatoma cell growth. *PloS one* **8**, e75628, doi:10.1371/journal.pone.0075628 (2013).

542 Tseng, H. H. *et al.* Next-generation Sequencing for microRNA Profiling: MicroRNA-21-3p Promotes Oral Cancer Metastasis. *Anticancer research* **37**, 1059-1066, doi:10.21873/anticanres.11417 (2017).

543 Kopkova, A. *et al.* Cerebrospinal Fluid MicroRNA Signatures as Diagnostic Biomarkers in Brain Tumors. *Cancers* **11**, doi:10.3390/cancers11101546 (2019).

544 Wang, W., Mu, S., Zhao, Q., Xue, L. & Wang, S. Identification of differentially expressed microRNAs and the potential of microRNA-455-3p as a novel prognostic biomarker in glioma. *Oncology letters* **18**, 6150-6156, doi:10.3892/ol.2019.10927 (2019).

545 Zhang, K. *et al.* miR-9 regulates ferroptosis by targeting glutamic-oxaloacetic transaminase GOT1 in melanoma. *Molecular carcinogenesis* **57**, 1566-1576, doi:10.1002/mc.22878 (2018).

546 Liu, N. *et al.* MicroRNA-9 suppresses uveal melanoma cell migration and invasion through the NF-kappaB1 pathway. *Oncology reports* **28**, 961-968, doi:10.3892/or.2012.1905 (2012).

547 Shiiyama, R. *et al.* Sensitive detection of melanoma metastasis using circulating microRNA expression profiles. *Melanoma research* **23**, 366-372, doi:10.1097/CMR.0b013e328363e485 (2013).

548 Gencia, I. *et al.* A preliminary study of microRNA expression in different types of primary melanoma. *Bosnian journal of basic medical sciences*, doi:10.17305/bjbms.2019.4271 (2019).

549 Wan, H. Y. *et al.* Regulation of the transcription factor NF-kappaB1 by microRNA-9 in human gastric adenocarcinoma. *Molecular cancer* **9**, 16, doi:10.1186/1476-4598-9-16 (2010).

550 Chen, X. *et al.* Oncogenic miR-9 is a target of erlotinib in NSCLCs. *Scientific reports* **5**, 17031, doi:10.1038/srep17031 (2015).

551 Nass, D. *et al.* MiR-92b and miR-9/9* are specifically expressed in brain primary tumors and can be used to differentiate primary from metastatic brain tumors. *Brain pathology (Zurich, Switzerland)* **19**, 375-383, doi:10.1111/j.1750-3639.2008.00184.x (2009).

552 Ma, L. *et al.* miR-9, a MYC/MYCN-activated microRNA, regulates E-cadherin and cancer metastasis. *Nature cell biology* **12**, 247-256, doi:10.1038/ncb2024 (2010).

553 Li, G., Wu, F., Yang, H., Deng, X. & Yuan, Y. MiR-9-5p promotes cell growth and metastasis in non-small cell lung cancer through the repression of TGFBR2. *Biomedicine & pharmacotherapy = Biomedecine & pharmacotherapie* **96**, 1170-1178, doi:10.1016/j.biopha.2017.11.105 (2017).

554 Wang, J., Wang, B., Ren, H. & Chen, W. miR-9-5p inhibits pancreatic cancer cell proliferation, invasion and glutamine metabolism by targeting GOT1. *Biochemical and biophysical research communications* **509**, 241-248, doi:10.1016/j.bbrc.2018.12.114 (2019).

555 Tang, S. *et al.* Combination of Four Serum Exosomal MiRNAs as Novel Diagnostic Biomarkers for Early-Stage Gastric Cancer. *Frontiers in genetics* **11**, 237, doi:10.3389/fgene.2020.00237 (2020).

556 Babion, I. *et al.* miR-9-5p Exerts a Dual Role in Cervical Cancer and Targets Transcription Factor TWIST1. *Cells* **9**, doi:10.3390/cells9010065 (2019).

557 Nishiuchi, A. *et al.* MicroRNA-9-5p-CDX2 Axis: A Useful Prognostic Biomarker for Patients with Stage II/III Colorectal Cancer. *Cancers* **11**, doi:10.3390/cancers11121891 (2019).

558 Wang, M. *et al.* PAK4, a target of miR-9-5p, promotes cell proliferation and inhibits apoptosis in colorectal cancer. *Cellular & molecular biology letters* **24**, 58, doi:10.1186/s11658-019-0182-9 (2019).

559 Wei, Y. Q. *et al.* MiR-9-5p could promote angiogenesis and radiosensitivity in cervical cancer by targeting SOCS5. *European review for medical and pharmacological sciences* **23**, 7314-7326, doi:10.26355/eurrev_201909_18837 (2019).

560 Chen, L. *et al.* Inhibition of miR-9-5p suppresses prostate cancer progress by targeting StarD13. *Cellular & molecular biology letters* **24**, 20, doi:10.1186/s11658-019-0145-1 (2019).

561 Guo, F., Hou, X. & Sun, Q. MicroRNA-9-5p functions as a tumor suppressor in papillary thyroid cancer via targeting BRAF. *Oncology letters* **16**, 6815-6821, doi:10.3892/ol.2018.9423 (2018).

562 Xie, Q., Lin, S., Zheng, M., Cai, Q. & Tu, Y. Long noncoding RNA NEAT1 promotes the growth of cervical cancer cells via sponging miR-9-5p. *Biochemistry and cell biology = Biochimie et biologie cellulaire* **97**, 100-108, doi:10.1139/bcb-2018-0111 (2019).

10. List of figures

11. List of tables

12. Abbreviations

3'-UTR, 3' untranslated region; 5FU, 5-fluorouracil; aa, Amino acid; Ab, Antibody; ACT, Adaptive cell transfer; ACTB, β-actin; ADAR, Adenosine deaminase acting on RNA enzymes; AGO2, Argonaute 2; ALAS1, Delta-aminolevulinate synthase 1; APA, Alternative cleavage and polyadenylation; APC, Antigen presenting cell; APM, Antigen processing and presenting machinery; ATCC, American Tissue Culture Collection; B-cell, B-lymphocyte; BCR, B cell antigen receptor; BiP, Binding immunoglobulin protein; BLH, Bleomycin hydrolase; BLS I, Bare lymphocyte syndrome type I; BRAF, B-Raf proto-oncogene, serine/threonine kinase; BRIM-3, BRAF inhibitor in melanoma-3; B-UTP, Biotinylated uridine-5'-triphosphate; CAF, Cancer-associated fibroblast; ccRCC, Clear cell renal cell carcinoma; CD, Cluster of differentiation; CDH1, E-cadherin; CDH2, N-cadherin; CDK4, Cyclin dependent kinase 4; CDKN2A, Cyclin dependent kinase inhibitor 2A; CDS, Coding sequence; CELF, CUG-BP, Elav-like family proteins; cisRNA, Cis-regulatory RNA; CML, Chronic myelogenous leukemia; CNX, Calnexin; CRC, Colorectal cancer; CREB1cAMP, responsive element binding protein 1; CRT, Calreticulin; CTL , Cytotoxic T-lymphocyte; CTLA-4, Cytotoxic T-lymphocyte associated protein 4; DC, Dendritic cell; DDP, Cisplatin; DGCR8, DiGeorge Critical Region 8; DMEM, Dulbecco's modified eagles medium; DNMT, DNA methyltransferase; DNMT1, DNA methyltransferase 1; dsDNA, Double stranded DNA; dsRNA, Double stranded RNA; DUB, Deubiquitinating enzyme; EBNA, Epstein–Barr nuclear antigen; EBV, Epstein-Barr virus; EMT, Epithelial–mesenchymal transition; ER, Estrogen Receptor; ERAAP, ER aminopeptidase associated with antigen processing; ERAP1, Endoplasmic reticulum aminopeptidase 1; ERAP2, Endoplasmic reticulum aminopeptidase 2; ERK pathway, Extracellular signal-regulated kinase pathway; FasL, Fas ligand; FcR, Fc receptor; FDA, Food and Drug Administration; FDR, False discovery rate; FFL, Firefly luciferase; FFPE, Formalin-fixed paraffin-embedded tissue; GAPDH, Glyceraldehyde-3-phosphate dehydrogenase; GAS, Gamma activated site; G-CSF, Granulocyte colonystimulating factor; GM-CSF, Granulocyte macrophage colony-stimulating factor; GRHL1, Grainyhead-like transcription factors 1; GRHL1, grainyhead-like transcription factors 1; HC, Heavy chain; HCC, Hepatocellular carcinoma; HCMV, Human cytomegalovirus; HER2, Human Epidermal Growth Factor Receptor 2; HLA-I, Human leukocyte antigen class I; HNRNP, Heterogeneous nuclear ribonucleoproteins; HNRNPC, Heterogenous ribonucleoprotein C; HNRNPF, Heterogenous ribonucleoprotein F; HNRNPL, Heterogenous ribonucleoprotein L; HSV, Herpes simplex virus; HuR, Human antigen R; IAP, Inhibitor of Apoptosis Proteins; ICC, Intrahepatic cholangiocarcinoma; IFN-γ, Interferon-γ; IGF2BP1, Insulin-like growth factor 2 mRNA binding protein 1; IGF2BP2, Insulin-like growth factor 2 mRNA binding protein 2; IGF2BP3, Insulin-like growth factor 2 mRNA binding protein 3; IGFR, Insulin-like growth factor receptor; IHC, Immunohistochemistry; IL-3, 10, 12, 15, 17, Interleukin-3, 10, 12, 15, 17; ILT, Ig-like transcripts receptor; im-miRs, Immune-modulatory miRNAs; IRF, Interferon-regulated factor; IRF1, Interferon regulatory factor 1; ISRE, IFN-stimulated regulatory element; ITGB3, Integrin Subunit Beta 3; ITIMs, Immunoreceptor tyrosine-based inhibition motifs; KIR, killer cell immunoglobulin-like receptor; LAP3, Leucine aminopeptidase 3; LILRB1, Leukocyte immunoglobulin like receptor B1; LMP-1, Latent membrane protein 1; LMP-2, Latent membrane protein 2; LMP2, Low molecular protein 2 (Proteasome subunit 9, PSMB9); LMP7, Low molecular protein 7 (Proteasome subunit 8, PSMB8); LMP10, Low molecular protein 10 (Proteasome subunit 10, PSMB10); LOH, Loss of heterozygosity; mAb, Monoclonal antibody; MALDI, Matrix-assisted laser desorption/ionization; MAPK, Mitogen-activating protein kinase; MBNL, Muscleblind-like proteins; MBP, Maltose binding protein; MCS, Multiple cloning site; MDS, Myelodysplastic syndrome; MDSC, Myeloid-derived suppressor cell; MEX-3B, Muscle excess protein 3B; MEX-3C, Muscle excess protein 3C; MHC-I, Major histocompatibility complex class I; microRNP, Microribonucleoprotein; miR, MicroRNA; MITF, Melanocyte Inducing Transcription Factor; miTRAP, MiRNA trapping by in vitro RNA affinity purification; mm, Millimeters; mRNA,

Messenger RNA; MS, Mass spectrometry; MS2-MBP, MS2 - Maltose binding fusion protein; MSI, Microsatellite instability; N/A, Not available; NBD, Nucleotide-binding domain; NCR, Natural cytotoxicity receptor; ncRNA, Non-coding RNA; NF1, Neurofibromin 1; NFIL3, Nuclear factor, interleukin 3 regulated; NFIX, Nuclear factor IX; NF-κB1, Nuclear factor kappa B subunit 1; NGS, Next generation sequencing; NK, Natural killer cell; NKT-cell, Natural killer T-cell; NLRC5, NOD–like receptor family and acid domain containing protein 5; NMSC, Non-melanoma skin cancers; NOTCH3, Notch receptor 3; NPC, Nasopharyngeal cancer; NRP1, Neuropilin 1; NSCLC, Non small cell lung cancer; nt, Nucleotide; PABP, Poly(A)-binding protein; PACT, Protein kinase, interferon-inducible double stranded RNA dependent activator; PAMP, pathogen-associated molecular patterns; pAPCs, Professional antigen-presenting cells; PBS, Phosphate-buffered saline; pcv, Packed cell volume; PD-1, Programmed death receptor 1; PDGF-R, Platelet-derived growth factor receptor; PDI, Protein disulfide isomerase; PD-L1, Programmed-death ligand 1; PI, Propidium iodide; piRNA, Piwi-interacting RNA; PLC, Peptide loading complex; PR, Progesterone Receptor; pre-miR, Precursor miRNA; pri-miR, Primary miRNA; prompts, Promoter-upstream transcripts; PRR, Pattern recognition receptor; PSMA 1-8, Proteasome 20S subunit alpha 1-8; PSMB 1-10, Proteasome 20S subunit beta 1-10; PSMC 1-6, Proteasome 26S subunit, ATPase 1-6; PSMD1-14, Proteasome 26S subunit, non-ATPase 1-14; PSME1-4, Proteasome activator subunit 1-4; PSMF1, Proteasome inhibitor subunit 1; PTEN, Phosphatase and tensin homolog; PU.1, Spi-1 proto-oncogene (or SPI1); QC, Quality control; RBD, RNA-binding domains; RCC, Renal cell carcinoma; RhCMV, Rhesus cytomegalovirus; RISC, RNA-induced silencing complex; RL, Renilla; RLU, Relative light Unit; RNA-AP, RNA affinity purification assay; RNP, Ribonucleoprotein; RPL13, 60S ribosomal protein L13; RPMI, Roswell park memorial institute; RRM, RNA recognition motif; rRNA, Ribosomal RNA; RT-qPCR, Reverse Transcription - quantitative polymerase chain reaction; RTK, Receptor Tyrosine Kinase; S100A7, S100 calcium-binding protein A7; SBS, Sequencing by synthesis; SCC, Squamous cell carcinomas; SDS-PAGE, Sodium dodecyl sulfate–polyacrylamide gel electrophoresis; SF3B1, Splicing factor 3B subunit 1; shRNA, short hairpin RNA; siRNA, Short interfering RNA; SKCM, Skin cutaneous melanoma; SLN, sentinel lymph node; Snail1, Snail family transcriptional repressor 1; snoRNA, Small nucleolar RNA; snRNA, Small nuclear RNA; sRNA, Small RNA; srRNA, Small rDNA-derived RNA; ssDNA, Single stranded DNA; ssRNA, Single stranded RNA; TA, Paclitaxel; TAM, Tumour-associated macrophages; TAP1, Transporter associated with antigen processing 1 (ABCB2); TAP2, Transporter associated with antigen processing 2 (ABCB3); TAPBPR, Tapasin-related protein (TAPBPL); Tc, Cytotoxic T-lymphocytes (CTL); T-cell, T-lymphocyte; TCGA, The Cancer Genome Atlas; TCR, T cell antigen receptor; telsRNA, Telomere specific small RNA; TFBS, Transcription factor-binding site; Tfh, T follicular helper cell; TGFBR2, Transforming Growth Factor Beta Receptor 2; Th, Helper T-lymphocyte; TIL, Tumour infiltrating lymphocyte; tiRNA, Transcription initiation RNA; TGF-β, Transforming growth factor β; TGFBR2, Transforming growth factor β receptor 1; TKI, tyrosine-kinase inhibitors; TLR, Toll-like receptor; TM, Transmembrane; TMD, Transmembrane domain; TME, Tumour microenvironment; TNF-α, Tumour necrosis factor–α; TNRC6, trinucleotide repeat containing 6A; TOF, Time of flight; TP53, Tumour protein p53; tpm, Transcripts per million; TPN, Tapasin; TPPII, Tripeptidyl peptidase II; TRBP, HIV-1 TAR RNA-binding protein; Treg, Regulatory T-lymphocytes; tRNA, Transfer RNA; tsRNA, tRNA-derived small RNA; TWIST1, Twist family bHLH transcription factor 1; UMI, Unique molecular identifiers; UV light, Ultraviolet light; VIM, Vimentin; VMP1, Vacuole membrane protein 1; XCL1, Lymphotactin; YBOX1, Y-box-binding protein 1; YBOX3, Y-box-binding protein 3; β2-m, β2-microglobulin.

Curriculum Vitae

Name:	Maria-Filothei Lazaridou
Born on:	29.04.1991 in Athens, Greece
Nationality:	Greek
Marital status:	Engaged

School education

1997-2003:	Primary School of Doukas Schools in Marousi, Athens, Greece
2003-2009:	High School of Arsakeia Schools in Psychiko, Athens, Greece

University education

2009-2013:	BSc in Chemistry, Department of Chemistry, National and Kapodistrian University of Athens, Athens, Greece (8.53/10) Bachelor Thesis: "Introduction of mutations in nucleic acid sequences by recombinant DNA techniques", Laboratory of Analytical Chemistry, Department of Chemistry, University of Athens, Athens, Greece Supervisor: Professor Dr. Penelope C. Ioannou
2014-2015:	MSc in Clinical Chemistry, Department of Chemistry, National and Kapodistrian University of Athens, Athens, Greece (9.82/10) Master Thesis: "Study of the expression of PLASTIN-3 and study of the methylation of RASSF1A in samples from patients with breast cancer and prostate cancer", Laboratory of Analytical Chemistry, Department of Chemistry, University of Athens, Athens, Greece Supervisor: Professor Dr. Evi S. Lianidou
2016-2020:	PhD in Institute for Medical Immunology, Department of Medicine, Martin-Luther-University Halle-Wittenberg, Halle (Saale), Germany PhD Thesis: "Posttranscriptional regulation of the components of the human leukocyte antigen class I antigen processing and presentation machinery as an immune escape mechanism in melanoma " Supervisor: Professor Dr. Barbara Seliger

Certificates

2018:	Certificate of Good Manufacturing Practise (GMP), GMP Course, Thomas Beer and Tobias Halfpap GbR, Halle (Saale), Germany
2019:	Certificate in animal well-fair and animal experiments - laboratory animal science of mice and rats (Tierschutz, Versuchtierkunde und tierexperimentelles Arbeiten), Centre for Basic Medical Research, Martin-Luther-University Halle-Wittenberg, Halle (Saale), Germany
Scholarships:	▪ 16 months scholarship funded by the State Scholarships Foundation of Greece (IKY). Scholarship's Duration: 02/01/2014 - 05/31/2015 ▪ 3 years scholarship from the graduate program RTG1591: Posttranscriptional control of gene expression: mechanisms and role in pathogenesis (GRK1591), funded by the German

Research Foundation (DFG, Project number: 105533105). Scholarship's Duration: 01/03/2016 - 28/02/2019

Conferences:

▪ Lazaridou M-F., Identification of immune modulatory microRNAs targeting the peptide transporter TAP1 in melanoma, 5th Symposium on Advances in Cancer Immunology and Immunotherapy, 5-7 December 2019, Athens, Greece (Talk)

▪ Subbarayan K.*, Lazaridou M-F.*, Massa C., Handke D, Müller A. and Seliger B.:"Transcriptional and post-transcriptional regulation of MHC class I expression in breast cancer and melanoma", TIMO XV, 25-27 April 2019, Halle (Saale), Germany (Poster, Award)

▪ Lazaridou M-F., Massa C., Gonschorek E., Mueller A., Biehl K., Stevens A., Friedrich M., Jasinski-Bergner S., Seliger B. Role of miR-200a-5p on the immune escape of melanoma. 10-15 March, Ettal, Germany (Poster)

▪ Lazaridou M-F., Massa C., Friedrich M., Handke D., Mueller A., Tretbar S., Huettelmaier S., Seliger B. Identification of novel miRNAs modulating the antigen processing and presentation machinery in melanoma, 8th course on non-coding genome, 13-20 February 2019, Paris, France (Poster)

▪ Lazaridou M-F., Discovering the post-transcriptional regulation of HLA class I APM components and its clinical relevance in melanoma as a PhD student in Germany, 16th Panhellenic Congress of Clinical Chemistry, 11-14 October 2018, Alexandroupolis, Greece (Talk)

▪ Lazaridou M., Bukur J., Handke D., Mueller A., Tretbar S., Friedrich M., Huettelmaier S., Meyer S., Seliger B.: "MicroRNAs regulating the expression of HLA class I antigen processing in melanoma", 4. Kongress für Doktorandinnen und Doktoranden der Medizinischen Fakultät der Martin-Luther-Universität Halle-Wittenberg, 10-11 November 2017, Halle (Saale), Germany (Poster)

▪ Lazaridou M., Subbarayan K., Rahn J., Handke D., Mueller A., Tretbar S., Friedrich M., Huettelmaier S., Meyer S., Seliger B.: "Post-transcriptional regulation of HLA class I APM components and its clinical relevance in tumors", 3rd Symposium on Advances in Cancer Immunology and Immunotherapy, 2-4 November 2017, Athens, Greece (Talk & Poster)

▪ Lazaridou M., Bukur J., Handke D., Mueller A., Tretbar S., Friedrich M., Huettelmaier S., Meyer S., Seliger B.: "MicroRNAs regulating the expression of HLA class I antigen processing in melanoma", 47th Annual Meeting of German Society for Immunology, 12-15 September 2017, Erlangen, Germany (Talk & Poster)

▪ Lazaridou M., Bukur J. Handke D. Mueller A., Meyer S., Huettelmaier, Seliger B., "Identification of microRNAs regulating expression of APM components and investigating their relevance in melanoma", 2nd Symposium on Advances in Cancer Immunology and Immunotherapy, 15-17 December 2016, Athens, Greece (Talk, Award)

List of publications

1. Lazaridou M-F., Massa C., Handke D., Mueller A., Friedrich M., Subbarayan K., Tretbar S., Dummer R., Koelblinger P., Seliger B. Identification of microRNAs targeting the transporter associated with antigen processing TAP1 in melanoma. *J Clin Med.* 2020, doi: 10.3390/jcm9092690.

2. Lazaridou M-F., Gonschorek E., Massa C., Friedrich M., Handke D., Jasinski-Bergner S., Dummer R., Koelblinger P., Seliger B. Identification of miR-200a-5p targeting the peptide transporter TAP1 and its association with the clinical outcome of melanoma patients. *OncoImmunology,* vol. 9, doi.org/10.1080/2162402X.2020.1774323, 2020.

3. Friedrich M.*, Simon Jasinski-Bergner S.*, Lazaridou M-F., Subbarayan K., Massa C., Tretbar S., Mueller A., Handke D., Biehl K., Bukur J., Donia M., Mandelboim O., Seliger B. Tumor-induced escape mechanisms and their association with resistance to checkpoint inhibitor therapy. *Cancer Immunology, Immunotherapy* 68:1689–1700, doi: 10.1007/s00262-019-02373-1, 2019.

4. Friedrich M., Lazaridou M-F., Jette R., Vaxevanis C., Heimer N., Jasinski-Bergner S., Seliger B. Identification of immunomodulatory RNA-binding molecules in tumors. *Methods in Enzymology*, doi: 10.1016/bs.mie.2019.05.042, 2019.

5. Jasinski-Bergner S., Vaxevanis C., Heimer N., Lazaridou M-F., Friedrich M., Seliger B. An altered miTRAP method for miRNA affinity purification with its pros and cons. *Methods in Enzymology*, doi: 10.1016/bs.mie.2019.05.016, 2019.

6. Tretbar U.S., Friedrich M., Lazaridou M-F., Seliger B. Identification of immune-modulatory miRNAs by miRNA enrichment via RNA affinity purification. *Methods in Molecular Biology*, vol. 1913, doi: 10.1007/978-1-4939-8979-9_6, 2019.

7. Markou A, Lazaridou M., Paraskevopoulos P. et al., Multiplex Gene Expression Profiling of In Vivo Isolated Circulating Tumor Cells in High-Risk Prostate Cancer Patients. Clin Chem., doi: 10.1373/clinchem.2017.275503, 2017.

8. Kouloulia S., Lazaridou M., Christopoulos T., Ioannou PC. Multi-allele dipstick assay for visual genotyping of four novel SIRT1 gene variant alleles as candidate biomarkers for sporadic Parkinson disease. Microchimica Acta, doi: 10.1007/s00604-017-2252-x, 2017.

9. Subbarayan K., Massa C., Lazaridou M-F. and Seliger B., Central role of miR-21-3p in the MHC class I-mediated immune escape linking the proteoglycan biglycan, TGF-β signaling with oncogenic transformation (submitted)

10. Jasinski-Bergner S., Lazaridou M-F., Friedrich M., Subbarayan K., Vaxevanis C., Mandelboim O., Seliger B., Immunological relevant microRNAs modulating immune surveillance. (in preparation)

11. Meyer S., Handke D., Mueller A., Biehl K., Bukur J., Kloor M., Lazaridou M-F., Steven A., Seliger B., Distinct molecular mechanisms of altered HLA class II expression in malignant melanoma (in preparation)

Declaration

Erklärung

Hiermit erkläre ich, dass ich mich mit der vorliegenden wissenschaftlichen Arbeit erstmals um die Erlangung des Doktorgrades bewerbe und diese Arbeit selbstständig und nur unter Verwendung der angegebenen Quellen und Hilfsmittel angefertigt habe. Außerdem habe ich die den benutzten Werken wörtlich oder inhaltlich entnommenen Stellen als solche kenntlich gemacht.

Declaration

I hereby declare that I am applying for the doctoral degree with the present scientific work for the first time and that I have worked independently, using only the specified sources and tools. In addition, I have marked the places taken literally or in terms of content as such from the works used.

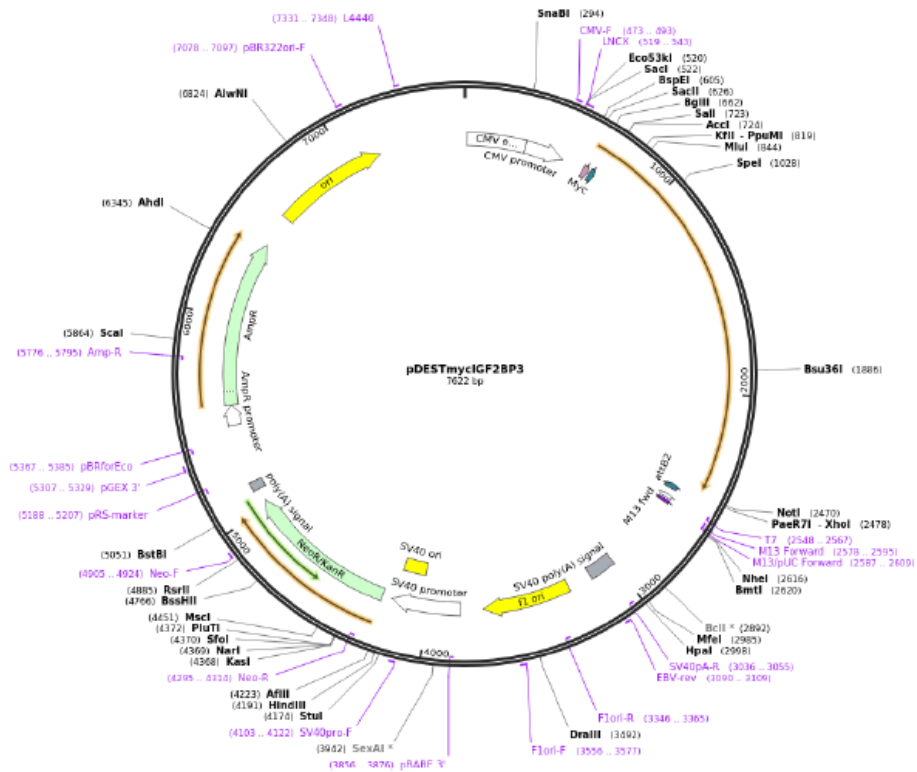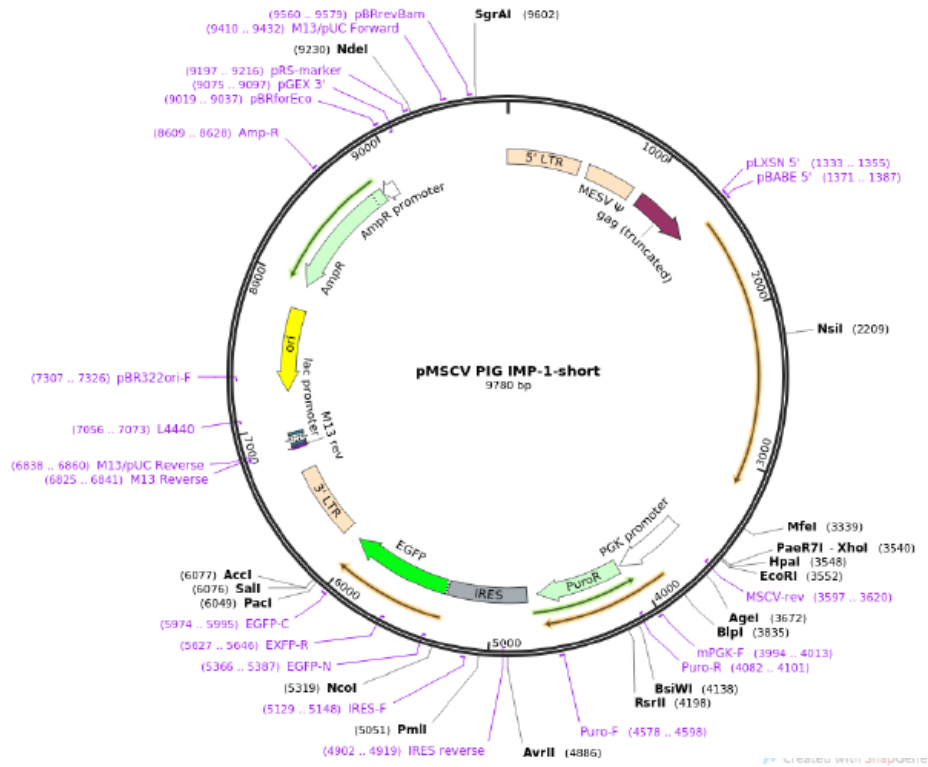Halle (Saale), 08.09.2020

Acknowledgements

Appendix

1. Plasmid cards of the constructs for the miTRAP assay
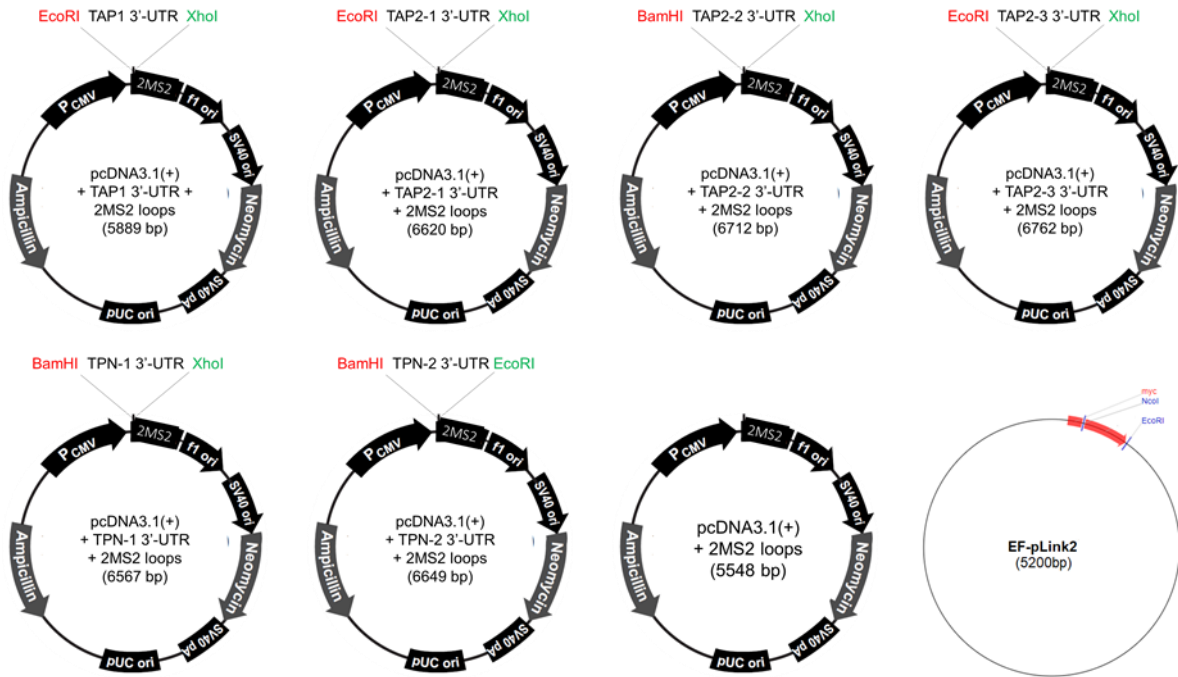
2. Plasmid cards of the constructs for the dual luciferase reporter assay
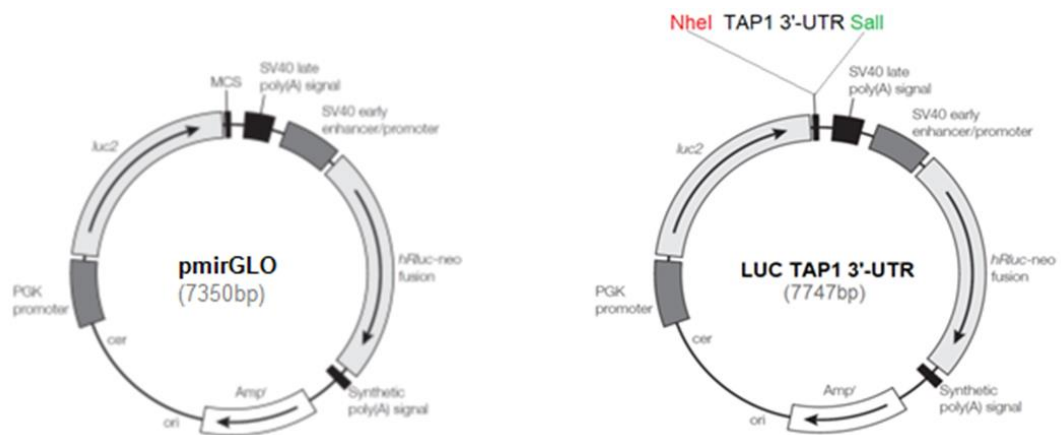
3. Plasmid cards for the expression vectors

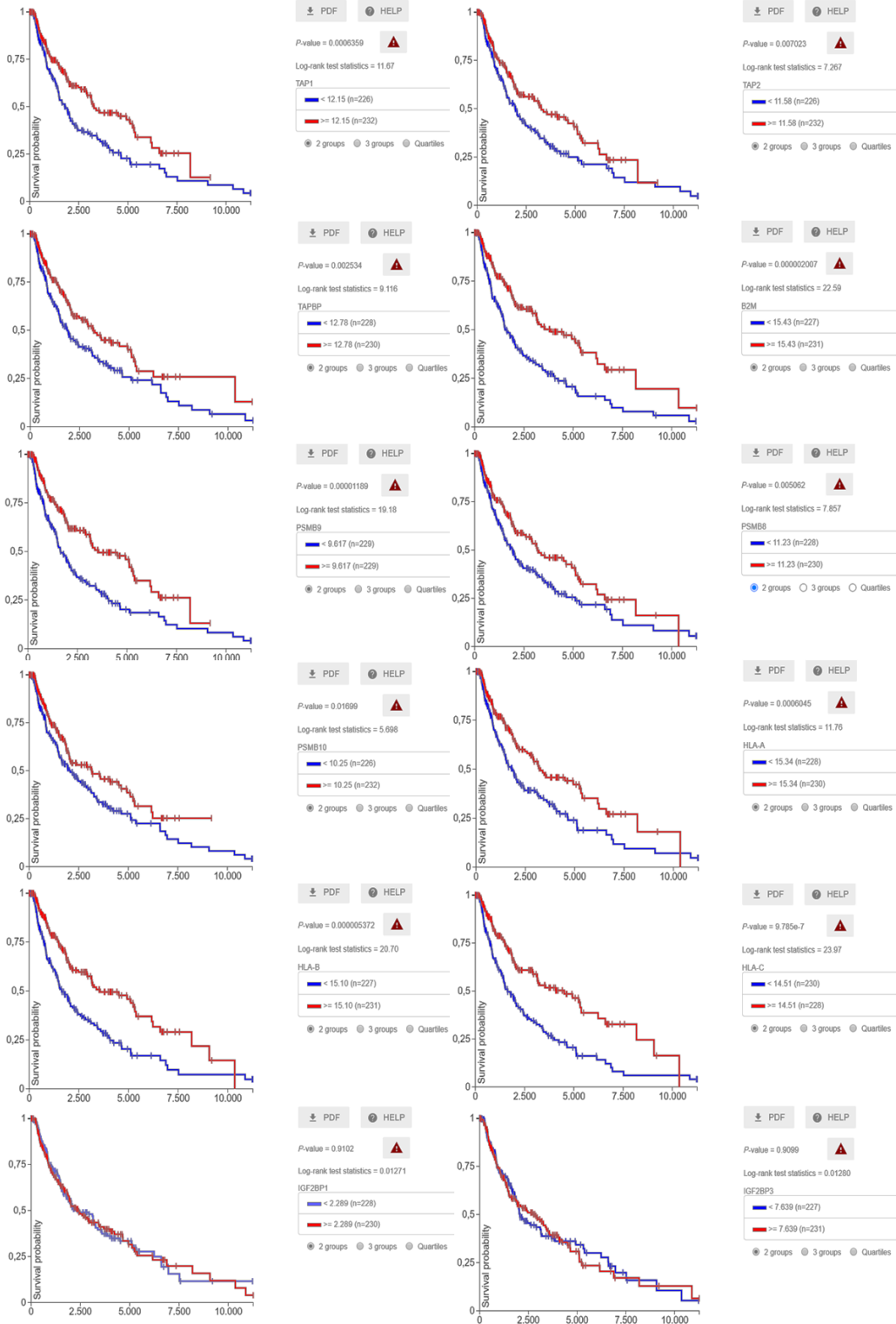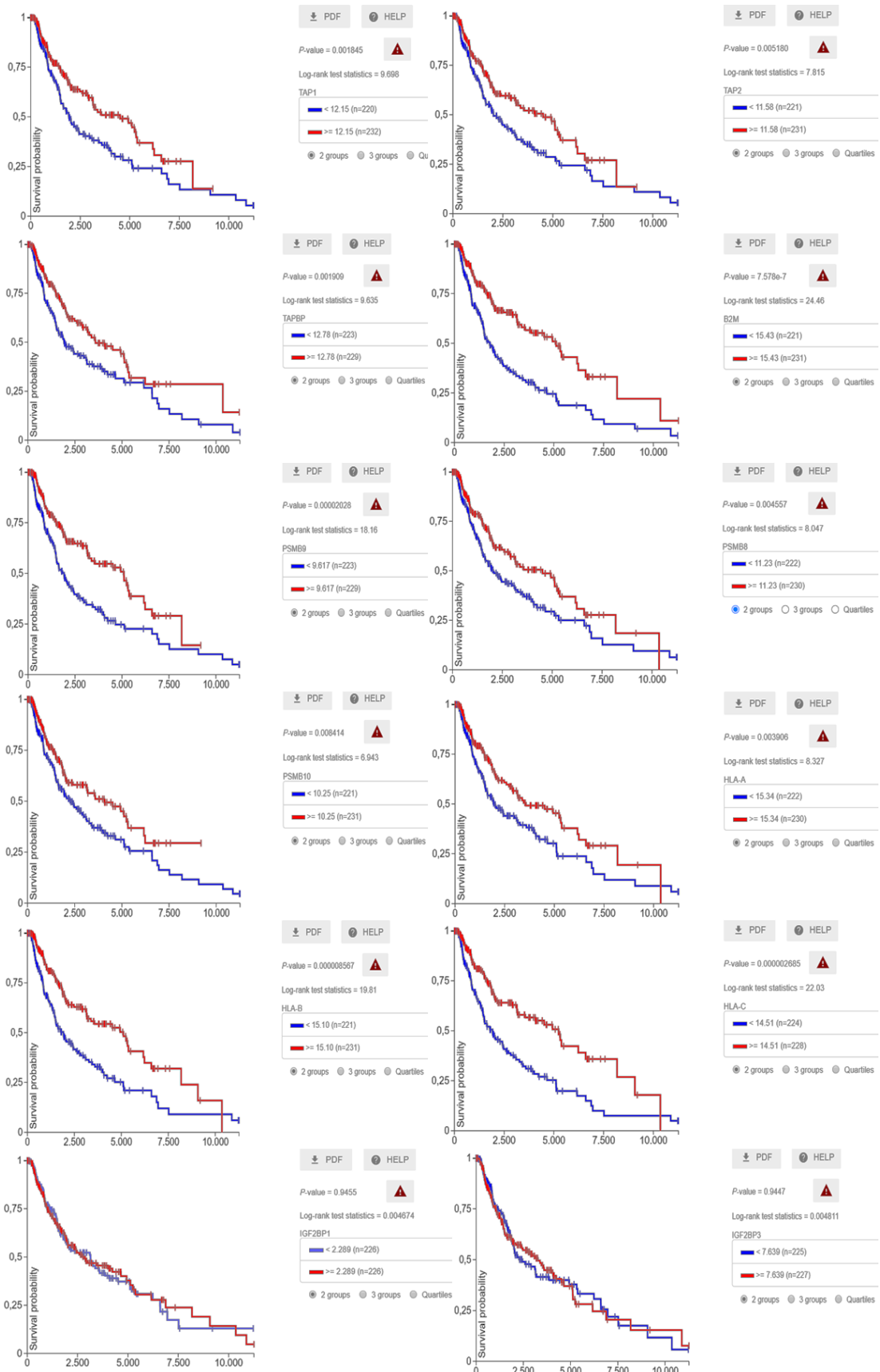

pMSCV PIG IMP-1-short
9780 bp

pDESTmycIGF2BP3
7622 bp

4. Kaplan Meier curves

The following KM curves were designed using the "Xenabrowser" database:

Overall Survival – TCGA – Melanoma (SKCM) – 470

Disease Specific Survival – TCGA – Melanoma (SKCM) – 470

P-value = 0.001845
Log-rank test statistics = 9.698
TAP1
< 12.15 (n=220)
>= 12.15 (n=232)
2 groups   3 groups   Qu

P-value = 0.005180
Log-rank test statistics = 7.815
TAP2
< 11.58 (n=221)
>= 11.58 (n=231)
2 groups   3 groups   Quartiles

P-value = 0.001909
Log-rank test statistics = 9.635
TAPBP
< 12.78 (n=223)
>= 12.78 (n=229)
2 groups   3 groups   Quartiles

P-value = 7.578e-7
Log-rank test statistics = 24.46
B2M
< 15.43 (n=221)
>= 15.43 (n=231)
2 groups   3 groups   Quartiles

P-value = 0.00002028
Log-rank test statistics = 18.16
PSMB9
< 9.617 (n=223)
>= 9.617 (n=229)
2 groups   3 groups   Quartiles

P-value = 0.004557
Log-rank test statistics = 8.047
PSMB8
< 11.23 (n=222)
>= 11.23 (n=230)
2 groups   3 groups   Quartiles

P-value = 0.008414
Log-rank test statistics = 6.943
PSMB10
< 10.25 (n=221)
>= 10.25 (n=231)
2 groups   3 groups   Quartiles

P-value = 0.003906
Log-rank test statistics = 8.327
HLA-A
< 15.34 (n=222)
>= 15.34 (n=230)
2 groups   3 groups   Quartiles

P-value = 0.000008567
Log-rank test statistics = 19.81
HLA-B
< 15.10 (n=221)
>= 15.10 (n=231)
2 groups   3 groups   Quartiles

P-value = 0.000002685
Log-rank test statistics = 22.03
HLA-C
< 14.51 (n=224)
>= 14.51 (n=228)
2 groups   3 groups   Quartiles

P-value = 0.9455
Log-rank test statistics = 0.004674
IGF2BP1
< 2.289 (n=226)
>= 2.289 (n=226)
2 groups   3 groups   Quartiles

P-value = 0.9447
Log-rank test statistics = 0.004811
IGF2BP3
< 7.639 (n=225)
>= 7.639 (n=227)
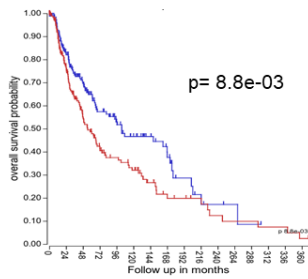2 groups   3 groups   Quartiles

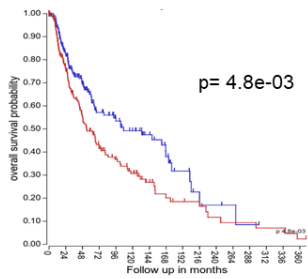Progression Free Interval – TCGA – Melanoma (SKCM) – 470
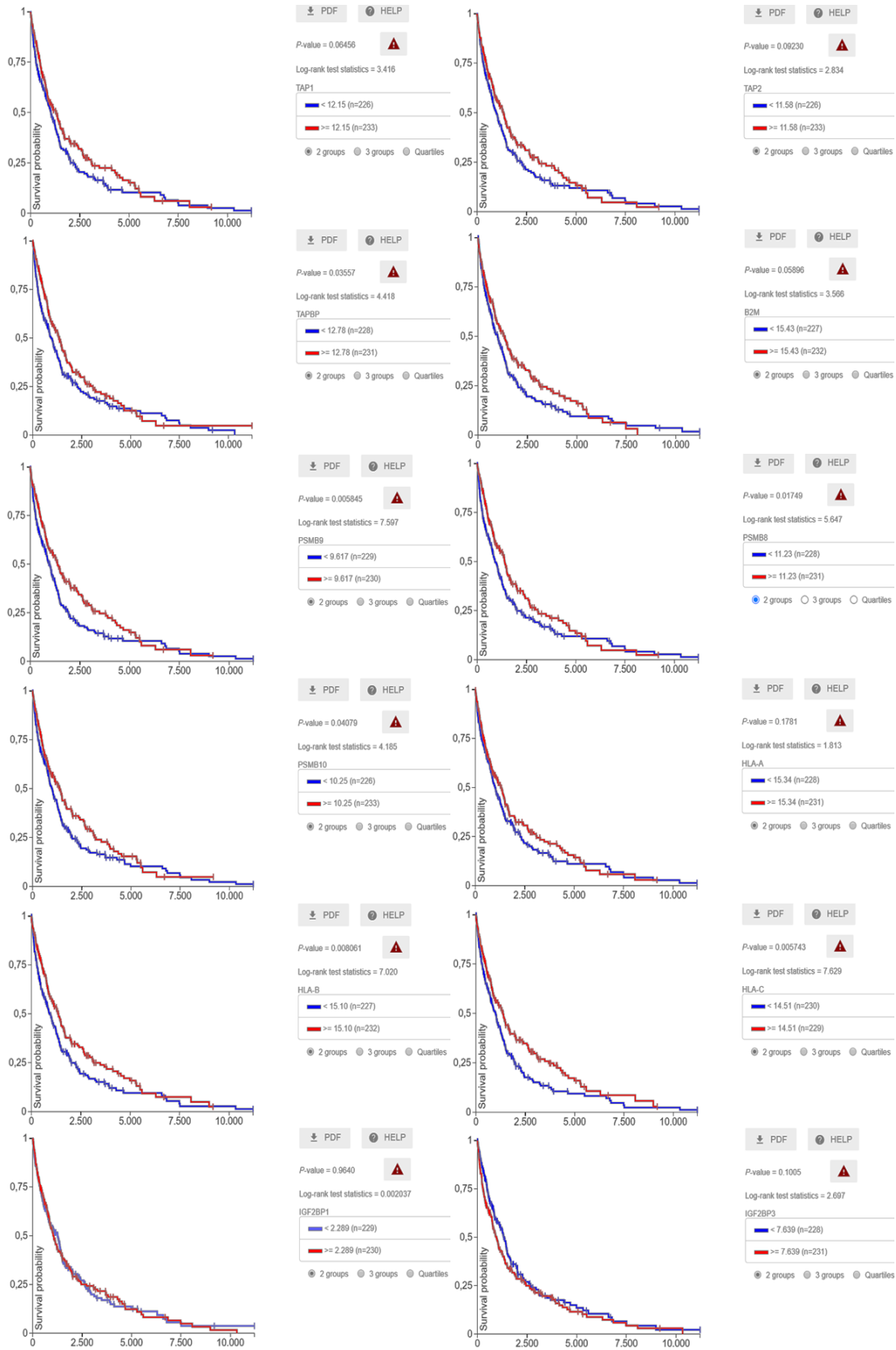
The following KM curves were designed using the "R2: Genomics Analysis and Visualization Platform" database:

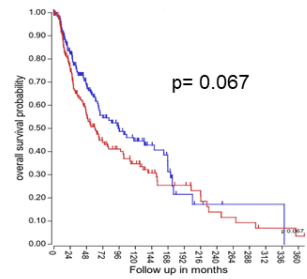## Overall Survival –TCGA – Melanoma (SKCM) – 375
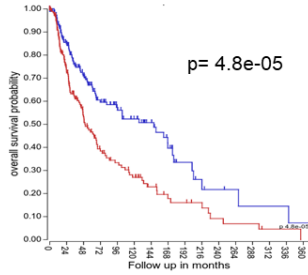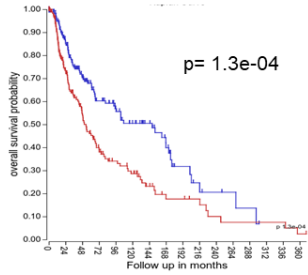

TAP1 Exp. Cutoff:4357.2736 — p= 8.8e-03

TAP2 Exp. Cutoff:3080.0570 — p= 4.8e-03

TPN Exp. Cutoff:6903.1043 — p= 0.067

β2-M Exp. Cutoff:43146.0615 — p= 4.8e-05

LMP2 Exp. Cutoff:806.8684 — p= 1.3e-04

LMP7 Exp. Cutoff:2334.1414 — p= 7.0e-03
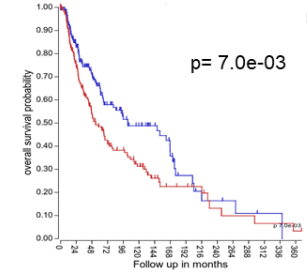
LMP10 Exp. Cutoff:1153.0183 — p= 0.095
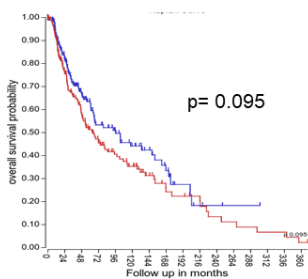
HLA-A Exp. Cutoff:39895.1145 — p= 1.7e-03
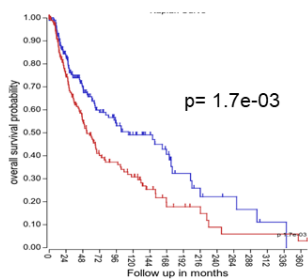
HLA-B Exp. Cutoff:33312.7405 — p= 7.1e-05
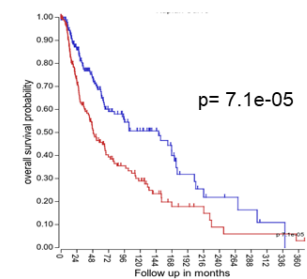
HLA-C Exp. Cutoff:22677.5417 — p= 2.0e-05
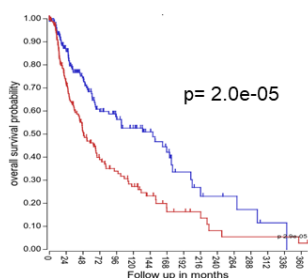
IGF2BP1 Exp. Cutoff:4.8914 — p= 0.904
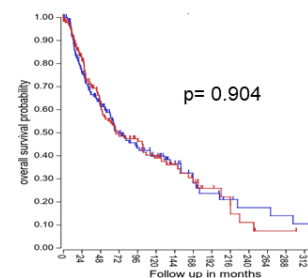
IGF2BP3 Exp. Cutoff:200.3355 — p= 0.746
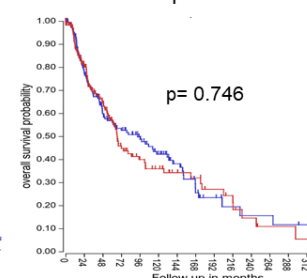
high (n=188), low (n=187)

5. <u>Length distribution histograms of miTRAP eluates</u>

The histograms have been designed and provided by Novogene Co., Ltd (Hong Kong, China) (for TAP1 and TAP2 groups) and from Dr. Andreas Dahl (Deep Sequencing Group, TU Dresden, Germany) (for TPN group).
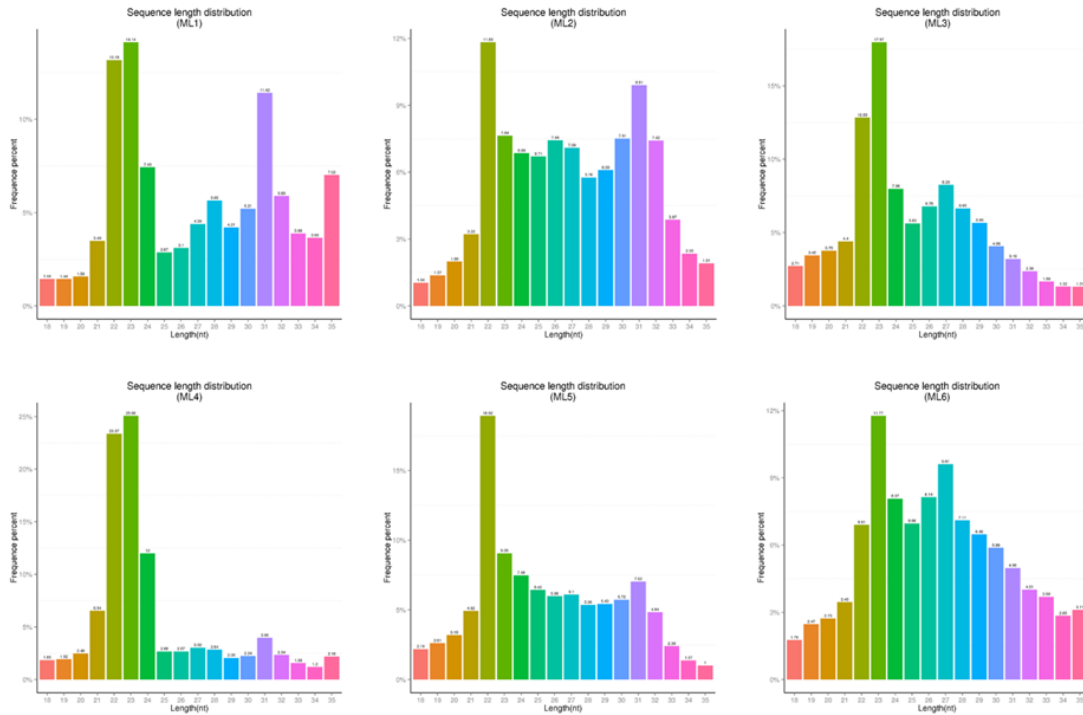
ML 1/4: MZ-Mel2 eluates, ML 2/5: TAP1 eluates, ML 3/6: MS2 eluates
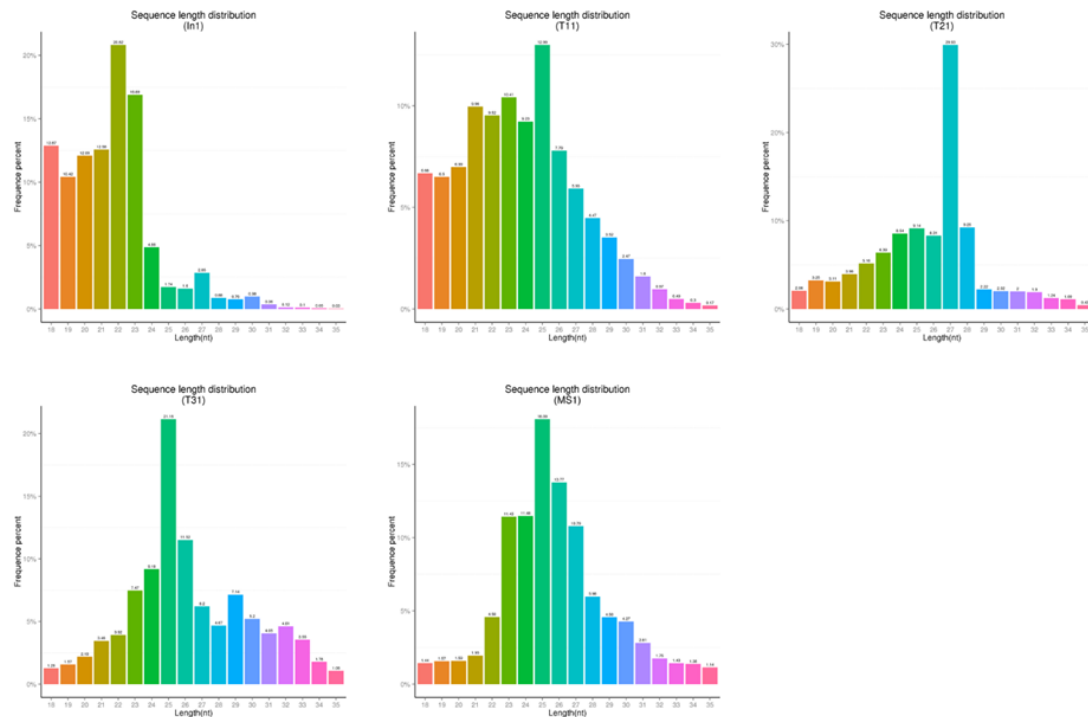
In 1/2: Mel1359 eluates, T1 1/2: TAP2-1 3'-UTR eluates, T2 1/2: TAP2-2 3'-UTR eluates, T3 1/2: TAP2-3 3'-UTR eluates, MS 1/2: MS2 eluates
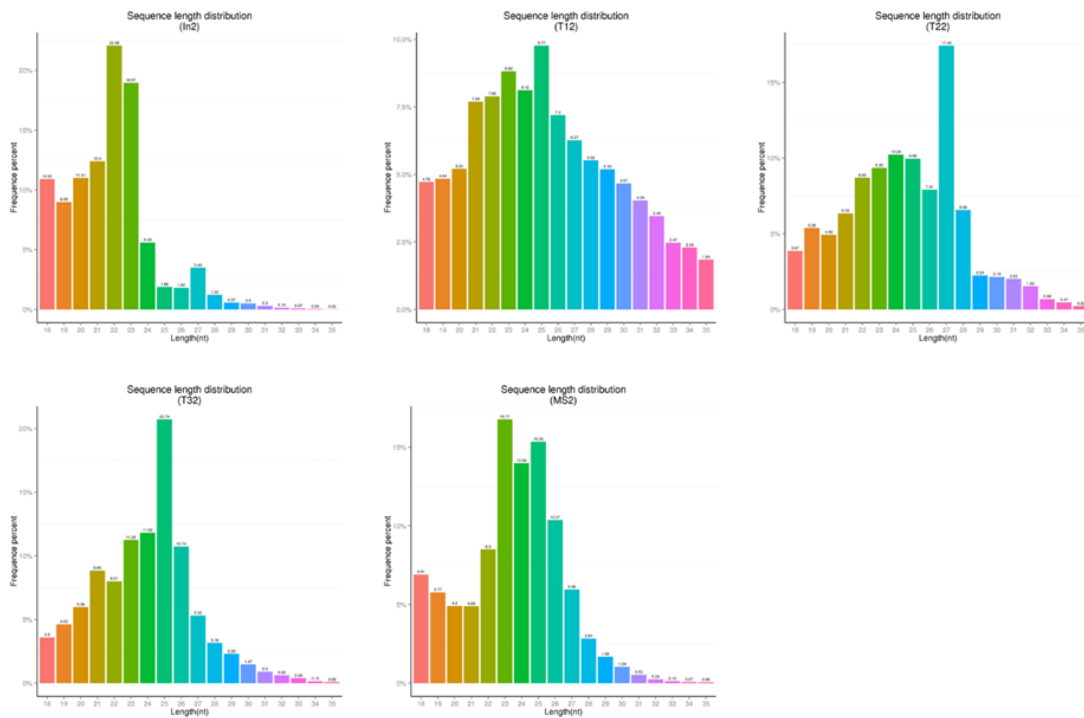
In 1/2: Mel1359 eluates, T1 1/2: TAP2-1 3'-UTR eluates, T2 1/2: TAP2-2 3'-UTR eluates, T3 1/2: TAP2-3 3'-UTR eluates, MS 1/2: MS2 eluates
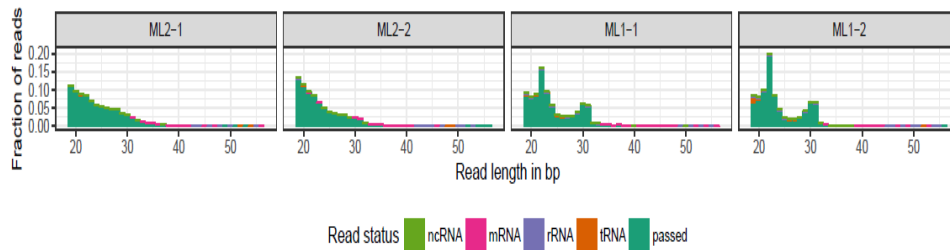
ML 2-1/2-2: TPN-2 3'-UTR eluates, ML 1-1/1-2: MKR eluates

6.   Clean reads after small RNA sequencing analysis of the miTRAP eluates

Table A.6. Data filtering summary

Sample	total reads	N%>10%	low quality	5' adapter contamine	3' adapter null or insert null	with polyA/T/G/C	clean reads
MZ-Mel2 Input Control (B.R.1)	13356676 (100.00%)	35 (0.0%)	14707 (0.11%)	1850 (0.01%)	580715 (4.35%)	20163 (0.15%)	12739206 (95.38%)
(B.R.2)	12642190 (100.00%)	34 (0.0%)	12745 (0.10%)	3605 (0.03%)	648187 (5.13%)	23573 (0.19%)	11954046 (94.56%)

Sample	total reads	N%>10%	low quality	5' adapter contamine	3' adapter null or insert null	with polyA/T/G/C	clean reads
TAP1 3'-UTR (B.R.1)	12812178 (100.00%)	49 (0.0%)	20014 (0.16%)	4095 (0.03%)	496141 (3.87%)	69330 (0.54%)	12222549 (95.40%)
(B.R.2)	12056561 (100.00%)	1293 (0.0%)	26718 (0.22%)	1023 (0.01%)	330297 (2.74%)	127399 (1.06%)	11569831 (95.96%)
MS2 Control (B.R.1)	13248792 (100.00%)	47 (0.0%)	35338 (0.27%)	7198 (0.05)	461336 (3.48%)	102201 (0.77%)	12642672 (95.43%)
(B.R.2)	13987605 (100.00%)	1525 (0.0%)	29702 (0.21%)	1585 (0.01%)	402453 (2.88%)	80346 (0.57%)	13471994 (96.31%)
MKR Input Control (B.R.1)	15284672 (100.00%)	0 (0.00%)	117292 (0.77%)	13338 (0.09%)	13166198 (86.14%)	8757 (0.06%)	1979087 (12.95%)
(B.R.2)	15295182 (100.00%)	0 (0.00%)	101667 (0.66%)	14445 (0.09%)	10298295 (67.33%)	17115 (0.11%)	4863660 (31.80%)
TAP2-1 3'-UTR (B.R.1)	18895925 (100.00%)	0 (0.00%)	93415 (0.49%)	21075 (0.11%)	608837 (3.22%)	74604 (0.39%)	18097994 (95.78%)
(B.R.2)	14752006 (100.00%)	4 (0.00%)	62506 (0.42%)	61950 (0.42%)	279707 (1.90%)	69666 (0.47%)	14278173 (96.79%)
TAP2-2 3'-UTR (B.R.1)	22086222 (100.00%)	0 (0.00%)	95903 (0.43%)	11490 (0.05%)	1173081 (5.31%)	24072 (0.11%)	20781676 (94.09%)
(B.R.2)	17461513 (100.00%)	3 (0.00%)	66084 (0.38%)	47756 (0.27%)	1580786 (9.05%)	17819 (0.10%)	15749065 (90.19%)
TAP2-3 3'-UTR (B.R.1)	18354593 (100.00%)	0 (0.00%)	95709 (0.52%)	49476 (0.27)	309734 (1.69%)	44402 (0.24%)	17855272 (97.28%)
(B.R.2)	18310557 (100.00%)	2 (0.00%)	68094 (0.37%)	24046 (0.13%)	619827 (3.39%)	20496 (0.11%)	17578092 (96.00%)
MS2 Control (B.R.1)	14791385 (100.00%)	23 (0.00%)	86136 (0.58%)	37697 (0.25%)	197902 (1.34%)	39060 (0.26%)	14730567 (97.56%)
(B.R.2)	16555845 (100.00%)	4 (0.00%)	75233 (0.45%)	127485 (0.77%)	2559761 (15.45%)	89629 (0.54%)	13703733 (82.77%)

Note:
(1) Sample: Sample id.
(2) total_reads: Total sequenced reads.
(3) N% > 10%: Percentage of reads with N > 10%.
(4) low quality: Percentage of low quality reads .
(5) 5'adapter contamine: Percentage of reads with 5'adapter contamine.
(6) 3'adapter null or insert null: Percentage of reads with 3'adapter null or insert null.
(7) with ployA/T/G/C: Percentage of reads with ployA/T/G/C.
(8) clean reads: Total clean reads and its percentage accounted for raw reads.
(9) B.R.1/2= Biological Replicate 1 or 2

7. _In silico_ analysis of the candidate miRs by available online tools

Table A7.1. _In silico_ predicted and strongly enriched miRs via the miTRAP assay for TAP1 3'-UTR

miR	miRWalk	miRanda	miRDB	RNA22	RNAhybrid	Targetscan	SUM
hsa-miR-21-3p	1	1	1	0	1	1	5
hsa-miR-22-3p	1	1	0	1	1	1	5
hsa-miR-140-3p	1	1	0	1	1	1	5
hsa-miR-590-3p	1	1	1	0	1	1	5
hsa-miR-26b-5p	1	1	0	0	1	1	4
hsa-miR-532-5p	1	1	0	0	1	1	4
hsa-miR-26a-5p	1	1	0	0	1	1	4
hsa-miR-516b-5p	1	0	0	0	1	0	2

Table A7.2. _In silico_ predicted and strongly enriched miRs via the miTRAP assay for TAP2 3'-UTR

miR	miRWalk	miRanda	miRDB	RNA22	RNAhybrid	Targetscan	SUM
hsa-miR-125b-5p	1	1	1	1	1	1	6
hsa-miR-200b-3p	1	1	1	1	1	1	6
hsa-miR-200c-3p	1	1	1	1	1	1	6
hsa-miR-584-5p	1	1	0	1	1	1	5
hsa-miR-629-5p	1	1	0	1	1	1	5
hsa-miR-128-3p	1	1	0	1	1	1	5
hsa-miR-125a-5p	1	1	0	1	1	1	5
hsa-miR-181b-5p	1	1	1	0	1	1	5
hsa-miR-29b-3p	1	1	0	1	1	1	5
hsa-miR-452-5p	1	0	0	1	1	1	4
hsa-miR-107	1	0	0	1	1	1	4
hsa-miR-542-3p	1	0	0	0	1	1	3

Table A7.3. _In silico_ predicted and strongly enriched miRs via the miTRAP assay for TPN 3'-UTR

miR	miRWalk	miRanda	miRDB	RNA22	RNAhybrid	Targetscan	SUM
hsa-miR-29a-3p	1	1	0	0	1	1	4
hsa-miR-125a-5p	1	1	0	0	1	1	4
hsa-miR-744-5p	1	1	0	0	1	1	4
hsa-miR-3180-3p	1	1	0	0	1	1	4
hsa-miR-24-3p	1	0	0	0	1	1	3
hsa-miR-26b-5p	0	0	0	0	1	0	1
hsa-miR-21-5p	0	0	0	0	1	0	1
hsa-miR-128-3p	1	0	0	0	0	0	1

8. <u>Association networks designed with the online available STRING database</u>

The selected differentially expressed proteins upon knock down (A, C) or overexpression (B, D) of IGF2BP1 or IGF2BP3 have been selected as input for each network, respectively. The confidence cutoff for showing interaction links has been set to 'high' (0.700). Each group of deregulated proteins was subjected to computational analysis using the STRING database of known and predicted protein-protein interactions. The interactions included direct (physical) and indirect (functional) associations; they derived from computational prediction and from interactions aggregated from other (primary) databases.

(A: siIGF2BP1= knock down of IGF2BP1 via siRNAs, B: pIGF2BP1= overexpression of IGF2BP1 via recombinant plasmid, C: pIGF2BP3= overexpression of IGF2BP3 via recombinant plasmid, D: siIGF2BP3= knock down of IGF2BP3 via siRNAs)

D   siIGF2BP3

9. Published cell type-specific targets of miR-26b-5p, miR-21-3p or miR-9-5p associated with cancer disease

Table A.9.1. Known cell type-specific targets of miR-26b-5p associated with cancer disease

Cancer	Profile	Target	Pathway	Correlation	Ref
melanoma	down	PDGFRA (*in silico*)	MAPK signalling pathway	Not available (N/A)	503
melanoma	down	TRIM44	AKT/mTOR pathway	positive with poor prognosis	504
melanoma	down	TRAF5	MAPK signalling pathway	negative with progression	505
murine melanoma	up	DNMT3b	DNA methylation pathway	negative	506
HCC	down	SMAD1	BMP4/SMAD1 signalling and Twist1-induced cellular EMT	negative with metastasis	507
HCC	down	VE-cadherin, SNAIL and MMP2	EMT	negative regulator of proliferation, angiogenesis and apoptosis	508
HCC	down	HSPA8, EpCAM	N/A	negative with migration, invasion and tumourigenicity	509

Cancer	Profile	Target	Pathway	Correlation	Ref
ICC	down	S100A7	N/A	suppressed the proliferation, migration and invasion	510
bladder	down	PLOD2	hypoxia, glycolytic pathway (indirectly)	suppressed the migration and invasion indirectly negatively with shorter OS	511
gastric	down		p53 signalling, hippo signalling, transforming growth factor-β signalling, and glycosaminoglycan biosynthesis-chondroitin sulfate/dermatan sulfate	negative with progression	512
multiple myeloma	down	JAG1	Notch pathway	positive with OS and PFS	513
breast	up	TRPS1	DNA-repair, cell cycle, mitosis, cell migration, angiogenesis and EMT pathways	positive with radiation exposure	514
lung	up	EZH2	N/A	suppression of proliferation, induction of apoptosis	515
papillary thyroid	down	β-catenin	β-catenin-signalling	negative with proliferation, migration, invasion, EMT and clinical stage	516
thyroid	down	pGsk3beta, β-catenin	Gsk3beta/β-catenin pathway	negative with lymph node metastasis	517
prostate	N/A	N/A	in pair with miR-107	negative with diagnosis	518
NSCLC	down	COMMD8	SP1-LINC00657-miR-26b-5p-COMMD8 axis	negative with cell proliferation, migration and progression	519
prostate	down	N/A	genes involved in PC onset (IGF1R, PTEN, TP53, RB1, E2F2 and EZH2)	negative with PSA levels, Gleason score and positively with low-risk patients	520
luminal breast	up	N/A	invasion and metastasis pathway	positive with metastasis	521
bladder	down	PDCD10	ERK pathway	negative with proliferation, positively with prognosis	522
bladder	N/A	N/A	N/A	positive with survival and prognosis	523
neuroblastoma	down	LIN28B	MYCN-LIN28B pathway	positive with overall survival	524
diffuse intrinsic pontine glioma	N/A	TFAP2C	N/A	development and progression	341
small cell osteosarcoma	up	N/A	cancer, mTOR and cell cycle signalling	SCO tumorigenesis	525
pancreatic	down	COX2	Cox-2 centered pathway	prognosis	526

Cancer	Profile	Target	Pathway	Correlation	Ref
HNSCC	down	N/A	N/A	N/A	[527]
hepatitis B virus-associated HCC	down	CCNE1	N/A	tumorigenesis	[528]
collecting duct RCC	up	PPARGC1A, ALDH6A1, and MARC2	cancer and cell cycle pathways	negative with overall survival	[529]
pituitary tumours	down	N/A	N/A	negatively with Ki-67 proliferative index	[530]
invasive bladder	up	N/A	N/A	diagnosis	[531]
NSCLC	down	COX2	N/A	suppress lung cancer cells proliferation, migration and invasion	[532]
glioma	down	EphA2	N/A	inverse with the grade of glioma	[533]
hepatocellular carcinoma	down	USP9X	EMT through Smad4/TGF-β signalling pathway	negative with EMT and the grade of HCC	[534]
NSCLC	down	MIEN1	NF-κB/MMP-9/VEGF pathway	negative with prognosis	[535]
prostate	down	ULK2	autophagy pathway	negative with autophagy	[536]

Table A.9.2. Known cell type-specific targets of miR-21-3p associated with cancer disease

Cancer	Profile	Target	Pathway	Correlation	Ref.
cutaneous melanoma	up	N/A	N/A	positive invasive and aggressive phenotype	[452]
non-melanoma skin cancer	up	GRHL1	PI3K/AKT/ mTOR signalling pathway	N/A	[537]
MSI-CRC	up	SMAD7	EMT	positive with migration and invasion, negatively with prognosis	[451]
ovarian	up	NAV3	N/A	positive to resistance to cisplatin	[453]
ovarian and prostate	up	RBPMS, RCBTB1, ZNF608	N/A	positive with proliferation and invasion	[454]
squamous cell carcinoma	up	TRAF4	cell cycle regulation and TGF-β signalling pathway	positive with high risk	[456]
early breast cancer	up	N/A	N/A	positive with early detection	[457]
triple negative breast cancer	up	N/A	cell protein metabolism, RNA transcriptional regulation, cell migration, MAPK signalling, ErbB signalling, prolactin signalling and adherents junctions	positive with low OS	[538]
colorectal carcinogenesis	up	N/A	N/A	N/A	[458]
CRC	up	RBPMS	Smad4/ERK signalling pathway	positive with proliferation, migration and invasion	[539]

Cancer	Profile	Target	Pathway	Correlation	Ref.
choriocarcinoma	up	STAT3	NK-kB, TGFβ-SMAD, RAS-RAF-MEK-ERK, PI3K-AKT, NWASP-ARP/2/3-(F)-actin, JAK-STAT	N/A	540
ccRCC	N/A	N/A	N/A	secretion as exosomal miR	459
HCC	down	MAT2A, MAT2B	N/A	N/A	541
laryngeal	up	FZD4	PI3K pathway	N/A	455
oral squamous cell carcinoma	up	N/A	N/A	positive with metastasis	542
brain metastasis	up	N/A	N/A		543
glioma	up	N/A	N/A	positive with prognosis, negatively with OS	544

Table A.9.3. A selection of known cell type-specific targets of miR-9-5p associated with cancer disease

Cancer	Profile	Target	Pathway	Correlation	Ref.
metastatic/primary melanoma	down/up	SNAIL1, NFkB1	NFkB1/SNAIL1 pathway	negative with progression	460
malignant melanoma	down	NRP1	N/A	negative with proliferation, migration, and invasion	461
malignant melanoma	down	SIRT1	N/A	negative with proliferation and migration	462
melanoma	N/A	GOT1	N/A	negative with ferroptosis	545
uveal melanoma	down	NFkB1, MMP-2, MMP-9, VGFA	NFkB1 pathway	negative with cell migration and invasion	546
metastatic melanoma	down	N/A	N/A	negative with metastasis	547
primary melanoma	up	N/A	N/A	N/A	548
gastric	down	N/A	NFkB1 pathway	negative with cell growth	549
NSCLC	up	FOXO1		positive with cell growth	550
primary brain	up	N/A	N/A		551
breast	up	CDH1	beta-catenin signalling	positive with amplification, tumour grade and metastatic status	552
NSCLC	up	TGFBR2	TGF-β/SMAD2/SMAD3 pathway	positive with proliferation, metastasis and invasion	553
pancreatic	down	GOT1	glutamine metabolism and redox homeostasis	negative with tumour stage and vessel invasion	554
early stage gastric	up	N/A	N/A	positive with tumour stage and diagnosis	555
squamous cell carcinoma (SSC)	up	TWIST1	EMT	positive with histotype and high risk HPV (HPV16) type, positively wirh cell viability and anchorage independence	556
adenocarcinoma	down			positive with tumour suppression (HPV18)	
CRC	up	CDX2	N/A	negative with prognosis in stage I-IV CRC	557

Cancer	Profile	Target	Pathway	Correlation	Ref.
CRC	down	PAK4	N/A	negative with cell proliferation and positively with apoptosis	558
cervical	up	SOCS5	EMT	positive with angiogenesis, invasion and primary tumour growth and radiosensitivity	559
prostate	up	STARD13	EMT	positive with cell proliferation, invasion and migration	560
papillary thyroid cancer	down	BRAF	RAF-MEK-ERK signalling pathway	negative with viability and positively with apoptosis	561
cervical	down	PTEN, POU2F1	N/A	negative with proliferation and migration	562

10. Immunohistochemistry Scoring System

Histology # .... Befunder: PK

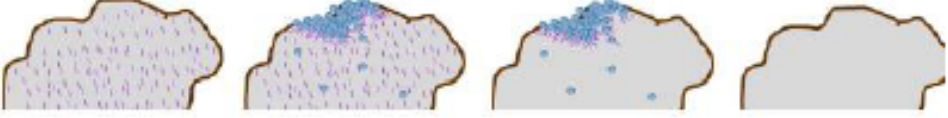**Ulceration** ☐ yes ☐ no ☐ equivocal

Intratumoral lymphocytes

CD8 - T-cell infiltrate ☐ brisk ☐ non-brisk ☐ absent

CD8-count/HPF ☐ 0 ☐ 1-10 ☐ 11-50 ☐ >50

CD4-count/HPF ☐ 0 ☐ 1-10 ☐ 11-50 ☐ >50

foxP3-count/HPF ☐ 0 ☐ 1-10 ☐ 11-50 ☐ >50

CD
PD-L1   Constitutive   Constitutive and induced   Induced   Negative

PD-L1 ☐ const. ☐ const.& ind. ☐ Induced ☐ negative

% of pos. Tu-cells ☐ 0 ☐ 1-5% ☐ >5%

Macrophages   Intratumoral

CD68/HPF ☐ 0 ☐ 1-10 ☐ 11-30 ☐ >30

CD163/HPF ☐ 0 ☐ 1-10 ☐ 11-30 ☐ >30

DCs   Intratumoral / HPF

CD123 (pDCs) ☐ 0 ☐ 1-5 ☐ 6-10 ☐ >10

CD11c ☐ 0 ☐ 1-5 ☐ 6-10 ☐ >10

Intratumoral   Peritumoral

CLEC 9A ☐ 0 ☐ 1 ☐ 0 ☐ 1

Tumor cell expression (%)

TAP-1 (NOB1) ☐ 0 ☐ 1-5 ☐ 6-20 ☐ >20

MxA ☐ 0 ☐ 1-5 ☐ 6-20 ☐ >20